A University of Sussex DPhil thesis

Available online via Sussex Research Online:

http://sro.sussex.ac.uk/

This thesis is protected by copyright which belongs to the author.

This thesis cannot be reproduced or quoted extensively from without first obtaining permission in writing from the Author

The content must not be changed in any way or sold commercially in any format or medium without the formal permission of the Author

When referring to this work, full bibliographic details including the author, title, awarding institution and date of the thesis must be given

Please visit Sussex Research Online for more information and further details

INVESTIGATING THE ROLE OF THE ATR-DEPENDENT DNA DAMAGE RESPONSE IN THE AETIOLOGY OF MICROCEPHALIC PRIMORDIAL DWARFISM DISORDERS

A thesis submitted to the University of Sussex for the degree of Doctor of Philosophy

By

Sarah A. Walker

July 2012

Declaration

I hereby declare that this thesis has not been and will not be submitted in whole or in part to another University for the award of any other degree.

Signed……..

S. A. Walker

Acknowledgements

Firstly I would like to thank all patients, their families and clinicians, without whom this work would not have been possible. Thanks to our collaborators for their mapping and sequencing expertise and for identifying those all-important mutations. Thank you to all the members of the Jeggo laboratory for their support and guidance, particularly Tom, Lisa and Queti who were always available for helpful scientific discussions and therapeutic tea breaks. Special thanks go to both Penny and Mark for their continual scientific guidance, support and encouragement. Finally a huge thank you to Jon, my wonderful husband, and Grace and Ellie my beautiful daughters, without whose support and love I could not have achieved this.

For Dad.

UNIVERSITY OF SUSSEX

SARAH ANN WALKER

DOCTOR OF PHILOSOPHY BIOCHEMISTRY

INVESTIGATING THE ROLE OF THE ATR-DEPENDENT DNA DAMAGE RESPONSE IN THE AETIOLOGY OF MICROCEPHALIC PRIMORDIAL DWARFISM DISORDERS

SUMMARY

Repair of damage to the DNA is essential for the maintenance of genomic stability, both during embryonic development and normal growth. The cell has therefore evolved a complex array of interconnected pathways to ensure the appropriate response to DNA damage is initiated, such as cell cycle checkpoint arrest, activation of DNA repair pathways or induction of apoptotic processes. These co-ordinated signal transduction pathways have been termed the DNA damage response (DDR). A previous study showed that ATR-dependent damage responses were frequently defective in cell lines from patients with Microcephalic Primordial Dwarfism (MPD) disorders. In this thesis I have further characterised ATR–dependent damage response signalling in several cell lines from patients with various MPD disorders. I have shown that novel mutations in *PCNT*, which encodes a structural centrosomal protein, result in an MPD disorder and have characterised the associated ATR-dependent DNA damage responses. I also contributed to the identification of mutations in *ORC1*, encoding a component of the DNA replication Origin Recognition Complex, in further MPD patients and examined origin licensing and S-phase progression in the patient derived cell lines. As a novel finding, I observed defects in the ATR-dependent G2/M checkpoint response in these cells. Additionally, I have characterised novel mutations in *ATRIP*, a gene encoding the obligate partner of ATR, in Seckel Syndrome patients, denoting a novel genetic defect in this condition. Finally, I have explored the role of PLK1 and AurA kinase in ATR-dependent G2/M checkpoint control and provided compelling evidence of mis-regulation of this pathway in various MPD-patient derived cell lines. Collectively these data provide important functional insights into the genetic defects that cause MPD disorders and further explore the link between defective ATR-dependent damage response signalling and microcephaly.

Contents

LIST OF FIGURES

LIST OF TABLES

ABBREVIATIONS

aa	Amino acid
AP	apurinic site
APE-1	Apurinic/apyrimidinic (AP) DNA endonuclease
APTX	Aprataxin
ASPM	Abnormal Spindle Microcephaly associated
A-T	Ataxia-telangiectasia
ATLD	Ataxia-telangiectasia-like disorder
ATM	Ataxia-telangiectasia mutated
ATR	Ataxia-telangiectasia mutated and Rad3-related
ATRIP	ATR interacting protein
AurA	Aurora A Kinase
BAH	Bromo-adjacent homology domain
BARD1	BRCA1-associated RING domain protein-1
BER	Base excision repair
BLM	Bloom's syndrome defective protein
bp	Base pair
BP	Basal progenitor cell
BRCA1/2	Breast cancer susceptibility protein 1/2
BRCT	BRCA1 C-terminal CHECK
BrdU	Bromodeoxyuridine
BSA	Bovine serum albumin
CDC	Cell division cycle protein
CDK	Cyclin dependent kinase
Cdk5Rap2	CDK5 regulatory subunit-associated protein 2
CDT1	chromatin licensing and DNA replication factor 1
cDNA	Complementary DNA
CENP-J	Centromere protein J
CEP63	Centrosomal protein of 63kDa
CEP152	Centrosomal protein of 152kDa
CEP164	Centrosomal protein of 164kDa
CEP192	Centrosomal protein of 192kDa
Chk1/2	Checkpoint kinase 1/2
CldU	Chlorodeoxyuridine
hCLK2	CDC-like kinase 2
CPD	Cyclobutane pyrimidine dimmer

CS	Cockayne Syndrome
CSA	Cockayne syndrome protein A
CSB	Cockayne syndrome protein B
CtIP	CtBP-interacting protein
DAPI	4’-6-diamino-2-phenylindole
DDR	DNA damage response
DNA	Deoxyribonucleic acid
DNA-PK	DNA-dependent protein kinase
DNA-PKcs	DNA-dependent protein kinase catalytic subunit
dsDNA	Double stranded DNA
DSB	DNA double strand break
EBV	Epstein-Barr virus
EDTA	Ethylene diamine tetraacetic acid
EGL	external granule layer
EGTA	Ethylene glycol tetraacetic acid
EME1	Crossover junction endonuclease 1
EXO1	Exonuclease 1
FA	Fanconi anaemia
FAAP24	Fanconi anaemia associated protein 24
FAAP100	Fanconi anaemia associated protein 100
FAN-1	Fanconi-associated nuclease 1
FANCD2	Fanconi anaemia complementation group D2
FANCI	Fanconi anaemia complementation group I
FANCJ	Fanconi anaemia complementation group J
FANCM	Fanconi anaemia complementation group M
FAT	FRAP, ATM, TRRAP domain
FATC	FAT C-terminal domain
FCS	Foetal calf serum
FEN-1	Flap endonuclease 1
FITC	Fluorescein isothiocyanate
FoxM1	Forkhead Box M1
GE	ganglionic eminence
GGR	Global genome repair
Gy	Gray
h	Hours
H2AX	variant form of histone H2A
γH2AX	Phosphorylated form of H2AX
HDAC6	Histone Deacetylase 6

HEAT	Huntingtin, Elongation factor 3, A subunit of protein phosphatase 2A and TOR1 (repeat motif)
HEF1	human enhancer of filamentation 1
HP1	Heterochromatin protein 1
HR	homologous recombination
HRP	Horseradish peroxidase
hTERT	Human telomerase reverse transcriptase
HU	Hydroxyurea
ICL	Interstrand crosslink
IdU	Iododeoxyuridine
IF	Immunfluoresence
IKNM	Interkinetic nuclear migration
IP	Immunoprecipitation
IR	Ionising radiation
KAP1	KRAB (Krüppel-associated box) domain-associated protein 1
KD	Kinase domain
LATS2	Large tumor suppressor homolog 2
LIGI	DNA Ligase I
LIGIII	DNA Ligase III
LIG4	DNA Ligase IV
LB	Luria-Bertani Broth
LBL	Lymphoblastoid line
MCM	Mini chromosome maintenance protein
MCPH1	Microcephalin
MDC1	Mediator of checkpoint protein 1
MDM2	E3 Ubiquitin-protein ligase Mdm2
MGS	Meier-Gorlin Syndrome
Min	Minutes
mL	Millilitres
MMC	Mitomycin C
MMR	DNA Mismatch repair
MOPD	Microcephalic osteodysplastic primordial dwarfism
MPD	Microcephalic Primordial Dwarfism
MRC	Medical research council
Mre11	Meiotic recombination 11 homolog A (S. Cerevisiae)
MRI	Magnetic resonance imaging
MRN	Mre11-Rad50-Nbs1 complex
mTOR	Mammalian target of rapamycin

MTOC	Microtubule-organising centre
MUS81	Crossover junction endonuclease Mus81
N	Neuron
NaCl	Sodium chloride
NBS	Nijmegen breakage syndrome
Nbs1	Nijmegen breakage syndrome protein 1
NDEL1	Nuclear distribution element-like 1
NE	Neuroepithelium
NEK2	NIMA (never in mitosis gene a)-related kinase 2
NER	Nucleotide excision repair
NHEJ	Non-homologus end-joining
NMD	Nonsense mediated decay
OB	Oligonucleotide-oligosaccharide
ORC	Origin recognition complex
ORCA	ORC-associated protein
PACT	pericentrin-AKAP450 centrosomal targeting
PALB2	Partner and localiser of BRCA2
PARP1/2	Poly (ADP-ribose) polymerase 1/2
PBS	Phosphate buffered saline
PCR	Polymerase chain reaction
PFA	Paraformaldehyde
PCNA	Proliferating Cell Nuclear Antigen
PCNT	Pericentrin
PIKK	Phosphoinositol 3-kinase like kinase
PKA	Protein kinase A
PLK1	Polo-like kinase 1
PNKP	polynucleotide kinase 3’-phosphatase
Polβ	DNA polymerase beta
PP1	Protein phosphatase 1
PP2	Protein phosphatase 2
PRD	PIKK-regulatory domain
preRC	pre-replication complex
qPCR	Quantitative polymerase chain reaction
RAD51	DNA repair protein RAD51 homolog 1
RFC	Replication factor C
RG	Radial glial cell
RNA	Ribonucleic acid
RNF8	Ring finger protein 8

RNF168	Ring finger protein 168
RPA	Replication protein A
RPMI	Roswell Park Memorial Institute media
RS-SCID	Radiosensitive severe combined immunodeficiency
RT	Room temperature
RT-PCR	Reverse transcription polymerase chain reaction
SAC	Spindle assembly checkpoint
SCE	Sister chromatid exchange
SCF	Skp, Cullin, F-box containing complex
SCKL	Seckel syndrome locus
SD	Standard deviation
SDS	Sodium dodecyl sulfate
SDS-PAGE	Sodium dodecyl sulfate polyacrylamide gel electrophoresis
SMG-1	Suppressor of morphogenesis in genitalia
SNP	single-nucleotide polymorphism
SS	Seckel syndrome
SSB	Single strand break
ssDNA	Single stranded DNA
TACC	Transforming acidic coiled-coil protein
TBS	Tris-buffered saline
TCR	Transcription coupled repair
TDP1	Tyrosyl-DNA phosphodiesterase 1
TFIIH	Transcription factor-IIH
Tipin	Timeless-interacting protein
TLK1	tousled-like kinase 1
TOP1	DNA topoisomerase 1
TOP3A	DNA topoisomerase 3-alpha
TopBP1	DNA topoisomerase II binding protein 1
TPX2	Targeting Protein for Xenopus kinesin-like protein 2
TRRAP	Transformation/transcription domain-associated protein
TTD	Trichothiodystrophy
UV	Ultraviolet radiation
WCE	Whole cell extract
WRN	Werner syndrome protein
WT	Wild type
XLF	XRCC4-like factor
XPA	Xeroderma pigmentosum complementation group A
XPF	Xeroderma pigmentosum complementation group F

XPG	Xeroderma pigmentosum complementation group G
XP	Xeroderma pigmentosum
XRCC1	X-ray cross–complementing group 1
XRCC4	X-ray cross–complementing group 4
53BP1	p53 binding protein 1
6-4PP	pyrimidine 6-4 pyrimidone photoproduct
8-oxoG	with 8-oxo-7,8-dihydroguanine
9-1-1	Rad9-Hus1-Rad1 complex

CHAPTER ONE

1. INTRODUCTION

Primordial dwarfism is a medical term used to describe individuals that display severe short stature at birth. This description has come to encompass many subtypes of human genetic disorder, including Seckel syndrome (SS) (OMIM 210600, 606744, 608664 and 613676), Microcephalic Osteodysplastic Primordial Dwarfism, Type II (OMIM 210720) and Meier-Gorlin Syndrome (OMIM 224690). These disorders are inherited in an autosomal recessive manner and common clinical features include intrauterine growth retardation, proportionate dwarfism, severe microcephaly and varying degrees of intellectual disability (Majewski and Goecke, 1982, Gorlin, 1992, Hall *et al.*, 2004). These disorders will be discussed in detail in due course.

Microcephaly is defined as a reduced head circumference of greater than 3 standard deviations below the normal mean for age, sex and length of gestation. The reduced head circumference is an external manifestation of an overall reduction in brain volume, which may or may not be accompanied by other neurological defects (O'Driscoll *et al.*, 2006). The exact cause of microcephaly is unclear and there are likely to be multiple causes, however changes to cell cycle duration, spindle position and the efficiency of DNA repair have all been shown to affect cortical expansion (Thornton and Woods, 2009).

1.1 MAMMALIAN BRAIN DEVELOPMENT

The bulk of work undertaken in order to understand the process of brain development has been performed using the mouse as a model. Therefore the following section will focus on this data. The mammalian brain develops from a single specialised embryonic cell layer called the neuroepithelium (NE). This layer is formed at the base of the ventricular zone, around the ventricles of the developing brain (O'Driscoll and Jeggo, 2008). Neural progenitor cells present in the neuroepithelium can divide either symmetrically to expand stem cell numbers and therefore brain volume, or asymmetrically in order to give rise to the specialized differentiated cells of the brain (Lu *et al.*, 2000) (Huttner and Kosodo, 2005) (Figure 1.1).

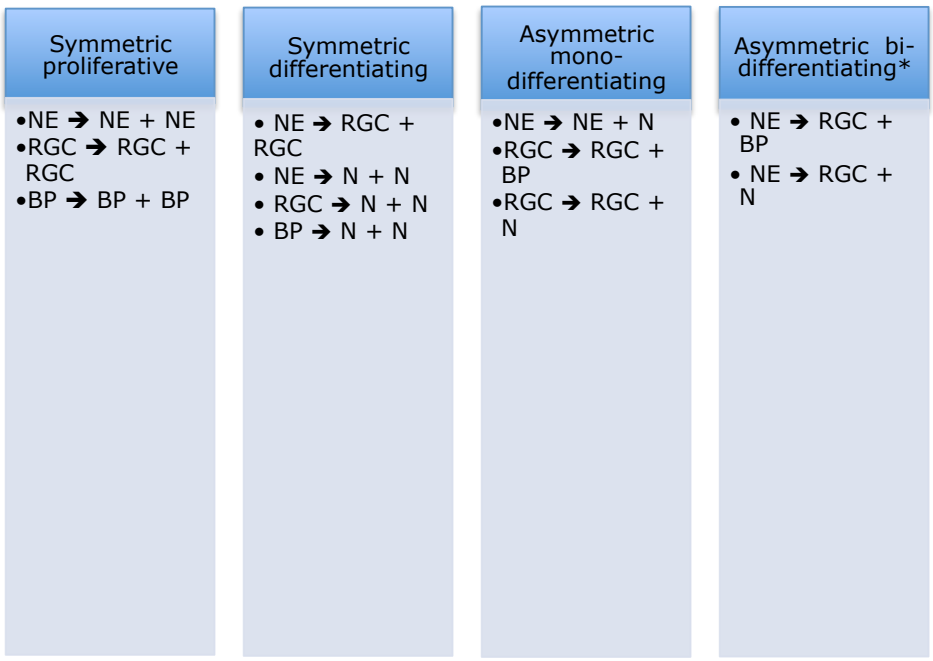

Figure 1.1 Progenitor cell divisions

NE: neuroepithelial cell, RGC: radial-glial cell, BP: basal progenitor, N: neuron. * Proposed but not reported

Adapted from Huttner & Kosodo, 2005 and Götz & Huttner, 2005.

NE progenitor cells are attached to the apical surface of the neuroepithelium and are polarized along the apico-basal axis (Thornton and Woods, 2009). They are anchored to the apical surface via adherens junctions, the integrity of which are required to maintain cell polarity (Zhadanov *et al*., 1999). The apical-basal polarity is an important factor in the decision between symmetric and asymmetric division, along with cleavage plane orientation, cell cycle length and interkinetic nuclear migration (Götz and Huttner, 2005).

The apical plasma membrane is a tiny portion of the whole cellular membrane but is a critical factor in determining symmetric versus asymmetric division (Kosodo *et al.*, 2004). In symmetric division, the apical membrane is bisected by vertical cleavage during cytokinesis, with two identical daughter cells each inheriting a segment. These cells therefore retain their NE progenitor cell characteristics and remain attached to the apical surface (Thornton and Woods, 2009). These symmetric divisions are proliferative and serve to expand the cellular population laterally.

In asymmetric division, two daughter cells with different fates are produced. The apical membrane is bypassed either by horizontal cleavage or a vertical cleavage (Figure 1.2). This results in one daughter cell inheriting all of the apical membrane and the adherens junction, thus remaining an NE progenitor. The other daughter cell, receiving no apical membrane, detaches from the ventricular surface, migrates in a sub-ventricular fashion and differentiates into a radial glial cell (RG), basal progenitor (BP) or neuron (N) (Götz and Huttner, 2005).

The precise location of the poles of the mitotic spindle is likely to be an important factor in determining the orientation of the cleavage plane in these highly polarised cells. The cleavage furrow during cytokinesis proceeds from the basal to the apical surface of the cell and this has been shown to be dependent on the positioning of the asters and midzone of the mitotic spindle (Bringmann and Hyman, 2005). Therefore, any small deviation of the mitotic spindle from its position of perpendicular to the apical-basal axis, can alter the cleavage furrow from bisecting the apical membrane to bypassing it, resulting in a switch from symmetrical to asymmetrical division (Götz and Huttner, 2005).

Cell cycle length has also been implicated in proliferative versus differentiating divisions. Differentiating divisions have been shown to have a longer cell cycle length than proliferative ones, indeed if G1 phase is artificially shortened, an

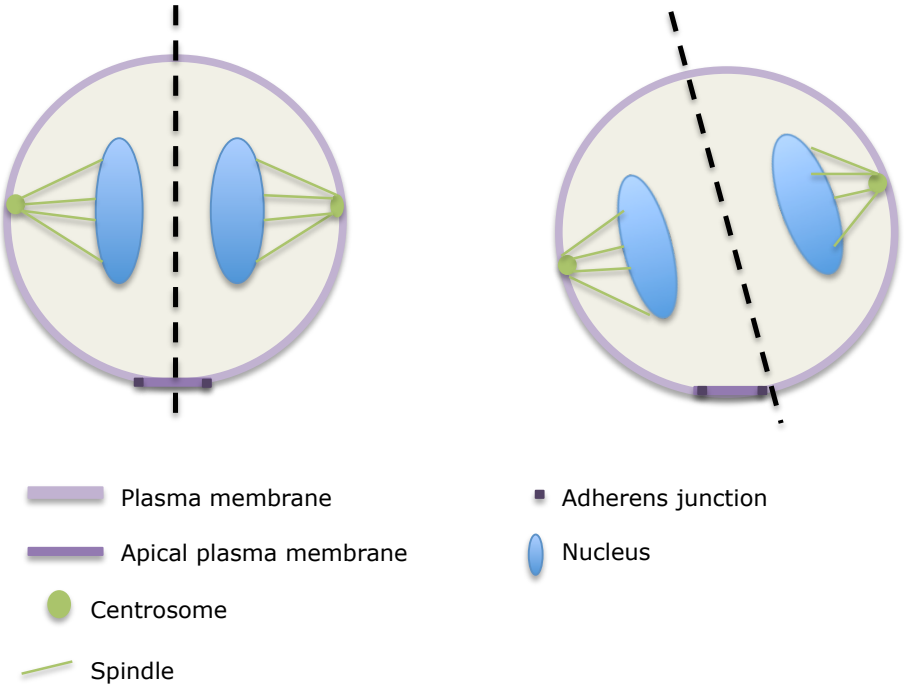

Figure 1.2 Symmetric and asymmetric division of progenitor cells

a) Symmetric division – the mitotic spindle is perpendicular to the apical-basal axis of the cell. Vertical cleavage results in inheritance of apical plasma membrane and adherens junctions by both daughter cells.

b) Asymmetric division – the mitotic spindle is not exactly perpendicular to the apical-basal axis. Vertical cleavage results in inheritance of apical plasma membrane and adherens junctions by one daughter cell only.

Figure and legend adapted from Götz and Huttner, 2005

increase in proliferative versus differentiating divisions is observed (Huttner and Kosodo, 2005). Recent findings also demonstrate that the duration of S phase is an important factor in the ability of neural progenitor cells to self-renew. This study found that the S phase duration of a self-renewing, proliferative neural progenitor was on average 3.3 fold longer than that of a neural cell committed to differentiate (Arai *et al*., 2011).

Interkinetic nuclear migration (IKNM) is observed in both NE cells and RG cells. The nucleus migrates to the basal side of the cell during G1 and S phase and then returns to the apical side during G2 phase. Mitosis is completed at the apical surface (Götz and Huttner, 2005). The exact function of IKNM is unclear although recent studies have implicated the process in the maintenance of the neural progenitor pool (Xie *et al.*, 2007) (Farkas and Huttner, 2008).

The positioning of the centrosomes within neural progenitor cells is critical for ensuring the fidelity of symmetric versus asymmetric division, via correct spindle orientation. It is thought that association of the centrosome with adherens junctions helps to maintain centrosome positioning during neurogenesis (Higginbotham and Gleeson, 2007). The centrosome will be discussed in detail in later sections.

The switch from symmetric to asymmetric division is therefore highly regulated by various different processes and the number of symmetric versus asymmetric divisions is critical for determining the final number of neurons in the brain (Cox *et al.*, 2006). For example, if a progenitor cell undergoes ten rounds of asymmetric division, it will produce ten neurons. If the progenitor cell divides symmetrically for all except the last round of division, approximately 512 neurons can be generated. The point at which the cell moves from symmetric to asymmetric division may therefore be critical in order to prevent microcephaly (Thornton and Woods, 2009).

1.2 THE DNA DAMAGE RESPONSE

Microcephaly is a clinical feature commonly observed in many DNA damage response disorders (O'Driscoll and Jeggo, 2008), suggesting that efficient DNA damage responses are essential for normal brain development.

Repair of damage to the DNA is essential for the maintenance of genomic stability, both during embryonic development and during normal growth. The cell is

continuously assaulted by both endogenous DNA damaging agents, such as reactive oxygen species and exogenous agents including ionising radiation, UV radiation or mutagenic chemicals. It is imperative that the integrity of the genome is maintained in order to prevent the introduction of mutations that could potentially lead to disease such as cancer. In some cases the most favourable outcome may be cell death, rather than allowing further proliferation of damaged cells. The cell has therefore evolved a complex array of interconnected pathways to ensure the appropriate response to DNA damage is initiated. This may include the induction of cell cycle checkpoint arrest, activation of DNA repair pathways or induction of apoptotic processes. This co-ordinated response of signal transduction and DNA repair pathways has been termed the DNA damage response (DDR) (Figure 1.3).

1.2.1 UV-induced DNA damage

UV radiation, particularly UV-B and UV-C, is absorbed by DNA resulting in its chemical and physical modification in the form of introduction of dimers (Rastogi *et al.*, 2010). Many types of photoproducts have been observed in the DNA following exposure to UV radiation. The most common of these are Cyclobutane pyrimidine dimers (CPDs), in which adjacent pyrimidine bases are joined together by a cyclobutane ring structure, and pyrimidine 6-4 pyrimidone photoproducts (6-4PPs) where the carbon in position 6 of the 5' pyrimidine is linked to the carbon in position 4 of the 3' pyrimidine (Figure 1.4). Both of these dimers distort the helical structure of the DNA as the bases are drawn together and create blocks to replication until their removal. Oxidation products can also be formed by reaction of the DNA reactive oxygen species (ROS) of which 8-oxo-7,8-dihydroguanine (8-oxoG) is the most common lesion formed (Figure 1.4) (Rastogi *et al.*, 2010). If unrepaired, this can lead to the conversion of the guanine base to a thymine and is therefore a potential cause of mutagenesis (Cheng *et al.*, 2005).

Repair of lesions of this nature is important as they can represent blocks to faithful replication of the DNA and can lead to the introduction of double-strand breaks (DSBs) through the collapse of stalled replication forks. Replication forks can stall when the polymerase becomes uncoupled from the helicase due to a distortion in helical DNA structure. Photolyase enzymes in mammals bind to CPDs or 6-4PPs and use energy from visible light to monomerise the cyclobutane ring, splitting the dimer (Rastogi *et al.*, 2010). This process is termed photoreactivation. Base excision repair (BER) and Nucleotide excision repair (NER) are important repair processes for UV-induced lesions and are discussed in detail below.

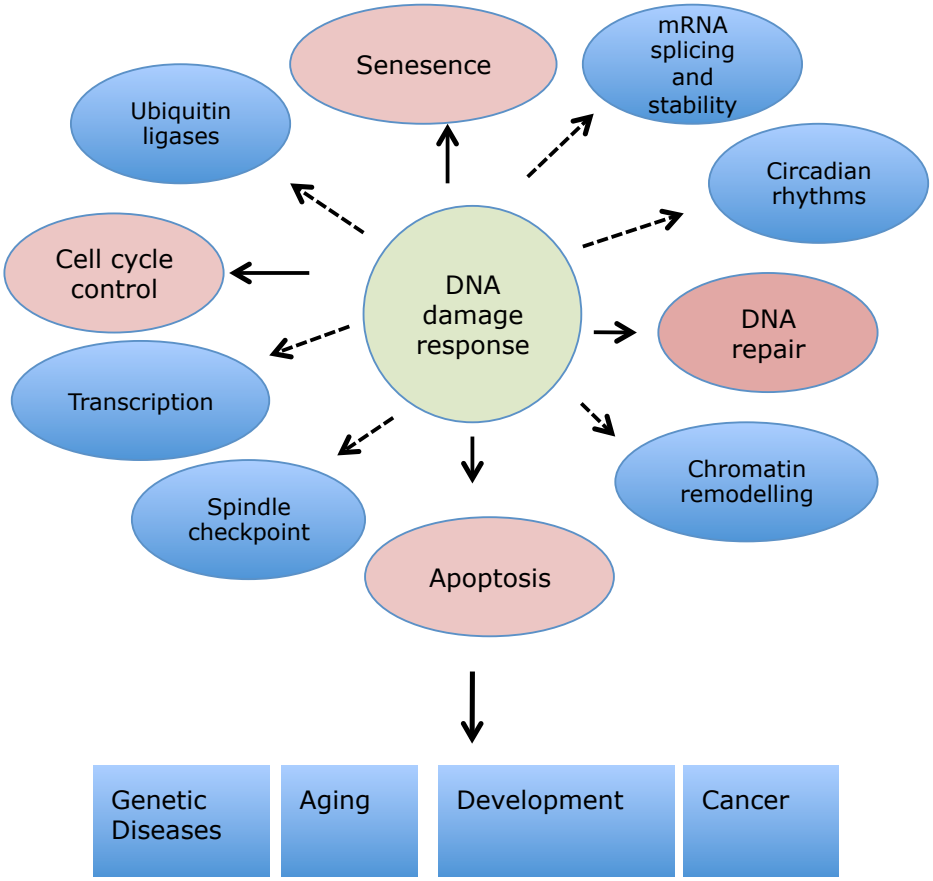

Figure 1.3 The DNA Damage Response (DDR).

The response to DNA damage involves control of the cell cycle, induction of DNA repair processes, senesence or apoptosis. A broader role of the DDR is increasingly evident involving pathways such as spindle checkpoints, transcription and circadian rhythm proteins.

Adapted from Harper & Elledge, 2007.

a)

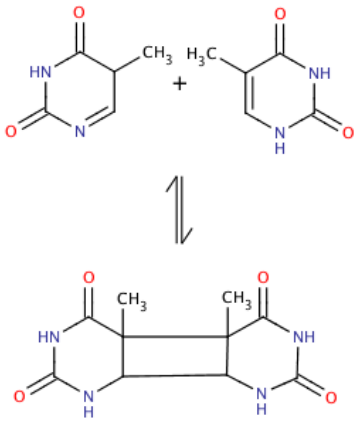

b)

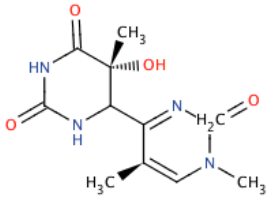

c)

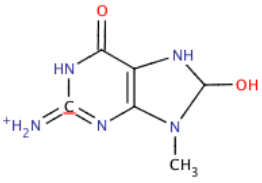

Figure 1.4 UV –induced photoproducts

a) T-T Cyclobutane pyrimidine dimer (CPD)
b) pyrimidine 6-4 pyrimidone photoproduct (6-4PP)
c) 8-oxo-7,8-dihydroguanine (8-oxoG)

UV irradiation also activates checkpoint mechanisms within the cell to delay the cell cycle in order to allow damaged bases to be repaired. This checkpoint activation will be discussed in detail in section 1.5.

1.2.2 Base excision repair

Base excision repair (BER) is the principal pathway that repairs bases damaged by alkylating agents, deamination and reactive oxygen species (Berquist and Wilson, 2012). Short-patch BER repairs lesions involving one nucleotide and long-patch BER repairs lesions involving two or more nucleotides (Figure 1.5). Both pathways are initiated by the removal of the damage by a DNA Glycosylase. DNA glycosylases cleave the N-glycosidic bond to remove the base, resulting in an abasic site (AP site) or a single-strand break. In short patch repair, AP endonuclease 1 (APE-1) then makes an incision at this site to create a gap in the DNA, which is detected by Poly(ADP-ribose) polymerase 1 (PARP1). PARP1 plays an important role in the recruitment of further repair factors to the damage site. End processing of the damaged termini is then performed by enzymes such as polynucleotide kinase 3'-phosphatase (PNKP) and aprataxin (APTX). This restores the 3' hydroxyl and 5'phosphate ends required for gap-filling and ligation steps to occur (Caldecott, 2008). X-ray cross–complementing group 1 (XRCC1), is a scaffold protein that interacts with end-processing enzymes and promotes their accumulation at damage sites. DNA polymerase beta (Polβ) is then recruited to the damage site. Polβ possesses both dRP lyase activity and polymerase activity and is thus able to fill the gap and remove the 5' phosphate to enable DNA ligase III (LIGIII) to seal the remaining nick.

In long-patch BER, the damaged flap 5' to the lesion is removed by Flap endonuclease 1 (FEN1) and this reaction is stimulated by Proliferating Cell Nuclear Antigen (PCNA) and PARP1 (Caldecott, 2008). PCNA interacts with specialised polymerases such as Polγ/ε or Polβ to extend and fill the gap by insertion of the correct nucleotides. The remaining nick is then sealed by DNA ligase 1 (LIG1).

Patients with mutations in the BER protein Aprataxin present with a disorder called Ataxia-oculomotor apraxia 1 (AOA1). The clinical features of this syndrome include cerebellar atropy, ataxia and peripheral axonal neuropathy. A similar syndrome Spinocerebellar ataxia with axonal neuropathy 1 (SCAN1) has also been described where patients also show cerebellar atrophy and peripheral neuropathy. These patients were found to have mutations in Tyrosyl-DNA phosphodiesterase 1 (TDP1),

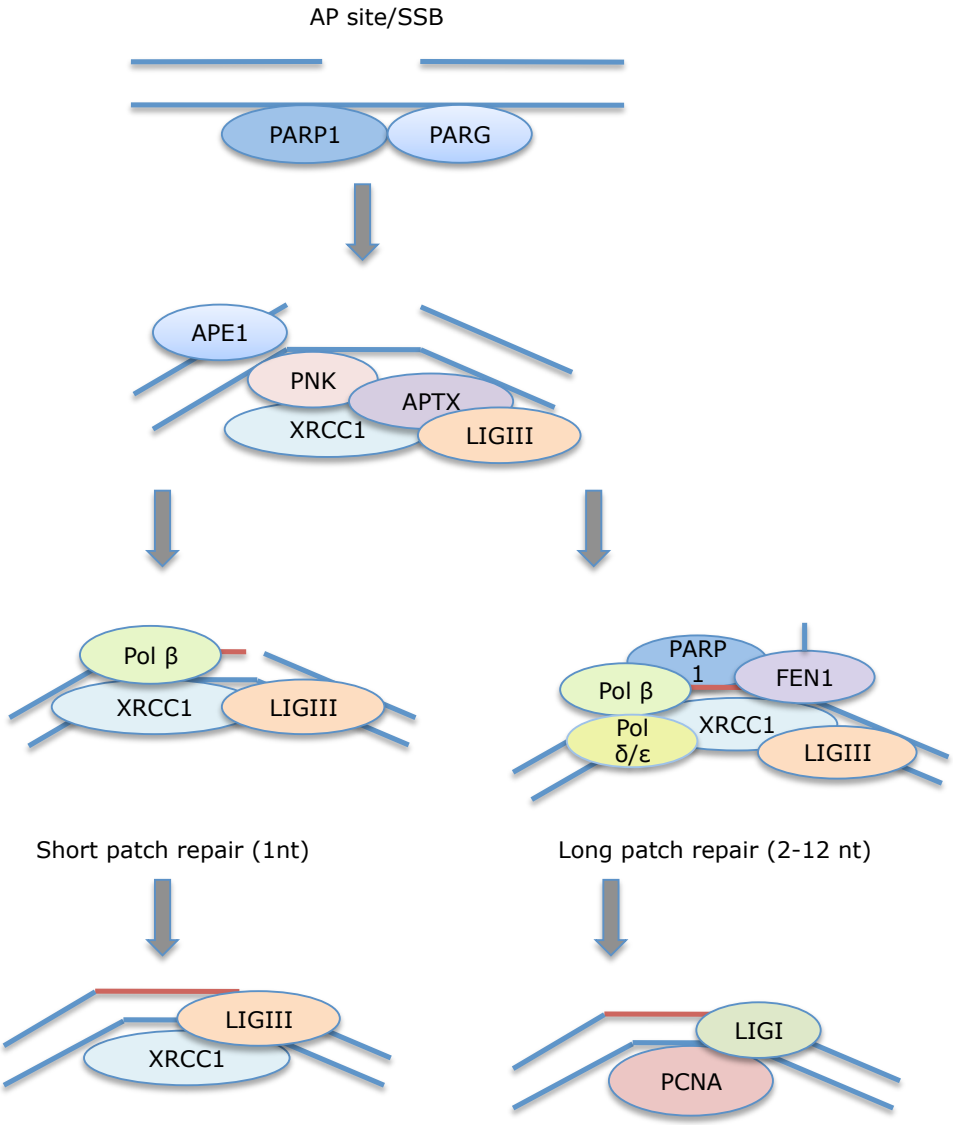

Figure 1.5 Base excision repair

Apurinic-apyrimidinic (AP) sites and single strand breaks are detected by poly(ADP-ribose) polymerase 1 (PARP1) which promotes accumulation of further repair factors. Poly(ADP-ribose) glycohydrolase (PARG) returns PARP1 to its pre-activated state, allowing further detection of SSBs. End processing of any damaged termini is then performed by polynucleotide kinase (PNK), AP endonuclease (APE1) and Aprataxin (APTX). Flap endonuclease 1 (FEN1) removes the 5′ flap in long patch repair. Pol β, Polδ or Polε fills in the gap and DNA ligase III(LIGIII) repairs the nick in short patch repair whilst DNA Ligase I (LIGI) repairs it in long patch repair.

Figure adapted from Caldecott, 2008.

a protein involved in the repair of DNA topoisomerase 1 (TOP1) associated SSBs (Caldecott, 2008).

1.2.3 Nucleotide Excision Repair

Nucleotide excision repair (NER) is the major repair pathway utilised for the removal of bulky lesions within the DNA that cause distortion of the DNA helix. These lesions include UV induced damage such as CPD's and 6-4PPs, as discussed earlier, and also DNA adducts caused by agents such as aromatic amines (Nouspikel, 2009). There are two distinct pathways of NER; Global genome repair (GGR) and transcription coupled repair (TCR). The core processes are the same for each pathway and involve; damage recognition, assembly of the pre-incision complex, removal of the damaged strand by the introduction of incisions on either side of the lesion, and finally the filling in of the resulting gap followed by its ligation (Hanawalt *et al.*, 2003) (Figure 1.6).

Global genome repair (GGR) is the NER pathway used in non-coding or silent gene regions of the DNA. The DNA damage recognition step in this pathway involves UV-damage DNA binding protein (UV-DDB1 and 2, also known as the XPE complex) and the DNA damage-binding protein XPC-HR23B (Cleaver *et al.*, 2009). Transcription coupled repair (TCR) occurs in transcriptionally active regions of the genome and is detected by the stalling of RNA polymerases I and II (RNAPI/II). Cockayne Syndrome A (CSA) and Cockayne syndrome B (CSB) are then recruited to displace the RNA polymerase to allow repair to continue. Once the damage has been detected the pathways converge and lesions are dealt with in the same manner. Transcription factor-IIH (TFIIH) is composed of ten subunits including XPB, XPD, p62, p44, p34, p52, p8, Mat1, Cdk7 and CyclinH. It is recruited to the damage and unwinds the DNA by virtue of its helicase activity (Rastogi *et al.*, 2010). RPA, XPA and XPG are then recruited, although the exact sequence of events is unclear. XPG cleaves the DNA around the damage site on the 3' side, whilst XPF-ERCC1 cleaves on the 5' side. The damage is then removed and the repair patch is filled and ligated by the BER machinery (Cleaver *et al.*, 2009).

Mutations in proteins involved in nucleotide excision repair give rise to distinct clinical diseases; Xeroderma Pigmentosum (XP), Cockayne Syndrome (CS) and Trichothiodystrophy (TTD). These disorders have diverse clinical features that include developmental and neurological problems, dwarfism, microcephaly and mental retardation (Cleaver *et al.*, 2009).

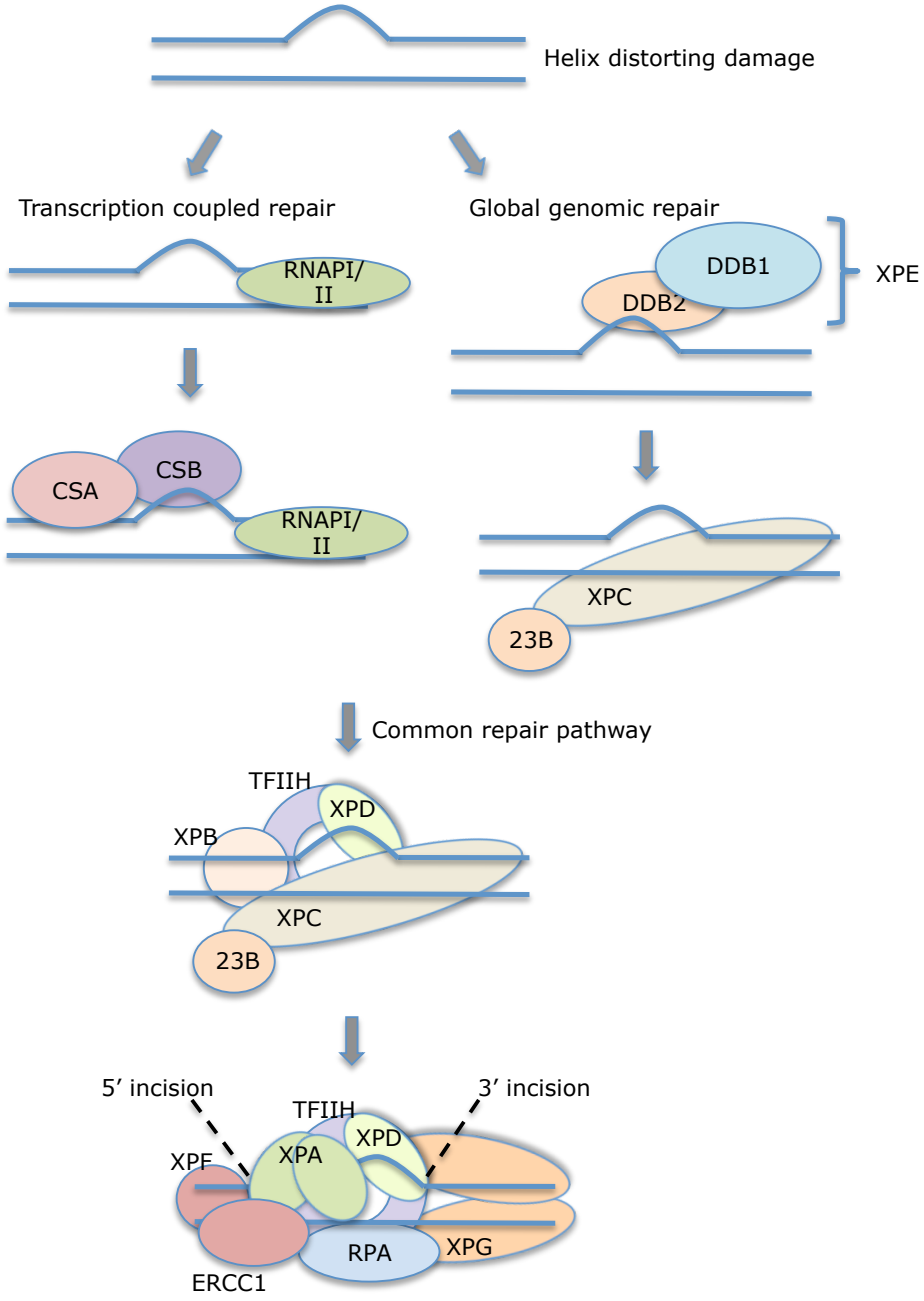

Figure 1.6 Nucleotide excision repair

Damage recognition by RNAPI/II (TCR) or XPC and XPE (GGR) is followed by recruitment of TFIIH which unwinds the DNA helix by the helicase activity of XPD. Cleavage of the damage site is then performed by the XPG (3′) and XPF-ERCC1 (5′) nucleases. BER machinery can then refill and ligate the repair patch.

Figure adapted from Cleaver et al, 2009.

1.2.4 Non-homologous End-joining

Double strand breaks can arise in the cell, either directly through exposure to ionising radiation or indirectly through the collapse of stalled replication forks. Non-homologous End–joining (NHEJ) is an error-prone process employed by the cell to ligate the ends of the DSB without the need for a homologous chromatid. This is particularly important in G1 where the sister chromatid is not available. DSBs in the DNA are recognised by the Ku70/80 heterodimer that binds to the DNA ends and recruits the DNA-dependent protein kinase catalytic subunit (DNA-PKcs). DNA-PKcs becomes activated through its interaction with the DNA and Ku. It phosphorylates Artemis as well as undergoing autophosphorylation. Artemis is a nuclease that resects the overhanging ends of the DNA in preparation for re-ligation. DNA polymerase μ (Polμ) fills in the gap and the ends are ligated by DNA Ligase IV/ X-ray repair, complementing defective repair in Chinese Hamster (LIG4/XRCC4) in conjunction with XRCC4-like factor (XLF) (Lieber, 2010, Lieber and Wilson, 2010) (Figure 1.7).

Patients with mutations in the NHEJ protein LIG4 display radiosensitivity, developmental delay and microcephaly (O'Driscoll *et al.*, 2001). Radiosensitive severe combined immunodeficiency (RS-SCID), where patients exhibit severe immunodeficiency without developmental delay, is caused by mutations in Artemis (Moshous *et al*., 2001).

1.2.5 Homologous Recombination

Homologous recombination (HR) is the repair process that is preferentially used in the S and G2 phases of the cell cycle for the repair of DSBs, when a homologous sister chromatid is available. In order for HR to proceed, the ends of the DSB must be resected in a 5’ to 3’ direction. This resection is undertaken by Exonuclease1 (Exo1) and the Mre11-Rad50-Nbs1 (MRN) complex (Ira *et al.*, 2004). CtIP also works in conjunction with MRN to promote resection (Sartori *et al.*, 2007). The single-stranded DNA (ssDNA) created by the resection activity then becomes coated with Replication protein A (RPA). This is then displaced by the Rad51 protein, which forms filaments along the DNA. These regions initiate HR by invading the strand of the homologous sister chromatid to form a D-loop structure. DNA polymerase δ extends the DNA strand from the 3’ end, using the donor DNA strand as a template. Double Holliday junctions are then formed when the break end interacts with the displaced strand from the intact homologous chromatid. Holliday

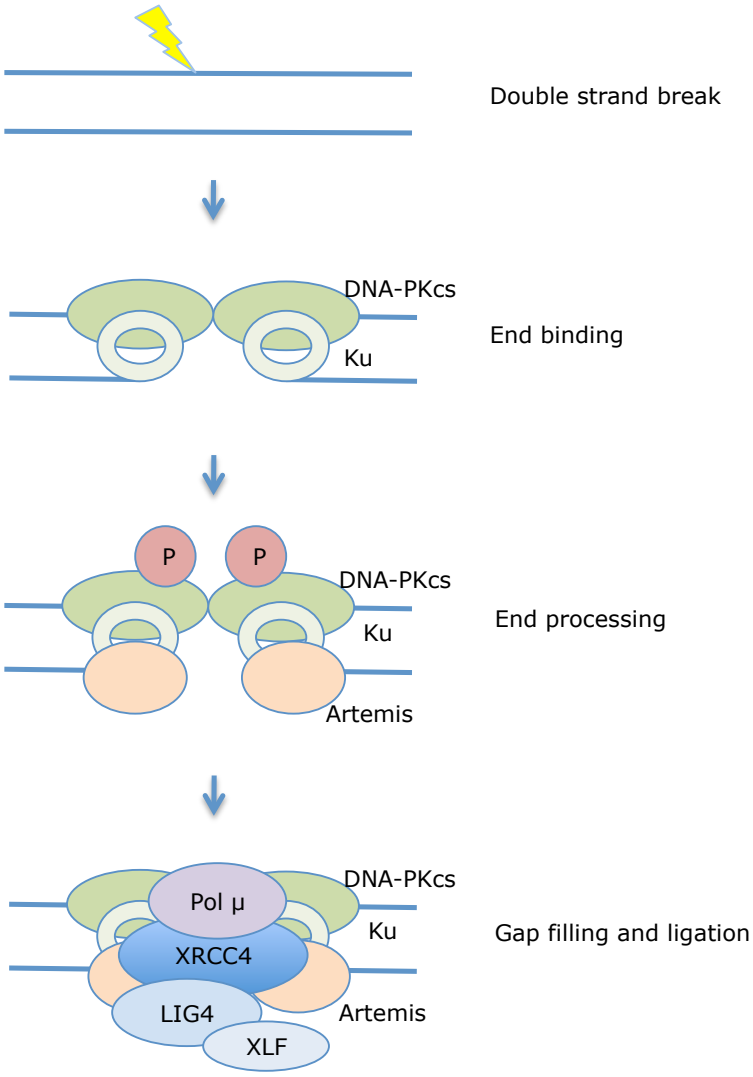

Figure 1.7 Non-homologous end joining of double strand breaks (DSBs).

DSBs in the DNA are recognised by Ku which binds to the DNA ends and recruits DNA-PKcs. DNA-PKcs is activated through its interaction with the DNA and it phosphorylates itself and Artemis. Artemis resects the ends of the DNA in preparation for re-ligation. Pol μ fills in the gap and the ends are ligated by XRCC4/LIG4 in conjunction with XLF.

Figure adapted from Lieber and Wilson, 2010.

junctions are resolved by cleavage of strands by either BLM-Top3 or Mus81-Eme1 nuclease complexes. The ends are then ligated yielding either crossover or noncrossover products (Mazón *et al.*, 2010) (Figure 1.8). Cells from patients with Bloom's syndrome, harbouring mutations in the RecQ helicase BLM, exhibit a high incidence of homologous recombination as evidenced by increased rates of sister chromatid exchanges (SCE's) (Bartram *et al.*, 1976).

1.3 ATM AND ATR: REGULATORS OF THE DNA DAMAGE RESPONSE

The main regulators of the DNA damage response are Ataxia telangiectasia mutated (ATM), Ataxia telangiectasia Rad3 related (ATR) and DNA-dependent protein kinase catalytic subunit (DNA-PKcs). These proteins are members of the phosphoinositol 3-kinase like kinase (PIKK) family of protein kinases, which also includes mammalian target of rapamycin (mTOR), suppressor of morphogenesis in genitalia (SMG1) and transformation/transcription domain-associated protein (TRRAP) (Lempiäinen and Halazonetis, 2009). These proteins share a common domain structure (Fig 1.9), which is conserved within the PIKKs and but is distinct from other protein kinases. These domains are the FRAP-ATM-TRRAP (FAT) domain, the kinase domain (KD), the PIKK-regulatory domain (PRD) and the FAT-C-terminal (FATC) domain (Lempiäinen and Halazonetis, 2009). The FAT, PRD and FATC domains are involved in regulating the activity of the kinase domain through protein-protein interactions and post-translational modifications. These kinases predominately phosphorylate substrates at –S/T-QN- sites where a serine or threonine residue is followed by a glutamate (Shechter *et al.*, 2004).

1.3.1 ATM activation

ATM and DNA-PKcs are activated by double strand breaks (DSBs), such as those induced by exposure to ionising radiation. ATM is recruited to DSBs via an interaction with the Mre11-Rad50-Nbs1 (MRN) complex, whilst DNA-PKcs is recruited by an interaction with Ku70/80 (Lovejoy and Cortez, 2009). These associated proteins have DNA end binding properties, essential for correct PIKK localisation to the damage (Falck *et al.*, 2005).

In undamaged cells, ATM is present as an inactive dimer (Goodarzi *et al*., 2004). Upon DNA damage, ATM undergoes autophosphorylation at serine 1981 and the dimer dissociates into active monomers (Bakkenist and Kastan, 2003). This

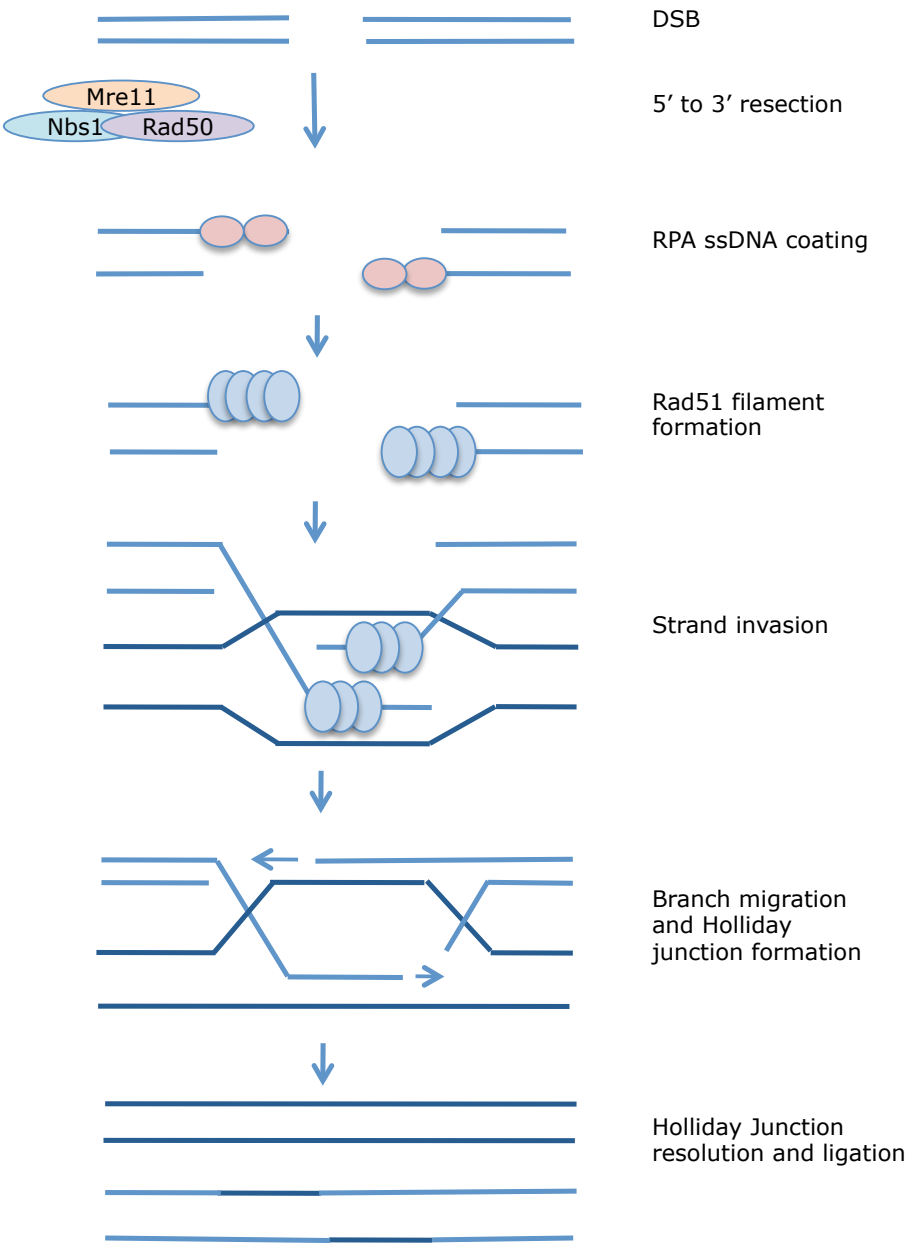

Figure 1.8 Homologous Recombination

DSB ends are resected by Exo1 and MRN nuclease yielding an ssDNA region that becomes coated with RPA. This is displaced by Rad51, mediated by BRCA2. Rad51 filaments promote strand invasion of the homologous chromatid. DNA synthesis by DNA polymerase δ extends the DNA strand. Holliday junctions are formed and resolved by BLM-Top3 or Mus81-Eme1 nucleases. Ligation of the ends completes the reaction.

Figure adapted from Sancar et al, 2004

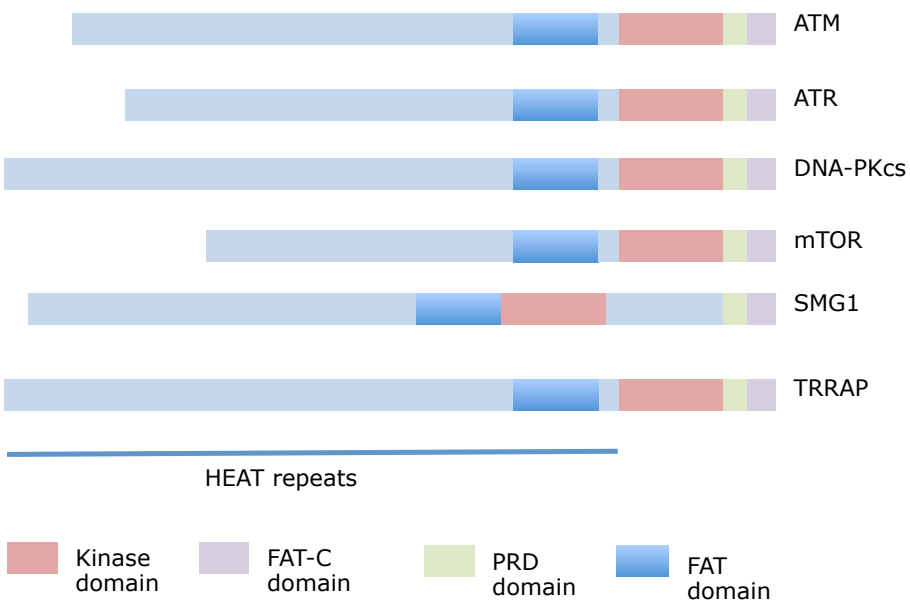

Figure 1.9 PIKK family domain structure

See text for information on domain function.

Figure adapted from Lempiainen and Halazonetis, 2009

phosphorylation is important to retain ATM at the damage site, although it is not required for its initial localisation (So *et al.*, 2009). ATM is then recruited to the DSB via an interaction with the C-terminus of Nbs1 of the MRN complex, the initial sensor of the damage (Cerosaletti *et al.*, 2006). ATM then phosphorylates histone H2AX to produce γH2AX and this phosphorylation recruits a mediator protein, mediator of DNA-damage checkpoint protein-1 (MDC1) to the break (Stewart *et al.*, 2003). H2AX can also be phosphorylated by DNA-PK in a redundant manner (Stiff *et al.*, 2004). Phosphorylated MDC1 recruits further proteins to the break site such as the ubiquitin ligase RING-finger-protein-8 (RNF8) and RING-finger-protein-168 (RNF168) (Mailand *et al.*, 2007, Doil *et al.*, 2009). RNF8 then ubiquitylates γH2AX, resulting in the recruitment of breast cancer susceptibility protein-1 (BRCA1) and p53 binding protein-1 (53BP1). RNF168 helps to maintain the ubiquitination of γH2AX and helps to stabilise the recruitment of BRCA1 and 53BP1 (Derheimer and Kastan, 2010). Thus, the ATM signalling cascade is critical to signal the presence of a subset of DSBs to further downstream repair processes such as non-homologous end-joining (NHEJ) or homologous recombination (HR) (Figure 1.10).

Ataxia telangiectasia (A-T) (OMIM 208900) is an autosomal recessive DNA damage response disorder that arises due to mutations in ATM. Cell lines from these patients have defects in all cell cycle checkpoints, are sensitive to killing by ionising radiation and also show defects in the repair of a subset of DSBs (Riballo *et al*., 2004). Clinical features of the disorder include progressive cerebellar ataxia, telangiectases, immune defects and cancer predisposition, however, unlike some of the other DNA damage response disorders that will be described later, AT patients do not display microcephaly (O'Driscoll and Jeggo, 2006).

1.3.2 ATR activation

ATR is activated in response to many kinds of DNA damage including base adducts, crosslinks, replication stress and persistent DSBs, where ssDNA regions are generated. However, it is primarily activated by the production of a common structure resulting from these different damage effects (Cimprich and Cortez, 2008). The excision of pyrimidine dimers induced by UV irradiation, mediated by the nucleotide excision repair pathway (Branzei and Foiani, 2008), the stalling of replication forks where a lesion causes the polymerase and helicase to become uncoupled, the resection of the end of a DSB by nucleases (Jazayeri *et al*., 2006); all of these cellular processes generate a region of single-stranded DNA that is next

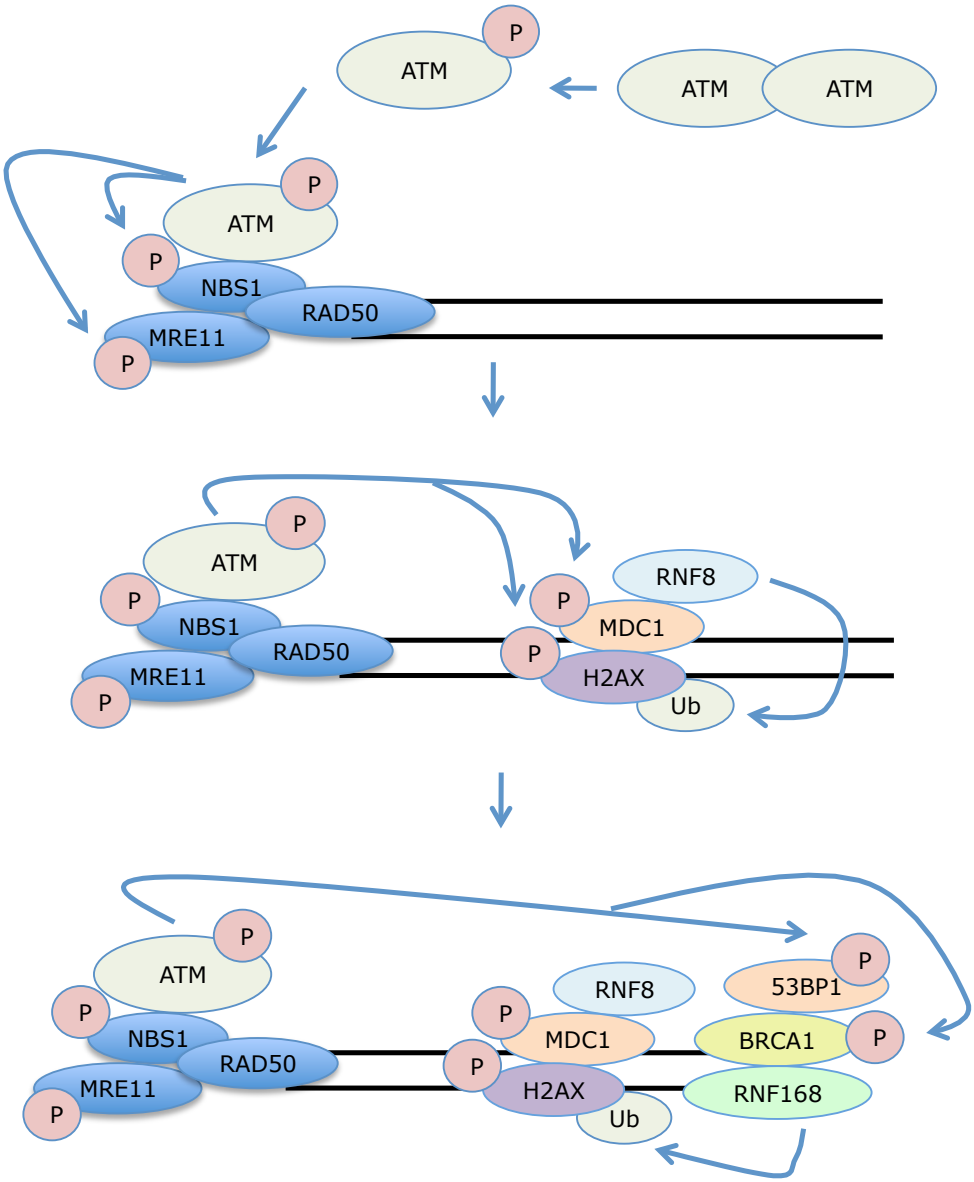

Figure 1.10 ATM-dependent recruitment of proteins to a DSB.
ATM exists in the cell as an inactive dimer. Upon induction of a DSB, ATM undergoes autophosphorylation and forms active monomers. ATM and the MRN complex are then recruited to the break where ATM phosphorylates MRE11, NBS1 and H2AX. The phosphorylation of H2AX enables recruitment of MDC1. MDC1 is phosphorylated by ATM and recruits RNF8. RNF8 mono-ubiquitinates γH2AX which results in the recruitment of 53BP1, BRCA1 and RNF168. RNF168 maintains the ubiquitination of γH2AX, stabilising 53BP1 and BRCA1 at the break.

Figure and legend adapted from Derheimer and Kastan, 2010.

to a region of double-stranded DNA with a 5' primer end (Figure 1.11). This is the DNA structure that is thought to activate ATR (Cimprich and Cortez, 2008).

When single-standed DNA (ssDNA) is detected in the cell it rapidly becomes coated with RPA. RPA is a heterotrimeric single-standed DNA binding complex that is composed of three subunits, RPA1 (70kD), RPA2 (32kD) and RPA3 (14kD). It plays important roles in DNA replication such as ssDNA stabilisation and replication initiation, as well as after DNA damage where it is essential for the assembly of signalling complexes onto damaged DNA (Namiki and Zou, 2006, Olson *et al.*, 2006). The N-terminal oligonucleotide-oligosaccharide fold (OB fold) domain of RPA1 directly binds to the N-terminus and two further domains of ATR-interacting protein (ATRIP), recruiting the ATRIP-ATR complex to ssDNA (Zou and Elledge, 2003, Namiki and Zou, 2006, Ball *et al.*, 2007). In cells, ATR exists in a stable complex with ATRIP and the expression of each protein is dependent on the other (Cortez *et al.*, 2001). The structure and function of ATRIP will be discussed in more detail in Chapter 4.

The Rad17-RFC2-5 clamp-loader complex is independently recruited to RPA-ssDNA, where it recruits and loads the Rad9-Hus1-Rad1 (9-1-1) complex onto the chromatin in the presence of a dsDNA-ssDNA junction (Zou *et al.*, 2002), (Burrows and Elledge, 2008). DNA topoisomerase II binding protein 1 (TopBP1) is then recruited to the damage via an interaction with the C-terminal tail of Rad9 (Greer *et al.*, 2003). Once all these proteins are assembled at the site of damage, an interaction between TopBP1 and both ATR and ATRIP stimulates ATR activation and the ATR kinase becomes fully active (Mordes *et al.*, 2008). Threonine 1989 on ATR was recently identified as a marker for the active kinase (Nam *et al*., 2011). ATR is auto-phosphorylated at this site after damage and this is promoted by the presence of multiple ATR-ATRIP complexes on RPA-ssDNA (Liu *et al.*, 2011). The phosphorylation was proposed to occur in *trans* along the RPA-ssDNA stretch. The T1989 phosphorylation then mediates the interaction of TopBP1 and ATR, resulting in full kinase activity.

1.4 ATR-DEPENDENT SIGNALLING

ATR has been shown to be essential for embryonic development. An elegant study demonstrated that ATR-/- embryos survive the earlier stages of development but die following implantation, at around day 7 postcoitem (Brown and Baltimore, 2000). ATR+/- heterozygous mice survive for longer but greater numbers of these

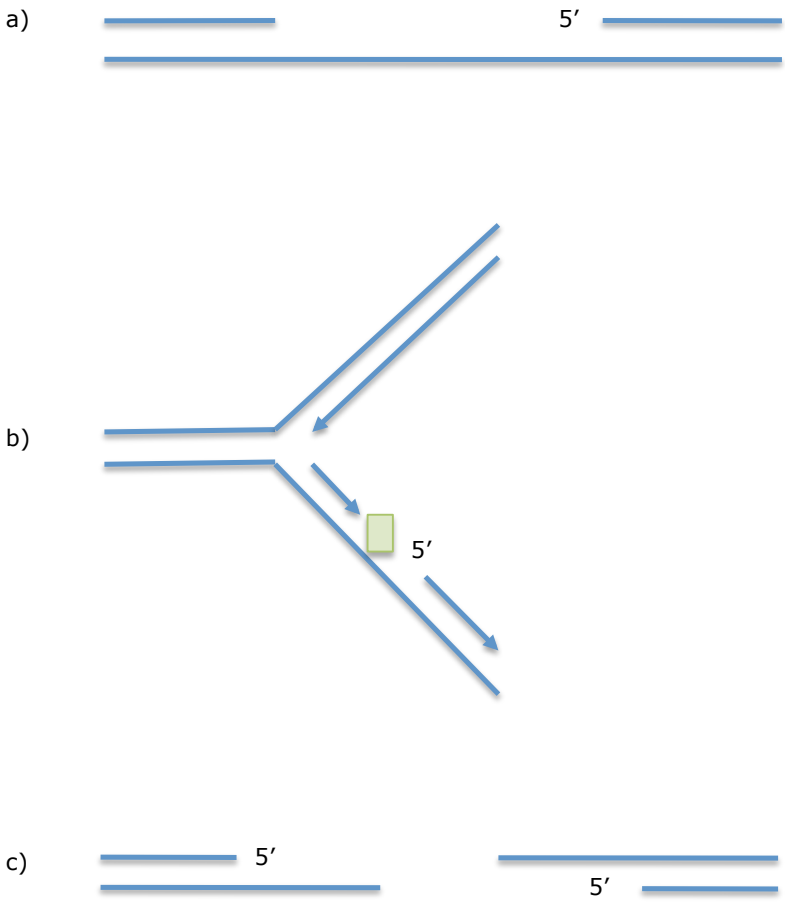

Figure 1.11 DNA structures that activate ATR

a) Single-stranded intermediate in nucleotide excision repair
b) End resection of double strand breaks
c) Regions of ssDNA generated during replication fork stalling

Adapted from Cimprich & Cortez, 2008.

animals had died by 18 months than the control or ATM+/- animals. The ATR+/- animals also showed higher tumour incidence than controls upon post-mortem examination. In contrast to ATR, ATM-/- mice are viable but display growth retardation and are infertile (Xu *et al.*, 1996). These studies demonstrate the essential nature of the ATR-dependent signalling pathway in development.

Recent studies have produced further mouse models to aid our understanding of the consequences of deficient ATR function. In one study, ATR was down regulated in all tissues in adult mice by the use of Cre-technology (Ruzankina et al., 2007). Stem and progenitor cell depletion was observed in tissues with high replicative capacity and a loss of the capacity of these tissues to renew. There was little effect on post-mitotic brain tissue. Premature aging-related phenotypes such as hair greying and osteoporosis were also observed. This study therefore eloquently illustrates the importance of ATR not only in development but also in ongoing cellular proliferation. In a further study, the ATR mutation that leads to aberrant splicing in the described ATR-Seckel patient (O'Driscoll *et al.*, 2003) was engineered into a mouse model termed $ATR^{s/s}$ (Murga *et al.*, 2009). The $ATR^{s/s}$ mice were born at sub-mendelian ratios and are phenotypically reminiscent of human Seckel syndrome, displaying severe growth retardation, microcephaly, receding foreheads and micrognathia. The mice did not survive beyond six months and also exhibited premature ageing related phenotypes such as hair greying and osteoporosis. Examination of embryonic fibroblast cells revealed an increased activation of the DNA damage response, as measured by H2AX phosphorylation, 53BP1 foci formation and chromosome breakage. It was proposed that this response was due to an increase in replication stress. When $ATR^{s/s}$ embryos were examined for the same replication stress indicators, the results were reproduced *in vivo* and also were shown to result in increased levels of apoptosis in the tissues examined.

A recently conducted study has demonstrated the importance of ATR in neural development. An elegant system was utilised to reduce embryonic expression of ATR in mice from E10.5. Mice were born with Seckel like features such as growth retardation, reduced brain size and defects in brain development, but died about 7 days later (Lee *et al.*, 2012). Post mortem examination of the brain revealed decreased cellularity of the cortex and the corpus callosum. Increased DNA damage, as evidenced by H2AX phosphorylation, was detected in the external granule layer (EGL) of the cerebellum and the ganglionic eminence (GE) of the cortex. However, other parts of the brain were not affected, indicating that ATR is required for the maintenance of specific neuroprogenitor cells. It was proposed that

this is due to the rapid proliferation of these cells, which exerts a higher dependency on ATR signalling potentially due to higher levels of replicative stress in these cell populations.

Once ATR has become fully activated as described in section 1.3.2 it can then phosphorylate many downstream targets to effect different cellular outcomes (Figure 1.12). Some important targets of ATR will be discussed in this section.

1.4.1 H2AX

The Histone H2A variant X (H2AX) can be phosphorylated by all the PIKKs as an early step in the DDR. It is phosphorylated on S139 in the C terminal tail and is then referred to as γH2AX (Fernandez-Capetillo *et al.*, 2003). This modification stretches for megabases along the chromatin, surrounding the damage site (Rogakou *et al.*, 1999). This is usually a DSB, formed either directly by external damage, after exposure to ionising radiation, or induced by processes such as recombination during meiosis or V(D)J recombination (Ward and Chen, 2001). Phosphorylation of H2AX has also been shown to be induced by the fragmentation of DNA during apoptosis (Rogakou *et al.*, 2000).

H2AX has also been shown to be phosphorylated in an ATR-dependent manner after exposure to UV or HU treatment and to form foci at replication forks during S phase (Ward and Chen, 2001). Further studies have demonstrated that ATR-dependent, UV-induced H2AX phosphorylation is cell cycle phase independent and is triggered by the generation of DNA repair-induced intermediates, specifically those produced by the NER pathway of DNA repair (Hanasoge and Ljungman, 2007).

The phosphorylation of H2AX is important in order to recruit and retain further DDR mediator and effector proteins to damage sites such as BRCA1, 53BP1, MDC1, Rad51 and the MRN complex (Fernandez-Capetillo *et al.*, 2003). H2AX-/- mice exhibit increased chromosomal instability, growth defects and defects in DNA repair (Bassing *et al.*, 2002, Celeste *et al.*, 2002), demonstrating the importance of H2AX in maintaining genome stability. After replication fork stalling, H2AX is also required for the induction of a p21-dependent cell cycle arrest (Fragkos *et al.*, 2009).

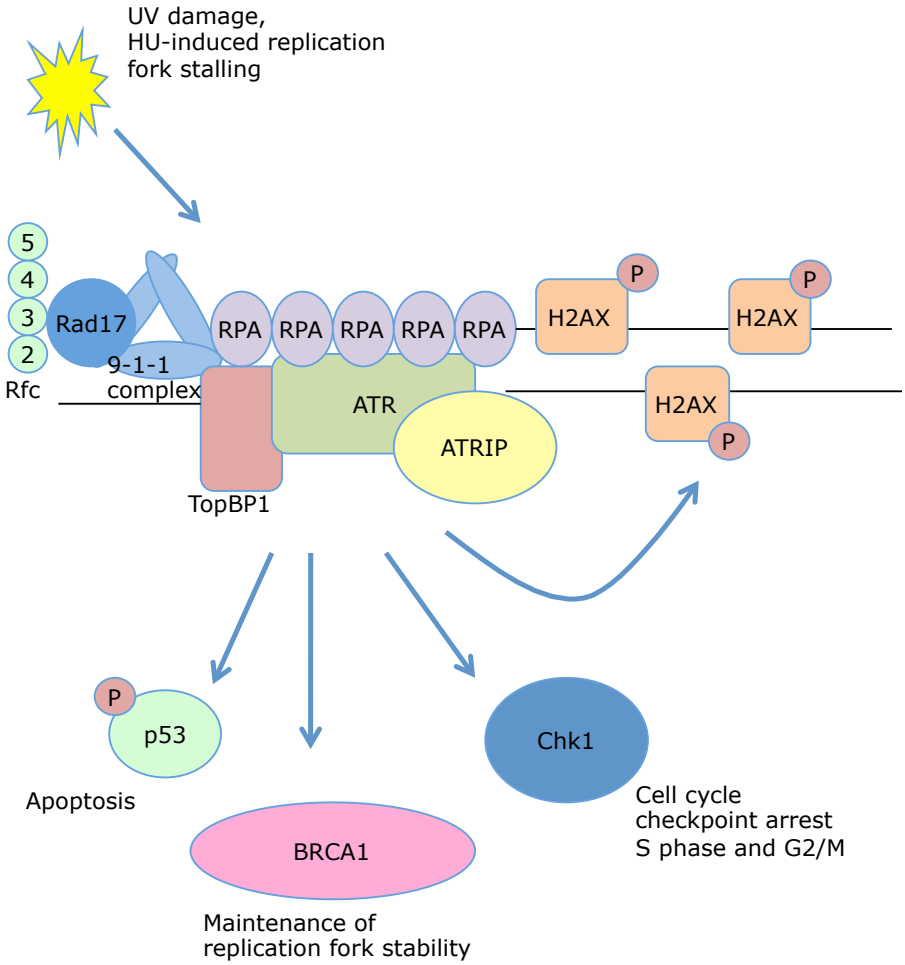

Figure 1.12 ATR–dependent signalling

Stretches of ssDNA formed by the stalling of replication forks or excision of UV damage is rapidly coated with RPA. The rad17-rfc complex loads the 9-1-1 complex onto the DNA. An interaction between TopBP1 and the tail of Rad9 recruits TopBP1 to the damage site. ATRIP is recruited via an interaction with RPA, recruiting the ATR-ATRIP complex to the site. When ATR, ATRIP and TopBP1 are localised together ATR becomes fully activated. ATR can then phosphorylate downstream targets such as p53, BRCA1 and Chk1.

1.4.2 Chk1

Checkpoint kinase 1 (Chk1) is an essential kinase that is phosphorylated by ATR both during an unperturbed cell cycle and in response to DNA damage (Liu *et al.*, 2000). ATR phosphorylates Chk1 on amino acids ser317 and ser345, resulting in its activation. It has been demonstrated that phosphorylation of ser345 is dependent on the initial phosphorylation of ser317, with speculation that this prior phosphorylation induces a conformational change in Chk1, allowing the second phosphorylation to occur (Wilsker *et al.*, 2008).

The efficient phosphorylation of Chk1 by ATR requires two other protein complexes. Claspin is a mediator protein that is found at the replication fork, binds to phosphorylated Rad17 (Wang *et al.*, 2006) and interacts with Chk1 after DNA damage (Kumagai and Dunphy, 2000). The interaction of Claspin with Chk1 requires three Chk1 binding motifs and the phosphorylation of Claspin on sites Thr916 and Ser 945/982 (Chini and Chen, 2006). The kinase responsible for these phosphorylation events is unknown, as these sites are not consensus sites for ATR. It is possible that Chk1 regulates itself in a positive feedback loop as it is able to phosphorylate Claspin on Thr916 *in vitro* (Chini and Chen, 2006).
This Claspin-mediated Chk1 phosphorylation event is promoted by the association of Timeless-interacting protein (Tipin)-Timeless complexes and Tipin-Claspin complexes on stretches of RPA-ssDNA. The association of these protein complexes on the chromatin is facilitated by the interaction of Tipin with the 34kDa subunit of RPA (Kemp *et al*., 2010).

Once Chk1 is phosphorylated it is released from the chromatin into the surrounding nuclear environment (Smits *et al.*, 2006). It has been proposed that the phosphorylation of Ser317 on Chk1 is important for its release from the chromatin, whilst phosphorylation at Ser345 is important for the subsequent cellular relocalisation of Chk1 to the cytoplasm and centrosomes (Niida *et al.*, 2007). The accumulation of Chk1 at the centrosome plays a role in preventing Cdk1 activation, thus controlling mitotic entry (Krämer *et al*., 2004). This mechanism will be discussed in detail in Chapter Three.

Chk1-/- mice are embryonic lethal (Liu *et al.*, 2000) before embryonic day 6.5, demonstrating that Chk1 is an essential kinase. Subsequent studies have revealed that phosphorylation of Chk1 at Ser345 may have an essential function as human cell lines harbouring this mutation could not be generated, although cell lines were

successfully created containing the Ser317 mutation (Wilsker *et al.*, 2008). Exogenously expressed Chk1 mutated at Ser345 is also unable to rescue the Chk1 lethal phenotype of knockout mouse embryonic cells. However Ser317 is dispensable for this function (Niida *et al.*, 2007).

Depletion of Chk1 also leads to replication fork slowing and stalling (Petermann *et al.*, 2006), as well as an increase in the number of replication-associated DNA strand breaks (Syljuåsen *et al.*, 2005). How Chk1 is involved in the regulation of replication is not clear. It is known to regulate origin firing during replication stress by inhibiting the activation of new replication factories (Ge and Blow, 2010). Chk1 is also required to maintain the rate of replication fork progression during an unperturbed S phase, with speculation that its role lies in the stabilisation of replication forks (Petermann *et al.*, 2006).

1.4.3 53BP1

p53-interacting protein 1 (53BP1) is a mediator protein that is involved in recombination, the activation of p53 (Harper and Elledge, 2007) and is rapidly recruited to sites of DNA damage, where it associates with γH2AX and serves as a scaffold to concentrate damage response proteins to the site (Sakasai and Tibbetts, 2008). It is phosphorylated by ATM following ionising radiation and is recruited to DSB's where it serves to amplify the ATM signal via the accumulation of the MRN complex (Noon *et al.*, 2010). 53BP1 also plays a role in both the initiation of G2/M checkpoint arrest at low IR doses and the maintenance of checkpoint arrest after high IR doses (Shibata *et al.*, 2010). Depletion of 53BP1 leads to checkpoint defects at low doses of IR as well as defects in DSB repair by NHEJ (Sakasai and Tibbetts, 2008).

The role of 53BP1 in the ATR-dependent signalling pathway is less clear. It has been shown that after induction of replication stress by UV or HU treatment, 53BP1 is phosphorylated by ATR at several sites, as early as 15 minutes post treatment (Jowsey *et al.*, 2007). It then localises to stalled replication forks, and this recruitment is partially dependent on both UBC13, a ubiquitin-conjugating enzyme and RNF8, an E3 ligase (Sakasai and Tibbetts, 2008). The formation of 53BP1 foci during S phase arrest is known to be dependent on both ATR and Chk1 (Sengupta *et al*., 2004). In this scenario, 53BP1 has an anti-recombinogenic role and recruits BLM (Bloom helicase protein) to HU-induced stalled replication forks. 53BP1 then

interacts with BLM and Rad51 in a Chk1 dependent manner and modulates Rad51 to control HR at these sites of replication stress (Tripathi *et al.*, 2008).

Similar to its role in ATM signalling, 53BP1 is required for replication-independent ATR checkpoint activation following UV treatment, possibly by serving to amplify ATR signalling (Stiff *et al.*, 2008). It was demonstrated that 53BP1 is recruited to sites of focused UV damage, independent of γH2AX, indicating that there may be different processes involved in the recruitment of 53BP1 to stretches of ssDNA to those for its recruitment to DSBs.

1.4.4 Fanconi Anemia Pathway proteins

The Fanconi Anemia (FA) pathway is critical for the repair of interstrand crosslinks (ICLs). These arise when the two strands of DNA become covalently linked due to the binding of agents such as Cisplatin, nitrous acid and aldehydes. ICLs are blocks to transcription and replication and therefore their removal is essential to maintain genome stability. The FA pathway is composed of at least fifteen different proteins. The FA core complex consists of eight FA proteins (FANCA/B/C/E/F/G/L/M) and two FA-associated proteins (FAAP24 and FAAP100). This complex forms an E3 ubiquitin ligase, the function of which is to monoubiquitinate two further FA proteins, FANCD2 and FANCI. Monoubiquitinated FANCD2 then becomes active and recruits Fanconi-associated nuclease 1 (FAN1) to the damage site. FANCD2 interacts with damage response proteins such as BRCA1, BRCA2 and FANCJ, which facilitate DNA repair via homologous recombination (Kee and D'Andrea, 2010).

Crosstalk occurs between the FA pathway and the ATR pathway, possibly allowing coordination of checkpoint mechanisms with repair. ATR is required for the monoubiquitination of FANCD2 after damage and ATR deficient cells are hypersensitive to ICLs (Andreassen *et al.*, 2004). ATR-ATRIP is required for the phosphorylation of FANCI and ATR has been shown to phosphorylate FANCI *in vitro* (Ishiai *et al.*, 2008, Shigechi *et al.*, 2012). FANCM and FAAP24 interact with a complex of ATR and HCLK2 and are required for activation of ATR-dependent S-phase checkpoint responses (Collis *et al.*, 2008).

The FA pathway has also been shown to be important in the survival and maintenance of neural progenitors. *FANCA-/-* and *FANCG-/-* mice present with features such as microcephaly with abnormal development of the cortex (Sii-Felice *et al.*, 2008).

Patients with mutations in the Fanconi Anemia proteins present with microcephaly, bone marrow failure and a high incidence of cancers. Cells from FA patients exhibit increased genomic instability in the form of hypersensitivity to ICL-inducing agents and increased chromosome aberrations (Kee and D'Andrea, 2010).

1.4.5 BRCA1

BRCA1 is a large protein that is involved in many cellular pathways, interacting with a variety of proteins including tumour suppressors, DNA repair proteins and cell cycle regulators. The N-terminal RING domain of BRCA1 confers E3 ubiquitin ligase activity, which is enhanced when BRCA1 is in complex with BRCA1-associated RING domain protein-1 (BARD1) (Wu *et al.*, 1996). BRCT domains within BRCA1 mediate protein-protein interactions. BRCA1 plays multiple roles in HR by forming complexes with multiple proteins. BRCA1 in complex with Abraxas and Receptor-associated protein-80 (RAP80) binds to DSBs and results in the ubiquitination of histones around the DSB (Wang *et al.*, 2007). BRCA1 in complex with CtIP and the MRN complex mediates resection of the 5' DNA end (Yun and Hiom, 2009). BRCA1 in complex with BARD1 and TOPBP1 plays a role in the repair of replication-associated damage (Greenberg *et al.*, 2006) and may mediate ATR dependent checkpoint signalling, although its function here is not known (Roy *et al.*, 2012).The recruitment of RAD51 to sites of DNA damage is also dependent on BRCA1 in complex with Partner and localiser of BRCA2 (PALB2) and BRCA2.

The function of BRCA1 in checkpoint responses to DNA damage is not well understood. It is known that BRCA1 is required for ATM/ATR to phosphorylate particular targets in response to damage, such as facilitating the phosphorylation of p53 on ser15 (Foray *et al*., 2003). This phosphorylation is required for inducing transcription of p21, a CDK inhibitor, and results in activation of the ionising radiation induced G1/S checkpoint (Siliciano *et al*., 1997). How BRCA1 is precisely involved here is not known although depletion of BRCA1-BARD1 results in reduced p21 induction (Fabbro *et al*., 2004). Cells with deficient BRCA1, BARD1, RAP80 or Abraxas also exhibit defects in G2/M checkpoint activation following exposure to IR (Kim *et al.*, 2006, Kim *et al.*, 2007a, Kim *et al.*, 2007b). BRCA1 interacts with ATRIP phosphorylated at Ser239 and disruption of this interaction leads to G2/M checkpoint defects (Venere *et al.*, 2007).

1.4.6 p53

p53 is a transcription factor that regulates the expression of a large number of genes involved in many cellular processes such as DNA repair, apoptosis, cell cycle progression, and cell senescence. Under unperturbed cell cycle conditions, p53 is degraded by the MDM2 ubiquitin ligase, rendering it functionally inactive. When cells are exposed to stress such as DNA damage, hypoxia, or oxidative damage, p53 levels accumulate due to the shut down of MDM2 mediated degradation (Hayon and Haupt, 2002).

In response to UV-induced DNA damage or stalled replication forks, ATR phosphorylates p53 on Ser15. This causes the accumulation of p53 and results in increased transcription of p53 gene targets such as p21. This is a CDK inhibitor and contributes to the G2/M checkpoint by the direct inhibition of CDK by binding to CDK-Cyclin complexes (Boulaire *et al.*, 2000). Gadd45 is another transcriptional target of p53 and is thought to inhibit the binding of CDK1 to cyclinB (Zhan *et al.*, 1999) p53 is also a transcriptional regulator of the 14-3-3 protein. This protein binds to CDK1, sequestering CDK1-CyclinB complexes in the cytoplasm and inhibiting mitotic entry.

If DNA damage persists or is at a high level, the cell may undergo apoptosis. ATR phosphorylation of p53 can induce transcription of pro-apoptotic genes such as Fas, Bax, Puma and Noxa. These can activate the extrinsic death receptor apoptosis pathway, resulting in the assembly of the DIS-complex that is composed of Fas-associated protein with death domain (FADD) and the pro-caspases 8 and 10. Activation of this pathway culminates in the digestion of the DNA by caspase-activated DNase (CAD) and the inactivation of proteins by their degradation by caspases 3 and 7. The intrinsic mitochondrial apoptosis pathway is also activated resulting in the formation of an apoptosome composed of pro-caspase-9, Apoptotic protease activating factor-1 (Apaf-1) and cytochrome C. This complex also activates caspases resulting in DNA and protein degradation (Roos and Kaina, 2012).

1.5 ATR-DEPENDENT CHECKPOINTS

Cell cycle checkpoints can be defined as a temporary delay or arrest of cell cycle progression in response to cellular stress (Sancar *et al.*, 2004). These important cellular surveillance points are at the G1/S transition, intra S phase and the G2/M

transition. Additional checkpoints also exist that monitor the level of origin licensing (licensing checkpoint) (Shreeram *et al.*, 2002), the fidelity of spindle assembly (spindle assembly checkpoint) (Rudner and Murray, 1996) and chromosome condensation and entry into mitosis (the antephase checkpoint) (Matsusaka and Pines, 2004). In this section I will discuss those checkpoints that are known to be dependent upon ATR signalling pathways.

1.5.1 The Intra-S-phase checkpoint

ATR plays an important role in the induction of S-phase checkpoints in response to replication stress. When a DNA polymerase encounters a block to replication, the helicase often continues to unwind the DNA and becomes uncoupled from the stalled polymerase. This results in the formation of a long stretch of single-stranded DNA that precedes the advancing fork (Paulsen and Cimprich, 2007). The generation of ssDNA causes the activation of ATR as described in section 1.3.2. Once activated, ATR initiates several cellular responses such as the phosphorylation and activation of Chk1. Chk1 then phosphorylates downstream targets such as Cdc25A, targeting it for ubiquitination and degradation by the Skp1/Cullin/F-box (SCF) complex (Busino *et al.*, 2003). Cdc25A is then unable to remove the inhibitory phosphorylations at Threonine 14 and Tyrosine 15 of Cdk2, which is in complex with either CyclinA or CyclinE (Sebastian *et al.*, 1993), resulting in inhibition of Cdk2 kinase activity (Falck *et al.*, 2002). This prevents the loading of Cdc45 onto the chromatin, resulting in a down regulation of DNA replication by the inhibition of late firing origins (Costanzo *et al.*, 2000, Mohammad *et al.*, 2007).

The activation of Chk1 can also lead to the inhibition of DNA elongation though the inhibition of tousled-like kinase (TLK1). TLK1 phosphorylates a chromatin assembly factor, Anti-silencing factor1 (Asf1). Upon DNA damage, TLK1 is inhibited resulting in dephosphorylation of Asf1 (Silljé and Nigg, 2001, Krause *et al.*, 2003, Cook, 2009).

1.5.2 The G2/M checkpoint

The G2/M checkpoint prevents cells that harbour DNA damage from undergoing mitosis and is activated by either ATM or ATR, depending on the damage detected (Sancar *et al.*, 2004).

The control of entry into mitosis is governed largely by the activity of the Cdk1-CyclinB complex. During normal cell cycle progression, the transcription of cyclinB1 begins in S phase and rises to its peak in G2 phase (Lindqvist *et al.*, 2009). Control of CyclinB protein levels is crucial as restriction of its availability limits the formation of Cdk1-CyclinB complexes. CyclinB shuttles between the nucleus and the cytoplasm. In S and G2 phase it is predominately found in the cytoplasm (Hagting *et al.*, 1998, Toyoshima *et al.*, 1998). As the centrosomes mature, in mid G2, CyclinB starts to accumulate there and by late G2, the highest concentration of CyclinB within the cell is located at the centrosomes (Jackman *et al.*, 2003). This is the location, in human cells, where phosphorylated CyclinB can be detected first.

CyclinB forms a complex with Cdk1 and in order for these complexes to become activated Threonine 161 in the T loop of Cdk1 must be phosphorylated. The Cdk-activating kinase (CAK) mediates this phosphorylation when a threshold concentration of Cdk1-cyclinB complexes is reached (Tassan *et al.*, 1994). Cdk1-CyclinB complexes are also negatively regulated by inhibitory phosphorylations on T14 and Y15 of Cdk1 by the Wee1 and Myt1 kinases (Lindqvist *et al.*, 2009). Active Cdk1-cyclinB complexes can regulate their own activity via positive feedback loops (Figure 1.13). Cdk1-cyclinB activation of the Cdc25 phosphatases can remove the inhibitory phosphorylation on T14 and Y15 of Cdk1, imposed by Wee1/Myt1. There are three Cdc25 isoforms present in mammalian cells; Cdc25A, Cdc25B and Cdc25C. Each of the isoforms can shuttle between the nucleus and the cytoplasm and all have also been found at the centrosome (Dutertre *et al.*, 2004, Boutros *et al.*, 2006, Busch *et al.*, 2007, Bonnet *et al.*, 2008, Shreeram *et al.*, 2008). Polo-like kinase 1 (Plk1) and Aurora A kinase (AurA) also regulate Cdk1-cyclinB activity and will be discussed in detail in Chapter 6.

The active Cdk1-CyclinB complexes build up steadily during G2 and translocate into the nucleus during mitotic entry. A further rapid activation of the majority of the Cdk1-CyclinB complexes takes place during the last thirty minutes before prometaphase, triggering mitotic entry (Lindqvist *et al.*, 2007).

The regulation of Cdk1-cyclinB activity has been proposed to be a switch-like bistable process (Lindqvist *et al.*, 2007). Bistability in this context can be defined as the Cdk1-cyclinB complexes existing as either active, inactive or nearing one of these states. This system is also influenced by hysteresis which can be defined as the resistance of these stable states to change, for instance, once Cdk1-cyclinB is active it remains active and the cell is likely to enter mitosis, regardless of small

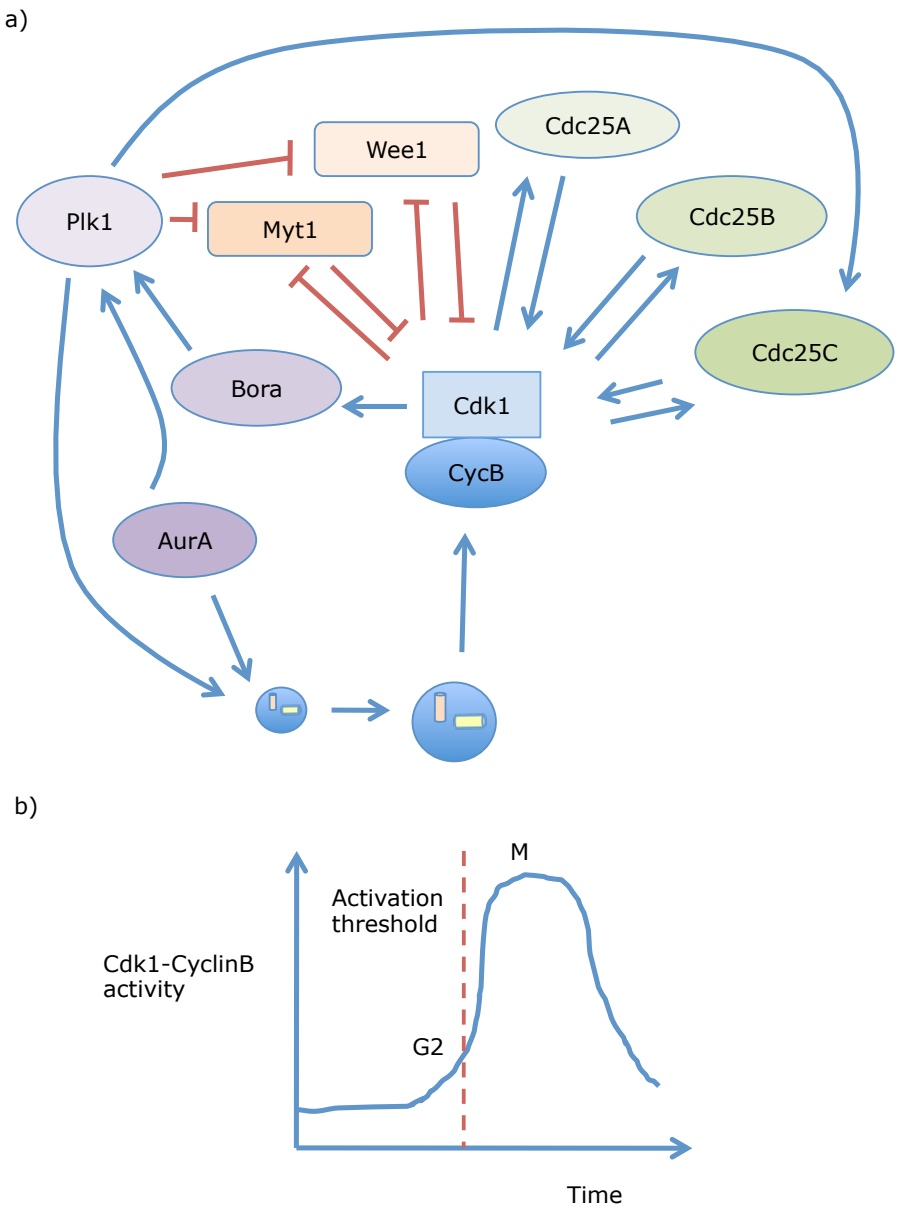

Figure 1.13 Cdk1-CyclinB control of mitotic entry

a) Feedback loops control activation of Cdk1-cyclinB complexes. Myt1 and Wee1 inhibit Cdk1-cyclinB activity whilst the Cdc25 phosphatases activate Cdk1. Once active Cdk1 can inhibit its inhibitors and activate its activators. Cdk1 also phosphorylates Bora, increasing its association with AurA and PLK1, leading to PLK1 activation. Active PLK1 increases Cdk1 activation via Wee1 inhibition and Cdc25 activation. Centrosome maturation increases local concentrations of CyclinB through AurA and PLK1 activity.
b) Cdk1-CyclinB activation is triggered when complexes reach a threshold level in G2 and remain active until completion of mitosis

Figure and legend adapted from Lindqvist, 2009.

fluctuations in Cdk1-cyclinB concentration (Lindqvist *et al.*, 2009). In terms of mitotic entry this means that Cdk1-cyclinB activation will occur once a threshold of complexes is reached and that once the feedback loops maintaining this activation are initiated, they will remain active until mitosis is completed (Figure 1.13).

The G2/M checkpoint initiated after UV damage is controlled by the same cyclin dependent kinases and has been shown to be ATR-dependent (Cliby et al., 1998). Upon detection of DNA damage, ATR is activated as previously described in section 1.2.1.1 and phosphorylates downstream targets such as Chk1. Active Chk1 then phosphorylates Cdc25A at Serines 76 and 123 (Zhao *et al.*, 2002, Donzelli *et al.*, 2004, Jin *et al.*, 2008). Phosphorylation of Cdc25A at these and other sites, stimulates its ubiquitination via the Skp1/Cullin/F-box (SCF) proteins and target it for degradation (Busino *et al.*, 2003). Chk1 also phosphorylates Cdc25C at Serine 216, leading to its nuclear export via cytoplasmic sequestration by the 14-3-3 protein (Peng *et al.*, 1997). The phosphorylation of Cdc25B is also inhibited after DNA damage, via inhibition of AurA phosphorylation of the Ser323 site on Cdc25B. This phosphorylation event was shown to be Chk1 dependent (Cazales *et al.*, 2005). By controlling the access of Cdc25 proteins to Cdk1, Chk1 can downregulate Cdk1-cyclinB activation, thus stalling mitotic entry to allow repair to damaged DNA (Figure 1.14). The phosphorylation of PLK1 is also inhibited after DNA damage in an ATR/Chk1 dependent manner, inhibiting its kinase activity (Tsvetkov and Stern, 2005). This will be discussed in detail in Chapter 6.

1.5.3 Further ATR-dependent checkpoints

Recent data has come to light that suggests that ATR may be involved in a checkpoint that monitors spindle assembly, independently of the Spindle Assembly checkpoint (SAC). Chromosome breakage was shown to induce ATR/ATM dependent phosphorylation of a centrosomal protein CEP63, displacing this protein from the centrosome. This leads to inhibition of spindle assembly and a delay in mitotic progression (Smith *et al.*, 2009).

1.6 ATR AND REPLICATION

DNA replication is a particularly sensitive phase of the cell cycle when endogenous barriers such as DNA-protein complexes or other replication blocks, such as base damage, can cause replication forks to stall and potentially to collapse, resulting in the introduction of DSBs. Replication can also proceed slowly at specific points in

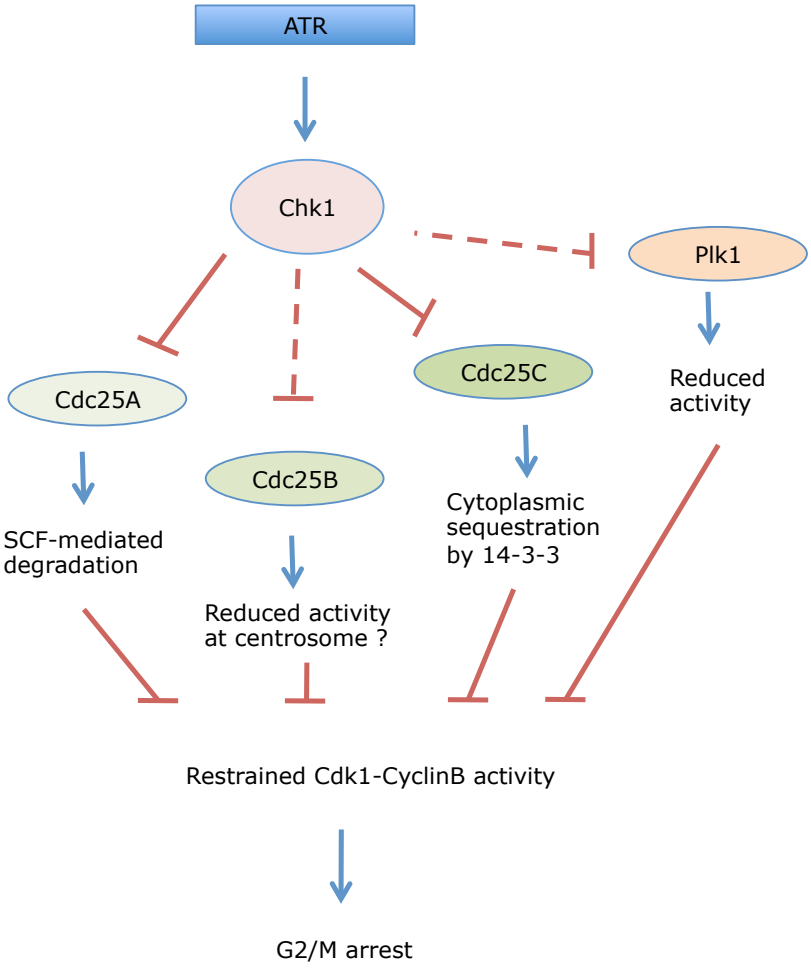

Figure 1.14 ATR-dependent G2/M checkpoint arrest

ATR is activated at regions of ssDNA. It then phosphorylates Chk1 at serines 317 and 345. Activated Chk1 phosphorylates Cdc25A, Cdc25B and Cdc25C, resulting in their inhibition via different mechanisms as shown. Inhibition of PLK1 kinase activity via Chk1 pathways also occurs. This results in Cdk1-CyclinB inhibition and delay to mitotic entry. Dashed lines indicate indirect relationships. Red lines indicate inhibition. Blue lines indicate activation.

the genome, such as repetitive sequences, fragile sites and natural pause sites, increasing the probability of the introduction of replication errors (Branzei and Foiani, 2005).

ATR and Chk1 are essential during unperturbed cell cycles. The loss of ATR or Chk1, even in the absence of damage, results in premature mitotic entry before the completion of replication, a phenotype termed 'mitotic catastrophe' (Cortez *et al.*, 2001, Niida *et al.*, 2005). The role of ATR and Chk1 in unperturbed cell cycles is thought to be related to its DNA damage response functions of Cdk regulation and control of DNA replication (Cook, 2009). When replication forks stall, ATR is rapidly recruited to these sites and once activated, phosphorylates many downstream targets. The activation of the ATR-dependent response enables checkpoint activation, as discussed in section 1.5.2, down-regulation of late origin firing, stabilisation of the stalled replication forks and activation of processes required to restart collapsed replication forks (Paulsen and Cimprich, 2007). In this section, I will discuss each of these processes in turn.

1.6.1 Origin licensing and origin firing

The identification of mutations in the Origin Recognition Complex (ORC) in Microcephalic Primordial dwarfism patients (Chapters Five and Six) has highlighted the relationship between ATR signalling and origin licensing. It is important for the cell to have sufficient licensed origins to complete replication in a timely manner, but also important that licensing is restricted in order that each origin only fires once in S phase to avoid re-replication. If a cell enters S phase with too few licensed origins this could lead to fork stalling as forks have to travel a longer distance to complete replication. A 'licensing checkpoint' has been proposed that delays G1, ensuring that cells only enter S phase once they have a sufficient number of licensed origins (Ge and Blow, 2009).

Origins become licensed once the pre-replication (preRC) complex has been assembled in G1. First the Origin Recognition Complex (ORC) binds to each origin. This is composed of six subunits, ORC1-6 and will be discussed in detail in Chapter 5. Cdc6 and Cdt1 then associate with ORC and promote the loading of the Mini-chromosome Maintenance complex (MCM) helicase. Once MCM is loaded at the origin it becomes licensed (Figure 1.15). At the G1/S transition, the activity of Cdc7/Dbf4 and cyclinE/Cdk2 then promote the association of Cdc45 and the GINS complex at origins that will fire.

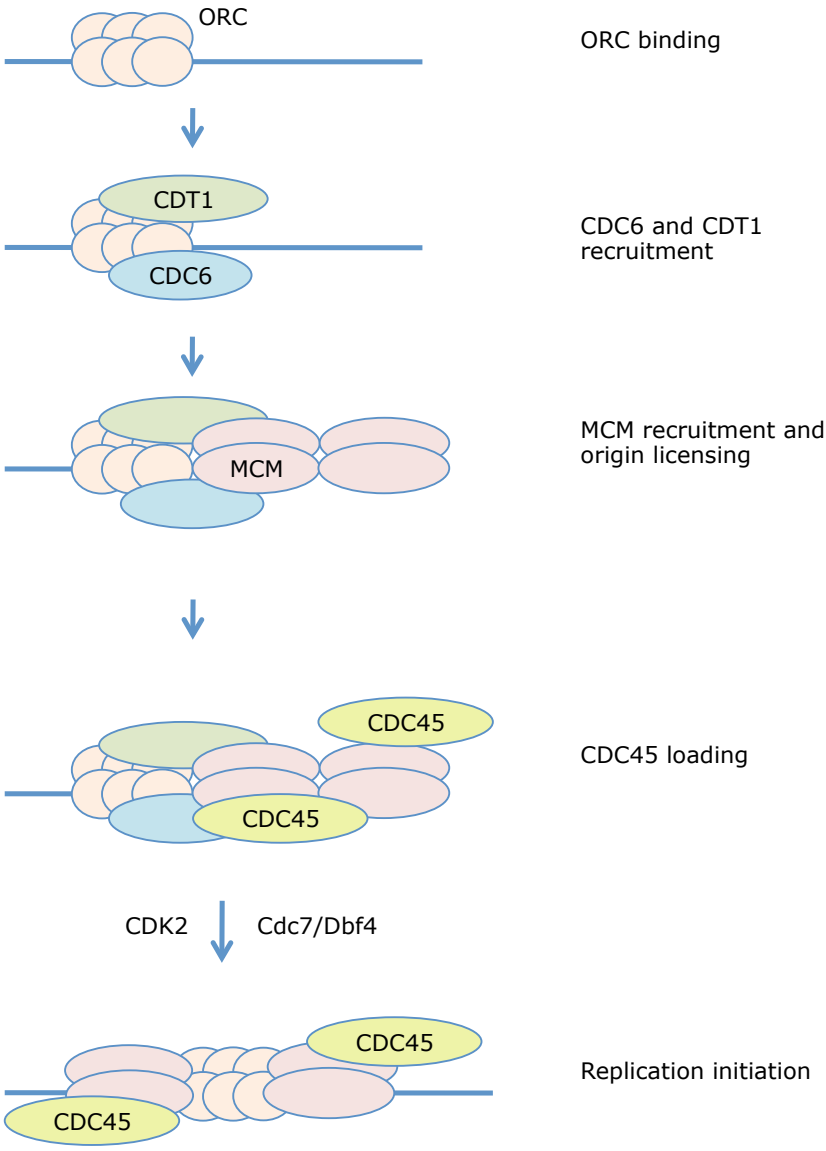

Figure 1.15 Pre-replication complex formation and the initiation of DNA replication

ORC binds to replication origins and recruits CDC6 and CDT1. Recruitment of the MCM2-7 complex to ORC forms the pre-replication complex (pre-RC). At this point the origin becomes licensed. The pre-RC changes to a pre-initiation complex (pre-IC) with the recruitment of CDC45. The initiation of DNA replication is triggered by CDK2 and Cdc7/Dbf4 kinases.

Figure adapted from Diffley and Labib, 2002.

When DNA damage is detected, the inhibition of Cdk2/CyclinE complexes by ATR/Chk1 dependent inhibition of the CDC25 phosphatases, prevents the association of Cdc45 and GINS with the pre-replication complexes on the chromatin, preventing further origin firing (Sancar *et al.*, 2004). Chk1 also inhibits Cdc45 loading via inhibition of Cdc7/Dbf4, independently of Cdk2 activity (Liu *et al.*, 2006, Heffernan *et al.*, 2007). Inhibition of Cdc45 loading is further achieved by the phosphorylation of Myeloid/lymphoid or mixed-lineage leukemia (MLL) by ATR. This stabilises MLL, resulting in its accumulation on the chromatin. Here it methylates histone H3 at lysine 4 at late replicating origins, inhibiting Cdc45 loading (Liu *et al.*, 2010).

Upon UV exposure, Cdt1 is targeted for degradation by the SCF (Skp2) E3 ubiquitin ligase complex and by the Cul4, DNA Damage binding protein 1 (DDB1) with the adaptor protein Cdt2 (Nishitani *et al.*, 2006). This UV-induced degradation can be inhibited by exposure to caffeine or the inhibition of Chk1 (Kondo *et al*., 2004), indicating that ATR-dependent signalling may play a role in Cdt1 regulation.

Cdc6 is also ubiquitinated and degraded after DNA damage. Cdc6 interacts with the E3 ligase Huwe1. *In vitro* experiments indicate that Huwe1 ubiquitinates Cdc6 after exposure to UV irradiation and if the expression of Huwe1 is suppressed in cells, Cdc6 degradation is compromised (Hall *et al.*, 2007). Cdc6 is also degraded in an APC/C dependent manner after exposure to ionising radiation (Petersen *et al.*, 2000, Duursma and Agami, 2005). After damage Cdc6 is also released from the chromatin, although the mechanism for this is unclear (Hall *et al.*, 2007). It is possible that the chromatin association of Cdc6, mediated by its interaction with ORC, is regulated by ATR and prevents further assembly of preRCs in the presence of damage (Cook, 2009).

1.6.2 Stabilisation of stalled replication forks

The stabilisation of stalled replication forks is critical in order to prevent fork collapse and hence DSB formation, one of the most deleterious forms of DNA damage. Fork stabilisation ensures that the DNA polymerases Polα and Polε remain associated with the fork in order for replication to restart when possible (Paulsen and Cimprich, 2007). In *Saccharomyces cerevisiae* Mec1/ATR is recruited to the replication fork where it phosphorylates Mrc1 (Claspin in humans). This stabilises the MCM complex and halts DNA unwinding, preventing replication fork collapse

(Ben-Yehoyada *et al.*, 2007). The mechanism for fork stabilisation in mammalian cells is not clear although the loss of both ATR and H2AX leads to increased chromosome translocation and chromatid breakage when replication is stalled (Chanoux *et al.*, 2009). ATRIP interacts with MCM7 and ATR phosphorylates MCM2 (Cortez *et al.*, 2004) raising the possibility that ATR regulates MCM-mediated unwinding of the DNA at the replication fork, perhaps inhibiting this process after damage to prevent dissociation of the helicase from the polymerase.

The long stretches of ssDNA that often form at replication forks are prone to rearrangement, resulting in the formation of aberrant structures that require intervention if replication is to be resumed. These structures are more likely to require some form of recombination repair, potentially resulting in base incorporation errors or the introduction of DSBs. ATR suppresses recombination by the phosphorylation of the RecQ helicases, Werner syndrome protein (WRN) (Ammazzalorso *et al.*, 2010) and Bloom syndrome protein (BLM) (Tripathi *et al.*, 2008), promoting their recruitment to the replication fork. It is thought that these 3' to 5' helicases act at replication forks to prevent the formation of aberrant structures, such as the 'chicken-foot' structure (Figure 1.16), which require the use of homologous recombination mechanisms to resolve them. WRN and BLM deficient cells exhibit an increased rate of sister chromatid exchanges and an increase in aberrant replication intermediates, demonstrating their importance in this process (Paulsen and Cimprich, 2007).

There is increasing evidence that the Fanconi Anemia (FA) complex proteins also play a role in the stabilisation of stalled replication forks, particularly where interstrand cross-links occur.

1.7 THE CENTROSOME

ATR and other DNA damage response proteins have been detected at the centrosome in recent years (Zhang *et al.*, 2007) and the importance of this organelle in damage response signalling is increasingly evident. In this section I will discuss aspects of centrosome biology and the relationship of the centrosome with the DNA damage response.

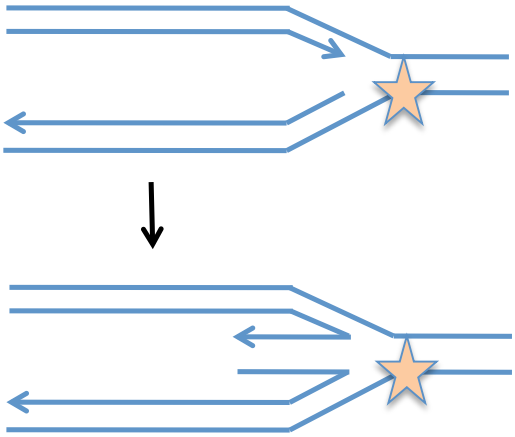

Figure 1.16 Chicken-foot DNA structure

Stalling of replication forks can lead to fork reversal and the formation of a 'Chicken-foot' DNA structure. These structure require homologous recombination for their resolution.

a)

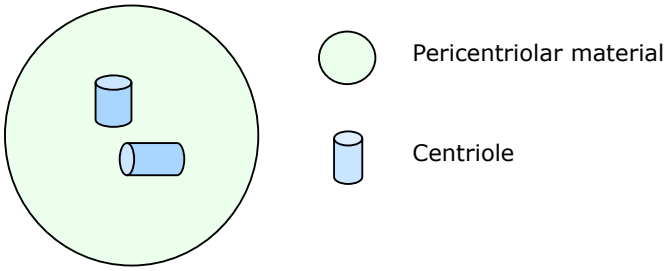

b)

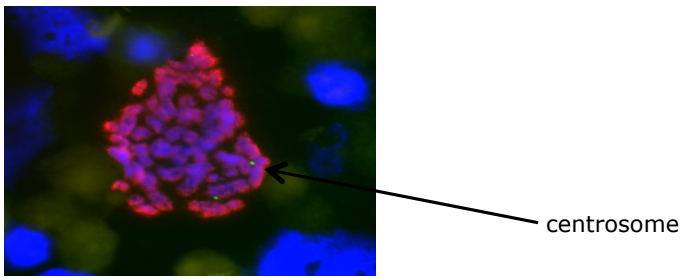

Figure 1.17 The centrosome

a) The centrosome indicating centrioles and pericentriolar material
b) Immunofluoresence image of mitotic cell showing centrosomes in green

1.7.1 The centrosome in cell division

The centrosome is a tiny (1-2μM) organelle that is comprised of two centrioles surrounded by a cloud of pericentriolar material (PCM) (Figure 1.17). The centrosome is thought to be composed of hundreds of proteins, including many coil-coil proteins such as Pericentrin, that serve as docking modules for the recruitment of further protein to the centrosome. The PCM contains γ-tubulin ring complexes (γTURCs) that nucleate the microtubules. In mammalian cells, the centrosome therefore plays a crucial role, acting as a microtubule-organising centre (MTOC). A key function of the centrosome is the formation of a functional bipolar mitotic spindle to ensure that chromosomes are segregated accurately during cytokinesis (Doxsey *et al.*, 2005). As each daughter cell receives one centrosome during mitotic division, the centrosome must be duplicated once each cell cycle. Centrosomal duplication is coupled with the initiation of DNA replication, linking the 'centrosome cycle' with the nuclear cell cycle (Figure 1.18). If centrosomes do not duplicate correctly or fail to separate, monopolar spindles can be formed which are unable to undergo cytokinesis (Figure 1.19b). These cells either activate a p53 dependent checkpoint, leading to arrest and cell death, or in the absence of p53 continue to cycle and become polyploid (Uetake and Sluder, 2004, Fukasawa, 2007). Defects in centrosome maturation, a process where centrosomes increase in size and microtubule nucleating capability, (Lee and Rhee, 2011) can also result in an inability to form proper bipolar spindles. If centrioles split prematurely, or centrioles are overduplicated during interphase, supernumary centrosomes can be created, often leading to the formation of multipolar spindles (Figure 1.19.c). Cells with tripolar spindles can enter cytokinesis but are likely to become severely aneuploid (Fukasawa, 2007), whilst cells with more than 3 poles are similar to cells with monopolar spindles and either do not enter cytokinesis or continue to cycle and become polyploid. An increase in the number of centrosomes does not always result in multipolar spindles. A process termed 'centrosome clustering' can occur where extra centrosomes are organised into two spindle poles. The cell thus forms 'psuedo-bipolar spindles' and can undergo cytokinesis (Krämer *et al.*, 2011). In cancer cells this strategy may increase genomic instability, as there can be an increased incidence of low-level chromosome mis-segregation (Silkworth *et al.*, 2009). This is because a single kinetochore is more likely to attach to more than one spindle pole during mitosis, an event termed 'merotelic attachment', resulting in a lagging chromosome at anaphase (Ganem *et al.*, 2009). There is a strong association between centrosome abnormality and the incidence of aneuploidy in cancer (Wang *et al.*, 2004).

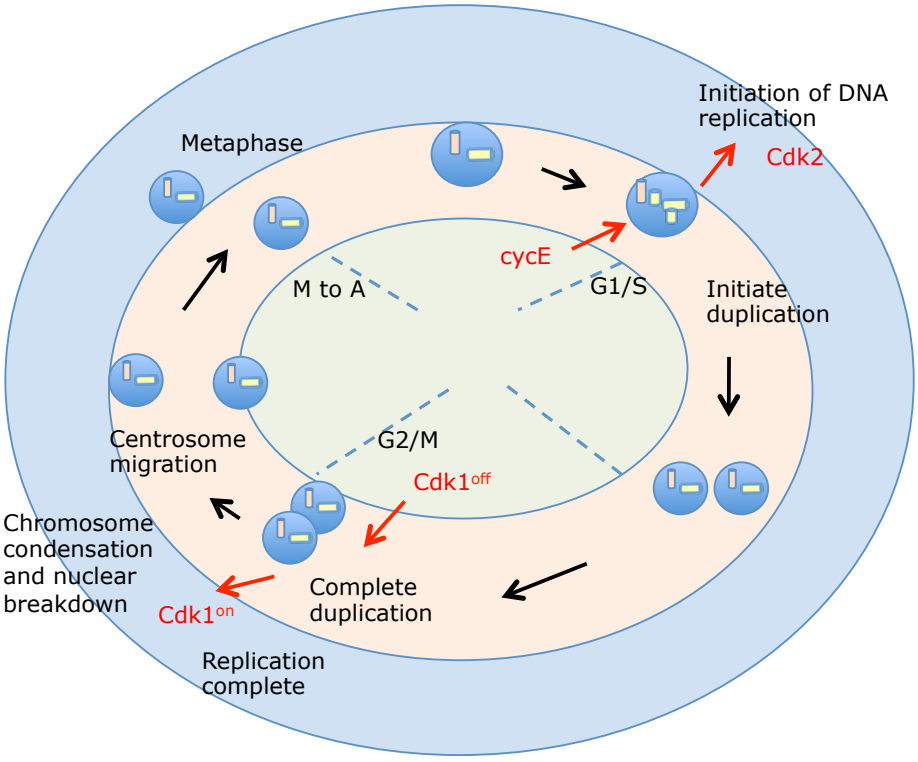

Figure 1.18 The centrosome cycle

Centrosome duplication is coupled with the initiation of DNA replication, linking the centrosome cycle (red) with the nuclear cycle (blue). This is achieved through the use of the common regulatory proteins, Cdks. Cell cycle mechanisms requiring centrosomes are shown in red.

Figure adapted from Doxsey et al, 2005.

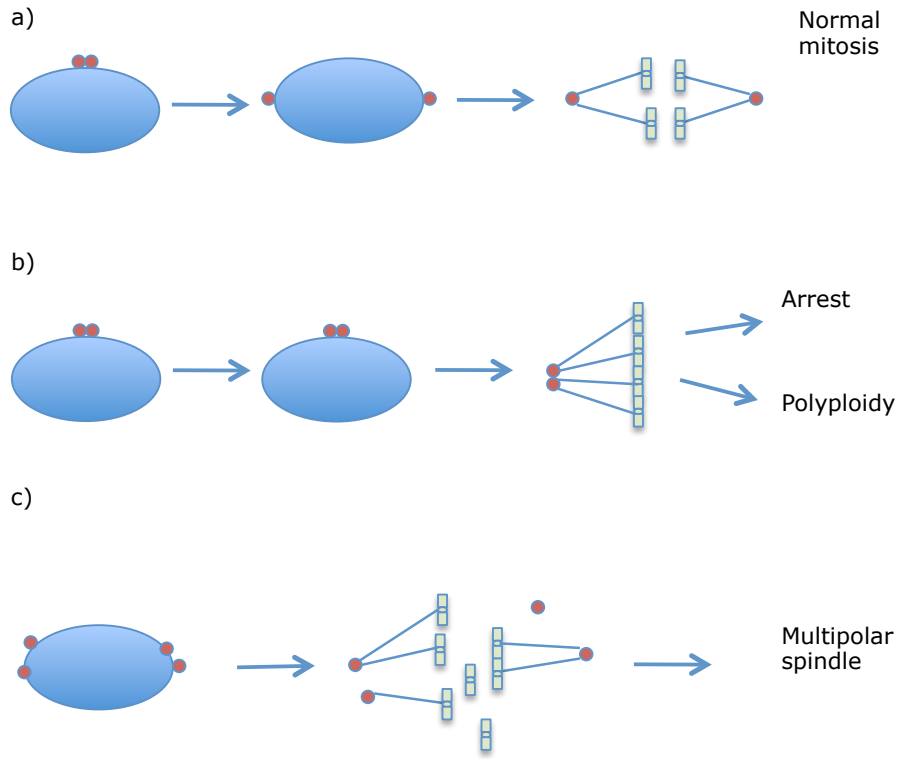

Figure 1.19 The centrosome in cell division

a) The centrosome in normal mitosis. Duplicated centrosomes disengage and migrate to opposite poles of the cell, resulting in a bipolar spindle.
b) Centrosomes fail to disengage during G2, resulting in a monopolar spindle and either cell arrest leading to death, or polyploidy.
c) Supernumary centrosomes due to centrosome overduplication, fragmentation or premature disengagement. Multipolar spindles are formed resulting in aneuploidy, arrest or polyploidy.

Figure adapted from Fukusawa, 2007

The role of the centrosome in asymmetric cell division such as during brain development is currently emerging. The position of the centrosome in neural progenitor cells is critical for maintaining the balance between symmetric and asymmetric cell division, an important factor in determining brain size (as discussed in section 1.1). In the first embryonic division of neuroblasts, astral microtubules emanating from the centrosome interact with sites formed on the apical membrane of the epithelium. This results in the positioning of the spindle in an apicobasal orientation, which is maintained by the centrosome through subsequent divisions (Knoblich, 2010) .

Centrosome positioning is also important in the neuronal migration processes of brain development. Cortical neurons migrate to the cortical plate in a stepwise process. The leading process extends forward followed by movement of the centrosome into the leading process. The nucleus then translocates towards the centrosome and the cycle repeats (Higginbotham and Gleeson, 2007). Defects in neuronal migration have been documented in the olfactory bulb of Pericentrin mutant mice (Endoh-Yamagami *et al.*, 2010) and in Human lissencephaly patients with mutations in *LIS1 (*Dobyns *et al., 1993)*. Both of these proteins are located at the centrosome.

1.7.2 The centrosome in cell cycle control

Involvement of the centrosomes in cell cycle control was demonstrated by experiments where centrosomes were removed from the cell by microsurgery or ablated by laser treatment. These cells fail to initiate DNA replication and remain arrested in G1 (Hinchcliffe *et al.*, 2001, Khodjakov and Rieder, 2001). One mechanism that has been proposed to induce this G1 arrest is the existence of a centrosome checkpoint that monitors the structural integrity of the centrosomes, arresting the cells via a p53/p38 dependent pathway (Mikule *et al.*, 2007). An alternative hypothesis is that the removal of the centrosome results in the elimination of the centrosomal Cdk2-CyclinE complexes, which are required for the initiation of DNA replication (Matsumoto and Maller, 2004). CyclinE contains a centrosomal localisation sequence (CLS) that is required for its localisation to the centrosome. CyclinE centrosomal localisation is required for the initiation of DNA replication within the nucleus, linking the nuclear and centrosome cycle together (Ferguson and Maller, 2010). Cdk2-CyclinE also has a key role in the initiation of centrosome duplication (Lacey *et al.*, 1999), an event that coincides with the

initiation of DNA replication. Whether the G1/S centrosomal checkpoint pathways proposed above are targeted by the DNA damage response is yet to be defined.

A role for the centrosome in G2/M checkpoint regulation has also been described. The initial activation of Cdk1-CyclinB in an unperturbed cell cycle occurs at the centrosome (Jackman *et al.*, 2003). This activation of Cdk1-CyclinB, mediated by the Cdc25 phosphatases, can be inhibited by Chk1, a fraction of which is also localised at the centrosome. DNA damage causes the accumulation of Chk1 at the centrosome and loss of the kinase activity of Chk1 at this location results in G2/M checkpoint defects (Krämer *et al.*, 2004, Löffler *et al.*, 2007). This element of centrosomal checkpoint control will be discussed in detail in Chapter Three.

There is, therefore, increasing evidence that centrosomes play an important role in cell cycle control alongside their role in mitotic spindle organisation. Centrosomes have been proposed to act as a 'molecular scaffold', enabling an increase in the local concentration of proteins and thus reducing non-specific interactions (Doxsey *et al.*, 2005). The role of the centrosome in the DNA damage response is also increasingly compelling with more studies detecting proteins that function in the DNA damage response at this organelle.

1.7.3 Centrosomes and Cilia formation

A further function of the centrosome is the formation of the primary cilia. In non-dividing cells the centrioles migrate to the cell surface. At this location the mother centriole (the older of the centriole pair) forms a basal body that directs cilia formation. The exact mechanism behind basal body formation is currently unclear. Primary cilia have important functions in development including maintenance of left-right symmetry and a role in an important signalling pathway called sonic-hedgehog signalling. Defects in cilia formation or signalling cause a range of human diseases termed 'ciliopathies'. Clinical features of these diseases include polydactyly, brain malformation, situs inversus and polycystic kidney disease (Nigg and Raff, 2009).

1.8 MICROCEPHALIC PRIMORDIAL DWARFISM DISORDERS

Mutations in centrosomal proteins are increasingly being identified in many diseases where microcephaly is a prominent clinical feature. In this section I will discuss a range of microcephalic primordial dwarfism disorders (see Table 1) and highlight

DISORDER	OMIM NO.	DDR-DEFECT	NEUROLOGICAL PHENOTYPE
Seckel syndrome (SS)	210600 606744 608664 613676	ATR signalling	Moderate to severe mental retardation
Nimegen Breakage syndrome	251260	ATM and ATR signalling and Artemis-ATM-dependent DSB repair	Moderate mental retardation
Primary Microcephaly (MCPH1)	251200	ATR-dependent checkpoint activation	Moderate mental retardation
Fanconi Anaemia	227646	Response to cross-linking agents	Normal
Xeroderma Pigmentosum (XP-A)	278700	Nucleotide excision repair and ATR signalling	Mild to moderate mental retardation
LIG4	606593	Non-homologous End Joining	Normal to mild mental retardation
XLF/Cernunnos-SCID	611291	Non-homologous End Joining	Normal to mild mental retardation
Bloom syndrome	210900	Unregulated homologous recombination	Mild to moderate mental retardation
Cockayne syndrome		Nucleotide excision repair	Severe mental retardation
Microcephalic Osteodysplastic Primordial Dwarfism II	210720	ATR signaliing??	Mild mental retardation
Meier-Gorlin syndrome	224690	ATR signalling??	Mild mental retardation
BPES? MDLS? WBS?		ATR haploinsuffiency	

Table 1 Microcephalic Primordial Dwarfism disorders
Adapted from (O'Driscoll & Jeggo, 2008).

the relationship between the clinical features observed, the DNA damage response and the centrosome.

1.8.1 Seckel Syndrome

Seckel syndrome (SS) (OMIM 210600) was first described by Helmut Seckel in 1960 (Seckel, 1960). It is an autosomal recessive genetic disorder that is clinically and genetically heterogenous with at least four different genetic susceptibility loci identified to date. It is characterised by severe intrauterine growth retardation, proportionate dwarfism and marked microcephaly with moderate to severe mental retardation. Patients were originally described as 'bird-headed dwarfs' due to the striking facial appearance conferred by a small head, beak like nose and a receding lower jaw (Figure 1.20) (Majewski and Goecke, 1982). Patients also display some skeletal abnormalities such as fifth finger clinodactly, thoracic kyphosis, ivory epiphysis and delayed ossification (Børglum *et al.*, 2001). No clear link between SS and cancer incidence has been defined, although a small number of patients have presented with acute myeloid leukaemia (Hayani *et al.*, 1994) and osteosarcoma (Faivre *et al.,* 2002).

The first genetic defect identified in SS was a hypomorphic, synonymous mutation in *ATR* (O'Driscoll *et al.*, 2003) at SCKL1 locus 3q22.1-q24. This mutation was shown to affect the splicing of the gene and ATR protein expression was dramatically reduced but crucially, not totally abolished (Figure 1.20b). Patient cell lines were shown to be defective in ATR-dependent damage responses such as H2AX phosphorylation following exposure to UV irradiation.

Further Seckel patient cell lines were subsequently examined and found to harbour defects in ATR-dependent signalling (Alderton *et al.*, 2004), although no further mutations in *ATR* were identified. All lines examined had defects in UV-induced G2/M checkpoint activation, displayed supernumerary mitotic centrosomes and showed high levels of fragmented DNA following treatment with hydroxyurea to induce replication fork stalling. This phenotype was termed 'nuclear fragmentation' and these cells were proposed to be of late S/early G2 origin. The cells were found to stain for prophase markers such as the lamin B1 nuclear envelope, but did not stain for mitotic markers such as phospho-histone H3 (ser10). The cells were also examined using the TUNEL assay but were found not to be apoptotic. It was proposed that these cells arose from a failure to recover from replication fork stalling coupled with a premature entry into prophase due to the lack of a

a)

b)

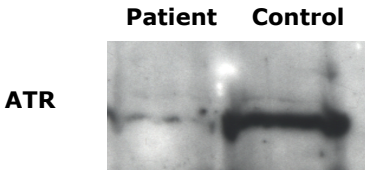

Figure 1.20 ATR-Seckel patient presenting with bird-like facial features.

a) Patient described in O'Driscoll et al, 2003.
b) Western blot showing reduced but not absent ATR protein expression

functional G2/M checkpoint (Alderton *et al.*, 2004). The nuclear fragmentation phenotype could be corrected by the introduction of wild type ATR cDNA into the ATR-S patient cells, confirming that ATR inactivation was responsible for this cellular phenotype.

Recently, we identified a new subset of Microcephalic Primordial Dwarfism (MPD) patients with Microcephalic osteodysplastic primordial dwarfism, type II (MOPDII) who were shown to harbour mutations in the *Pericentrin (PCNT)* gene, which maps to chromosome 21q22.3 (Griffith *et al.*, 2008). These cell lines also display defects in ATR-dependent signalling. The identification of this novel genetic defect provided the first example of a defect in a structural centrosomal protein resulting in defects in DNA damage response signalling and will be discussed in full in chapter three.

Subsequently, mutations in *CENPJ* mapping to chromosome 13q12.2 (SCKL4, OMIM 613676) have also been described in one consanguineous SS family. A homozygous mutation in intron 11 of the *CENPJ* gene was detected, causing aberrant splicing and the production of three mutant transcripts (Al-Dosari *et al.*, 2010). Mutations in *CENPJ* have also been identified in Primary Microcephaly patients (Bond *et al.*, 2005, Gul *et al.*, 2006, Darvish *et al.*, 2010). It has been speculated that these mutations may only affect transcripts expressed in the brain, whereas the mutation found in the SS family may also affect transcripts involved in proliferation throughout the body (Al-Dosari *et al.*, 2010), resulting in the different clinical phenotypes. CENPJ is also a centrosomal protein that plays a key role in maintaining centrosome integrity (Cho *et al.*, 2006), in mitotic spindle nucleation (Hung *et al.*, 2000) and is thought to be involved in cell cycle control (Chen *et al.*, 2006).

A further subset of SS patients with mutations in the *CEP152* gene on chromosome 15q21.1-q21.2 has also been identified (Kalay *et al.*, 2011). It was demonstrated that CEP152 has an important role in maintaining genomic integrity, although an involvement in ATR-dependent signalling was not directly investigated (Kalay *et al.*, 2011). CEP152 is another centrosomal protein that has been shown to act as a scaffold to recruit and retain other proteins at the centrosome (Cizmecioglu *et al.*, 2010). Mutations in *CEP152* have also been identified in Primary Microcephaly patients (MCPH4) (Guernsey *et al.*, 2010).

SS patients with genetic susceptibility loci mapped to chromosome 18p11-q11 (SCKL2, OMIM 606744) were recently discovered to harbour point mutations in

CTIP (Qvist *et al*., 2011). This gene encodes a protein that has known functions in DNA repair. CtIP localises at DSBs and interacts with the MRN complex to promote the resection of the break ends (Sartori *et al.*, 2007). This results in a region of ssDNA that rapidly becomes coated with RPA, leading to ATR activation. In the SS patients examined, a mutated C-terminally truncated form of the CtIP protein is expressed that impairs the processing of the DSB, reducing the formation of RPA-ssDNA. This results in reduced ATR activation and a hypersensitivity to DNA damage (Qvist *et al.*, 2011).

Other SS genetic susceptibility loci have been mapped to 14q21-q22 (SCKL3, OMIM 608664) but no mutations have yet been discovered in these patients.

1.8.2 Microcephalic Osteodysplastic Primordial Dwarfism (Type II)

Microcephalic osteodysplastic primordial dwarfism, type II (MOPDII) (OMIM 210720) is clinically similar to SS but is regarded as a distinct disorder. Severe pre and post-natal growth retardation is a common feature but distinct clinical features of MOPDII include disproportionate limbs, a normal head size at birth which progresses to true, disproportionate microcephaly and distinct skeletal features such as bony dysplasia and loose-jointedness which are also progressive with age (Hall *et al.*, 2004). There is also an increased likelihood of vascular problems in MOPDII patients, such as aneurysms and moyamoya disease, which can be potentially life-threatening (Hall *et al.*, 2004). Moyamoya disease is an idiopathic disorder of the blood vessels supplying the brain. Narrowing of the blood vessels occurs which can result in cerebral ischaemia. This manifests in patients as seizures, haemorrhage, aneurysms and stroke (Brancati *et al.*, 2005).

Mutations in the *PCNT* gene have been identified in MOPDII patients (Rauch *et al.*, 2008), prompting speculation that the PCNT-Seckel patients identified are actually PCNT-MOPDII patients. However, this conclusion was based on clinical findings and genotyping alone (Willems *et al.*, 2010). Examination of ATR-dependent signalling in these cell lines may help to define whether a genotype-phenotype impact can distinguish between these two syndromes, and is important in view of the need to monitor the vascular problems observed in MOPDII patients. This will be discussed further in Chapter Three.

1.8.3 Meier-Gorlin Syndrome

Meier-Gorlin Syndrome (MGS) (OMIM 224690) is also referred to as Ear-Patella-Short stature syndrome. It is an autosomal recessive disorder with clinical features including pre- and post-natal growth retardation, absent patella (kneecaps) and microtia (small ears). Patients may also manifest other clinical features such as microcephaly, small mouth, skeletal abnormalities and micrognathia (abnormal smallness of the jaws) (Faqeih *et al.*, 2005).

Recently, mutations in components of the pre-replication complex, including ORC1, ORC4, ORC6, CDC6 and CDT1, have been identified in a group of MGS patients. ORC1 was also found to be mutated in a subset of Seckel Syndrome patients and will be discussed in Chapter 5. ORC1 is known to be located at the centrosome where it plays a role in control of centrosome duplication (Hemerly *et al.*, 2009). Cell lines from MGS patients have been shown to display defects in ATR-dependent damage response signalling (See Chapter 5 and 6).

1.8.4 Primary Microcephaly

Autosomal recessive primary microcephaly is a genetic disorder characterised by the presentation of microcephaly (at least 3 standard deviations below the mean) accompanied by mild to moderate mental retardation. Patients do not show any other clinical features, such as skeletal abnormalities, which are common in the other disorders described above. This disorder is genetically heterogeneous with at least seven loci identified to date. These are summarised in Table 2. Approximately one third of MCPH cases have not yet been linked to one of these loci, indicating that more genes may still await identification (Thornton and Woods, 2009). Most of the mutations that cause MCPH lead to either a dramatic reduction in the level of protein present or are functionally null (Nicholas *et al.*, 2009). All of the proteins identified thus far are localised at the centrosome, further demonstrating the importance of this organelle in neurogenesis.

The first molecular defect to be identified in primary microcephaly patients was *Microcephalin* (Jackson *et al.*, 2002). *Microcephalin* encodes a BRCT domain containing protein (MCPH1), which has been shown to play a variety of roles in cell cycle progression and DNA damage response pathways. It has been demonstrated to localise to foci induced by DNA damage by binding to γH2AX (Wood *et al.*, 2007)

	OMIM I.D	LOCUS	GENE	OCCURANCE
MCPH1	251200	8p23	MICROCEPHALIN	Rare
MCPH2	604317	19q12	WDR62	10%
MCPH3	604804	9q33.3	CDK5RAP2	Rare
MCPH4	604321	15q21.1	CEP152	Rare
MCPH5	608716	1q31	ASPM	50%
MCPH6	608393	13q12.2	CENPJ	Rare
MCPH7	612703	1p32	STIL	Rare

Table 2 MCPH genes
(Adapted from Thornton & Woods, 2009)

and is required for the recruitment of many downstream DNA damage response proteins (Wu *et al.*, 2009).

MCPH1 patient cells display defects in ATR-dependent G2/M checkpoint activation and Cdc25A stabilisation (Alderton *et al.*, 2006). It was demonstrated that Microcephalin plays an important role in the regulation of mitotic entry via the regulation of Cdk1. Patient cells exhibit a premature chromosome condensation (PCC) phenotype that correlates with dramatically reduced levels of phosphorylated Y15-Cdk1 in late S and G2 phases of the cell cycle. Subsequent studies have demonstrated that Microcephalin interacts with Pericentrin in order to recruit Chk1 to the centrosome and this may be important for the timely control of mitotic entry (Tibelius *et al*., 2009).

Mutations in *ASPM* (Abnormal Spindle Microcephaly associated) are the most common cause of primary microcephaly (Thornton and Woods, 2009). ASPM localises to the spindle poles during mitosis and is involved in the organisation of the spindle and its positioning within the cell (Higgins *et al.*, 2010). It is highly expressed during the period of rapid expansion of the cerebral cortex in the mouse brain (Bond *et al.*, 2002) and is then down-regulated at the point where the divisions switch from symmetric proliferation to asymmetric (Fish *et al.*, 2006). In the absence of ASPM, cells prematurely switch to asymmetric division due to an increase in the number of cells that bypass the apical membrane (Figure 1.1) (Fish *et al.*, 2006). Mutations in mouse ASPM revealed defects in the ability of the protein to localise to the midbody, resulting in microcephaly and a striking loss of germ cells (Pulvers *et al.*, 2010).

Mutations in *Cdk5Rap2* and *CENPJ* were also identified in primary microcephaly patients (Bond *et al.*, 2005). CDK5RAP2 is involved in recruitment of gamma tubulin ring complexes (γTURC) to the centrosome via an interaction with Pericentrin (Buchman *et al.*, 2010), aids in the maintenance of centrosome cohesion (Graser *et al.*, 2007) and regulates the assembly of microtubules (Fong *et al.*, 2009). It is expressed in the embryonic mouse brain and its depletion leads to a reduction in the proportion of apical progenitor cells, which have the capacity to self-renew, and an increase in the proportion of basal progenitor cells, which tend to differentiate. There was also an increased level of apoptosis observed in Cdk5Rap2 deficient mouse embryos (Buchman *et al.*, 2010).

1.9 AIMS

The aim of this thesis was to carry out a functional characterisation of SS patient cell lines to gain insight into the underlying genetic defects. Based on a previous finding that multiple SS patient cell lines display ATR-dependent G2/M checkpoint defects, I aimed to examine ATR-dependent DNA damage responses in multiple, genetically uncharacterised, SS patient cell lines. In order to attempt to identify the underlying genetic defects in these patients, a two-pronged approach was undertaken. Firstly, the analysis of ATR-dependent signalling was assessed by the use of assays to determine if there are defects in upstream or downstream signalling events. This enables a determination of the likely position of the genetic defect within the ATR signalling pathway. Secondly, patient samples from large families with multiple affected members were sent to collaborating genetics laboratories to include in genetic mapping studies. Once genetic defects were identified, a characterisation of the impact of mutations was undertaken in order to gain insight into both the genetic and molecular basis underlying SS and related Microcephalic primordial dwarfism disorders.

CHAPTER TWO

MATERIALS AND METHODS

2.1 TISSUE CULTURE

2.1.1 Cell lines

Lymphoblastoid cell lines (LBLs) used were wild-type (WT; GM2188), ATR-Seckel (ATR-S; DK0064) and Ataxia Telangiectasia-mutated (ATM; GM03189D), obtained from the Coriell Cell Repository (New York, NJ). Patient LBLs and primary fibroblasts were derived from patients with informed consent. $PCNT^{E220X-/-}$ (CV1559, affected), $PCNT^{E220X-/+}$ (CV1584, unaffected brother of CV1559), $PCNT^{S629fs-/-}$ (CV1576, affected), $PCNT^{S629fs-/+}$ (CV1582, unaffected mother of CV1576) and $PCNT^{C1990fs-/-}$ (12061, affected) (Griffith *et al.*, 2008). CV1720 was derived from an affected patient with mutations in ATRIP, CV1780 was derived from unaffected the father of CV1720 and CV1783 was derived from the unaffected mother of CV1720 (Ogi *et al*, 2012 in submission). $ORC1L^{E127G-/-}$ (CV1759, affected), $ORC1L^{E127G-/+}$ (CV1794, unaffected father of CV1759) and $ORC1L^{E127G-/+}$ (CV1795, unaffected mother of CV1759) (Bicknell *et al.*, 2011b). $CDC6^{T323R-/-}$ (13107 affected), $ORC4^{Y174C-/-}$ (18380 affected), $CDT1^{R462Q + Y520X}$ (20792 affected) and $ORC6^{F86X + Y232S}$ (20744 affected) (Bicknell *et al.*, 2011a). LBLs were cultured in RPMI 1640 medium supplemented with 15% fetal calf serum (FCS), 1% penicillin/streptomycin and 1% L-Glutamine.

Primary fibroblasts used were WT (1BR3 and 48BR), ATR-Seckel (F02-98), 42552 ($PCNT^{C1990fs-/-}$), ASB ($PCNT^{E220X-/-}$) and AJ620 (ORC1-P4 $^{R105Q/R720Q}$). Primary fibroblasts were cultured in MEM medium supplemented with 15% fetal calf serum (FCS), 1% penicillin/streptomycin and 1% L-Glutamine.

HeLa and MG63 cell lines were cultured in MEM medium supplemented with 10% fetal calf serum (FCS), 1% penicillin/streptomycin and 1% L-Glutamine.

All cell lines were grown at 37°C in 5% CO_2 incubators. All tissue culture reagents were supplied by Gibco, Invitrogen.

2.1.2 Treatment with DNA-damaging agents

UV irradiation was performed using a UV-C source (0.5J/m^2/s).
γ-irradiation was performed with a ^{137}Cs source at a dose rate of ~2Gy/min.
Hydroxyurea was obtained from Sigma-Aldrich (Poole, UK).

2.2 IMMUNOFLUORESENCE AND MICROSCOPY

2.2.1 Standard Immunofluoresence

LBLs were swollen in 75mM KCL for five minutes and then cytospun onto poly-L-lysine coated slides. The cells were then fixed in 3% paraformaldehyde (PFA), 2% sucrose for ten minutes. Cells were permeabilised using 0.2% Triton-X100 for 30 sec followed by extensive washing with phosphate buffered saline (PBS). Cells were blocked with 2% bovine serum albumin (BSA) in PBS for ten minutes prior to incubation with primary antibody (Table 3) (1:100, 40 min). Secondary antibodies (1:200, 20 min) used were FITC, Cy3 or TRITC conjugated and were obtained from Sigma-Aldrich. Nuclei were counterstained with DAPI. Images were captured with a Zeiss axioplan fluorescent microscope using Simple PCI software.

2.2.2 Centrosomal immunofluoresence

LBLs were swollen in 75mM KCL for five minutes and then cytospun onto slides. The cells were then fixed in 3% PFA, 2% Sucrose for ten minutes followed by extensive PBS washing. Cells were then fixed using ice cold 70% methanol for 1 min followed by extensive PBS washing. Cells were permeabilised using 0.2% Triton-X100 for 45 sec followed by extensive washing with PBS. Cells were blocked with 2% BSA in PBS for ten minutes prior to incubation with primary antibody (1:100, 40 min). Secondary antibodies (1:200, 20 min) used were FITC, Cy3 or TRITC conjugated and were obtained from Sigma-Aldrich. Nuclei were counterstained with DAPI. Images were captured with a Deltavision microscope using Softworx software. Quantification of centrosomal signal was achieved using ImageJ software.

2.2.3 UV-induced G2/M checkpoint arrest

LBLs were seeded into complete medium and incubated for 2-4 hrs prior to irradiation with 5J/m^2 UV-C or 3gy IR. Cells were then cultured for a further two

hours in complete medium before harvesting, or for 24hr in complete medium with the addition of 1.5μM Nocodazole (Sigma). Cells were pelleted, swollen in 75mM KCL for five minutes and then fixed in Carnoys fixative (Methanol:Acetic Acid, 3:1). Nuclei were stained with DAPI and slides were prepared using a cytospin. The mitotic index was then determined for each cell line by counting at least 500 cells. A decrease in the number of mitotic cells was taken as indicative of activation of the G2/M checkpoint.

2.2.4 Supernumerary mitotic centrosomes

LBLs were incubated for 24hrs in complete medium supplemented with 1.5μM nocodazole and processed for immunofluorescence microscopy with anti-γ tubulin antibodies. The number of centrosomes present in 50-100 mitotic cells was scored for each cell line.

2.2.5 HU-induced 53BP1 foci formation

LBLs were untreated or treated with 5mM Hydroxyurea for 2hr. Cells were then washed once in PBS and slides prepared using a cytospin. Cells were fixed in 3% PFA, 2% Sucrose for ten minutes followed by extensive PBS washing. Slides were then stained using the standard immunofluoresence techniques described above using an anti-53BP1 primary antibody. Cells with > 5 53BP1 foci were counted as positive and the percentage of positive cells was assessed for each cell line.

2.2.6 HU-induced H2AX phosphorylation

LBLs were untreated or treated with 5mM Hydroxyurea for 2hr. Cells were then washed once in PBS and slides prepared using a cytospin. Cells were fixed in 3% PFA, 2% Sucrose for ten minutes followed by extensive PBS washing. Slides were then stained using the standard immunofluoresence techniques described above using an anti-γH2AX primary antibody. Cells with pan-nuclear γH2AX staining were counted as positive and the percentage of positive cells was assessed for each cell line.

2.2.7 Replication fork stability assay

Cells were labelled with CldU (50μM) for 20 min, pelleted and washed in PBS, followed by incubation in complete medium supplemented with 10μM Aphidicolin (Sigma) for 2 hr. Cells were then pelleted and swollen in 75mM KCL plus 100μM IdU for ten minutes to allow fork reinitiation and IdU incorporation. Cells were then fixed in Carnoys fix and slides prepared using a cytospin. Cells were permeabilised and then incubated in 2.5M HCL for 40 min to denature the DNA. Cells were then blocked in 2% BSA/PBS for 1hr prior to primary antibody incubation (Both at 1:100, 4 C, overnight). The CldU label was detected with a TRITC-conjugated secondary antibody and the IdU label detected with a FITC-conjugated antibody. Nuclei were counterstained with DAPI. Images were captured with a Zeiss axioplan fluorescent microscope using Simple PCI software. The percentage of cells with both red and green labels was scored.

2.2.8 DNA fibre analysis

Cells were labelled with IdU (25μM) for 20 min at 37°C and then pulse-labelled with CldU (250μM) for 20 min. Cells were then washed twice with ice-cold PBS and were resuspended in ice-cold PBD at a concentration of 0.5 to 1 $x10^6$ cells/ml. A 2μL drop of cell suspension was placed in the centre of the top quarter of a microscope slide. The drop was left to dry at room temperature for 7 min. 7.5μL of spreading buffer (200mM Tris-HCL pH7.5, 50mM EDTA, 0.5% SDS) was added to the drop and mixed by gentle stirring with a pipette tip. This was incubated for a further 5 min at room temperature. The slide was then tilted to an angle 10-20° to the horizontal by raising the top end by approximately 0.75cm, in order for the drop to run to the bottom of the slide in 4 min. The slide was then air-dried and fixed in methanol/acetic acid 3:1 for 10 min. For immunostaining of DNA fibres, slides were washed twice with water for 5 min and then denatured using 2.5M HCL for 1 hour. Slides were rinsed twice with PBS-Tween (0.1%) and then incubated in blocking solution (PBS/1% BSA/0.1% Tween) for 30 min. Primary antibody incubation with mouse anti-BrdU to detect IdU incorporation and rat anti-BrdU to detect CldU incorporation was performed overnight at 4°C. Slides were washed twice with PBS-T. Slides were incubated with secondary antibodies for 30 min at 37°C in a humid chamber. Slides were then washed 5 x 2min with PBS-T. To detect single-stranded DNA slides were incubated with mouse anti-ssDNA (polydT) antibody for 30 min at 37°C in a humid chamber. Slides were washed 5 x 2 min with PBS-T and then incubated with mouse secondary antibody for 30 min at 37°C in a humid chamber.

Slides were then washed 5 x 2 min with PBS-T and mounted using Prolong Anti-Fade Gold (Molecular Probes). Images were captured with a Deltavision microscope using Softworx software. Fibres were analysed according to (Maya-Mendoza *et al.*, 2007).

2.3 PROTEIN TECHNIQUES

2.3.1 Whole Cell Extracts (WCE)

Cell pellets were either stored at -80°C or directly lysed in 50-100uL of lysis buffer (50mM Tris-HCL pH7.5, 120mM NaCl, 0.5% NP-40, 1mM DTT, 1mM NaF, 1mM β-Glycerophosphate, 0.2mM PMSF and protease inhibitor cocktail from Sigma) for 1hr on ice. Cell lysates were centrifuged for 2 min at 13000rpm at 4°C. The supernatant was transferred to a clean, cold eppendorf tube. The protein concentration was then determined using Bradford Protein Assay reagent (Bio-Rad Laboratories) at a UV absorbance of 595nm. Extracts were either stored at -80°C or directly boiled in 2x SDS loading buffer (5% SDS, 10% Glycerol, 10% β-mercaptoethanol, 125mM Tris-HCL ph6.8 and 0.2% bromophenol blue) and loaded onto SDS-PAGE gels.

2.3.2 Chromatin extraction

1 x 10^7 cells were untreated or irradiated with 20J/m^2/s UV-C and incubated for 1hr in complete medium. Cells were then washed in PBS and resuspended in 100μL hypotonic buffer. Lysates were incubated on ice for 15min and then pelleted. The supernatant (soluble fraction) was removed and retained. The remaining pellet was washed once in hypotonic buffer before resuspension in 100μL hypertonic buffer. After incubation on ice for a further 15 min, the chromatin extract was pelleted and resuspended in 100μL of 2x High SDS loading buffer. The samples were then sonicated and 10μL resolved by SDS-PAGE for western blotting.

2.3.3 Chromatin Fractionation

LBLs (1 x 10^7) were washed with PBS and once with 1 ml low salt buffer (LSB). Pelleted cells were resuspended in six times the packed cell volume of LSB + 0.1 mM MC-LR and 1 x protease inhibitor cocktail, and immediately centrifuged for 10 min at 10,000 rpm (supernatant = S10). The pellet was gently resuspended (by tapping, but not pipetting, to prevent chromatin decondensation) in a volume (V) of

high-salt buffer (HSB: 50 mM Tris-HCl [pH 8.0], 5% [v/v] glycerol, 1 mM EDTA, 10 mM MgCl2, 400 mM KCl, 1x protease inhibitors and 0.1 mM MC-LR) equal to 0.25 V of LSB used to lyse the cells. Samples were immediately centrifuged for 10 min at 10,000 rpm (supernatant = P10). The pellet was then resuspended in nuclease buffer (same V as HSB) containing 10 U/ml MNase and incubated at 37°C for 10 min. Samples were then centrifuged for 5 min at 10,000 rpm (supernatant = C1). The pellet was resuspended in nuclease buffer (V same as used for HSB) containing 100 U/ml MNase and incubated at 37°C for 45 min before an equal V of solubilization buffer (nuclease buffer + 2% [v/v] NP-40, 2% [v/v] Triton X-100, 600 mM NaCl) was added. Samples were vortexed briefly and centrifuged for 5 min at 10,000 rpm (supernatant = C2). The remaining pellet was resuspended in solubilization buffer (same V as HSB) and an equal V of denaturing buffer (50 mM Tris [pH 6.8], 1% [v/v] SDS, 100 mM DTT, 10% glycerol) before brief sonication, boiling for 5 min, and centrifuging at 10,000 rpm for 5 min (supernatant = C3) (Goodarzi *et al.*, 2008).

2.3.4 SDS-PAGE and Western Blotting

Whole cell extracts (50μg) or chromatin extracts (5-10μL) were resolved by SDS-PAGE (Laemelli method) before transfer onto either HyBond 0.45uM PVDF (GE Healthcare) or 0.2uM Protran nitrocellulose membranes (Whatman). Membranes were blocked in either 5% BSA or 5% non-fat milk in Tris-buffered saline plus 0.1% Tween-20 (TBS-T) for 1hr. Membranes were then probed with primary antibody in 5%BSA/TBS-T overnight at 4 C. Membranes were washed with TBS-T, 3 times for ten minutes. Membranes were then probed with HRP-conjugated secondary antibodies followed by three further TBS-T washes. Signal was then detected using either Pierce ECL Detection Reagents or ECL plus detection reagents (GE Healthcare).

2.3.5 Cdc25A stability assay

Cells were either untreated or irradiated with 10J/m^2/s UV-C and then incubated in complete medium with 100μg/ml cycloheximide for 20 min. Cells were pelleted and resuspended in WCE extraction buffer in the continued presence of cycloheximide. 50μg WCE was resolved using SDS-PAGE and western blotted with anti-cdc25A antibodies (Alderton *et al.*, 2006).

2.4 Plasmids

pCMV ATRIP WT plasmid was obtained from David Cortez. pCGT ORC1 WT plasmid was obtained from Andrew Jackson. pcDNA3 ATR WT plasmid was obtained from Anthony Carr.

2.5 Site-directed mutagenesis

The Quikchange Lightning Site-Directed mutagenesis kit (Stratagene) was used to incorporate patient mutations into WT plasmids. Details of primers used for site-directed mutagenesis are shown in Table 4.

2.6 Complementation analysis

LBL cultures were either untransfected or transfected with 1μg of appropriate cDNA using GeneJuice transfection reagent (Novagen/Merck Chemicals), according to the manufacturers instructions. Transfections were repeated 24hr and 48 hr later. Cultures were therefore transfected three times in total. Cultures were then subjected to G2/M checkpoint analysis as described in section 2.2.3.

2.7 Fluorescence-activated cell sorting (Facs) analysis of S-phase progression

LBLs were pulse-labelled with 50μM BrdU for 30 min and then incubated in the presence of 0.2μg Colcemid for 6hr to prevent mitotic exit. Samples were collected at 0,2,4 and 6hr post BrdU label and were fixed in 70% ice-cold Ethanol. Cells were then treated with 2M HCL for 30 min followed by incubation in 0.1M Sodium Tetraborate for 2 min. Cells were washed with PBS/1%BSA and then incubated with fluorescein isothiocyanate (FITC)-conjugated monoclonal anti-BrdU (Becton Dickinson) for 30 min. Cells were washed with PBS/1%BSA and then counterstained with 10 μg/ml propidium iodide with 0.5 mg/ml RNase in PBS for 15 min prior to Facs analysis. Cells were gated to eliminate any doublets and then the BrdU labeled population gated and quantified. The rate of S-phase progression was calculated as the loss of cells from the early S-phase compartment.

2.8 Small interfering RNA studies

HeLa or MG63 cells were transfected with 10nM of siRNA duplex using siPort NeoFX transfection reagent according to the manufacturers instructions (Ambion, UK). The oligonucleotides used were Invitrogen Stealth™ duplexes, designed using an invitrogen algorithm (https://rnaidesigner.invitrogen.com/rnaiexpress/index.jsp).

Oligos used were: PCNT sense: UCACAAUCAGUGACCACCAACCGGA.
ORC1 sense: CGUAUGUUGCUAAAUUGCUUGAGUU
CEP192 sense: GAGACUCCUACGGUGUCCAUUCAAG

The control oligonucleotide was ON-TARGETplus siCONTROL Non-targeting siRNA #2 (Dharmacon).

Antibody	**Details**	**Supplier**	**Identifier**
53BP1	Rabbit polyclonal	Bethyl	BL181
ATR	Goat polyclonal	Santa Cruz	N19
ATRIP	Rabbit polyclonal	Bethyl	A300-095A
Aurora A	Mouse monoclonal	Abcam	Ab13824
Phospho Aurora A (Thr288)	Rabbit monoclonal	Cell signalling	S3079
BrdU (detects IdU)	Mouse monoclonal	BD Biosciences	Clone B44
BrdU (detects CldU)	Rat polyclonal	Abcam	Clone BU1/75
FITC-BrdU	Mouse monoclonal	BD Biosciences	347583
Cdc25A	Mouse monoclonal	Abcam	DCS120 + DCS121
Cdc25A	Mouse monoclonal	Santa Cruz	F6
Cdc25B S230		B Ducommon	
Chk1 phospho ser317	Rabbit polyclonal	Cell signalling	2344S
Chk1	Rabbit polyclonal	Santa Cruz	FL476
hCLK2	Rabbit polyclonal	Abcam	Ab65082
FANCD2	Rabbit polyclonal	Novus	NB-100-182
HDAC1	Rabbit polyclonal	Abcam	Ab19845
Histone H3	Rabbit monoclonal	Abcam	Y173
HP1	Rabbit polyclonal	Santa Cruz	FL191
Gamma H2AX	Mouse monoclonal	Upstate	05-636
Gamma Tubulin	Rabbit polyclonal	Sigma	T5192
Gamma Tubulin (GTU-88)	Mouse monoclonal	Abcam	Ab11316
Kap1	Rabbit polyclonal	Abcam	Ab10484
Mcm2	Goat polyclonal	Santa Cruz	N19
ORC1	Goat polyclonal N terminal	Santa Cruz	N17
ORC1	Rabbit polyclonal C terminal	Santa Cruz	H80
ORC2	Rabbit polyclonal	Santa Cruz	H300
Pericentrin	Rabbit polyclonal	Abcam	Ab4448
Phospho PLK1 (Thr210)	Rabbit polyclonal	Cell signalling	S5472
PLK1	Mouse monoclonal	Abcam	Ab14210
ssDNA	Mouse monoclonal	Millipore	MAB3034
Timeless	Rabbit polyclonal	Abcam	Ab72458
Secondary antibodies			
Anti-mouse IgG1-A546	Goat	Invitrogen	A21123
Anti-rat A488	Chicken	Invitrogen	A21470
Anti-Mouse IgG2a-A647	Goat	Invitrogen	A21241
Anti-mouse FITC	Goat	Sigma	F0257
Anti-rat TRITC	Rabbit	Sigma	T5778
Anti-rabbit Cy3	Sheep	Sigma	C2306
Anti-goat HRP	Polyclonal rabbit	Dako	P0449
Anti-rabbit HRP	Polyclonal swine	Dako	P0217
Anti-mouse HRP	Polyclonal goat	Dako	P0447

Table 3 Antibodies

Target	Primer sequence
ATRIP C2229T-F	GTCAGCATGCTCATCTGAGGGCTTCCTGATG
ATRIP C2229T-R	CATCAGGAAGCCCTCAGATGAGCATGCTGAC

Table 4 SDM primers

CHAPTER THREE

RESULTS I: Mutations in *Pericentrin (PCNT)* cause Microcephalic Primordial Dwarfism

3.1 INTRODUCTION

A splicing mutation in ATR was identified in a Seckel Syndrome patient in our laboratory (O'Driscoll *et al.*, 2003) and subsequent analysis of further Seckel syndrome patient cell lines showed defects in ATR-signalling but without mutations in ATR (Alderton *et al*., 2004). Two large, consanguineous families of Middle Eastern origin were therefore selected for further study in order to attempt to identify further genetic defects underlying Seckel syndrome. Two children from family 1 were clinically diagnosed with Seckel syndrome, whilst family 2 had one affected child. The lymphoblastoid (LBL) cell lines from one affected child plus one parent from each family were assessed for UV-induced G2/M checkpoint defects, nuclear fragmentation and supernumary centrosome phenotypes. They were then included in a genetic mapping study in order to identify potential causative gene candidates. Using this approach we identified mutations in the *Pericentrin (PCNT)* gene, which maps to chromosome 21q22.3, in collaboration with Andrew Jackson's group at the MRC Human Genetics Unit in Edinburgh. I will present data in this chapter to show that the identification of this novel genetic defect provided the first example of mutations in a structural centrosomal protein causing a defect in DNA damage response signalling.

Mutations in *PCNT* were also identified in a group of patients diagnosed with Microcephalic Osteodysplastic Primordial Dwarfism Type II (MOPDII) (Rauch *et al.*, 2008b). These patients are similar to Seckel syndrome in that the clinical features include microcephaly and severe growth retardation. Distinct clinical features of MOPDII include disproportionate limbs and distinct skeletal features such as bony dysplasia and loose-jointedness that are progressive with age. The microcephaly in these patients presents as a normal head size at birth which progresses to true, disproportionate microcephaly (Hall *et al.*, 2004). There is also an increased likelihood of vascular problems in MOPDII patients, such as aneurysms and moyamoya disease, which can be potentially life-threatening (Hall *et al.*, 2004).

Further clinical evaluation of the PCNT-Seckel patients described here resulted in their reclassification as MOPDII patients (Willems *et al*., 2010).
Pericentrin (PCNT) is a large 360kd coiled-coil protein that exists in multiple isoforms (Flory and Davis, 2003). It is an integral component of the pericentriolar material of the centrosome and acts as a scaffold, transporting proteins to the centrosome via an interaction with Dynein and anchoring them there (Purohit *et al.*, 1999). Depletion of PCNT results in disruption of centrosome structure and defects in organization of the spindle (Doxsey *et al.*, 2005b). One of the important functions of PCNT is therefore to anchor γTubulin ring complexes (γTURCs) at the centrosome, thereby providing sites for microtubule nucleation (Takahashi *et al.*, 2002, Zimmerman *et al.*, 2004).

PCNT has been shown to interact with a diverse range of proteins including Protein kinase A (Diviani *et al.*, 2000) and Protein kinase C (Chen *et al.*, 2004). Subsequent to publication of data included in this chapter, CDK5RAP2 (Buchman *et al.,* 2010*)*, CHK1 and Microcephalin (MCPH1) (Tibelius *et al*., 2009) were all found to interact with PCNT. CDK5RAP2 and MCPH1 are both centrosomally localised proteins that are mutated in some Primary Microcephaly patients (Jackson *et al.*, 2002, Bond *et al.*, 2005). NEK2 kinase is sequestered by PCNT at the centrosome, preventing premature splitting of the centrosomes before late G2 phase (Matsuo *et al.*, 2010).

In recent years, the centrosome has increasingly been demonstrated to be an important cellular site for the control of cell cycle progression, with evidence for roles in G1 to S phase progression, G2 to M phase progression and metaphase to anaphase transition (Doxsey *et al.*, 2005b). Initial findings regarding the importance of the centrosome for control of mitotic entry were provided from reports that the earliest detection of active Cdk1-CyclinB1 complexes occurred at the centrosome during prophase (Jackman *et al.*, 2003). Chk1 was reported to inhibit Cdk1 activity when both proteins were present at the centrosomes in interphase cells. This inhibition of Cdk1/Cyclin B1 prevents the progression of cells from G2 to mitosis. Chk1 was found to be absent from the centrosomes of mitotic cells, allowing the cells to progress from G2 to mitosis (Krämer *et al.*, 2004a). It was elegantly demonstrated that targeting wild type Chk1 to the centrosome via fusion with a PACT (pericentrin-AKAP450 centrosomal targeting) domain prevented activation of Cdk1 and resulted in polyploidy and multiple centrosomes. Targeting of kinase-dead Chk1 to the centrosome resulted in premature activation of Cdk1 and premature mitotic entry (Krämer *et al.*, 2004a). Chk1 inhibition also activated

Cdk1 associated with the centrosome and resulted in premature mitotic entry. The inhibition of mitotic entry was found to be via a Chk1-Cdc25B mechanism, rather than a direct effect of Chk1 on Cdk1. Cdc25A (Shreeram *et al.*, 2008), Cdc25B (Dutertre *et al*., 2004), and Cdc25C (Bonnet *et al.*, 2008) have all been reported to localize to the centrosome. Cdk1 is also recruited to the centrosome via an interaction with the CEP63 protein (Löffler *et al.*, 2007a).

The Kramer laboratory then went on to demonstrate that DNA damage causes the accumulation of phosphorylated Chk1 at the centrosome (Löffler *et al.*, 2007b). They concluded that the accumulation of total Chk1 at the centrosome was ATM/ATR independent, however, the accumulation of phosphorylated Chk1 at the centrosome was dependent on ATR/ATM (Löffler *et al.*, 2007a). Whether this phosphorylation of Chk1 by ATM/ATR occurs at the centrosome or in the nucleus was not established. The authors then targeted kinase-dead Chk1 to the centrosome using the PACT domain and observed a G2/M checkpoint defect after UV irradiation (Löffler *et al.*, 2007a).

PCNT is highly expressed in mouse embryo cells and is localized at the base of primary cilia. It was shown in PCNT mutant mice that PCNT is required for the assembly of cilia of olfactory neurons but not for global cilia formation (Miyoshi *et al*., 2006). PCNT has been shown to interact with intraflagellar transport proteins, depletion of which result in PCNT mislocalisation and inhibition of primary cilia formation (Jurczyk *et al*., 2004). Disruption of the primary cilia structure is associated with a range of disorders termed ‘Ciliopathies’, where phenotypes include polycystic kidney disease, pre and post axial polydactyly, and skeletal and neurodevelopmental disorders (Duldulao *et al.*, 2010).

A PCNT mutant mouse engineered with a two base pair deletion in exon 31, resulting in a frame-shift at codon 2214 has recently been described by Endoh-Yamagami and colleagues (Endoh-Yamagami *et al*., 2010). Homozygote mice display progressive embryonic growth retardation and a high incidence of perinatal lethality. Both homozygous and heterozygous embryos had smaller brains than their wild type counterparts. Another penetrant feature of the PCNT homozygous mice is preaxial polydactyly, a phenotype that is associated with the ciliopathy Joubert syndrome (Duldulao *et al.*, 2010).

Finally, a role for PCNT in glucose regulation has been demonstrated. PCNT is expressed in primary mouse pancreatic islet and insulinoma cells where it

associates with insulin granules. Depletion of PCNT results in a loss of intracellular insulin (Jurczyk *et al*., 2010). Premature diabetes with severe insulin resistance has been noted in patients with PCNT mutations (Huang-Doran *et al*., 2011).

The aim of this chapter was to carry out an in-depth functional characterisation of consanguineous Seckel syndrome patient cell lines to enable identification of novel genetic defects using gene-mapping techniques. Once a genetic defect had been identified an investigation into how it impacts on the ATR-dependent DNA damage response was conducted.

3.2 RESULTS

3.2.1 Mutations in Pericentrin in Microcephalic Primordial Dwarfism patients

Two families within our panel of Seckel Syndrome patient cell lines were of great interest as they were both large and consanguineous (Figure 3.1a). This makes them ideal candidates for genetic mapping studies where data from large numbers of genetically dissimilar individuals greatly increases the power of the study (Jin *et al.,* 2004). The patients displayed microcephaly and short stature, following intrauterine growth retardation (Figure 3.1b). In family 1 the patient (subsequently identified as E220X-/-) had a receding forehead with a high nasal bridge and prominent nose. An MRI scan revealed atrophy of the white matter and thinning of the corpus callosum. There was some developmental delay at 8 months of age with the patient unable to sit unaided. The facial features were thought to not entirely fit with a diagnosis of Seckel syndrome, although features common in Seckel syndrome patients such as fifth finger clinodactyly were present (Personal communication; Dr Nouriya Al Sanna). The patient from family 2 (S629fs) also had a prominent nose, small ears and a receding forehead. A deep voice with small 'broken' teeth was also observed. Skeletal surveys on all patients were normal (Griffith *et al*., 2008).

After confirming the 'Seckel status' of the patients by G2/M checkpoint assay and supernumary mitotic centrosome assessment, DNA was sent to our collaborators for further study. The MRC Human Genetics Unit in Edinburgh performed an SNP-microarray genome-wide homozygosity scan at 50kbp resolution, using Affymetrix chips, on the two families (Griffith *et al.*, 2008). Using this approach they identified a novel Seckel locus between markers rs1598206 and rs2330591 on chromosome

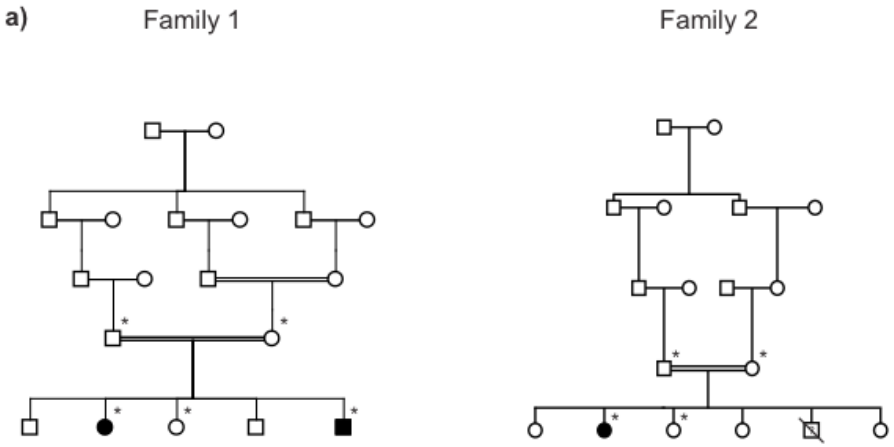

b)

Figure 3.1 Family pedigrees of PCNT mutated patients

a) Pedigrees of families with PCNT mutations. Asterix shows patients included in genome-wide SNP genotyping and linkage analysis

b) 13 year old patient with PCNT mutation showing growth retardation and microcephaly when compared to her 11 year old unaffected sibling (Family two).

Images adapted from Griffith and Walker, Nature Genetics, 2008.

21q22.3-qter. This region spans 2.9 Mbp of DNA and contains 55 known Refseq genes. Within this region was a gene encoding a centrosomal protein *Pericentrin (PCNT)*. Due to the consistent observation of supernumary mitotic centrosomes as a cellular phenotype of Seckel syndrome patients (Alderton *et al.*, 2004), and an established link between centrosomal gene mutation and primary microcephaly phenotypes (Zhong *et al.*, 2005), *PCNT* was considered to be a potential Seckel syndrome candidate gene. Sequencing of *PCNT* in each family revealed mutational changes.

A homozygous nonsense mutation (E220X) was identified in family 1 (Saudi Arabian) (CV1559). A homozygous single base-pair deletion (S629fs) was identified in family 2 (Kuwait) (CV1576). This deletion causes a frameshift and is thought to result in a premature protein truncation after an additional 65 amino acids. A further patient was then identified with a homozygous single base-pair insertion (C1190fs), which again results in a frameshift (12061) (Figure 3.2a).

3.2.2 PCNT expression is reduced in PCNT mutated patient cell lines

The levels of PCNT protein expression in each patient were examined by immunoblotting in order to verify the impact of the mutational change and to determine whether any residual protein could be detected (Figure 3.2b). Two bands of the correct predicted sizes were detected in control cell extracts that were not present in any patient cell line extracts. The levels of PCNT protein are therefore significantly disrupted by the mutations described, although the possibilty that residual protein is present cannot be excluded. Indeed, further work in our laboratory on patient primary fibroblasts has found that residual protein can be detected when these cells are examined using immunofluorescence with anti-pericentrin antibodies (T. Stiff, personal communication). This is perhaps unsurprising, as a structural centrosomal protein would be predicted to be essential for cell viabilty. Indeed, disruption of the PCNT gene in mice by the use of gene trap technology leads to embryonic lethality. Affected embryos display severe intrauterine growth retardation and microcephaly (Delaval and Doxsey, 2010).

3.2.3 PCNT mutated cells display a defective UV-induced G2/M checkpoint but a proficient IR-induced G2/M checkpoint

ATR-Seckel cells have previously been shown to display a defective G2/M checkpoint response both 24 hours (Alderton *et al.*, 2004) and 2 hours (Stiff *et al.*,

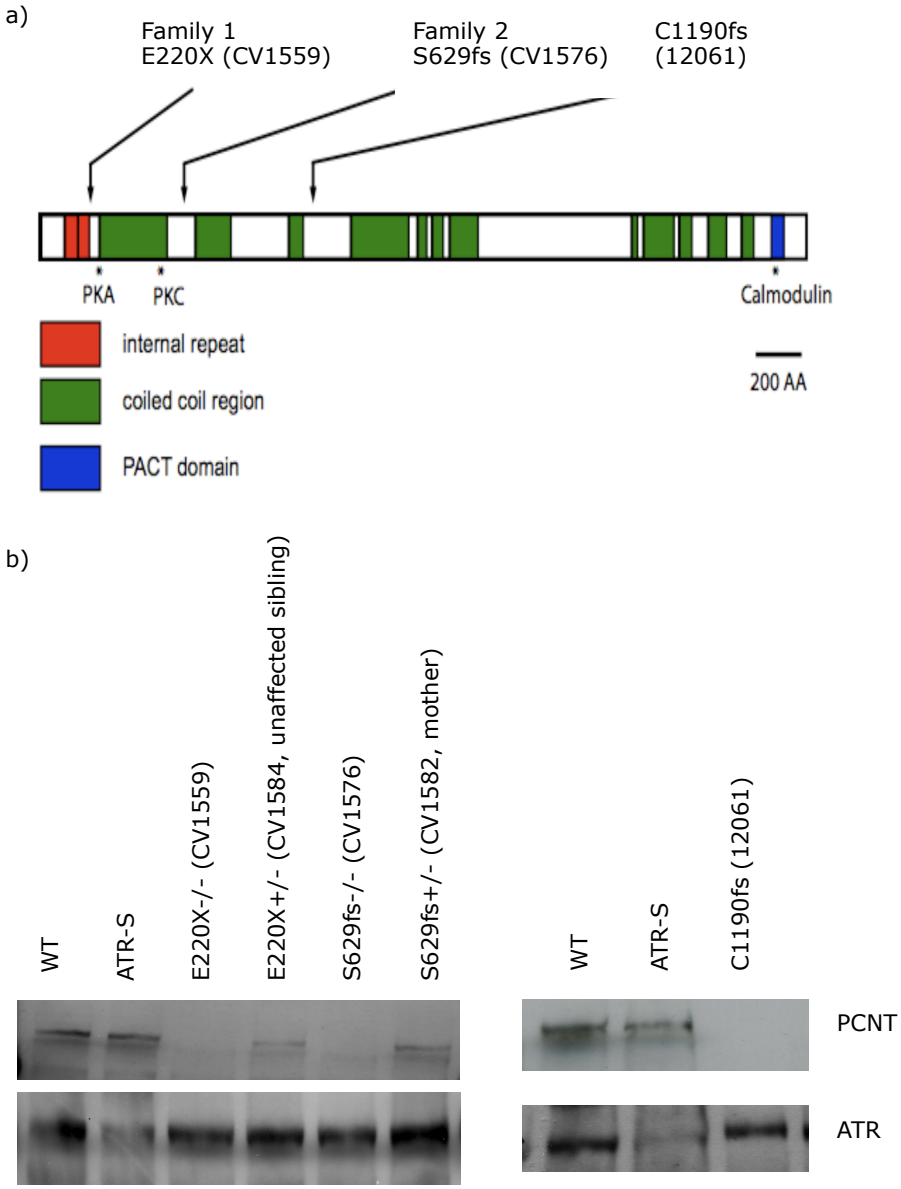

Figure 3.2 PCNT protein schematic and expression levels

a) Schematic of Pericentrin showing protein structure and the position of mutations found in the patients.
b) Levels of PCNT expression were examined by resolving whole cell extracts from WT, ATR-Seckel (ATR-S), unaffected heterozygous relative (E220X+/-, S629fs+/-) and PCNT-mutated cell lines (E220X-/-, S629fs-/- and C1190fs-/-) on 6% SDS-PAGE gel followed by transfer onto nitrocellulose membrane. Membranes were then probed with a PCNT antibody. ATR was used as a loading control.

2008) post UV irradiation. PCNT mutated cell lines were examined for their ability to activate G2/M checkpoint arrest at 2 hours after treatment with UV, reflecting a replication-independent arrest, and also 24 hours after treatment with UV, reflecting cells that may have progressed through both S phase and G2 phase before arresting. The patient cell lines examined failed to arrest effectively after exposure to UV at either time point post irradiation, similar to the response seen in ATR-Seckel patient cell lines and in contrast to wild-type cell lines (Figure 3.3 a, b). PCNT mutated cells are therefore compromised in their ability to activate ATR-dependent signaling in response to UV damage, resulting in a defective checkpoint response. This result demonstrated a surprising link between mutation in a core centrosomal structural protein and defects in the ATR-dependent signaling pathway.

In order to assess whether PCNT is required for activation of the ATM signaling pathway, PCNT mutated cells were examined for the ability to activate a G2/M checkpoint arrest after exposure to ionizing radiation, which introduces double-strand breaks into the DNA. PCNT mutated cells arrested normally following IR induced damage, in contrast to ATM mutant cell lines (Figure 3.4), indicating that PCNT is required for ATR-dependent pathway function but is not specifically required for ATM-dependent damage responses.

3.2.4 PCNT depletion in HeLa cells recapitulates the defective UV-induced checkpoint phenotype observed in PCNT mutated patient cell lines

In order to confirm the requirement for PCNT in ATR-dependent signaling, PCNT was depleted in HeLa cells using siRNA oligonucleotides. Cells were then irradiated with either UV or ionizing radiation and the G2/M checkpoint response examined 2 hrs later. The G2/M checkpoint response to UV irradiation was defective whilst the cellular response to ionizing radiation was normal (Figure 3.5). These results correspond to those observed in the patient cell lines and confirm that PCNT is specifically required for ATR-dependent signaling responses, but not ATM-dependent ones.

3.2.5 H2AX is phosphorylated normally in PCNT mutated cells

The phosphorylation of H2AX is a key upstream step in both the ATR and ATM signaling pathways and is important for the recruitment of proteins such as 53BP1,

a)

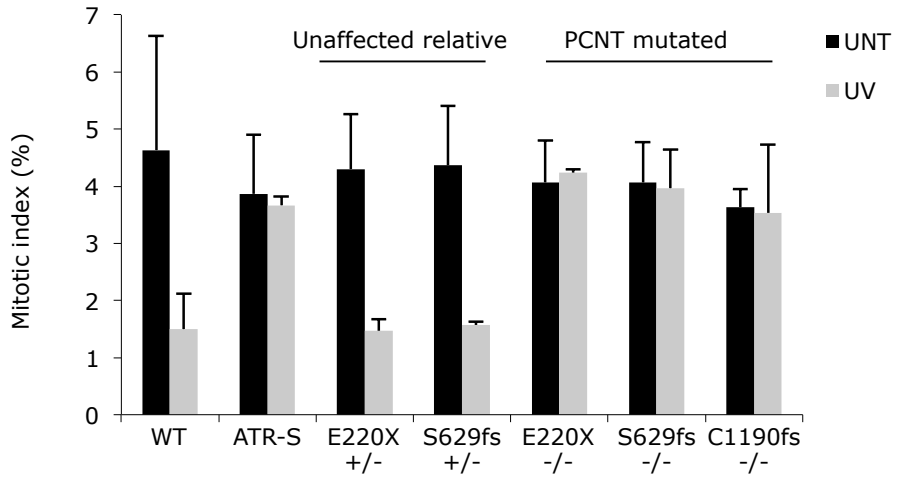

b)

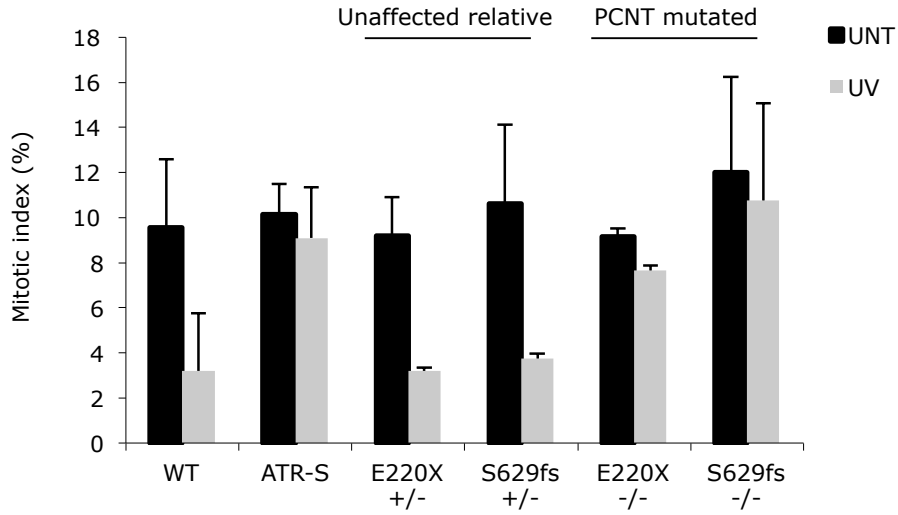

Figure 3.3 PCNT mutated cells display a defective UV-induced G2/M checkpoint

a) WT, ATR-S, unaffected heterozygous relative and PCNT mutated cell lines were examined for G2/M checkpoint arrest, 2hrs after treatment with 5J/m^2 UV irradiation. A decrease in the number of mitotic cells was taken as indicative of a G2/M arrest.
b) The same cell lines were examined for G2/M checkpoint arrest, 24hrs after treatment with 5J/m^2 UV irradiation and in the presence of 1.5μM nocodazole.

Graphs a represents the mean of three independent experiments. Graph b represents the mean of two independent experiments.
The error bars represent the standard deviation.

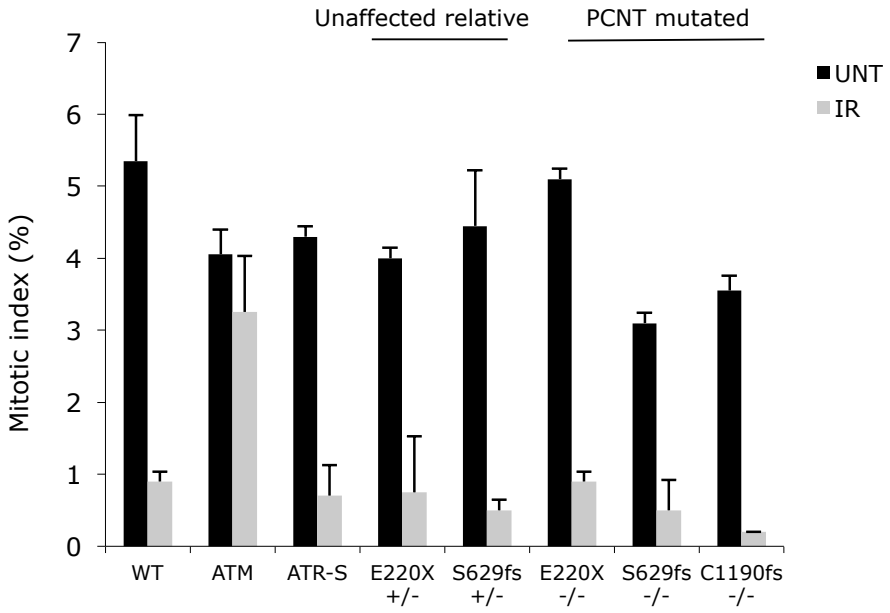

Figure 3.4 PCNT mutated cells display a proficient IR-induced G2/M checkpoint

WT, ATM, ATR-S, unaffected heterozygous relative and PCNT mutated cell lines were examined for G2/M checkpoint arrest, 2hrs after treatment with 3Gy IR irradiation. A decrease in the number of mitotic cells was taken as indicative of a G2/M arrest.

The graph represents the mean of three independent experiments.
The error bars represent the standard deviation.

a)

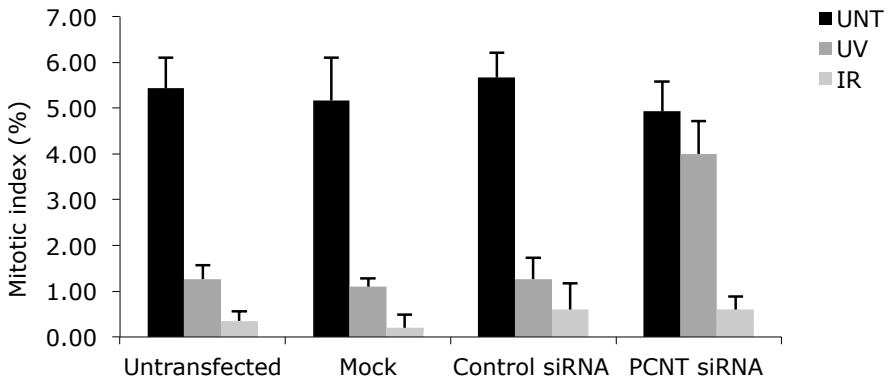

b)

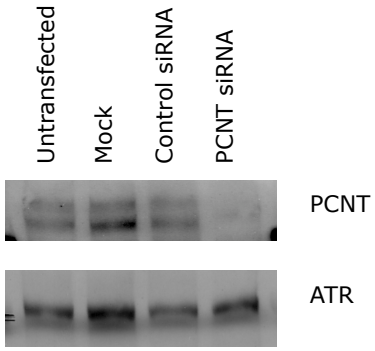

Figure 3.5 RNAi Depletion of PCNT in HeLa cells impairs ATR-dependent G2/M arrest

a) Hela cells were either untransfected, mock transfected (mock) or exposed to Control or PCNT siRNA oligonucleotides for 72hrs. Cells were then examined for G2/M arrest 2hrs after exposure to 5J/m^2 UV or 3 Gy IR. A decrease in the number of mitotic cells was taken as indicative of a G2/M arrest. Graph represents the mean of three independent experiments. Error bars represent the standard deviation.

b) Western blot confirming PCNT depletion. ATR was used as a loading control.

MDC1 and BRCA1 to the site of the damage (Fernandez-Capetillo *et al.*, 2003). The ability of PCNT mutated cells to phosphorylate H2AX following exposure to hydroxyurea was examined. This ATR-dependent phosphorylation was normal in patient cell lines, similar to wild-type controls and in contrast to ATR-Seckel cells (Figure 3.6). This indicates that ATR kinase is functional and able to phosphorylate a key upstream substrate in these cells.

3.2.6 Chk1 is phosphorylated normally in PCNT mutated cells

In order to further delineate at which point in the ATR signaling pathway PCNT could be functioning, the phosphorylation of Chk1 after UV irradiation was examined. Patient cells were assessed for their ability to phosphorylate Chk1 at ser317 after exposure to UV irradiation using western blotting and were shown to phosphorylate this key checkpoint kinase normally. PCNT depleted HeLa cells were then also examined, and Chk1 was again phosphorylated normally in the absence of PCNT (Figure 3.7). These results indicate that PCNT is dispensable for the phosphorylation of Chk1 at ser317 in the ATR-dependent response to UV irradiation.

3.2.7 Total Chk1 levels at the centrosome are reduced in PCNT mutated patient cell lines

As Chk1 has been shown to localize to the centrosomes of interphase cells (Krämer *et al.*, 2004b), and PCNT is known to recruit proteins to the centrosome (Diviani *et al.*, 2000), we speculated that PCNT might be required to anchor Chk1 to the centrosome.

PCNT mutated patient fibroblasts were examined for Chk1 levels at the centrosome using a previously characterised monoclonal antibody for total Chk1 (Krämer *et al.*, 2004b). Over 15% of cells in the PCNT mutated lines had a total absence of Chk1 signal, in contrast to below 5% of cells in WT and ATR-Seckel control cell lines (Figure 3.8). These results indicate a requirement for PCNT to localize Chk1 to the centrosome of these cells. This observation was subsequently published by Tibelius et al in 2009.

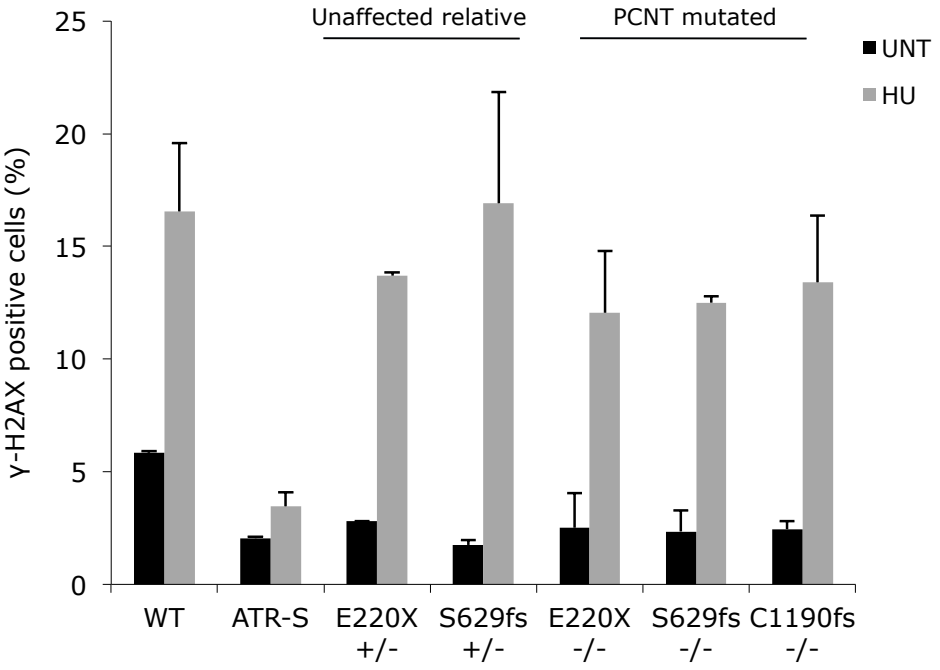

Figure 3.6 H2AX phosphorylation is normal in PCNT mutated cells.

WT, ATR-S, unaffected heterozygous relative and PCNT mutated cell lines were untreated (UNT) or exposed to 5mM Hydroxyurea (HU) and incubated at 37°C for 2hr. Phosphorylation of H2AX on ser139 was detected using immunofluoresence with specific antibodies. The percentage of cells staining positively for H2AX phosphorylation was determined for each cell line. The graph represents the mean of three independent experiments. Error bars represent the standard deviation.

a)

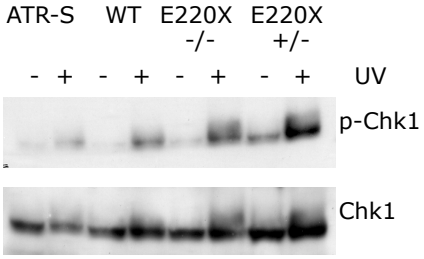

b)

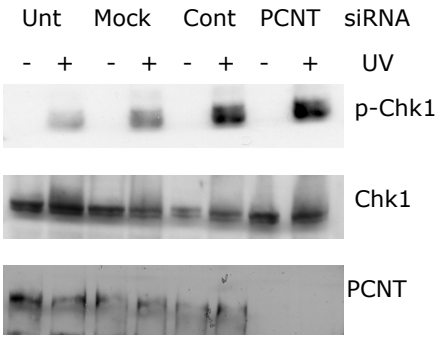

Figure 3.7 UV-induced Chk1 phosphorylation is normal in PCNT mutated patient cell lines and PCNT depleted lines.

a) Lymphoblastoid patient cell lines were treated with 5J/m^2 UV and cell pellets harvested 1hr later. Whole cell extracts were then resolved on a 8% SDS-PAGE and transferred onto a PVDF membrane. Membranes were then probed with an anti-phospho Chk1 (ser317) antibody. Total Chk1 levels were used as a loading control.

b) Hela cells were either untransfected (Unt), mock transfected (mock) or exposed to Control (Cont) or PCNT siRNA oligonucleotides for 72hrs. Cells were then treated with 10J/m2 UV and cell pellets harvested 1hr later. Whole cell extracts were then resolved on a 8% SDS-PAGE and transferred onto a PVDF membrane. Membranes were then probed with an anti-phospho Chk1 (ser317) antibody. Total Chk1 levels were used as a loading control. Extracts were immunoblotted for PCNT to confirm depletion.

a)

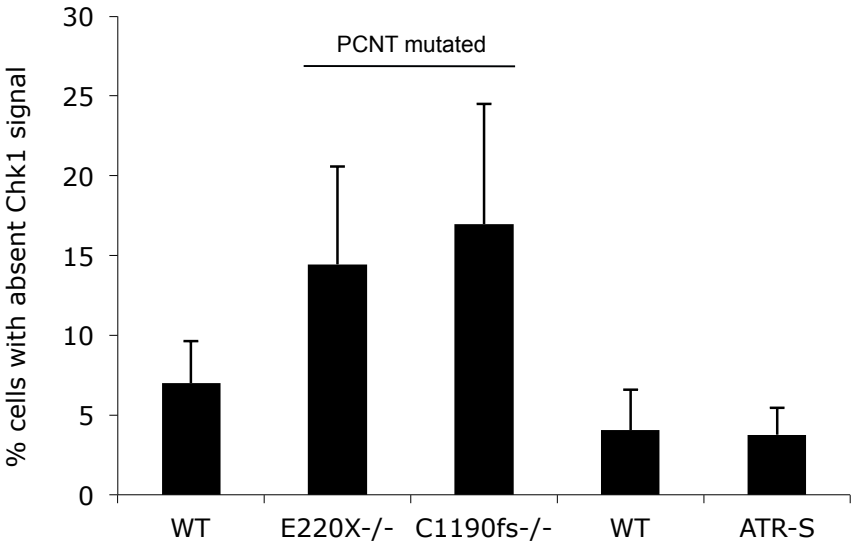

b)

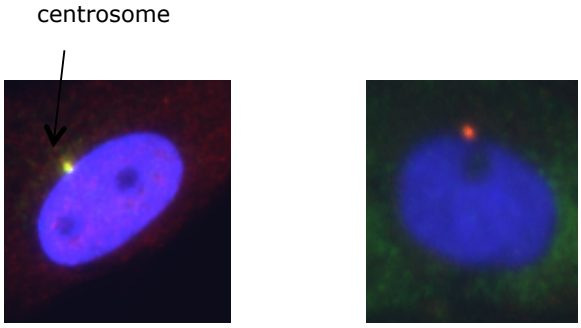

Figure 3.8 PCNT mutated cells display reduced levels of Chk1 at the centrosome

a) Patient primary fibroblasts (WT: 48BR, 1BR3; PCNT mutated: E220X-/-, C1190fs-/-; ATR Seckel: F02-98) were stained using techniques to identify the centrosomal pool of Chk1 (green). Centrosomes were identified by co-staining with a γ-tubulin marker (red). The percentage of cells with a total absence of Chk1 signal at the centrosome was evaluated. The graph represents the mean of three independent experiments. Error bars represent the standard deviation.

b) Immunoflurescent images showing 1BR3 control cell with Chk1 (green) and γ-tubulin (red) signal overlap and PCNT-Seckel cell with only red γ-tubulin signal.

3.2.8 Cdc25A degradation is normal in PCNT mutated cells

As Chk1 was phosphorylated normally in PCNT mutated cells, but its localization to the centrosome was compromised, downstream targets of Chk1 were further examined in order to establish whether Chk1 function is normal in these cells.

After damage Cdc25A is phosphorylated by Chk1 at multiple sites including serine 123 (Mailand *et al*., 2002). These phosphorylations target the phosphatase for ubiquitin-proteasome mediated degradation via the Skp1/Cul1/F-box (SCF) complex (Busino *et al*., 2003), resulting in a G2/M arrest. The stability of Cdc25A during the cell cycle or after damage can therefore be monitored by the addition of cycloheximide to culture media, in order to prevent new protein synthesis and thus visualize the degradation of the cellular pool of Cdc25A. This Chk1-dependent degradation process has previously been shown to be defective in ATR-Seckel cells (Alderton *et al*., 2006). PCNT mutated patient cells were examined for their ability to degrade the Cdc25A phosphatase during normal cellular growth. In WT and PCNT mutated lines, Cdc25A was degraded normally in contrast to ATR-Seckel cells (Figure 3.9). HeLa cells depleted of PCNT and treated with UV irradiation, also displayed normal degradation of Cdc25A, confirming the result observed in the patient cell line. This result indicates that Chk1 dependent degradation of Cdc25A is normal in the PCNT mutated lines and that this is therefore not a contributing factor in the loss of the G2/M checkpoint in these cells.

3.2.9 PCNT mutated cells display reduced levels of Cdc25B pS230 at the centrosome

The inhibitory phosphorylation of S230 on Cdc25B by Chk1 has been demonstrated to occur during normal cell growth (Löffler *et al*., 2006). The phosphorylation at ser230 was detected at the centrosome as well as in the cytoplasm and was demonstrated to inhibit the activity of Cdc25B, although the mechanism for this is unclear (Schmitt *et al*., 2006).

In order to assess if the reduced levels of Chk1 detected at the centrosome in PCNT mutated cells resulted in a reduction in the phosphorylation of a Chk1 target protein, the level of phosphorylated S230 Cdc25B present at the centrosomes was examined in PCNT mutated primary fibroblast cells using a previously characterised antibody (Schmitt *et al.*, 2006). The percentage of PCNT mutated cells with a total

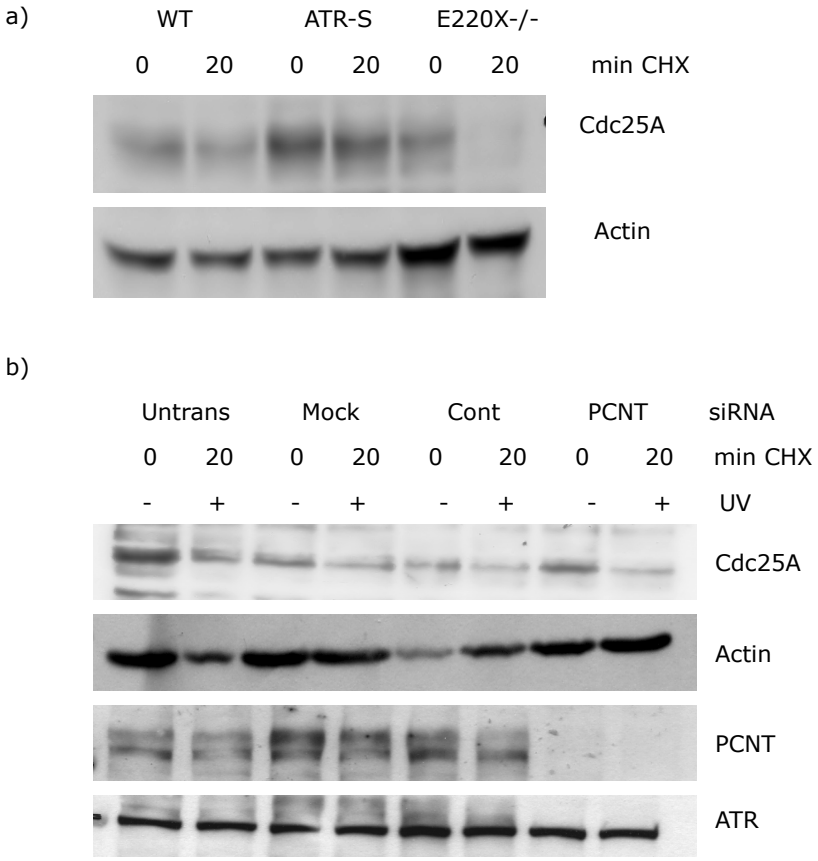

Figure 3.9 Cdc25A stability is normal in a PCNT mutated patient cell line and PCNT depleted line.

a) WT, ATR-Seckel (ATR-S) and PCNT mutated (E220X-/-) LBL lines were treated with 100 ug/mL Cycloheximide for 20 min and cell pellets were then harvested in the continued presence of cycloheximide. Whole cell extracts were resolved on a 10% SDS-PAGE gel and transferred onto PVDF membrane. Membranes were probed with antibodies against Cdc25A. Actin was used as a loading control.

b) Hela cells were either untransfected (Untrans), mock transfected (mock) or exposed to Control (Cont) or PCNT siRNA oligonucleotides for 72hrs. Cells were treated with 10J/m2 UV and then incubated in 100ug/mL cycloheximide for 20 min. Cell pellets were then harvested in the continued presence of cycloheximide. Whole cell extracts were resolved on a 10% SDS-PAGE gel and transferred onto nitrocellulose membrane. Membranes were probed with antibodies against Cdc25A. Actin was used as a loading control. Extracts were also immunoblotted to confirm PCNT depletion, using ATR as a loading control.

a)

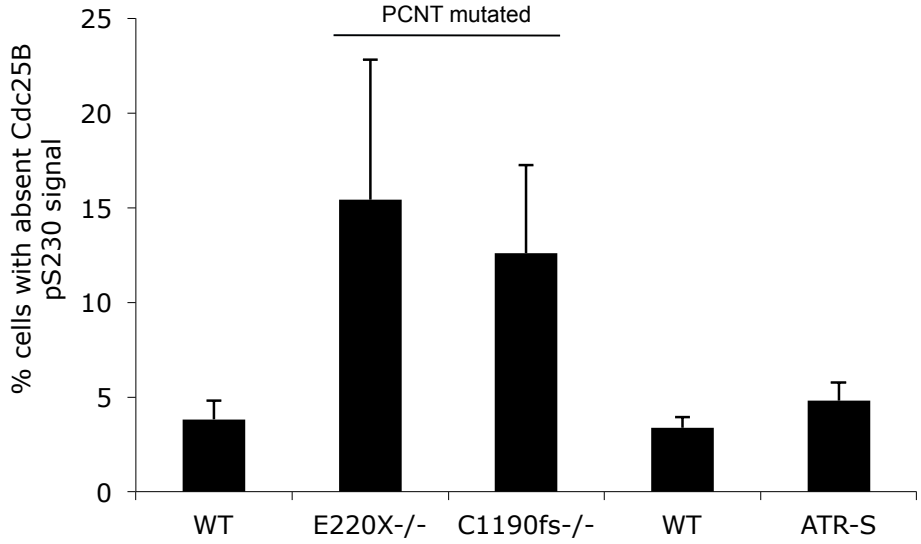

b)

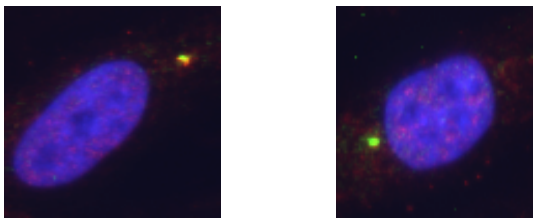

1BR3 control cell PCNT-mutated cell

Figure 3.10 PCNT mutated cells display reduced levels of Cdc25B pS230 at the centrosome

a) Patient primary fibroblasts fibroblasts (WT: 48BR, 1BR3; PCNT mutated: E220X-/-, C1190fs-/-; ATR Seckel: F02-98) were stained using techniques to identify the centrosomal pool of Cdc25B phosphoS230 (red). Centrosomes were identified by co-staining with a γ-tubulin marker (green). The percentage of cells with a total absence of Cdc25B pS230 signal at the centrosome was evaluated. The graph represents the mean of three independent experiments. Error bars represent the standard deviation.

b) Immunoflurescent images showing a 1BR3 control cell with Cdc25B pS230 (red) and γ-tubulin (green) signal overlap and a PCNT-mutated cell with only green γ-tubulin signal.

absence of pS230 Cdc25B at the centrosome was approximately 15% in contrast to less than 5 % in WT and ATR-Seckel control lines (Figure 3.10). This reduction in Cdc25B phosphorylation is comparable to the reduction of Chk1 signal observed at the centrosome (Figure 3.8). This result suggests that the reduction in Chk1 signal at the centrosome in these cells results in a reduction in the phosphorylation of its downstream target. The biological relevance of this is however unclear, as no changes to Cdc25B pS230 signal could be detected after exposing cells to DNA damage (data not shown) and this aspect of signalling warrants further investigation.

PCNT mutated primary fibroblast cells were then subjected to PCNT-siRNA treatment for 72 hours to deplete any residual protein remaining. These cells were then examined for pS230 Cdc25B levels at the centrosome using the same antibody as Figure 3.10. This treatment significantly increased the number of cells with a total absence of pS230 Cdc25B signal (Figure 3.11), confirming that loss of Chk1 from the centrosome due to PCNT depletion impacts on downstream phosphorylation events at the centrosome. This data was subsequently independently demonstrated and published by Tibelius and authors in 2009 (Tibelius *et al.*, 2009).

3.2.10 53BP1 foci formation in response to replicative stress is impaired in PCNT mutated cells

The formation of 53BP1 foci at sites of replication stress is known to be dependent on both Chk1 and ATR (Sengupta *et al.*, 2004, Tripathi *et al.*, 2008). ATR-Seckel cells have previously been shown to exhibit reduced 53BP1 foci formation following treatment with hydroxyurea (Alderton *et al.*, 2006). 53BP1 foci formation was therefore examined in PCNT mutated LBLs, following treatment with hydroxyurea to stall replication forks, as a readout for the activity of the Chk1 kinase, and also to determine if the lack of a key centrosomal protein has an impact on replication stress signalling.
Strikingly, both PCNT mutated and ATR-Seckel cells display impaired 53BP1 foci formation capability following replication stress (Figure 3.12). This is in contrast to wild-type and unaffected parental control lines where foci formed as expected. This result indicates that the signalling that is required to target 53BP1 to replication-stress induced damage is impaired in PCNT mutated cells. It further suggests that defects in centrosomal structure may impact upon events at the replication fork.

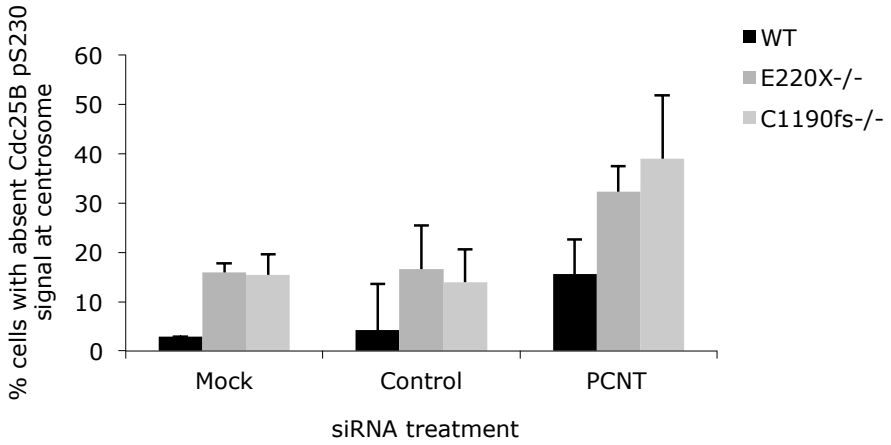

Figure 3.11 PCNT-mutated cells display a further reduction in levels of Cdc25B pS230 at the centrosome, following depletion of residual PCNT expression.

Residual PCNT expression in patient primary fibroblasts was depleted by 72hr PCNT siRNA incubation. Cells were stained using techniques to identify the centrosomal pool of Cdc25B phosphoS230 (red). Centrosomes were identified by co-staining with a γ-tubulin marker (green). The percentage of cells with a total absence of Cdc25B pS230 signal at the centrosome was evaluated. The graph represents the mean of two independent experiments. Error bars represent the standard deviation.

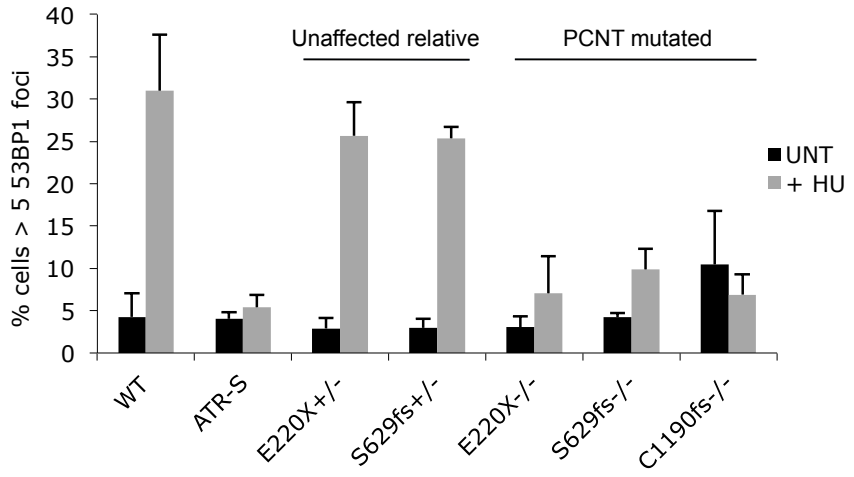

Figure 3.12 53BP1 foci formation in response to replication stress is impaired in PCNT-mutated cells.

WT, ATR-S, unaffected heterozygous relative and PCNT-mutated cell lines were exposed to 5mM hydroxyurea for 2hr. 53BP1 foci were examined using immunofluoresence with a specific antibody. The percentage of cells with more than 5 foci was determined for each cell line. The graph represents the mean of three independent experiments. Error bars represent the standard deviation.

3.2.11 Stalled replication forks in PCNT mutated cells recover normally after replication stress

The recovery of stalled replication forks after Aphidicolin-induced replication arrest is ATR and Chk1 dependent (Feijoo *et al.*, 2001, Stiff *et al.*, 2005). This recovery can be monitored by labelling replication forks with a deoxyuridine analogue, Chlorodeoxyuridine (CldU), stalling replication forks by treatment with aphidicolin and the labelling recovering forks with a second deoxyuridine analogue, Iodouridine (IdU). Each label can then be detected using immunofluoresence techniques and the percentage of recovered forks determined by scoring the overlay of red and green signal. ATR-Seckel cells have been shown to exhibit defects in the ability to recover from stalled replication forks (Stiff *et al.*, 2005), implicating ATR-dependent signalling in their stabilisation. PCNT mutated cells were therefore assessed for the ability to recover stalled replication forks following replication stress, particularly as 53BP1 foci formation in these cells was shown to be impaired (Figure 3.12). In wild-type and PCNT mutated cells, forks recovered from the replication block to the same extent, in contrast to ATR-Seckel cells which displayed defects in fork recovery (Figure 3.13). This result demonstrates that HU-induced stalled replication forks in PCNT mutated cells are stabilised normally. It is possible that the centrosomal pool of Chk1 is therefore not required for the functions of Chk1 that are related to replication. This result further suggests that the clinical features observed in these patients are not due to increased genomic instability due to the collapse of stalled replication forks.

3.3 DISCUSSION

In this chapter I have demonstrated that mutations in PCNT, a structural centrosomal protein, result in defects in ATR-dependent damage response signalling. I have shown that the mutations identified in *PCNT* result in some cellular phenotypes associated with Seckel syndrome such as supernumerary mitotic centrosomes and a UV-induced G2/M checkpoint defect. However, the upstream steps in the ATR signalling pathway, such as H2AX phosphorylation, are not defective in these cells. I have also shown that mutations in *PCNT* result in reduced Chk1 localisation to the centrosome, resulting in reduced Chk1 dependent phosphorylation of Cdc25B at the centrosome.

By studying PCNT mutated patient cell lines, a structural centrosomal protein has been implicated in the ATR-dependent DNA damage response for the first time. The

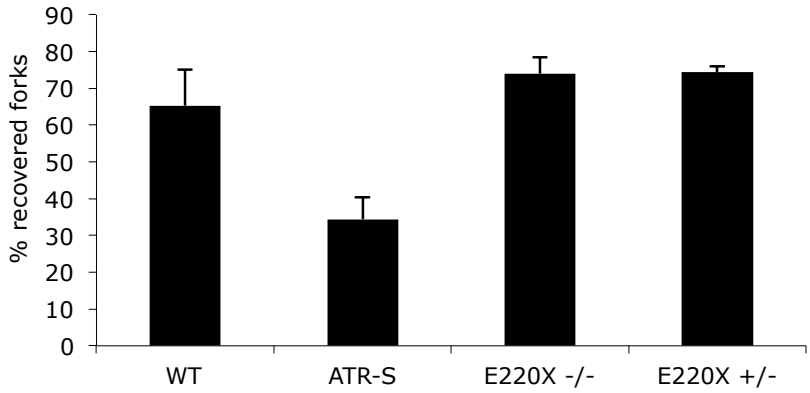

Figure 3.13 Recovery of stalled replication forks is normal in PCNT-mutated patient cell lines.

WT, ATR-S, E220X-/- and E220X+/- LBLs were labelled with CldU for 20 min to label replication forks. Cells were then pelleted, washed and incubated with APH for 2 hr to stall ongoing forks. Cells were pelleted and swollen in KCL plus IdU for ten minutes to allow fork reinitiation and IdU incorporation. Replication recovery is monitored by the overlap of CldU (red) and IdU (green) labelling. The graph represents the mean of three independent experiments. Error bars show the standard deviation.

evidence to link defects in ATR signalling with the clinical features displayed by the patients is compelling. Two genes have now been linked to Seckel syndrome by this laboratory: *ATR* and *PCNT*.

At the same time that Seckel sydrome patients harbouring *PCNT* mutations were reported, mutations in *PCNT* were also reported to cause another genetic syndrome Majewski Osteodysplastic Primordial Dwarfism Type II (MOPDII) (Rauch *et al.*, 2008a). These patients also present with microcephaly and extreme pre and post-natal growth retardation. Interestingly these patients are born with a proportionately normal head circumference, which then progresses to true microcephaly after birth (Hall *et al.*, 2004). Mental retardation in these patients appears to be less marked than in Seckel patients (Rauch *et al.*, 2008b). It will be interesting to obtain further MOPDII patient cell lines in order to analyse the ATR-dependent damage response in these patients and perform a genotype/phenotype analysis of PCNT mutations. This could determine whether all the PCNT mutations observed result in ATR-dependent damage response defects and whether this correlates with severity or frequency of clinical features in the patients.

Willems *et al*. (2010) undertook a retrospective analysis of clinical data and concluded that PCNT-Seckel patients had been mis-diagnosed and could actually be classified as MOPDII patients, based on clinical features such as skeletal abnormalities, facial features and intellectual disability (Willems *et al.*, 2010). However it appears that head circumference at birth was not examined in this study. As MOPDII is defined by proportionate head size at birth, progressing to a relative microcephaly after one year (Galasso *et al.*, 2008) is this clinical feature critical for distinction between the two disorders? A clinical distinction, if there is found to be one, could be argued as essential due to the extra surveillance required of MOPDII patients due to the occurrence of vascular problems, such as Moyamoya disease (Hall *et al.*, 2004). This is a disease leading to constriction of blood vessels in the brain that can lead to hemorrhage. These vascular problems can result in death. Perhaps further investigation of ATR-dependent signalling in these cell lines, as suggested above, could provide further insight and allow these disorders to be distinguished by the use of a diagnostic test.

There are currently two proposed models for the function of PCNT in cell division. The first model proposed to explain the function of PCNT is that the lack of this protein results in centrosome structural defects, resulting in defects in mitotic spindle assembly and orientation. Examination of MOPDII patients harbouring PCNT

patients revealed various mitotic defects, such as disorganized microtubules, incorrect orientation of metaphases and disorganized cytokinesis, in 71% of fibroblast cells (Rauch *et al.*, 2008b). The reduction of gamma-tubulin at the centrosome observed in our PCNT mutated patients (Griffith *et al.*, 2008) could also result in defective microtubule nucleation and disruption of mitotic spindle assembly (Takahashi *et al.*, 2002, Doxsey *et al.*, 2005a). Disruption of spindle assembly may result in the formation of multipolar spindles and therefore lead to aneuploidy or cell death during mitosis (Figure 3.14a). Interestingly, all cell lines examined with defects in ATR-dependent signaling show a nuclear fragmentation phenotype, postulated to be a result of premature mitotic entry due to failure of G2/M checkpoint activation in the presence of replication associated damage (Alderton *et al.*, 2004). Defects in spindle orientation were observed in PCNT-MOPDII patients (Rauch *et al.*, 2008b). PCNT depletion leads to loss of astral microtubules (Zimmerman *et al.*, 2004), which are known to be important for proper orientation of the spindle (Toyoshima and Nishida, 2007). Defects in spindle orientation can lead to a shift from symmetric division to asymmetric division, resulting in an overall decrease in the progenitor stem cell population (Cox *et al.*, 2006) (See Introduction).

The second model is that indicated from the data presented in this chapter. Reduction in the level of PCNT at the centrosome results in a defective ATR-dependent G2/M checkpoint response to UV damage (Figure 13.4b). This is due to reduced levels of Chk1 at the centrosome, which in normal circumstances is anchored there via an interaction with PCNT (Tibelius *et al.*, 2009). The lack of local Chk1 concentration at the centrosome contributes to a failure to inhibit the Cdc25-dependent activation of Cdk1-CyclinB1 complexes, and a resultant failure to inhibit unscheduled mitotic entry. This is demonstrated by reduced levels of Ser230 phospho Cdc25B at the centrosome observed in PCNT mutated patient cell lines. However, this phenotype is not observed in all cells, suggesting that this pathway may act redundantly, perhaps with the other Cdc25 proteins. The lack of a G2/M checkpoint in these cells may reduce the overall number of cells during embryonic development due to an increase in mitotic catastrophe, as damaged cells enter mitosis inappropriately. This increased cell death could potentially contribute to the short stature and microcephaly observed in the patients.

The role of PCNT in the formation of the primary cilia could also potentially contribute to the clinical features displayed by PCNT-Seckel patients. The primary cilium is anchored in place by a modified centrosome called the basal body

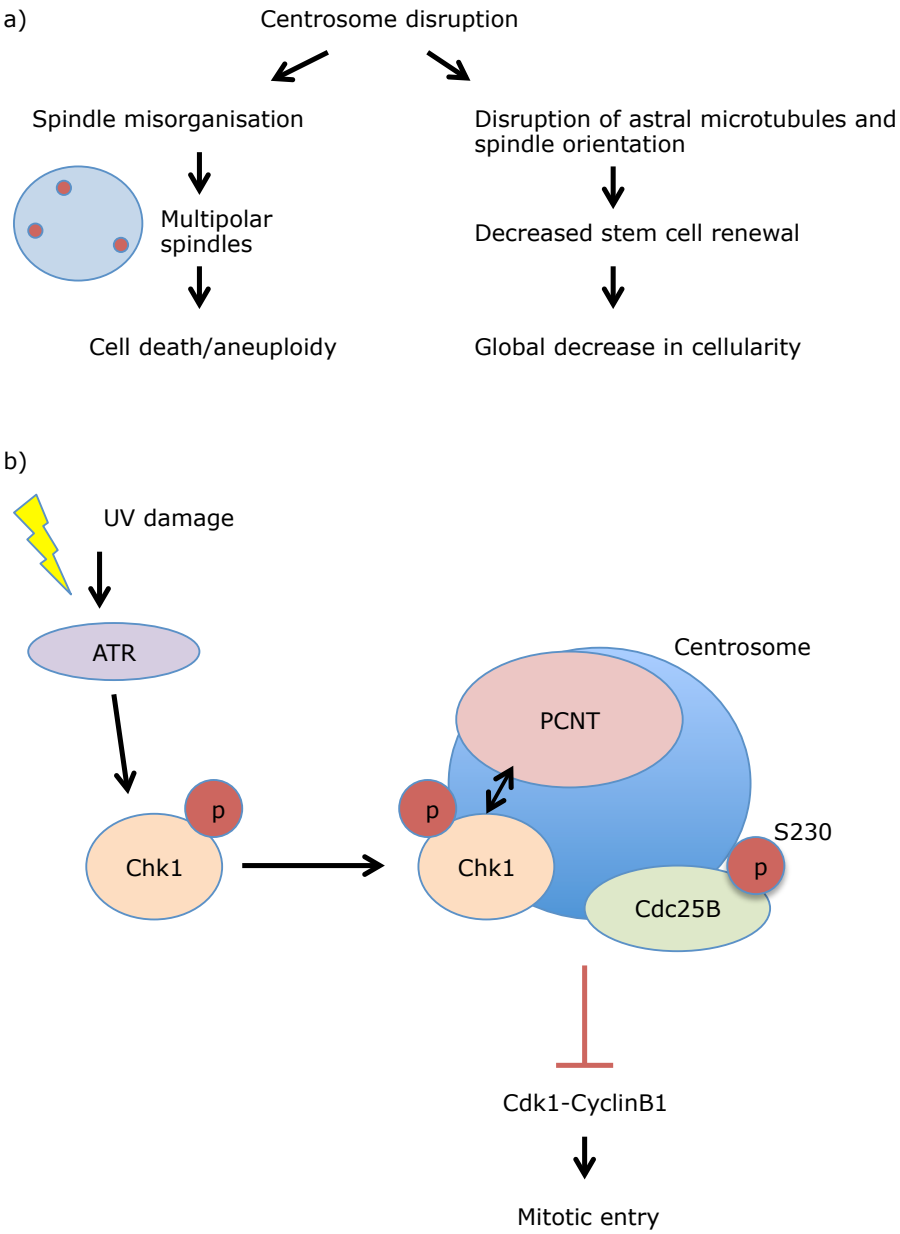

Figure 3.14 Models of PCNT function at the centrosome.

a) Centrosome defects result in spindle defects resulting in multipolar spindles and cell death. Loss of astral microtubules results in spindle orientation defects, increasing asymmetric cell division and resulting in reduced cell numbers. Figure adapted from Delaval and Doxsey, 2009.
b) UV or HU induced DNA damage results in activation of ATR kinase which then phosphorylates downstream targets such as Chk1. This phosphorylation is required for the accumulation of Chk1 at the centrosome. PCNT anchors Chk1 to the centrosome preventing activation of Cdk1-Cyclin B via the CDC25 proteins, and preventing progression into mitosis. In the absence of Chk1 at the centrosome cells do not arrest at the G2/M checkpoint.
Figure adapted from Griffith and Walker, Nature Genetics, 2008

(Duldulao *et al.*, 2010). The cilia have recently been shown to play important roles in major signaling pathways and also in brain development (Lee and Gleeson, 2011). There are some overlapping features between ciliopathies and Seckel syndrome such as skeletal defects, polydactyly and some degree of mental retardation. Recent data from our laboratory indicate that PCNT mutated patients do exhibit some defects in cilia formation and function (T. Stiff, data not shown). It appears that HU-induced stalled replication forks are stabilized effectively in PCNT mutated cells, however the deficiency in 53BP1 foci formation after HU treatment implies that the signalling cascade from stalled forks may be compromised. It is possible that 53BP1 is activated by Chk1 at the centrosome before relocating to stalled replication forks, or that an unknown factor is required for Chk1 to signal efficiently to 53BP1, and this may occur via the centrosome. 53BP1 depletion in human cells results in a partial defect in the intra S-phase checkpoint and a defect in the G2/M checkpoint response to low doses of IR (Jowsey *et al*., 2007). Although the G2/M checkpoint in the PCNT mutated lines was proficient after 3 Gy IR, an examination of the G2/M checkpoint response to low doses of irradiation could be informative to see if the defects in 53BP1 foci formation observed impacts upon these checkpoints.

Further investigation of the regulation of S-phase events is warranted in PCNT mutated cells. Interestingly, centrosomal localisation of Cyclin E has been shown to occur in mammalian cells from G1 through S phase (Matsumoto and Maller, 2004) and centrosomal localization of Cyclin E/Cdk2 is required for the initiation of DNA synthesis (Ferguson and Maller, 2010). These studies indicate that indeed the centrosome plays a role in the regulation of S phase events, as well as in G2/M checkpoint regulation. It is possible that PCNT is involved in the initiation of DNA replication or intra S-phase checkpoint induction. As ATR also has important roles in replication, which may impact on the clinical features observed in Seckel patients, an investigation of the role of PCNT in replication dynamics could be informative.

In conclusion, in this chapter I have shown that mutations in *PCNT*, in patients with microcephalic primordial dwarfism, result in defects in the ATR-dependent damage response. This provides the first description of a connection between a structural centrosomal protein and DNA damage response signaling.

CHAPTER FOUR

RESULTS II: Mutations in *ATRIP* cause Seckel Syndrome

4.1 INTRODUCTION

Seckel syndrome (SS) patient cell lines received by our laboratory are screened for ATR-dependent G2/M checkpoint arrest and supernumary mitotic centrosomes. Immunoblotting of proteins already established as genetic defects causal in Primordial Dwarfism syndromes, such as ATR and PCNT, is carried out. This enables the identification of patients with known genetic defects in order to help with genetic counselling of families, but also provides functional cellular data to aid with inclusion of patients in ongoing genetic mapping studies.

LBL cells were obtained from a consanguineous family of Saudi-Arabian origin with a clinical diagnosis of SS in one patient (CV1720) (Figure 4.1). The patient displayed severe microcephaly and short stature with a receding forehead and a prominent nose. There was some dental crowding with micrognathia. The patient had small ear lobes and fifth finger clinodactyly. A skeletal survey revealed a delayed bone age. An MRI scan of the brain showed generalised atrophy of the cerebrum. The pituitary was an unusual shape with an absent fossa (See Table 5). Extracts from LBL cell line CV1720 were therefore resolved by SDS-PAGE and immunoblotted with antibodies against ATR and PCNT. A decreased level of ATR was observed in the patient extracts compared to WT (Figure 4.2). Blots were reprobed to assess ATRIP protein levels, as ATR and ATRIP proteins are dependent on each other for stability (Cortez *et al.*, 2001). ATRIP protein levels were also markedly decreased in the patient extracts (Figure 4.2).

To determine if causal mutations in *ATR* or *ATRIP* could account for the decrease in protein level observed, samples were sent for sequencing to our collaborator in Japan, Tomoo Ogi. No mutations were detected in *ATR* in any of the samples tested. However, two mutations were identified in *ATRIP* that were also present as heterozygous changes in the parents (Figure 4.3).

	ATRIP-SS	ATR-S	27-4BI	19-8BI
Ethnicity	Gujarati-Indian (consanguineous)	Pakistani (consanguineous)	English	English
Birth. **OFC (cm)** **Wgt (Kg)** **Hgt (cm)**	 27.1 2.06 NR	 24 *(-8SD)* 1.1 *(-3SD)* NR	 NR 1.15 36	 24.2 0.77 NR
Age. **OFC** **Wgt Hgt**	**14mts** -9SD -5SD -5SD	**9yrs** -12SD -3.3SD NR	**20mts** -10SD -8SD -8SD	**4.5yrs** -10SD -7SD -8SD
Face	Micrognathia, receding forehead, prominent nose.	Micrognathia, receding forehead, prominent nose.	Micrognathia, prominent nose, hypoplastic alae nasi, low set columella, short palpebral fissures.	Micrognathia, blepharophimosis, short palpebral fissures. High anterior hairline.
Teeth	Dental crowding.	Dental crowding and malocclution.	4 teeth at 20 months.	Dental crowding.
Ears	Small lobes.	Posteriorly rotated with absent lobes.	Small, round, low set with poorly formed antihelix tragus & antitragus. Absent lobes.	Small ears with absent lobes
Hands	Bilateral 5th finger clinodactyly.	Multiple ivory epiphysis.	Small, tapering fingers.	Bilateral 5th finger clinodactyly. 5th metacarpels appear short.
Skeletal Survey	Delayed bone age (wrist & hips), symmetric dwarfism.	Microcrania with fuse sutures. Mild thoracic kyphosis. Ribs angulated posteriorly. Narrow iliac blades, cox valga and minor subluxation of the hips.	NA. Symmetric dwarfism. Small patellae. No joint hypermobility or kyphoscoliosis.	NA. Symmetric dwarfism. Small patella. Marked hip & shoulder flexibility. No kyphosis.
Endocrinology	Normal IGF1, TFT, LH, FSH & cortisol.	NA	NA	NA
MRI	14mts:generalised cerebral atrophy. Delayed myelination in the anterior limb of the internal capsule. Pituitary present but of unusual shape with absent fossa.	NA	NA	2yrs: abnormal gyration in posterior aspect of the cingulated gyrus extending into the parietal occipital region. Hypoplastic corpus collasum.
Other	NR	Developmental delay. Walked at 7yrs.	NR	Developmental delay. Sat at 15mts, walked at 3yrs 10mts. High pitched voice, asthma, multiple chest infections, feeding difficulties-reflux (gastrostomy fed).

NR; not recorded. NA; not assessed.

Table 5. ATR-ATRIP Seckel clinical features. Adapted from Ogi et al, 2012.

a)

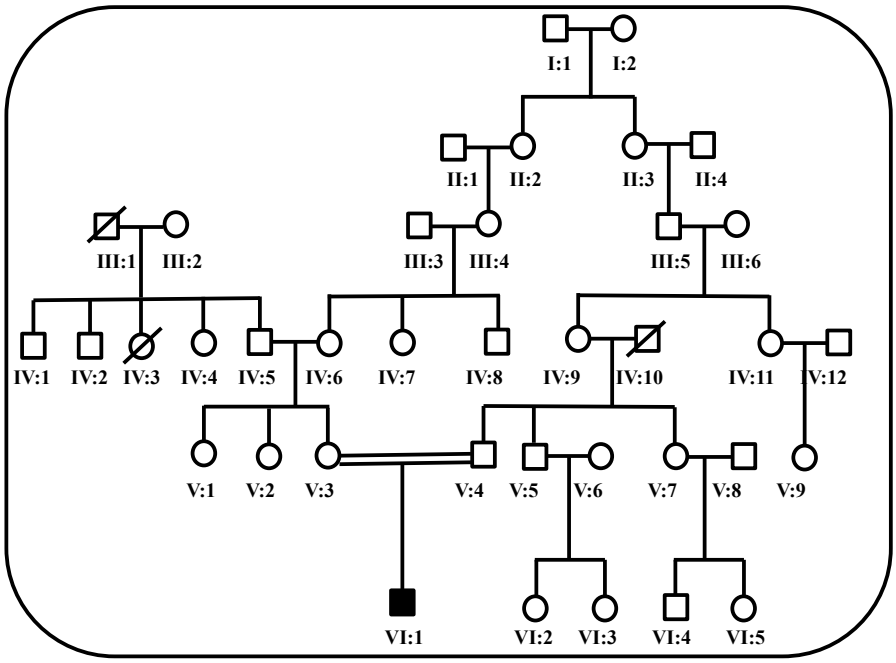

b)

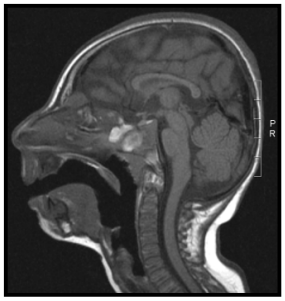

Figure 4.1 ATRIP patient pedigree and features

a) Pedigree of ATRIP family
b) ATRIP-S patient brain scan showing generalised cerebral atrophy

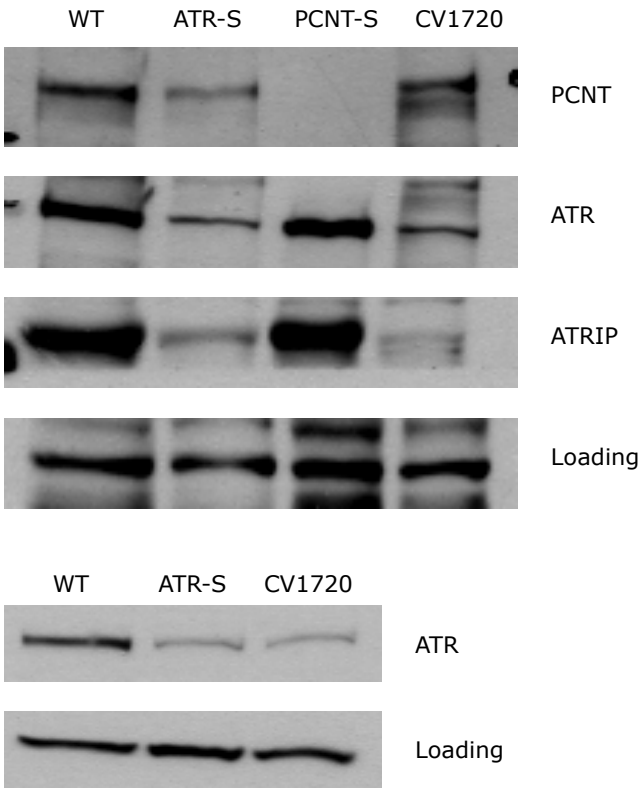

Figure 4.2 ATRIP and ATR expression is reduced in CV1720 patient cells

Levels of ATRIP and ATR expression were examined by resolving whole cell extracts from WT, ATR-S and CV1720 (ATRIP-S) cell lines on 6-8% SDS-PAGE gels followed by transfer onto nitrocellulose membranes. Membranes were then probed with a ATR or ATRIP antibody. The loading control was taken from a non-specific band.

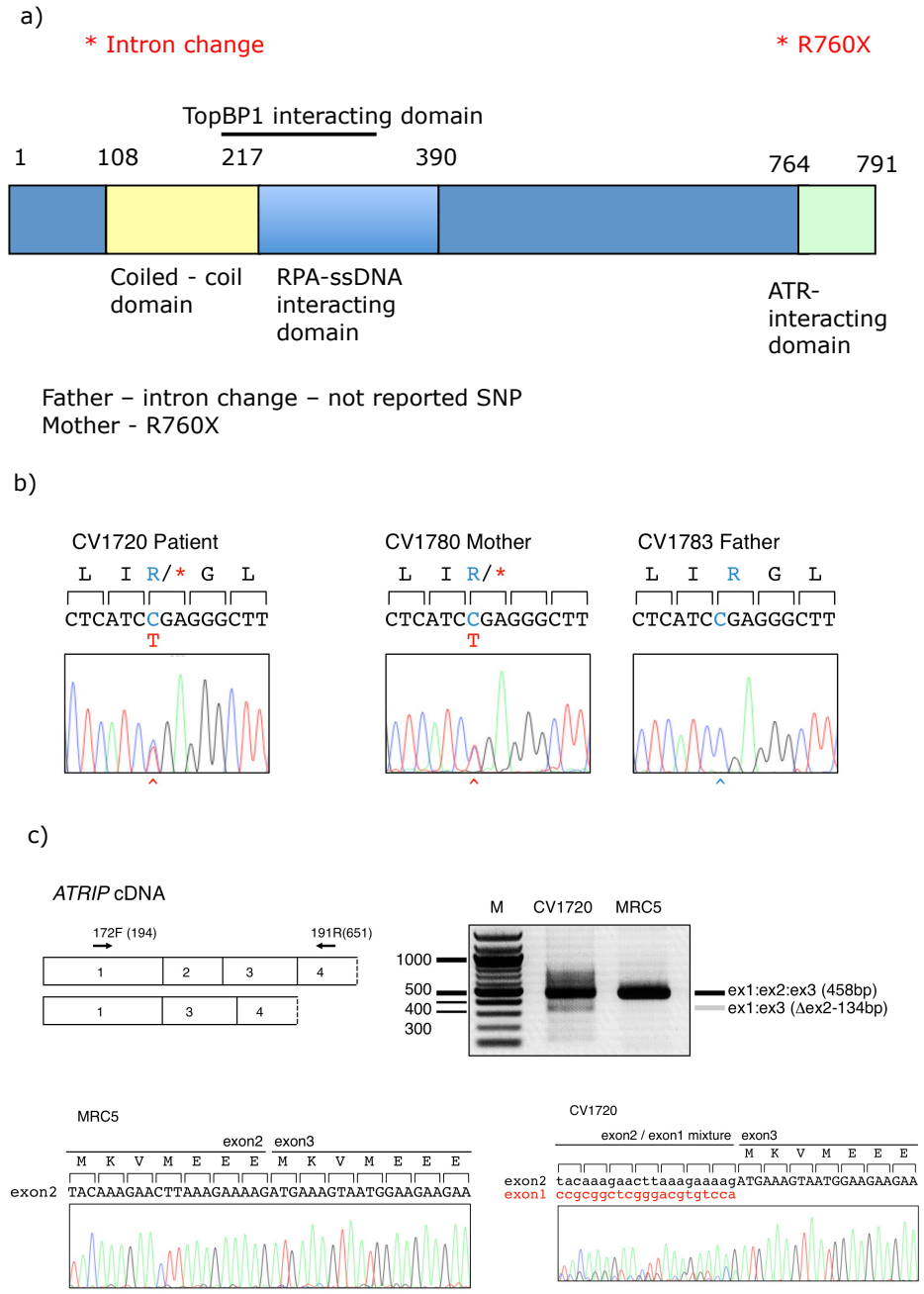

Figure 4.3 ATRIP protein schematic and mutations identified

a) Schematic of ATRIP protein showing positions of mutations identified in CV1720 patient.
b) C2278T mutation present in patient and mother only.
c) Exon 1 to 3 RT-PCR showing two PCR products in CV1720 patient. Sequence of smaller fragment showing exon 2 loss in CV1720 patient.

Sequencing of genomic DNA identified a heterozygous point mutation in exon 12, C2278T (Figure 4.3b). This change produced a stop codon, predicted to result in a truncated protein R760X. This mutation was detected as a heterozygous change in the mother but was not present in the father.

To investigate the impact of this mutational change, qPCR was performed using allele specific primers. Primer pairs P1 and P3C were used to selectively amplify the WT C2278 allele, whilst primer pairs P2 and P3C were designed to amplify only the mutated C2278T allele. The WT qPCR product was detected in all samples whilst the C2278T product was detected only in the patient and the mother. The WT and C2278T mRNA products were expressed at near equal levels in the mother, indicating that nonsense mediated decay (NMD) of the mutant C2278T transcript does not occur (Figure 4.4a).

Sequencing of introns 1 and 2 from the family material identified a novel mutational change in intron 2. This change was positioned 13bp from the intron-exon boundary of exon 2 and was present in the patient and the father but not the mother. The change was not a reported SNP. Therefore further investigation of the impact of this mutational change was performed. Both laboratories carried out RT-PCR analysis of the exon 1 to 3 region of *ATRIP*. Amplification of exons 1 to 3 produced a smeared PCR product with two distinct size products, a 458bp product that corresponds to full length exon1-3, and a smaller fragment of 325bp (Figure 4.3c and data not shown). Sequencing of these RT-PCR products revealed that the smaller product contained exon 1 directly spliced to exon 3 but missing exon 2. This suggested that mis-splicing is occurring in the patient cells, possibly due to the intron change detected.

The mutation leading to the production of a mis-spliced RT-PCR product in the patient results in the deletion of exon 2 of *ATRIP*. Exon 2 codes for a region of ATRIP including amino acids 108 to 137 of the coiled-coil domain. This domain has been shown to be important for oligomerisation of ATRIP and also to be required for Chk1 phosphorylation (Ball and Cortez, 2005). If the mutant mRNA is translated into a protein with a defective coiled-coil domain then this could impact on protein function.

Further primers were designed to the exon 2/3 boundary (P4) and within exon 3 (P6C) to selectively amplify the correctly spliced mRNA. A primer pair with one primer designed to the exon 1/3 boundary (P5) and one within exon 3 (P6C, as

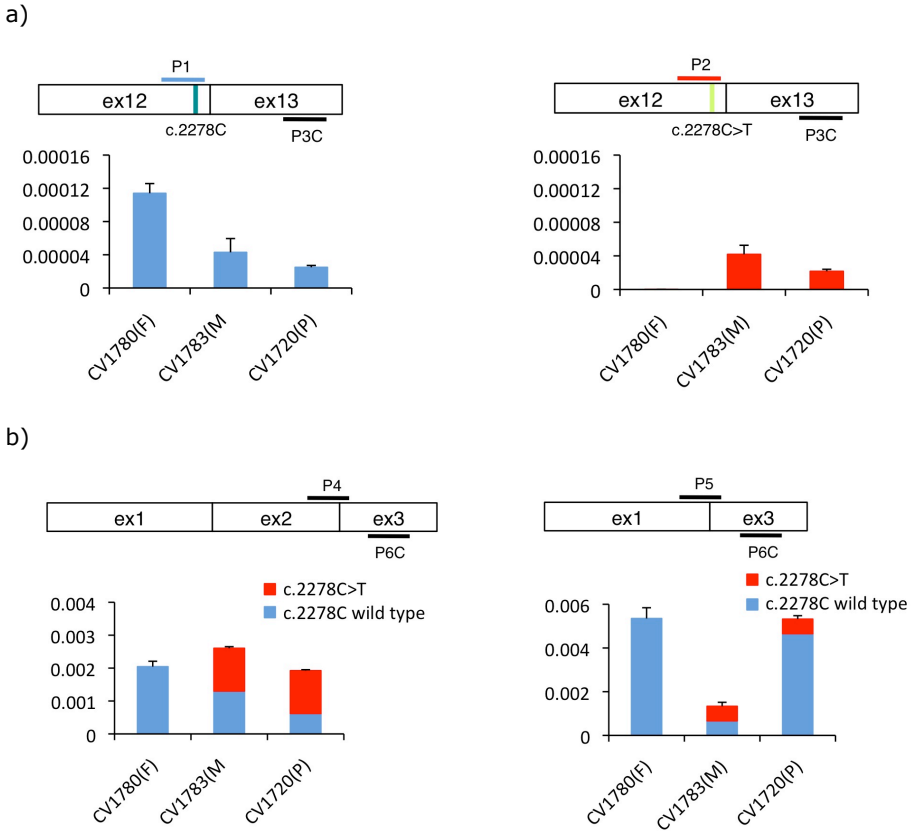

Figure 4.4 Quantitative PCR analysis of ATRIP mutant alleles

a) Selective quantitative amplification of the WT or 2278C>T ATRIP alleles. Primers located in ATRIP exon 12 and 13 were designed to selectively amplify the WT (c.2278C) (P1 and P3C) versus the mutated (c.2278C>T) (P2 and P3C) alleles. The WT PCR product is shown in blue and the c.2278C>T PCR product in red. The exon 12 mutated allele is only observed in the patient and mother cDNA whilst the WT allele is observed in the patient, mother and father cDNA although the level is reduced in the patient and mother.

b) qRT-PCR analysis of ATRIP splicing variants from patient CV1720 and parental cells. qRT-PCR analysis of the level of the normally spliced (encompassing exons 1- 2-3) and the aberrantly spliced (Δexon2) ATRIP cDNA in the patient and parent cells. PCR primers were designed at the exon2-exon3 or exon1-exon3 boundaries to selectively amplify the splicing variants. Transcripts from HPRT1 were used as a quantification control. The correctly spliced transcript from the paternal allele of the patient (wild type c.2278C, blue fraction in the cumulative bar labelled, 'patient', at the left panel) was estimated to be ~25% of the normal level.

Figure and legend from Tomoo Ogi.

above) were used to selectively amplify the mis-spliced mRNA product. Similar levels of correctly spliced mRNA were detected in all samples, however, the mis-spliced mRNA product was more abundant in both the patient and the father (Figure 4.4b).

Further qPCR experiments were conducted to clarify if the mis-spliced mRNA product, predicted to generate an out of frame cDNA, is subject to NMD. Fluorescent Cycleave PCR probes were designed and qPCR conducted in the absence or presence of Puromycin, an antibiotic that prevents NMD. Allele specific probes were designed to distinguish between the WT and the C2278T alleles (Figure 4.5). In the mother the WT and C2278T allele products were detected at equal levels, regardless of the presence or absence of Puromycin. This further confirms that the C2278T allele product is not subject to NMD. In the patient, the WT allele product was reduced compared to the mutant allele in the absence of puromycin but was detected at equal levels in the presence of puromycin. These results indicate that the mRNA from the paternal allele in the patient is subject to NMD, due to aberrant splicing. No changes in either allele product could be detected in the father, likely due to any changes being below the threshold of detection for this assay.

All of the above work on mutational analysis was conducted by Tomoo Ogi.

ATRIP, a protein of approximately 85 kDa, was identified in ATR immunoprecipitates and ATR and ATRIP were found to be mutually dependent on each other for their stability (Cortez *et al.*, 2001). It was proposed that ATR/ATRIP exists in cells in a stable complex and that depletion of ATRIP produced the same G2/M checkpoint defects as observed with depletion of ATR. It was also shown that ATR could phosphorylate ATRIP (Cortez *et al.*, 2001). Two splice variants of the protein were detected. A splice variant resulting in loss of exon 11 was subsequently shown to be expressed at levels of less than 5% of the full length mRNA, and the expressed protein is unable to bind to ATR and therefore is unlikely to have any biological function (Ball *et al.*, 2005).

When ssDNA is created in the cell, such as by damage or stalling of replication forks, the single stranded region is swiftly coated with RPA. Recruitment of ATR/ATRIP to ssDNA is dependent on an interaction between RPA and ATRIP (Zou and Elledge, 2003). The region of ATRIP that functions as an RPA-ssDNA binding domain includes the first 107 amino acids. This domain was shown to be essential for localising ATRIP at ssDNA sites within the nucleus as ATRIP lacking this domain

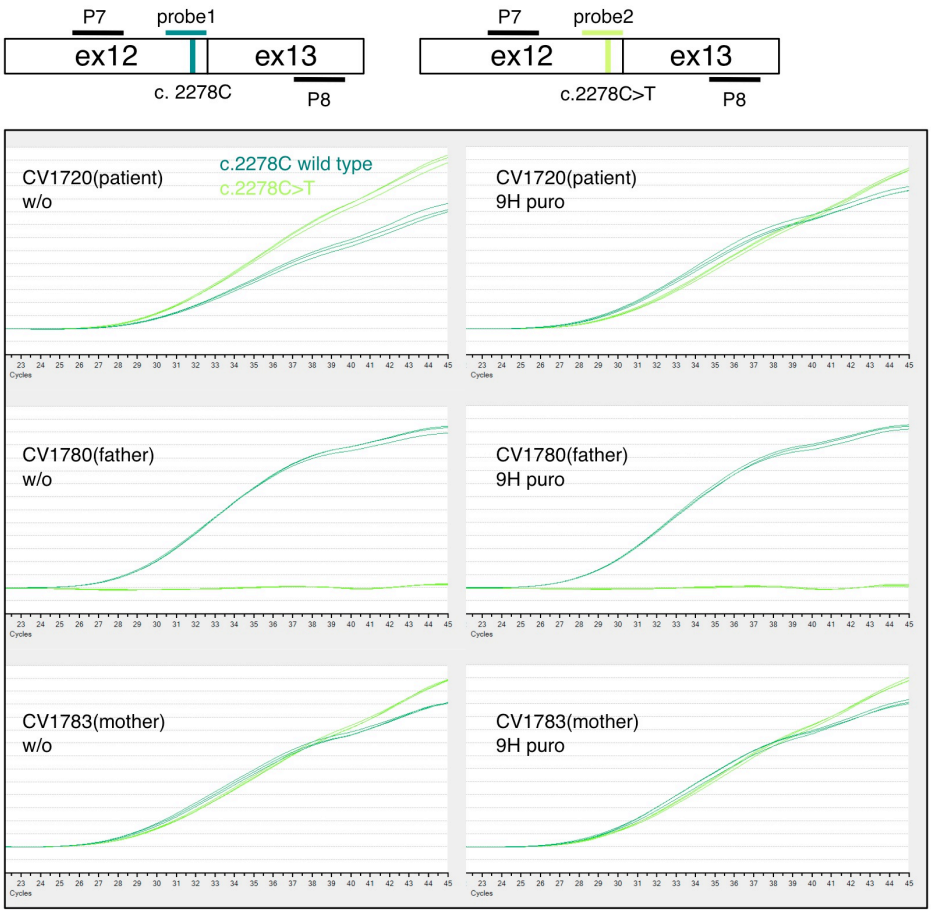

Figure 4.5 The mis-spliced paternal allele is subject to nonsense mediated mRNA decay (NMD).

Cycleave-qPCR confirmed that the ATRIP c.2278C>T mutant allele was expressed exclusively in the patient and the mother. The ATRIP exon12-13 fragment was amplified with a PCR primers P7/P8 as shown in the figure. A set of fluorescent probes were used to distinguish the WT versus c.2278C>T allele (probe1 and probe2, respectively). In the patient, the paternal mRNA transcript level (emerald lines) is low because of NMD (top left). Puromycin treatment eliminated the NMD and the paternal transcript level returned to the normal level.

Figure and legend from Tomoo Ogi

was mainly confined to the cytoplasm. However, no nuclear localization signal has been identified in this domain (Ball *et al.*, 2005). Further investigation revealed that there are multiple sites within ATRIP that are able to interact with RPA-ssDNA. The region containing amino acids 218 to 390 was also mapped as an RPA-ssDNA interacting domain (Namiki and Zou, 2006).
ATRIP oligomerises in cells independently of ATR and this oligomerisation is mediated by the coiled-coil domain of ATRIP from amino acid 108 to 217 (Ball and Cortez, 2005).The oligomerisation of ATRIP is required for the formation of stable ATR/ATRIP complexes and the coiled coil domain is essential for effective ATR dependent Chk1 phosphorylation (Ball and Cortez, 2005). An ATR-interacting domain was also determined to reside at the C-terminal region of ATRIP (Ball *et al.*, 2005). When ATRIP mutants lacking the C-terminal domain were constructed and expressed in cells, recruitment of ATR to damage was prevented and defects in ATR-dependent phosphorylation of Chk1 were observed (Falck *et al.*, 2005). These results indicated that in order for ATR to be recruited to ssDNA, a functional interaction between ATR and ATRIP is required (Falck *et al.*, 2005). As similar motifs exist in ATM and DNA-PK, facilitating their interaction with Nbs1 and Ku respectively, it was postulated that this conserved domain serves as a 'kinase-docking module' that is required for a more stable interaction between these binding partners with multiple interaction sites (Falck *et al.*, 2005).

Topoisomerase binding protein 1 (TopBP1) stimulates ATR kinase activity through binding to the ATR/ATRIP complex. This binding is dependent on ATRIP (Kumagai *et al.*, 2006). The region on ATRIP that interacts with TopBP1 was identified as amino acids 203-348, adjacent to the coiled coil domain (Mordes *et al.*, 2008). This ATRIP 'regulatory region' is conserved in the yeast protein Ddc2 and mutations within this region result in sensitivity to replication stress in both yeast and human cells (Mordes *et al.*, 2008).

ATRIP also interacts with minichromosome maintenance 7 (MCM7) possibly facilitating the phosphorylation of MCM2 by ATR (Cortez *et al.*, 2004). This function of ATRIP could be important for targeting of ATR to replication fork associated damage.

ATRIP is phosphorylated by Cdk2 on Serine 224, but this phosphorylation is not required for ATRIP to bind to RPA, localise to damage sites or bind to ATR. However, phosphorylation of ATRIP S224 is required for effective G2/M checkpoint responses at later times following exposure to IR. (Myers *et al.*, 2007).

In yeast Rad26-ATRIP, an important function for a conserved c-terminal motif was recently uncovered. Herring and colleagues discovered that this motif is required for a microtubule-associated damage response but not an overall damage response. Loss of Rad26-ATRIP resulted in sensitivity to microtubule toxins, segregation errors and a failure to delay mitotic entry in the presence of microtubule damage (Herring et al., 2010).

The aim of this chapter was to identify the genetic defect in CV1720 patient cells. Once the mutational changes in *ATRIP* were identified, an important aim was to examine how these mutational changes impact on protein expression, function and the ATR-dependent damage response.

4.2 RESULTS

4.2.1 Timeless and hCLK2 protein levels are normal in CV1720 patient cell line

Timeless protein and hCLK2 protein levels in CV1720 LBL extracts were examined by immunoblotting to determine if a reduction in either of these protein levels could be a cause of the reduced ATR/ATRIP protein levels detected in this cell line. Timeless is a circadian protein that interacts with ATR/ATRIP and depletion of Timeless by siRNA results in defects in Chk1 phosphorylation (Unsal-Kaçmaz *et al.*, 2005). HCLK2 is another circadian protein that interacts with ATR/ATRIP and TopBP1 (Collis *et al.*, 2007, Rendtlew Danielsen *et al.*, 2009). It was reported that this interaction helps to stabilise ATR protein. Neither protein was reduced by a significant amount in CV1720 LBL extracts (Figure 4.6) therefore they were considered not likely to be mutated and were excluded from further analysis.

4.2.2 Further assessment of ATR and ATRIP protein levels in CV1720 and parental cell lines

In order to further assess the extent of protein depletion in CV1720 LBLs, extracts were prepared from WT and CV1720 cells and loaded in increasing amounts on SDS-PAGE gels for immunoblotting analysis. When 100μg of extract was loaded, an amount at which the WT protein level was saturated, minimal ATRIP protein could be detected in the patient (Figure 4.7a). Increasing the amount of extract loaded

a)

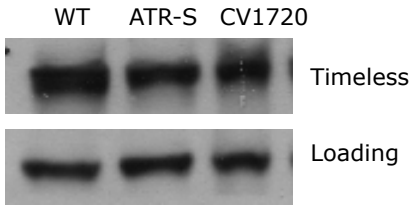

b)

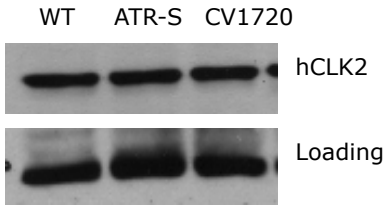

Figure 4.6 Timeless and hCLK2 expression are normal in CV1720 patient cells

Levels of Timeless and hCLK2 protein expression were examined by resolving whole cell extracts from WT, ATR-S and CV1720 (ATRIP-S) LBL cell lines on 8% SDS-PAGE gels followed by transfer onto nitrocellulose membranes. Membranes were then probed with a Timeless or hCLK2 antibody. The loading control used was a non-specific band.

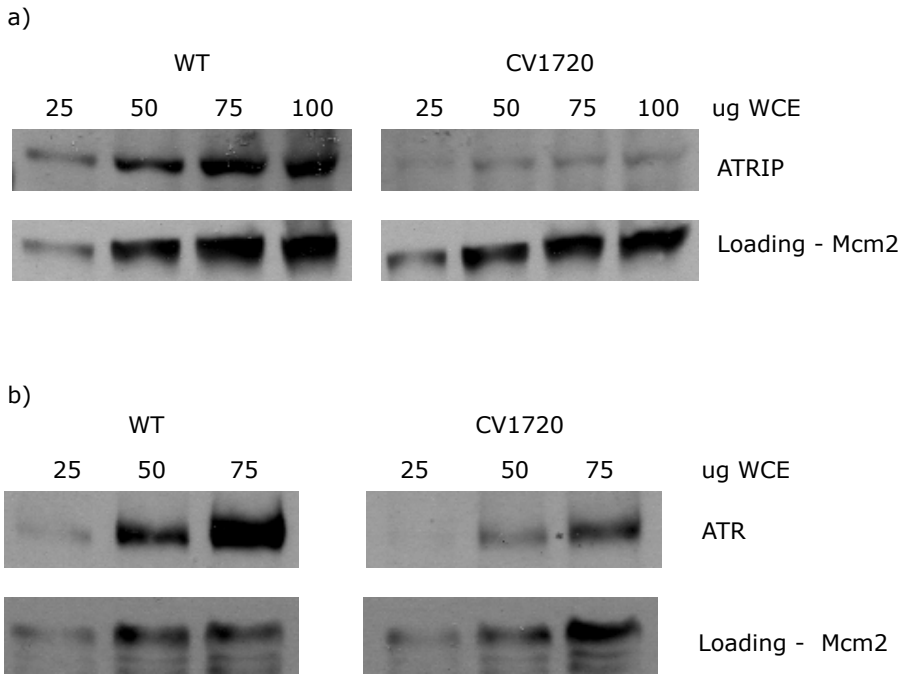

Figure 4.7 ATRIP and ATR protein levels are dramatically reduced in CV1720 patient cells

Levels of ATRIP and ATR expression were examined by resolving increasing amounts of whole cell extracts from WT and CV1720 (ATRIP-S) LBL cell lines on 6- 8% SDS-PAGE gels followed by transfer onto nitrocellulose membranes. Membranes were then probed with either ATR or ATRIP antibody. The loading control used was Mcm2.

corresponded with increasing levels of ATR protein in the patient, although the levels were still much reduced compared to WT (Figure 4.7b). When parent cell lines were examined, both ATR and ATRIP levels were reduced by approximately 50% in each parent (Figure 4.8). This corresponds with the genetic analysis of heterozygous mutations in each parent and suggests that each mutation impacts on ATRIP stability, and therefore also ATR stability. Quantification of ATRIP and ATR protein levels from at least three independent immunoblotting experiments is shown in Figure 4.9.

4.2.3 Assessment of the ATR-dependent DNA damage response in CV1720 patient cells

Due to the observed reduction in ATR protein levels, CV1720 patient cells were assessed for the response to damage induced by UV or HU using several assays to examine ATR-dependent DNA damage responses. The phosphorylation of H2AX is a key upstream step in both the ATR and ATM signalling pathways and is important for the recruitment of proteins such as 53BP1, MDC1 and BRCA1 to the site of the damage (Fernandez-Capetillo *et al.*, 2003). The phosphorylation of H2AX after UV irradiation or HU treatment is ATR-dependent (Ward and Chen, 2001). The formation of 53BP1 foci at sites of replication stress is known to be dependent on both Chk1 and ATR (Sengupta *et al.*, 2004, Tripathi *et al.*, 2008). ATR-Seckel cells have previously been shown to exhibit reduced H2AX phosphorylation and reduced 53BP1 foci formation following treatment with hydroxyurea (Alderton *et al*., 2006). Therefore these ATR-dependent phosphorylation responses were examined in CV1720 patient cells. H2AX phosphorylation and 53BP1 foci formation responses were defective in CV1720 cells, similar to ATR-S cells and in contrast to the WT. These results demonstrate that ATR is not functional in this cell line and is not able to phosphorylate key target proteins (Figure 4.10).

Supernumary mitotic centrosomes are also a common phenotype that we have observed in SS cell lines (Alderton *et al.*, 2004). CV1720 patient cells were therefore examined and found to display supernumary mitotic centrosomes, to a similar level to the ATR-S cells (Figure 4.10).

ATR-dependent modification of target proteins was also compromised in CV1720 cells with reduced phosphorylation of Chk1 following exposure to UV (Figure 4.11a,b) and reduced monoubiquitination of FANCD2 following exposure to HU (Figure 4.11c).

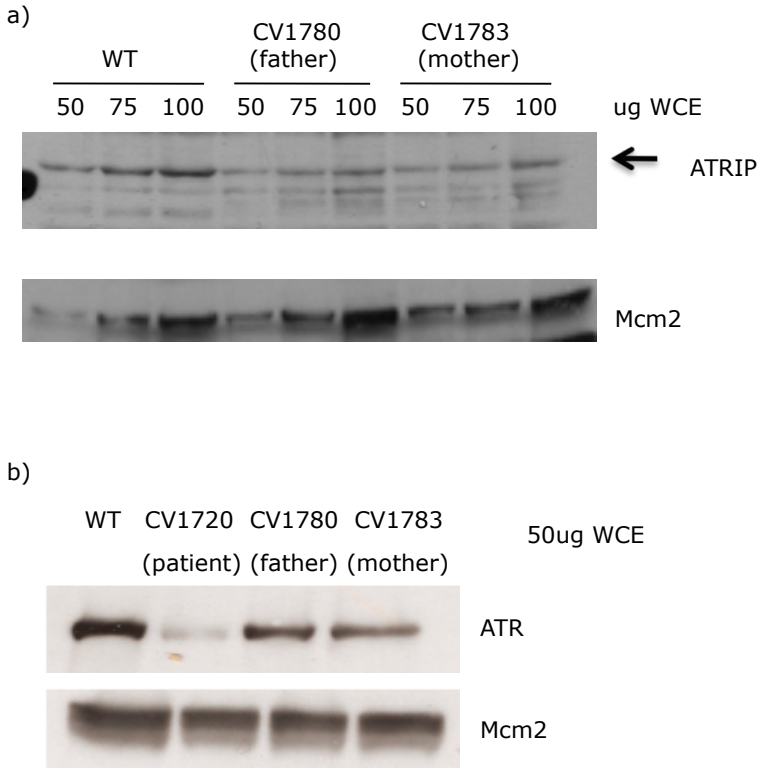

Figure 4.8 ATRIP and ATR protein levels are reduced in CV1780 and CV1783 heterozygous parental cells

a) Levels of ATRIP protein expression were examined by resolving increasing amounts of whole cell extracts from WT and CV1720 parental LBL cell lines (CV1780 and CV1783) on 8% SDS-PAGE gel followed by transfer onto nitrocellulose membrane. Membranes were then probed with an ATRIP antibody. The loading control used was Mcm2.
b) Levels of ATR protein expression were examined by resolving whole cell extracts from WT, CV1720 (ATRIP-S) and CV1720 parental (CV1780;CV1783) LBL cell lines on 6& SDS-PAGE gel followed by transfer onto nitrocellulose membrane. Membranes were then probed with ATR antibody using Mcm2 as a loading control.

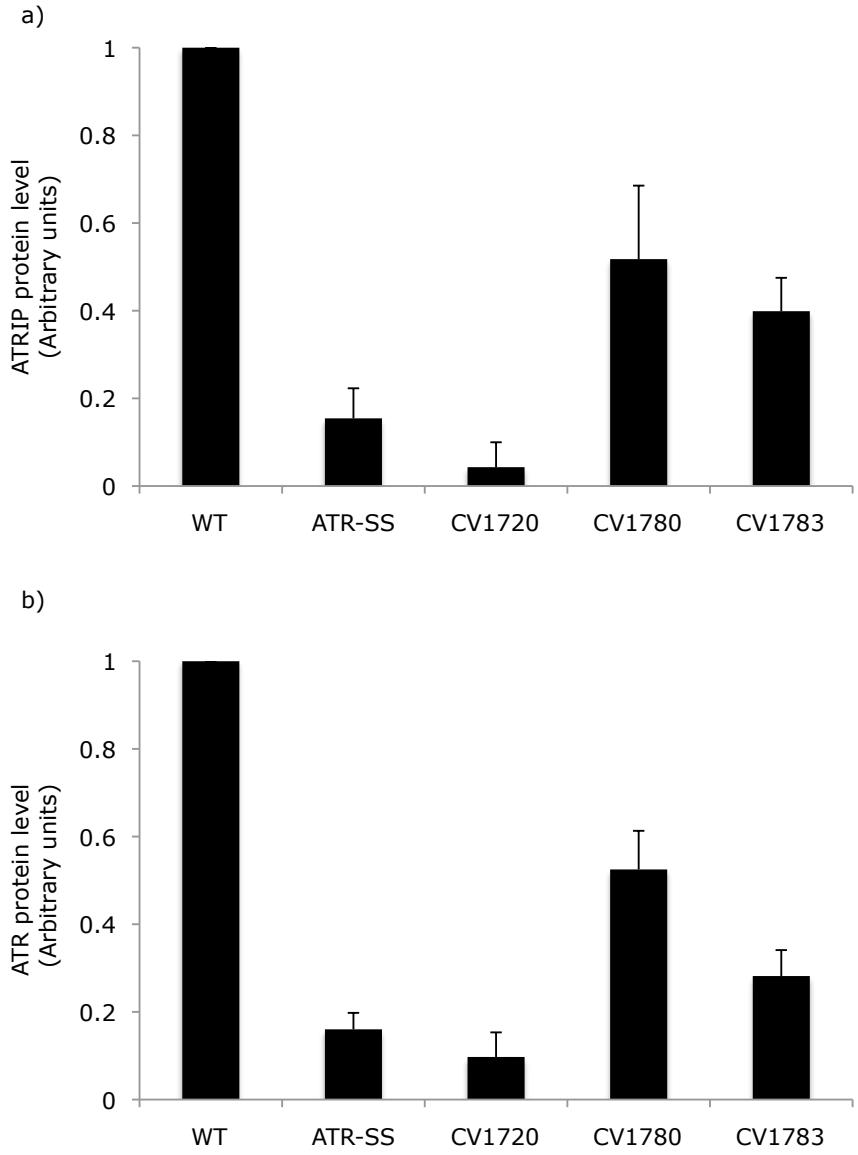

Figure 4.9 Quantification of ATRIP and ATR protein levels

At least three western blots were scanned and protein levels of ATRIP (a) and ATR (b) were quantified in WT, ATR-S, ATRIP-S (CV1720) and ATRIP-S parental (CV1780;CV1783) LBLs using SimplePCI software. Data shown is arbitrary units. Error bars represent the standard deviation.

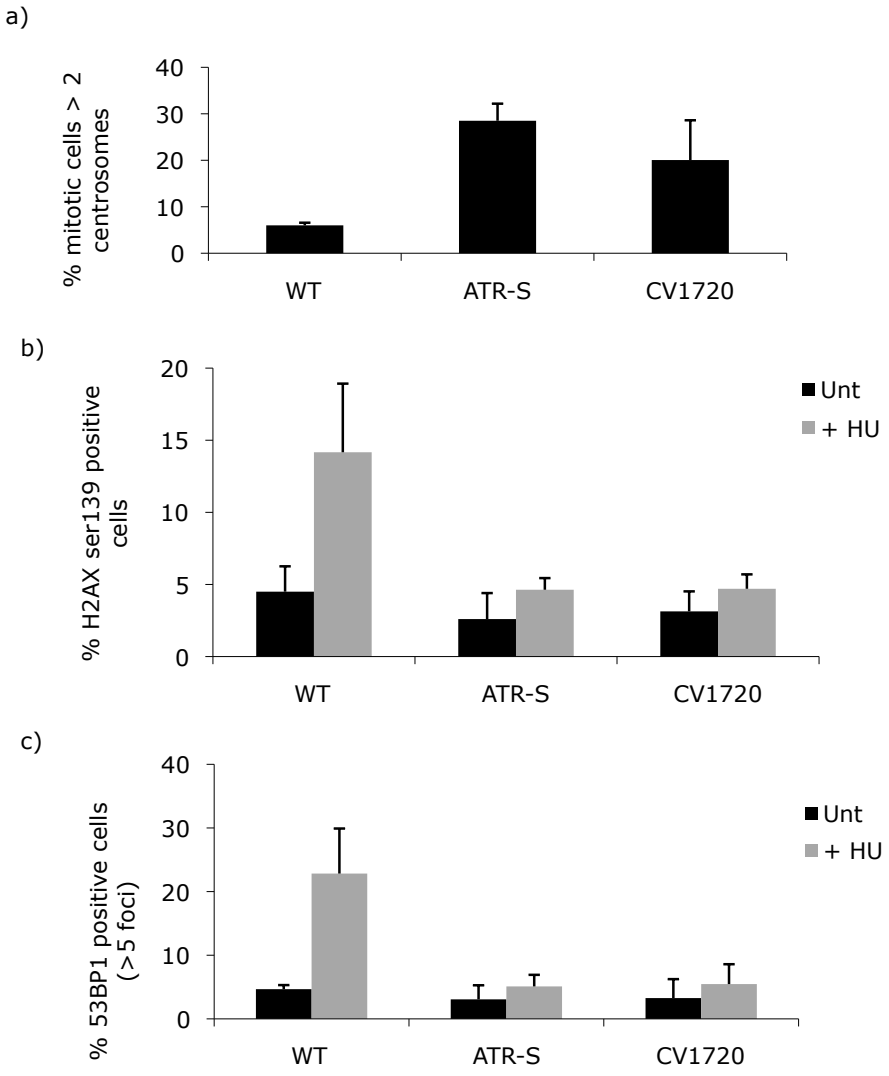

Figure 4.10 The ATR-dependent DNA damage response in CV1720 patient cells

a) CV1720 patient cells display supernumary mitotic centrosomes. Cells were treated with nocodazole for 24hrs to increase the number of mitotic cells. Centrosomes were then examined by immunofluorescence using antibodies to γ-tubulin. The number of cells containing more than two centrosomes was assessed. b) ATR-dependent H2AX phosphorylation is defective in CV1720 patient cells. WT, ATR-S and CV1720 (ATRIP-S) cell lines were treated with 5mM Hydroxyurea and incubated at 37°C for 2hr. Phosphorylation of H2AX on ser139 was detected using immunofluoresence with specific antibodies. The percentage of cells staining positively for H2AX phosphorylation was determined for each cell line. c) 53BP1 foci formation in response to replication stress is defective in CV1720 cells. WT, ATR-S and CV1720 (ATRIP-S) cell lines were exposed to 5mM hydroxyurea for 2hr. 53BP1 foci were examined using immunofluoresence with a specific antibody. The percentage of cells with more than 5 foci was determined for each cell line. Each graph represents the mean of three independent experiments. Error bars represent the standard deviation.

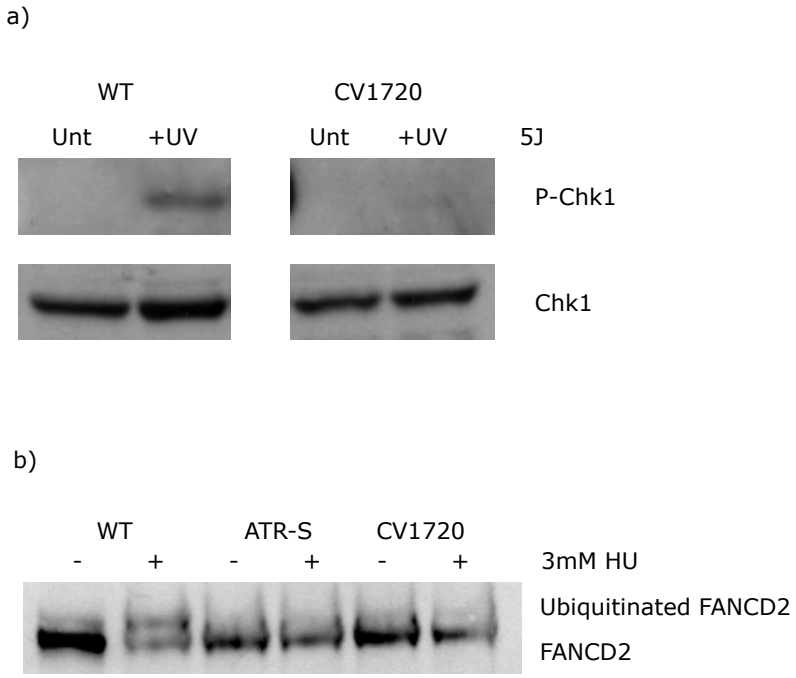

Figure 4.11 ATR dependent modification of target proteins is defective in CV1720 patient cells

a) Chk1 is not phosphorylated effectively in CV1720 patient cells. WT, and CV1720 (ATRIP-S) LBL cells were treated with $5Jm^{-2}$ of UV. Chk1 phosphorylation was assessed by immunoblotting with specific antibodies. Total Chk1 levels are used as a loading control.
b) ATR dependent FANCD2 monoubiquitination is defective in CV1720 patient cells. WT, ATR and CV1720 (ATRIP-S) LBL cells were treated with 3mM HU for 1hr. FancD2 ubiquitination was assessed by immunoblotting using specific antibodies.

These results all clearly show that ATR is unable to efficiently phosphorylate its targets in CV1720 patient cells and that CV1720 patient cells display phenotypes that are typical of Seckel syndrome patient cells.

4.2.4 CV1720 patient cells fail to activate the ATR-dependent G2/M checkpoint

ATR-Seckel cells have previously been shown to display a defective G2/M checkpoint response both 24 hours (Alderton *et al.*, 2004) and 2 hours (Stiff *et al.*, 2008) post UV irradiation. CV1720 patient cells were examined for their ability to activate an ATR-dependent G2/M checkpoint arrest, 24 hours after irradiation with UV. The patient cell line examined failed to arrest effectively after exposure to UV, similar to the response seen in ATR-S patient cell lines and in contrast to wild-type cell lines (Figure 4.12a). CV1720 patient cells are compromised in their ability to activate an ATR-dependent checkpoint in response to UV damage.

4.2.5 The G2/M checkpoint defect in CV1720 patient cells can be complemented by transfection with WT ATRIP cDNA

To confirm that the reduced expression of ATRIP in CV1720 patient cells causes an ATR-dependent G2/M checkpoint defect and to investigate further if the ATRIP C2278T (R760X) mutational change results in a loss of G2/M checkpoint control, the C2278T mutation was incorporated into WT ATRIP cDNA using site directed mutagenesis.

Wild type control, ATR-S and CV1720 patient cells were then transfected with either WT ATRIP, or mutant ATRIP-R760X DNA plasmids and examined for the ability to activate an ATR-dependent G2/M checkpoint arrest, 24 hours post UV irradiation (Figure 4.12b). Transfection with WT ATRIP rescued the G2/M checkpoint defect in both ATR-S and ATRIP-S cells, probably as the additional ATRIP available to the cells enabled residual ATR protein to be stabilised more effectively. Transfection with mutant ATRIP-R760X failed to fully rescue the G2/M checkpoint defect in either the ATR-S or CV1720 patient cells. These results demonstrate that the reduced level of ATRIP in the patient cell line cause the G2/M checkpoint defect observed and that the mutant ATRIP-R760X protein is not able to restore ATRIP checkpoint function in these cells.

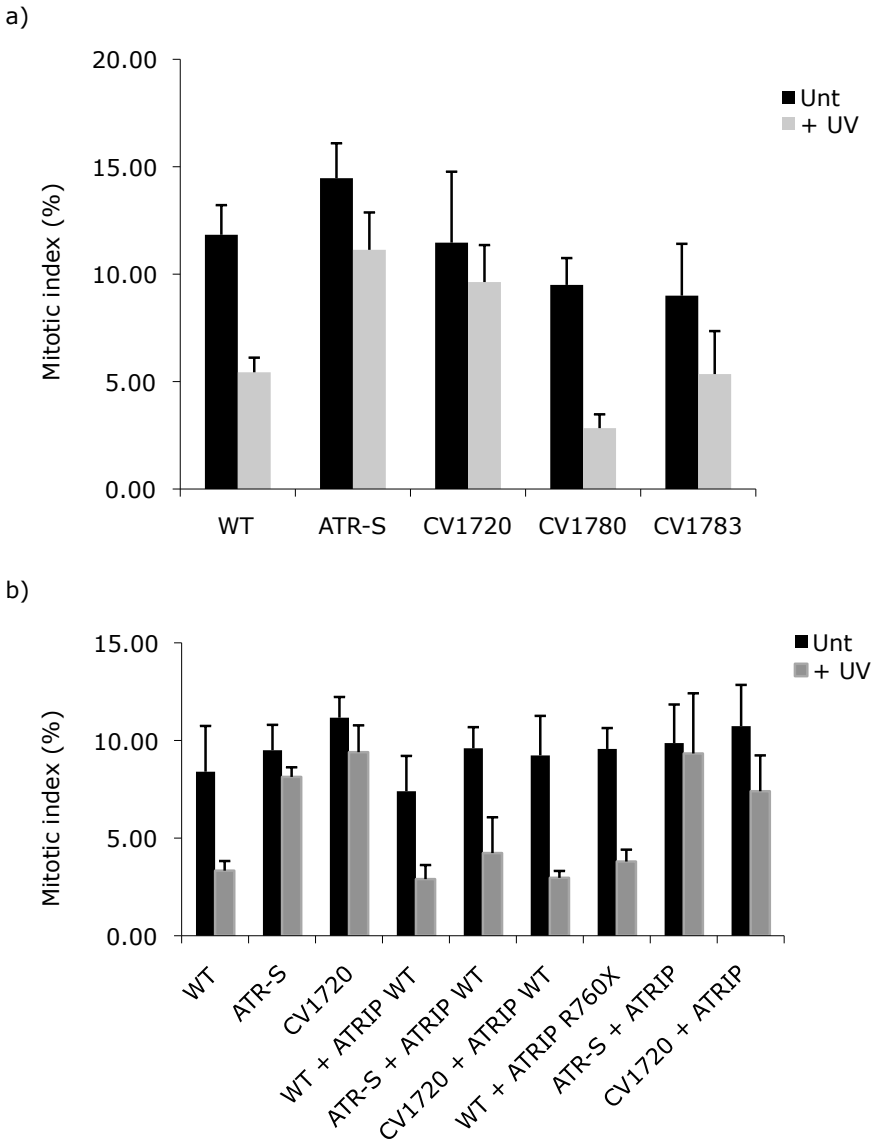

Figure 4.12 CV1720 patient cells fail to activate the ATR-dependent G2/M checkpoint

a) WT, ATR-S, unaffected heterozygous relative and CV1720 (ATRIP-S) cell lines were examined for G2/M checkpoint arrest, 24hrs after treatment with 5J/m^2 UV irradiation and in the presence of 1.5μM nocodazole. A decrease in the number of mitotic cells was taken as indicative of a G2/M arrest.

b) WT, ATR-S and CV1720 (ATRIP-S) cells were transfected with WT ATRIP or mutant ATRIP-R760X DNA plasmids and examined for ATR-dependent checkpoint arrest, 24hrs after exposure to 5Jm^2 UV and in the presence of 1.5μM Nocodazole. A decrease in the mitotic index is indicative of G2/M checkpoint arrest.

Graphs represent the mean of three independent experiments. Error bars represent the standard deviation.

4.2.6 R760X ATRIP impairs ATR-ATRIP protein interaction

The C2278T mutational change detected in *ATRIP* was predicted to result in a truncation of ATRIP at R760X, resulting in a loss of the C terminal of the protein. This region of ATRIP has previously been shown to be required for interaction of ATRIP with ATR and its loss results in defects in ATR recruitment to ssDNA and Chk1 phosphorylation (Falck *et al.*, 2005). We therefore reasoned that R760X ATRIP would not interact with ATR as efficiently as the WT protein.

To investigate if the C2278T mutational change in *ATRIP* results in an inactivating mutation, the C2278T mutation was incorporated into ATRIP WT cDNA using site directed mutagenesis. HA-tagged WT or R760X ATRIP was then co-transfected with WT ATR cDNA in HEK293T cells. Immunoprecipitation with HA-agarose was performed and then the level of ATR binding to ATRIP assessed by western blotting (Figure 4.13). The amount of ATR present in samples transfected with R760X ATRIP was significantly lower than that observed in WT ATRIP transfected samples. This result indictates that the R760X mutation reduces binding of the mutant ATRIP to ATR. The immunoprecipitation work was conducted in Tomoo Ogi's laboratory.

In conclusion, in this chapter I have shown that the mutations identified in *ATRIP* in this SS patient result in reduced protein levels and therefore impact on ATR stability, resulting in reduced protein levels of ATR. This leads to defects in ATR-dependent signalling such as reduced phosphorylation of ATR target proteins such as Chk1 and a failure to activate the G2/M checkpoint after UV exposure.

4.3 DISCUSSION

Mutations in ATR were first identified in a single SS family in 2003 but since that time no further patients with mutations in ATR had been identified. The results in this chapter identify mutational changes in *ATRIP* as a further cause of SS. In this chapter I have shown that the mutational changes detected in *ATRIP* lead to reduced expression of ATRIP protein, resulting in reduced expression of ATR. This is not unexpected, as each protein is known to be dependent on the other for its stability (Cortez *et al.*, 2001). However, this finding had previously not been verified *in vivo*. I have shown that the defect in ATRIP expression results in defective ATR-dependent damage response signalling and contributes to a defective ATR-dependent G2/M checkpoint response. I have also shown that the R760X mutation is not able to rescue the ATR-dependent G2/M checkpoint defect,

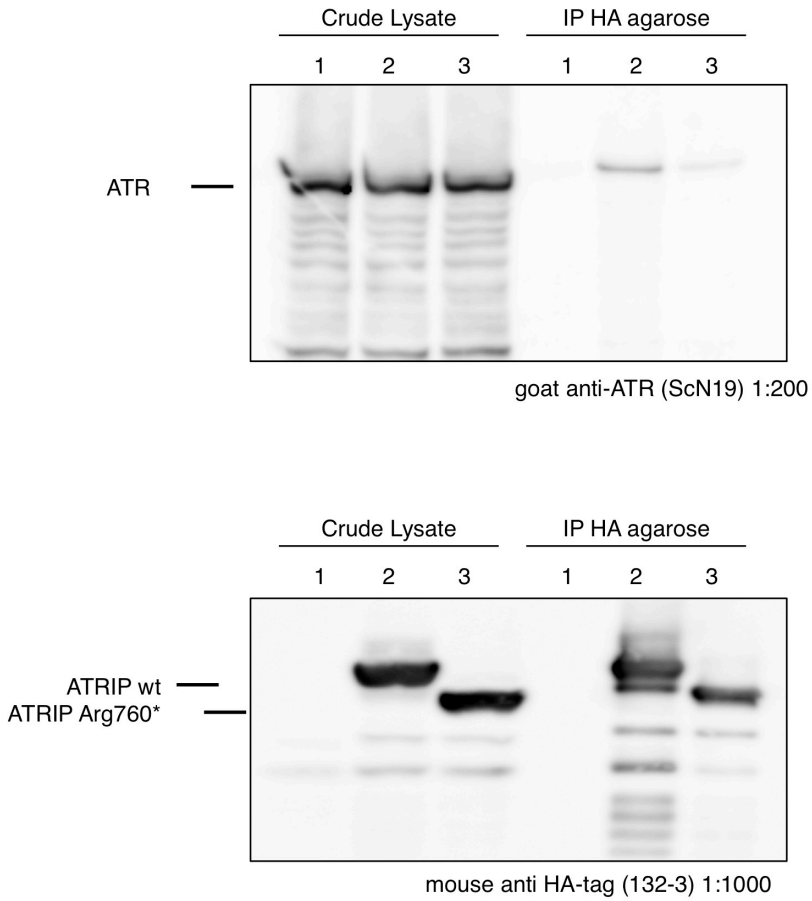

Figure 4.13 R760X ATRIP impairs ATR-ATRIP protein interaction

Crude lysates were prepared from HEK293T cells either mock transfected (lane 1), transfected with WT (lane 2) or R760X mutated (lane 3) ATRIP cDNA (HA-tagged) together with ATR cDNA. Extracts were immunoprecipitated with agarose-conjugated rabbit anti-HA-tag antibody (MBL). Interactions were detected by immunoblotting with antibodies against ATR (top panel) and HA-tag (ATRIP, bottom panel).

Figure and legend from Tomoo Ogi.

confirming that this mutational change is impacting in the patient. These observations are also important as they confirm, in patient cells, the *in vitro* experiments showing that ATR and ATRIP are mutually dependent for stability and therefore the importance of ATRIP for ATR-dependent signalling.

The clinical features of SS are heterogenous and there is considerable overlap between SS and other Microcephalic primordial dwarfism disorders such as Majewski Osteodysplastic Primordial Dwarfism type II (MOPDII) and Meier-Gorlin syndrome (MGS). Clinical features that are common to all of these disorders are microcephaly and primordial dwarfism, however there are further clinical features, which can be used to distinguish between each of these disorders. Therefore the identification of further patients with ATR/ATRIP defects is useful to define clinical features of Seckel syndrome and potentially further discriminate between these disorders. At the same time as our ATRIP patient was identified, two further ATR patients were also identified with compound heterozygous mutations in ATR (G. Stewart, Figure 4.14). Details of the clinical features of all ATR patients, including the original 2003 patient (O'Driscoll *et al.*, 2003) and the ATRIP patient described here, are shown in Table 5.

ATR-ATRIP Seckel patients can be defined as having extreme microcephaly and short stature, microtia (small ears), micrognathia (small receding chin) and dental crowding. Skeletal abnormalities in the newly described patients are also more severe than in the original ATR patient, highlighting a possible role for ATR in bone development. Bone abnormalities were also observed in a mouse model engineered to contain the splicing mutation from the original ATR patient (Murga *et al.*, 2009). Clinical features such as small patellae and absent earlobes present in the newly identified ATR patients are also characteristic features of MGS. However, the microcephaly and growth delay noted in MGS patients tends to be less marked than in the Seckel patients (Table 6). The ATRIP-Seckel patient described here also had some brain abnormalities such as generalised atrophy of the cerebellum and an unusually shaped pituitary gland with an absent fossa. These features could reflect problems in brain development *in utero*, with the pituitary defects possibly contributing to the growth abnormalities observed, although levels of hormones measured in the patient were normal (Table 5).

These observations raise the possibility that MGS and Seckel are the same syndrome, with defects in ATR signalling, and that the clinical spectrum of these primordial dwarfism disorders are simply wider than previously acknowledged.

	ORC1 - MGS	Pre-RC MGS	ATR/ATRIP SS
No of patients	10	25	4
OFC (cm) *	-5.4 to -11 SD	+1.7 to -5.0 SD	-10 to -12 SD
Height (cm) *	-4.5 to -9.6 SD	-0.4 to -6.4 SD	-5 to -8 SD
Weight (kg) *	0.8 to -11 SD	-0.3 to -9.9 SD	-3.3 to -8 SD
Intellectual disability	Ranges from none to mild/ moderate	None	Developmental delay (2/4)
Facial Features	Small and abnormal ears (9/10), micrognathia (5/10), down slanted palpebral fissures (1/10)	Small and abnormal ears(25/25), micrognathia (20/25), down slanted palpebral fissures (8/25)	Small and/or abnormal ears (4/4), micrognathia (4/4), receding forehead (4/4), prominent nose (4/4), short palpebral fissures (2/4)
Skeletal abnormalities	Delayed bone age (3/10), Slender long bones (2/10) , absent patellae (6/10), genu recurvatum (4/10)	Delayed bone age (11/25), slender long bones, absent patellae (24/25)	Delayed bone age (1/4), 5th finger clinodactyly (2/4), symmetric dwarfism (3/4), small/abnormal patellae (2/4), kyphosis (1/4), hip abnormality (2/4), narrow pelvis (iliac blades) (1/4)
MRI	Normal in 2 patients examined	NA	Generalised cerebral atrophy, delayed myelination, abnormal gyration (2 patients examined)
Other	High pitched voice (1/10), full lips (7/10), cryptochordism (2/4 examined), mammary hypoplasia (2/2 examined), feeding and respiratory problems during infancy (8/10)	Full lips (14/25), cryptochordism (7/14 examined), mammary hypoplasia (8/8 examined), feeding (20/25) and respiratory (9/25) problems during infancy	Dental crowding (4/4), feeding and respiratory problems during infancy (1/4)

•standard deviations from the age-related normal population mean, NA = not assessed MGS data from Bicknell et al, 2011 (a and b;, Guernsey et al, 2011; De Munnik et al, 2012.

Table 6 MGS and Seckel syndrome clinical features

a)

b)

Figure 4.14 Newly identified ATR patients

a) ATR-Seckel patient 27-4BI
b) ATR-Seckel patient 19-8BI

Mutations identified in components of the origin recognition complex have been identified in MGS patients and are described in this thesis. ATR-signalling pathway function is also examined in these patients and will also be discussed later. The overlapping clinical features observed in these patients could reflect the requirement for both ATR and replication proteins in ensuring genome stability during the rapid phase of replication during embryonic development.

In summary, in this chapter I have shown that mutations in *ATRIP* result in reduced protein levels of both ATRIP and ATR, causing defects in ATR-dependent DNA damage response signalling. The identification of further ATR/ATRIP patients is useful in allowing further definition of the clinical features of this MPD disorder.

CHAPTER FIVE

RESULTS III: Mutations in *ORC1L* cause Microcephalic Primordial Dwarfism

5.1 INTRODUCTION

DNA replication is initiated from sequences within the genome termed replication origins. In bacteria and yeast these are sites of specific nucleotide sequences whilst in humans and higher organisms this is not the case, although an AT-rich sequence is preferable for pre-replication complex binding (Vashee et al., 2003). How origins are defined in the human genome is not completely understood but epigenetic factors are thought to be important (Takeda and Dutta, 2005). Origins are licensed for replication in G1 phase of the cell cycle by the assembly of a multiple protein pre-replication complex (preRC) (Cook, 2009). The first protein of the preRC to bind to the origin is the Origin Recognition Complex (ORC1-6). The binding of ORC to the chromatin then recruits the further licensing factors CDC6, and CDT1. The MCM2-7 complex is a presumptive replicative protein helicase that is then loaded onto the chromatin to complete preRC assembly. Licensing of the origin is considered complete once the MCM helicase has been loaded onto the chromatin (Nishitani and Lygerou, 2002).

ORC is composed of six subunits, ORC1 to ORC6, of which ORC1 is the largest (Vashee *et al.*, 2001). ORC1 is the only subunit of the complex that contains a bromo-adjacent homology (BAH) domain, a highly conserved domain amongst mammals. The BAH domain has been shown to be important for both protein stability and for the binding of ORC1 to the chromatin (Noguchi *et al.*, 2006).

In human cells ORC1 levels are thought to fluctuate in a cell cycle specific manner, whilst the levels of subunits ORC2-5 remain constant throughout the cell cycle. In quiescent cells, early S-phase arrested cells and mitotic cells, ORC1 is present at a basal level. The cellular level of ORC1 protein begins to increase in early G1, rising to a maximal level, 10 fold higher than the basal, after 9 hours (G1/S) (Tatsumi *et al.*, 2003). ORC1 is then selectively degraded during S phase returning to a basal level. However, in hamster cells and some human tumour cell lines, the levels of

ORC1 remain constant throughout the cell cycle (Okuno *et al.*, 2001, Li and DePamphilis, 2002, McNairn *et al.*, 2005).

The human ORC complex is assembled in an ordered fashion with ORC2 and ORC3 first binding to each other and recruiting ORC5. ORC4 and ORC1 are then recruited in an ATP-dependent manner (Siddiqui and Stillman, 2007). This complex then binds to the chromatin in an ORC1 dependent manner. The binding of ORC1 to the chromatin is dependent on ORCA, a recently identified WD-repeat protein (Shen *et al.,* 2010). A further ORC subunit, ORC6 interacts weakly with the ORC2-5 complex.

In human cells ORC1 is stably bound to the chromatin in G1 phase, as part of the preRC (Ohta *et al.*, 2003). Upon entry into S phase, ORC1 dissociates from the chromatin and is then polyubiquitinated by the SCF/Skp2 complex during S phase (Méndez *et al*., 2002). It is then degraded via proteolysis. The dissociation of ORC leads to disassembly of the pre-replication complexes (Siddiqui and Stillman, 2007), helping to prevent inappropriate origin refiring. During mitosis the hyperphosphorylation of ORC1 by Cdk1/CyclinA prevents the binding of ORC1 onto the chromatin, thus preventing assembly of preRC's until mitosis is completed (Li *et al.*, 2004). The binding of ORC1 to the chromatin is then restored during the transition between mitosis and the following G1 (Méndez *et al.*, 2002).

Additional non-replicative roles for ORC have also been described. The ORC complex interacts with HP1 via the BAH domain of ORC1. HP1 associates with heterochromatin and localises to centromeres and telomeres, is involved in silencing of transcription at these heterochromatic regions and has a critical function in heterochromatin formation and maintenance (Kwon and Workman, 2008). Depletion of ORC1 results in loss of HP1 from heterochromatic foci suggesting a role for ORC1 in the maintenance of constitutive heterochromatin (Prasanth *et al.*, 2010).

Many of the ORC subunits have been found to localise to the kinetochores and knockdown of ORC2 results in mitotic defects suggesting a role for ORC in spindle attachment to kinetochores, possibly coordinating this with the completion of replication (Prasanth *et al.*, 2002, Prasanth *et al.*, 2004).

Sister chromatid cohesion is directly mediated by ORC in the budding yeast by a mechanism that is independent of cohesin (Suter et al., 2004). In Xenopus extracts pre-replication complexes are required for recruitment of cohesin to the chromatin,

thus ORC is indirectly required for this process in this system (Takahashi *et al.*, 2004).

ORC1 has been demonstrated to control centrosome numbers by the prevention of centriole reduplication (Hemerly *et al.*, 2009). The duplication of centrosomes is Cyclin E dependent but the duplication of centrioles is dependent on Cyclin A (Hanashiro *et al.*, 2008). It was suggested that Cdk2-CyclinA-dependent localisation of ORC1 to the centrosomes prevents Cdk2-CyclinE-dependent reduplication of centrosomes during late G1 and early S phase, when levels of Cyclin E in the cell are still high (Hemerly *et al.*, 2009).

ORC1 has also been shown to have a role in the induction of apoptosis, when in an unbound and unmodified form. ORC1 can trigger apoptosis via the Caspase-3 pathway, when it is not in complex with the other ORC subunits, when it is ubiquitinated in S phase or phosphorylated in M phase, and when it accumulates in a perinuclear location (Saha *et al.*, 2006).

In this chapter, patient cell lines from a consanguineous Saudi-Arabian family of nine members were examined for ATR-dependent UV-induced G2/M checkpoint activation and the presence of supernumary mitotic centrosomes, in order to confirm the Seckel syndrome status of the proband and to direct further studies towards the identification of the underlying genetic defect. The family were then included in a genetic mapping study in collaboration with Andrew Jackson's group at the MRC Human Genetics Unit in Edinburgh, in order to identify potential causative gene candidates. This approach lead to the identification of mutations in *ORC1L* in this family, segregating as expected for an autosomal recessive disorder. Further screening identified another three microcephalic primordial dwarfism families harbouring *ORC1* mutations.

5.2 RESULTS

5.2.1 Clinical features of MPD family 1

A consanguineous Saudi-Arabian family of nine, in which two children had Microcephalic Primordial Dwarfism (MPD) with a clinical diagnosis of SS, were referred to our laboratory for investigation into the underlying genetic defect. Both patients displayed marked growth retardation, severe microcephaly and additional

clinical features such as small ears (Patients P1 and P2, Table 7). Both patients were judged to be of normal intellect. These clinical features, common in SS, are overlapping with Meier-Gorlin Syndrome (MGS), which has been discussed in the introduction to this thesis.

5.2.2 Mutations in ORC1L identified in MPD family 1

Cells from patient P1 were confirmed to possess UV-induced G2/M checkpoint defects (see section 5.2.7) and were then sent to our collaborators in the MRC Human Genetics Unit in Edinburgh. Here they performed genome-wide genotyping on the consanguineous Saudi-Arabian family of nine members, using Affymetrix Genechips. The MRC Human Genetics Unit analysed SNP genotypes and performed multipoint linkage analysis to identify a region of homozygosity on chromosome 1p32. This region was then refined using microsatellite markers to a 15.6-cM region between D1S706 and D1S2890, containing 105 annotated genes (Bicknell et al, 2011). Several candidate genes were sequenced including *RAD54L* and *STIL* but no pathogenic mutations were identified. Sequencing of *ORC1* identified a homozygous A>G mutation in exon 4 resulting in an amino acid substitution, E127G in patient P1 (subsequently referred to as ORC1-P1) and patient P2. Further screening revealed mutations in *ORC1* in four other MPD families (Figure 5.1, Table 7). Many of the mutations identified were within the BAH domain of ORC1 (Figure 5.2a). There is currently no crystal structure for human ORC1 so the mutations were modelled into the crystal structure from the chicken polybromo BAH domain and the yeast Sir3 BAH domain (Figure 5.2b) using the Phyre server. The mutations identified were predicted to cause loss of protein folding (F89S), and loss of protein-protein interaction sites (R105Q). The mutation E127G was not thought to affect protein folding or interactions directly, although the loss of charge caused by the mutation could potentially cause some protein interaction loss (personal communication: Anthony Oliver).

5.2.3 ORC1 protein expression is reduced in ORC1-P1 patient cell lines

Cells from patient ORC1-P1 (E127G) were pre-treated with increasing levels of protease inhibitor for 30 minutes and pellets obtained. These were then separated into a soluble fraction and an insoluble fraction that contained chromatin bound proteins. Reduced levels of ORC1 were revealed in both the soluble and insoluble fractions examined, indicating that the mutations in the BAH domain of ORC1 in

Patient	Family No & Country of Origin	Mutation	Gestation/ Wgt (wks) / (kg)	Postnatal Morphometric Details Age (yrs) Hgt (cm) Wgt (cm) OFC (cm)	Facial Features	Other Notable Clinical History	Skeletal Analysis
P1	Family 1 Saudi Arabia (Consanguineous)	E127G (c.380A>G)	40/2.64 (-1.9SD)	4.5 85.5 (-4.5) 9.6 (-5.9) 42 (-7.1)	Small chin, mildly small ears, full lips	46XY. Mild, non-specific icythyosis. Suboptimal growth hormone stimulation test, Normal IGF1. No response GH therapy	-
P2	Family 1	E127G (c.380A>G)	39/2.18 (-2.5)	0.66 52 (-7.6) 3.1 (-9.3) 36 (-7.6)	Small anterior fontanelle, relatively small ears	46XX. Gastro-oesophageal reflux. Normal MRI Brain	-
P3	Family 2 Syria/USA (Consanguineous)	F89S (c.266T>C)	40/1.58 (-4.5)	4.5 73 (-7.6) 5.9 (-11) 38.5 (-11)	Mild micrognathia small ears, mild synophrys, full lips	Bronchomalacia. Gastro-oesophageal reflux. Craniosynostosis surgery	Hyper-extended dislocated knees at birth. Tibia posteriorly dislocated- surgically corrected, at surgery, patella present
P4	Family 3 USA	R105Q/ R720Q (c.314G>A/ C.2159G>A)	36/1.46 (-3.2)	7.1 94 (-5.3) 10.9 (-6.6) 46.2 (-5.4)	Normally shaped ears with small lobules, narrow auricular canals, Normal teeth, bifid uvula, full lips No micrognathia, nose slightly prominent	46XX. Normal sister chromatid exchange analysis. Severe conductive hearing loss. High pitched voice. Normal muscle biopsy, metabolic screen, endocrine screen, normal brain MRI	Skeletal survey mildly gracile long bones, minimal metaphyseal widening, some undertubulation in the midshaft for some long bones. Delayed bone age. Patella present on clinical examination
P5	Family 4 UK	R105Q (c.314G>A)	28/1 (-0.6)	13 102.9 (-6.6) 18.4 (-6.1) 43.5 (-7.3)	Normal/large ear size, short philtrum, normal teeth, full lips.	Lobectomy for lobar emphysema. Severe prematurity, consequently associated with intraventricular haemorrhage resulting in left hemiplegia	Slender long bones, cupped distal metaphyses of metacarpals, short 4th metacarpal. Patella present.

Table 7 ORC1 patient clinical features

a)

* = mutations found in ORC1 Seckel patients
1) E127G
2) F89S
3) R105Q/R720Q
4) R105Q/691X
5) R105Q

BAH = Bromo adjacent homology
AAA+ = ATP binding domains
Cdc6 = interaction domain
RXL motif = Cyclin binding

b)

	ORC1-P1	ORC1-P4
Height	85.5 (-4.5)	94 (-5.3)
Weight	9.6 (-5.9)	10.9 (-6.6)
OFC	42 (-7.1)	46.2 (-5.4)

Height in cm, weight in kg, OFC in cm
standard deviations below mean in brackets

Figure 5.1 ORC1 patient and mutations identified

a) Schematic of ORC1 showing protein domains and position of mutations found in ORC1 patients.

b) ORC1-P1 patient picture and clinical measurements from two patients

```
                                                          89
Human        EGDDDENPYVAKLLELFEDDSDPPPKKRARVQWFVRFCEVPA
Chimpanzee   EGDDDENPYVAKLLELFEDDSDPPPKKRARVQWFVRFCEVPA
Dog          EGDDDENPYVAKLVELFEDDSEPHSKKRARVQWFIRFCEVPV
Mouse        QGEDNKKPYVAKLIELFQNGAEVPPKKCARVQWFVRFLEIPV
Rat          QGEDNQKPYVAKLIELFENGSEVPPKKYARVQWFVRFCEIPI

                   105                          127
Human        CKRHLLGRKP-GAQEIFWYDYPACDSNINAETIIGLVRVIP
Chimpanzee   CKQHLLGRKP-GAQEIFWYDYPACDSNINAETIIGLVRVIP
Dog          SKRHLLGRKP-AAQEIFWYDYPACNSNINAETIIGRVQVVA
Mouse        SKRHLLGRSP-PAQEIFWYDCSDWDNKINVETIIGPVQVVA
Rat          PKRHLLGRRP-SAQEIFWYDCSDCDNDIHVETIIGPVQVVA
```

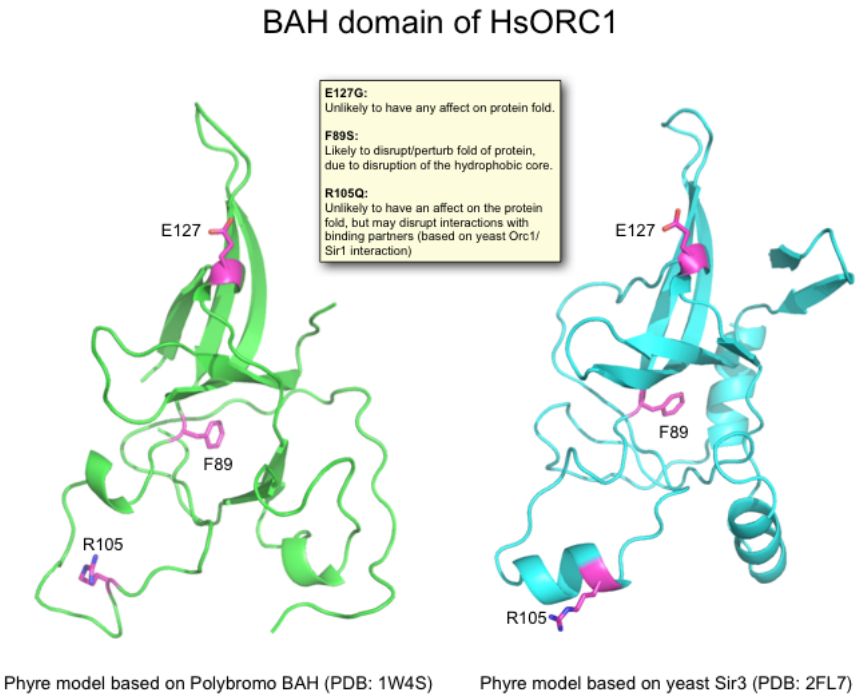

Figure 5.2 ORC1 BAH domain and mutation modelling

a)Alignment of ORC1 orthologs showing BAH domain of ORC1 and position of mutations in this region
b)Phyre server modelling of ORC1 BAH domain mutations. Personal communication, Anthony Oliver http://www.sbg.bio.ic.ac.uk/phyre

this patient results in reduced protein stability, consistent with a previous study (Noguchi *et al.*, 2006). Pre-treatment with MG-132, a proteosome inhibitor that reduces the degradation of ubiquitinated proteins (Tsubuki *et al.*, 1996), had no effect on protein levels indicating that increased protein degradation is not a factor in the reduced protein expression observed. A reduction in the level of ORC2 bound to the chromatin was also observed, indicating that the assembly of the preRC onto chromatin is impaired (Figure 5.3a,b). Parental cell lines exhibited a partial reduction in the level of ORC1 bound to the chromatin (Figure 5.3c). Micrococcal nuclease digestion of chromatin fractions revealed a dramatic reduction in the levels of ORC1 tightly bound to the chromatin (Figure 5.3d). The levels of ORC2 and MCM2 bound to the chromatin in these fractions was also markedly reduced, further demonstrating a reduced ability to efficiently form preRC's in these cells (Figure 5.3d). Examination of fibroblasts from the ORC1-P4 patient (R105Q/R720Q) by immunoblotting showed normal ORC1 protein levels but a decrease in the amount of chromatin-bound ORC1 and ORC2 (Figure 5.3e). This result suggests that the mutations detected in *ORC1L* in this patients result in a decreased ability of ORC1 protein to bind to the chromatin and a reduced ability for the ORC complex to assemble onto the chromatin.

5.2.4 ORC1-P1 cells exhibit defects in S-phase progression

The reduced ability to form preRC's on the chromatin suggested that origin licensing and origin firing might be compromised in these cells. We reasoned that if cells from the patient are not able to replicate efficiently, this could be a plausible explanation for the growth retardation and microcephaly phenotypes observed. This could be of increased importance during development, where cell cycle phases are often shorter than in somatic cells (Takahashi *et al.*, 1995). Data generated in our laboratory indicated that ORC1 deficient cells do not activate replication origins efficiently. ORC1-P4 cells were examined for replication licensing capacity using an assay that measures the requirement for cellular ORC to license a viral replication origin (episomes from Epstein-Barr virus) to enable its replication (Dhar et al., 2001) and were found to have drastically reduced capacity to initiate replication from this origin (Bicknell *et al.*, 2011b).

A fraction of the total pool of licensed origins are actually fired during each round of replication, with as many as 90% of licensed origins remaining dormant (Blow and Ge, 2008). Therefore the marked reduction in ORC1 protein levels in these cells may not confer any major growth abnormalities. However, dormant origins may be

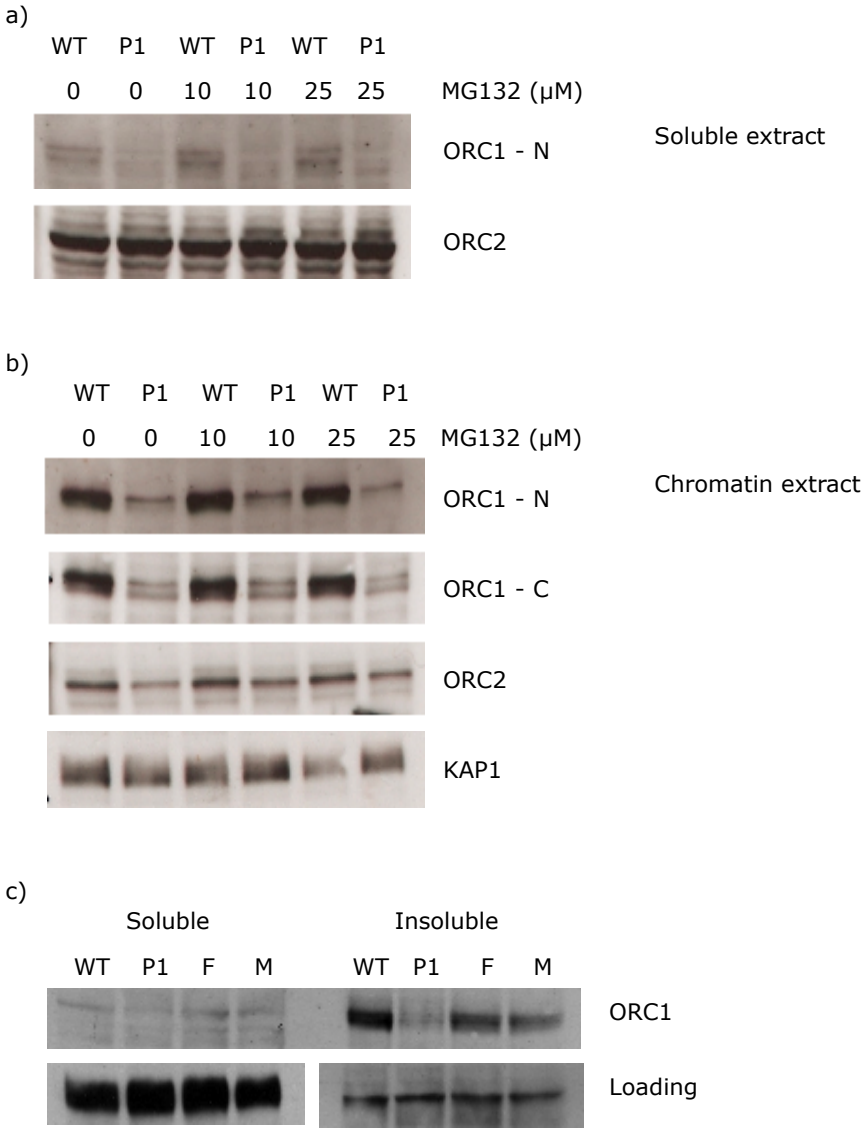

Figure 5.3 ORC1 expression and pre-RC complex assembly in ORC1 deficient cell lines

WT and Patient cells were pre-treated with increasing levels of MG132 protease inhibitor and separated into soluble (a) or insoluble fractions containing chromatin bound proteins (b). Extracts were resolved on 8% SDS-PAGE and transferred onto nitrocellulose membrane. Membranes were then probed with ORC1 (ORC1-N detects epitope at N terminus, ORC1-C detects epitope at C terminus) and ORC2 antibodies. ORC1-N was used for all subsequent blots. ORC2 served as a loading control for the soluble fraction. Heterozygous parental (mother M, father F) control cell extracts (c) also showed reduced ORC1 protein expression.

d)

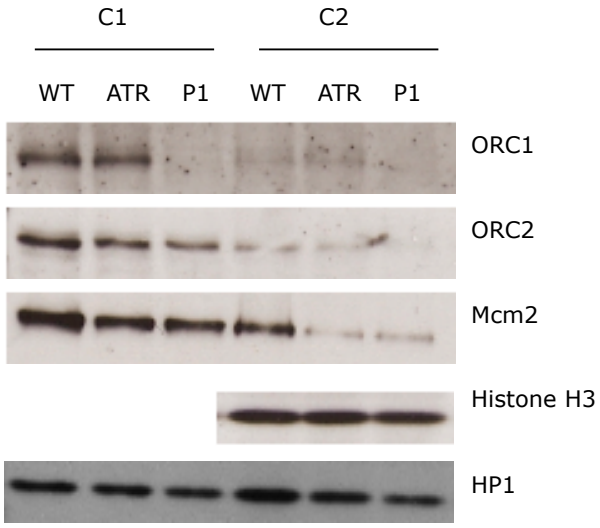

e)

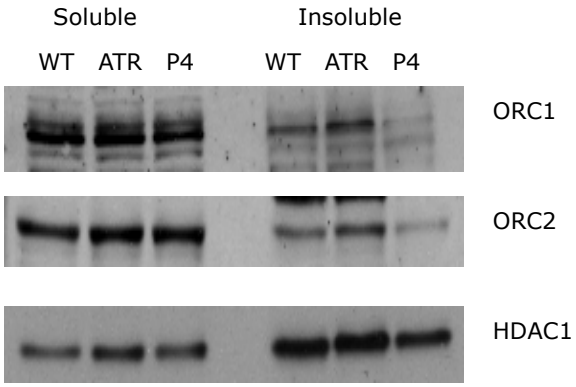

Figure 5.3 (cont) ORC1 expression and pre-RC complex assembly in ORC1 deficient cell lines

(d) WT and ORC1-P1 extracts were subjected to a two step micrococcal nuclease (Mnase) extraction procedure to obtain chromatin enriched fractions of increasing Mnase resistance (C1 and C2). These fractions were then resolved and immunoblotted for ORC and pre-replication complex components. (e) Cell extracts from ORC1- P4 fibroblasts were examined as in (a,b).

utilised in S phase in response to replication fork stalling or slowing (Woodward et al., 2006). Therefore we addressed whether the reduced licensing capacity observed in the ORC1-P1 cells, would affect the rate at which the cells progress through S phase. In order to address this question, the time taken for WT and ORC1-P1 cells to progress through S phase was examined. Cells were pulse-labelled for 30-minutes with BrdU to label S phase cells and then samples were taken over a six hour time period, in the presence of Colcemid to block cells in mitosis. Samples were then processed for Facs analysis using FITC-conjugated BrdU antibodies with propidium iodide staining. The rate of loss of BrdU positive early S phase cells was measured as an indicator of S phase progression (Figure 5.4b). ORC1-P1 cells were shown to progress through S phase more slowly than the WT control cell line (Figure 5.4a and b), although gross cell doubling times for each cell line were normal (data not shown). Further work was then undertaken in our laboratory, using sucrose gradient sedimentation to monitor the size of replication intermediates (T. Stiff). This work demonstrated that following 60 minutes of growth in medium containing labelled thymidine, the DNA from ORC1-P1 cells did not increase in size to the same degree as DNA from WT control cells (Figure 5.5). These results indicate that the rate of replication in ORC-P1 cells appears to be slower than in WT cells. This could be due to the presence of multiple origins but with a reduced rate of replication fork progression from those origins, or that there is reduced origin availability. The reduced ability to form pre-replication complexes on chromatin (Section 5.2.3), along with reduced capability to activate those origins (this section) is consistent with reduced origin availability.

5.2.5 The replication forks in ORC1-P1 cells are inherently less stable than those in WT cells

In order to gain further insight into the replication dynamics of ORC1-P1 cells, replication structures from WT and ORC1-P1 cells were directly analysed using techniques for the spreading of DNA fibres. Cells were double labelled first with IdU and then with CldU to enable visualisation of ongoing forks. DNA fibre spreads were prepared according to established protocols (Maya-Mendoza *et al.*, 2007). Replication structures were scored according to the classification by Maya-Mendoza et al, 2007, where 1 = elongating fork, 2 = fork growing from one origin, 3 = terminal fusion, 4 = isolated and 5 = interspersed. 100 fibres were analysed in preliminary experiments. In WT cells, 75% of structures observed were elongating forks, consistent with ongoing replication. 10% of structures contained two forks growing from the same origin and 5% of structures were terminal fusions indicating

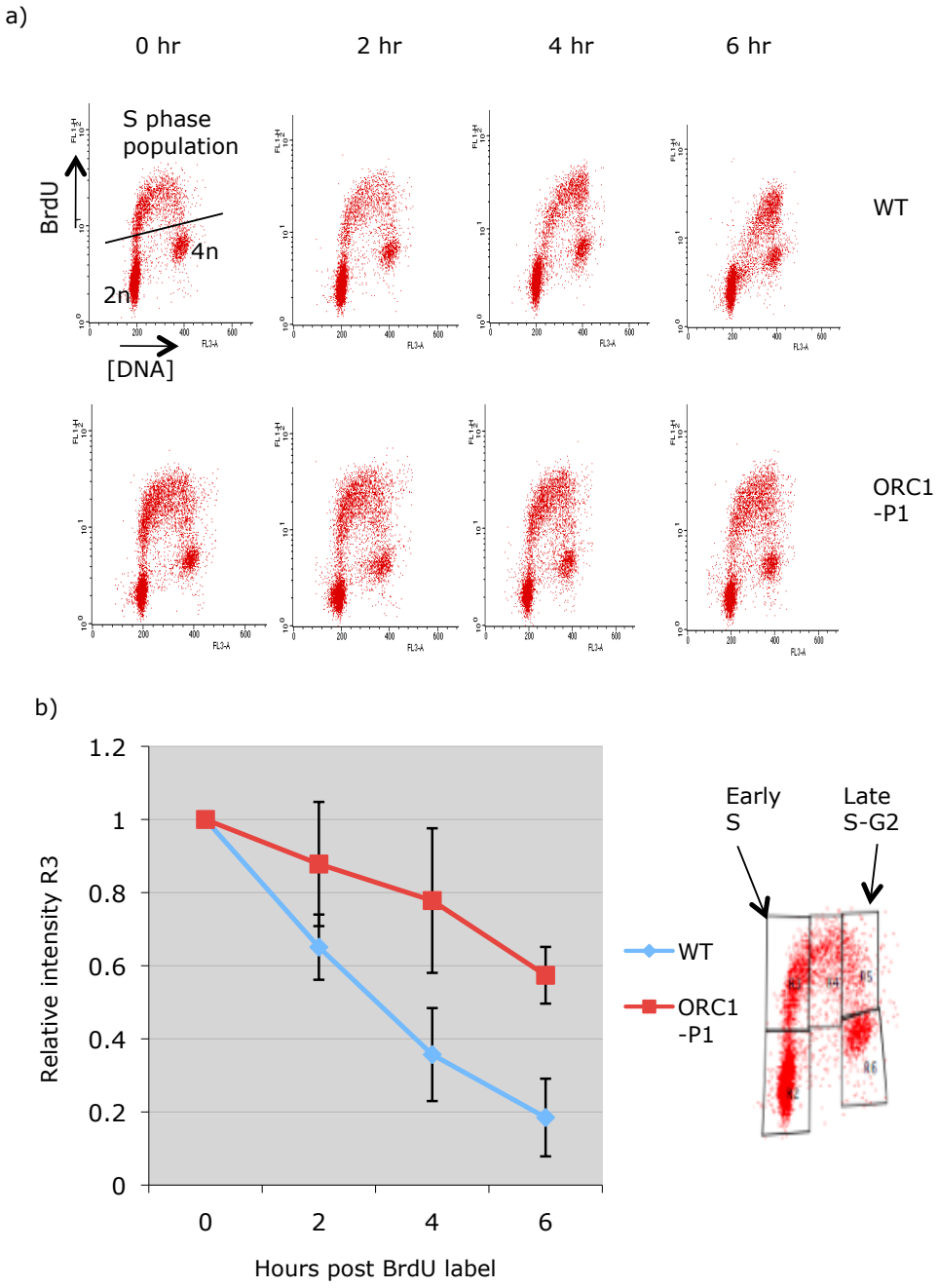

Figure 5.4 S phase progression is compromised in ORC1-P1 cells.

a) WT and ORC1-P1 patient cell lines were pulse-labelled with BrdU for 30 minutes. Cells were prevented from exiting mitosis by the addition of 0.2µg/mL Colcemid. Samples were collected for BrdU Facs analysis at 2 hr time intervals.

b) The rate of loss of early S phase cells (from R3 compartment) represents S phase progression. The graph represents the mean of three independent experiments. Error bars represent the standard deviation.

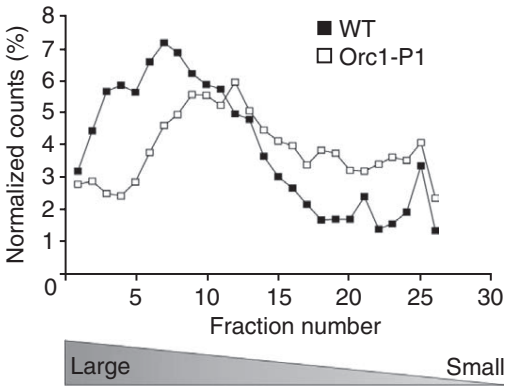

Figure 5.5 ORC1-P1 DNA fragments are smaller than WT fragments

WT or ORC1-P1 LBLs were labeled with [3H]TdR for 1 h and subjected to sucrose-gradient sedimentation following fragmentation and concurrent lysis. Newly fired origins sediment within fractions 25–30, precluding an estimation of new origin firing. DNA from WT LBLs increases in size more rapidly compared to ORC1-P1 DNA. Plot shows a representative profile from three experiments.

Figure and legend taken from Bicknell et al, Nature Genetics 2011. Experiment performed by T Stiff.

the fusion of two forks and thus termination during the labelling period. Very few isolated forks were observed in the WT cell fibre preparations (Figure 5.6). In contrast, preparations from the ORC1-P1 cells contained fewer elongating forks (55%) and a higher proportion of isolated and interspersed (closely spaced active origins) structures than WT cells. These preliminary findings raise the possibility that forks frequently stall and occasionally collapse during the labelling period (Maya-Mendoza *et al.*, 2007) suggesting that the replication forks in ORC1-P1 cells could be less stable than those in WT cells. An alternative explanation for this result could be that fewer origins are fired within the labelling period in the ORC1-P1 cells, resulting in detection of fewer elongating forks. This aspect of replication dynamics in ORC1-P1 cells is interesting but requires further investigation in order to draw firm conclusions.

5.2.6 Assessment of the ATR-dependent DNA damage response in ORC1-P1 cells

In order to determine if the observed reduction in ORC1 protein in these cells has any impact on the ATR-dependent DNA damage response, as we have observed with other SS cell lines (Alderton *et al.*, 2004), ORC1-P1 cells were assessed for the response to damage induced by UV or HU using several assays. The phosphorylation of H2AX after exposure to HU is ATR dependent (Ward and Chen, 2001). The formation of 53BP1 foci at sites of replication stress is dependent on both Chk1 and ATR (Sengupta *et al.*, 2004, Tripathi *et al.*, 2008). ATR-Seckel cells have previously been shown to exhibit reduced H2AX phosphorylation and reduced 53BP1 foci formation following treatment with hydroxyurea (Alderton *et al.*, 2006). H2AX phosphorylation, Chk1 phosphorylation and 53BP1 foci formation responses were all normal in the ORC1-P1 cells, demonstrating that both ATR and Chk1 kinases are activated appropriately in this cell line (Figure 5.7 b,c,d). ORC-P1 cells display supernumary mitotic centrosomes, to a similar level to the ATR-S cells, (Figure 5.7a), possibly reflecting the established role for ORC1 in the prevention of centrosome reduplication (Hemerly *et al.*, 2009).

5.2.7 ORC1-P1 cells fail to activate the ATR-dependent G2/M checkpoint

ATR-Seckel cells have previously been shown to display a defective G2/M checkpoint response both 24 hours (Alderton *et al.*, 2004) and 2 hours (Stiff *et al.*, 2008) post UV irradiation. In order to determine if the reduction in ORC1 protein

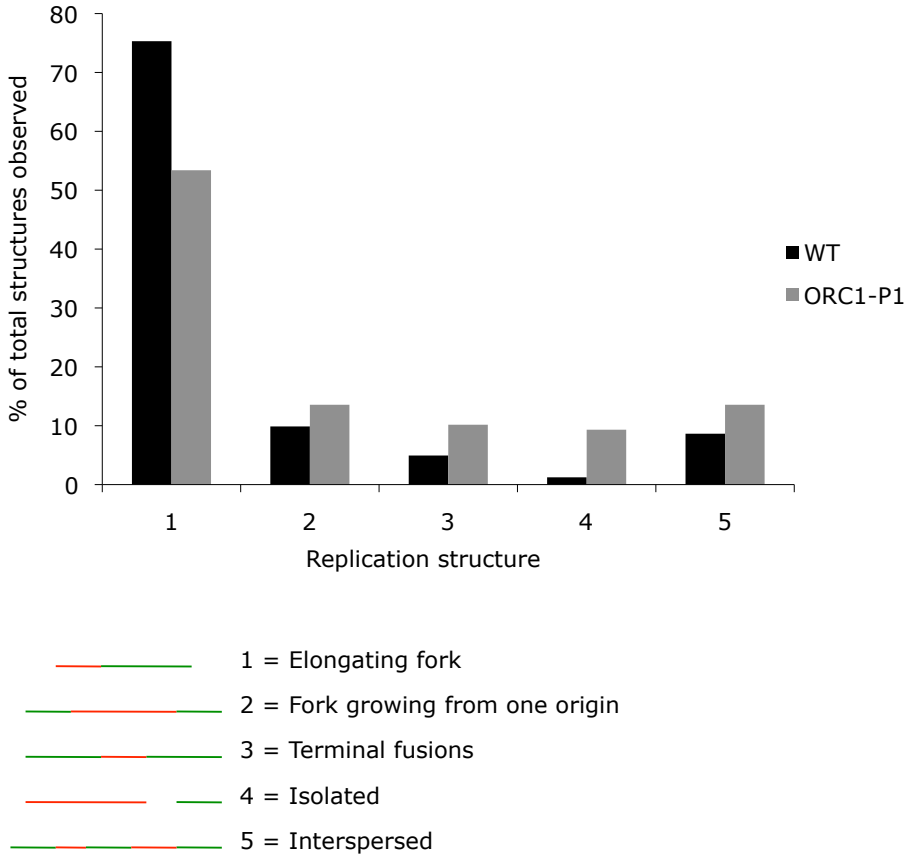

Replication structure classification
(Maya-Mendoza, 2007)

Figure 5.6 The replication forks in ORC1-P1 cells are inherently less stable than those in WT cells

WT and ORC1-P1 LBL cells were labelled with IdU and then CldU for 20 min periods. DNA was then isolated from the cultures and spreads prepared as in Maya-Mendoza et al, 2007. Spreads were immunostained using BrdU antibodies and images captured using Deltavision microscope and Softworx. Replication structures were examined according to classification by Maya-Mendoza et al, 2007. 100 fibres were scored for each cell line.

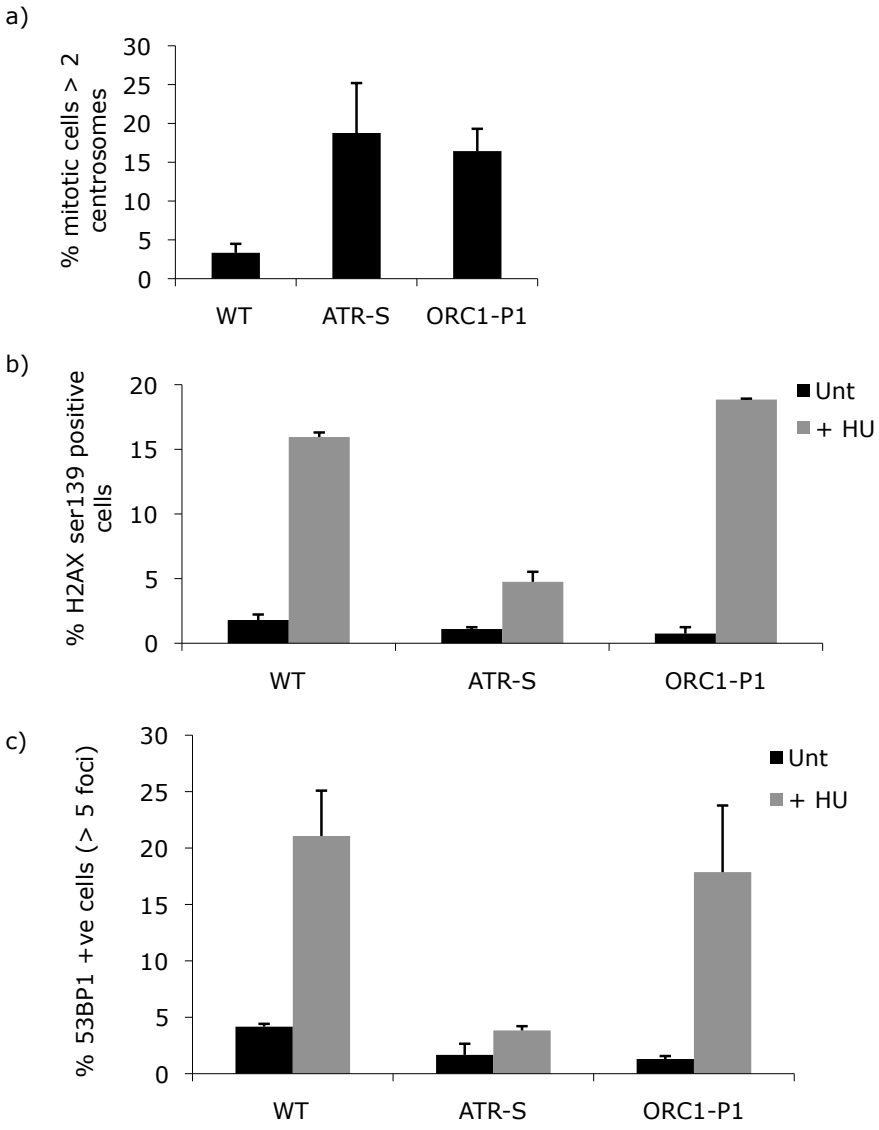

Figure 5.7 The ATR-dependent DNA damage response in ORC1-P1 cells

a) ORC1-P1 cells display supernumary mitotic centrosomes. Cells were treated with nocodazole for 24hrs to increase the number of mitotic cells. Centrosomes were then examined by immunofluorescence using antibodies to γ-tubulin. The number of cells containing more than two centrosomes was assessed. b) H2AX phosphorylation is normal in ORC1-P1 cells. WT, ATR-S and ORC1-P1 cell lines were treated with 5mM Hydroxyurea and incubated at 37°C for 2hr. Phosphorylation of H2AX on ser139 was detected using immunofluoresence with specific antibodies. The percentage of cells staining positively for H2AX phosphorylation was determined for each cell line. c) 53BP1 foci formation in response to replication stress is normal in ORC1-P1 cells. WT, ATR-S and ORC1-P1 cell lines were exposed to 5mM hydroxyurea for 2hr. 53BP1 foci were examined using immunofluoresence with a specific antibody. The percentage of cells with more than 5 foci was determined for each cell line. Each graph represents the mean of three independent experiments. Error bars represent the standard deviation.

d)

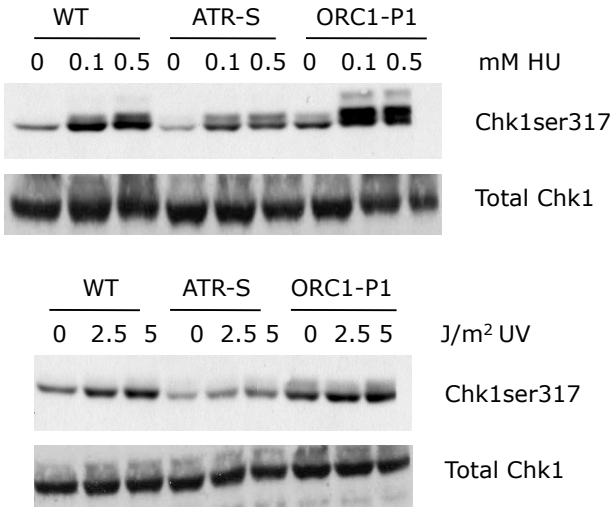

Figure 5.7 The ATR-dependent DNA damage response in ORC1-P1 cells (cont)

d) Chk1 is phosphorylated normally in ORC1-P1 cells. WT, ATR-S and ORC1-P1 cells were treated with increasing doses of HU or UV. Chk1 phosphorylation assessed by immunoblotting with specific antibodies. Total Chk1 levels are used as a loading control.

levels observed resulted in similar checkpoint defects, ORC1-P1 cells were examined for their ability to activate a G2/M checkpoint arrest, 24 hours after irradiation with UV. The patient cell line examined failed to arrest effectively after exposure to UV, similar to the response seen in ATR-Seckel patient cell lines and in contrast to wild-type cell lines (Figure 5.8). ORC1-P1 cells are therefore compromised in their ability to activate an ATR-dependent checkpoint in response to UV damage.

5.2.8 The G2/M checkpoint defect in ORC1-P1 cells can be complemented by transfection with WT ORC1 cDNA

To confirm that the reduced expression of ORC1 in ORC1-P1 patient cells causes an ATR-dependent G2/M checkpoint defect, wild type control, ATR-S and ORC1-P1 cells were transfected with either empty vector, WT ATR or WT ORC1 cDNA plasmids and examined for the ability to activate an ATR-dependent G2/M checkpoint arrest, 24 hours post UV irradiation. Transfection with WT ATR rescued the G2/M checkpoint defect in ATR-S cells but not in ORC1-P1 cells. Transfection with WT ORC1 rescued the G2/M checkpoint defect in ORC1-P1 cells but not in ATR-S cells. Transfection of the empty vector did not rescue the G2/M checkpoint defect in ORC1-P1 cells (Figure 5.9). These results demonstrate that the reduced expression of ORC1 in the patient cell line contributes to the checkpoint defect observed.

5.2.9 Depletion of ORC1 impairs ATR-dependent G2/M checkpoint arrest

In order to provide further confirmation that loss of ORC1 results in an ATR-dependent G2/M checkpoint defect, MG63 osteosarcoma weed cells were treated with control or ORC1 targeting siRNA oligonucleotides for 72hrs in order to deplete ORC1 protein levels. Residual protein was still detectable at this time-point although protein levels were reduced dramatically (Figure 5.10b). Cells were then exposed to 5J UV or 3Gy ionising radiation and examined for G2/M arrest 2hrs post irradiation. Untransfected, Mock and Control siRNA treated cells all arrested after exposure to UV or IR, as expected. ORC siRNA treated cells arrested normally after IR exposure but failed to arrest efficiently after exposure to UV irradiation (Figure 5.10a). This recapitulates the result observed in the patient cell line and confirms the requirement of ORC1 for ATR-dependent G2/M checkpoint activation.

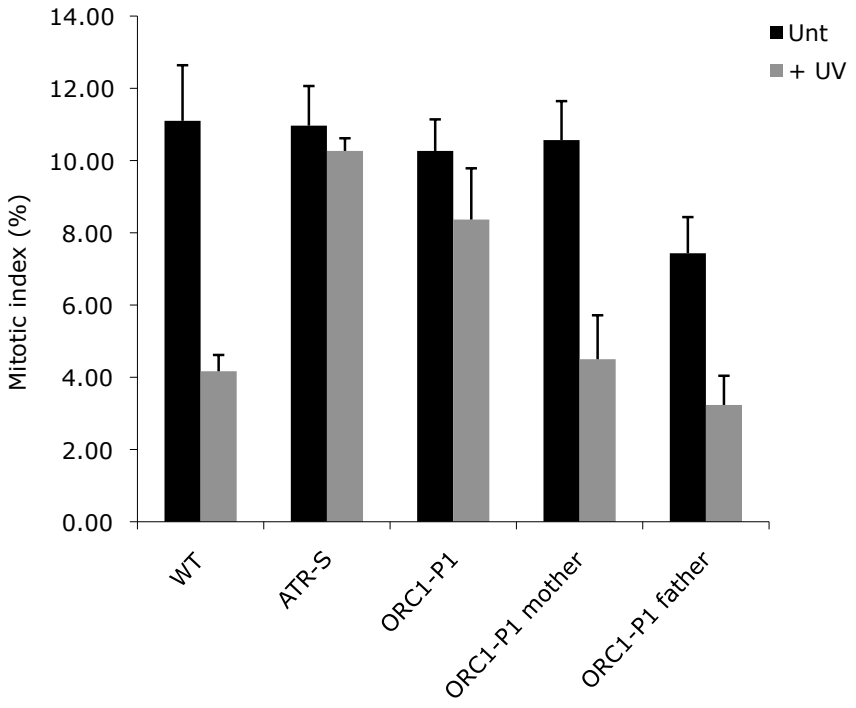

Figure 5.8 ORC1-P1 cells fail to efficiently activate the ATR-dependent G2/M checkpoint

WT, ATR-S, unaffected heterozygous relative (Mother, Father) and ORC1-P1 cell lines were examined for G2/M checkpoint arrest, 24hrs after treatment with $5J/m^2$ UV irradiation and in the presence of 1.5μM nocodazole. A decrease in the number of mitotic cells was taken as indicative of a G2/M arrest.

Graph represents the mean of three experiments. Error bars represent the standard deviation.

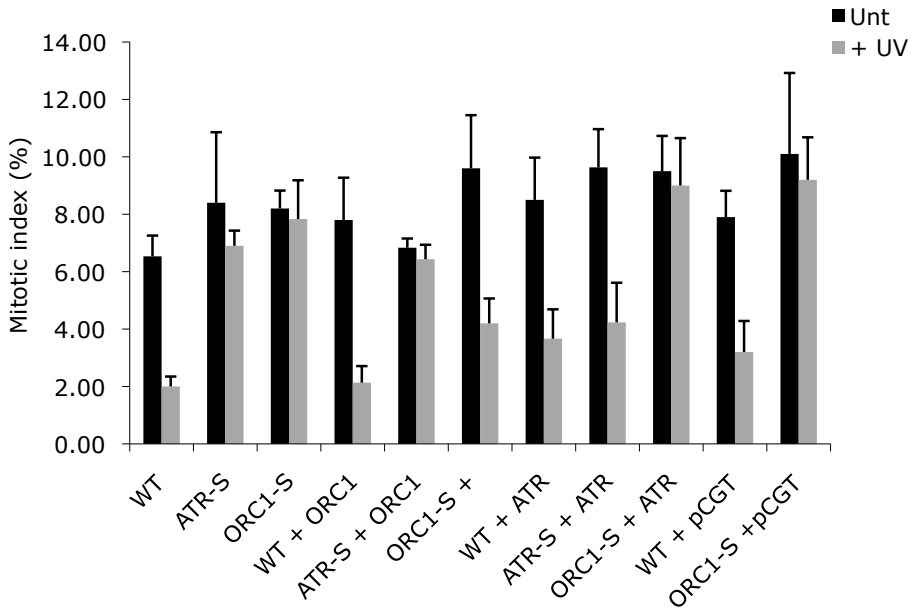

Figure 5.9 Transfection with WT ORC1 can complement the G2/M checkpoint arrest defect in ORC1-P1 cells

WT, ATR-S and ORC1-P1 cells were transfected with empty vector (pCGT), WT ATR or WT ORC1 DNA plasmids and examined for ATR-dependent checkpoint arrest, 24hrs after exposure to 5Jm^2 UV and in the presence of 1.5μM Nocodazole. A decrease in the mitotic index is indicative of G2/M checkpoint arrest.

The graph represents the mean of three independent experiments. Error bars represent the standard deviation.

a)

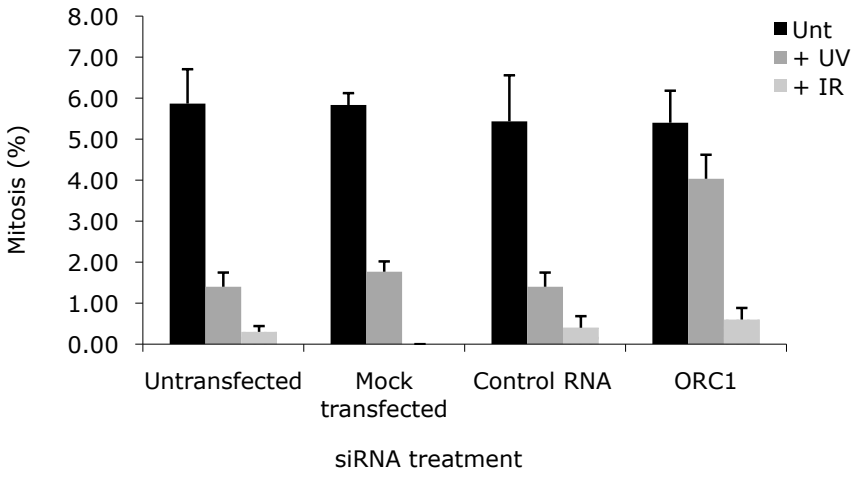

b)

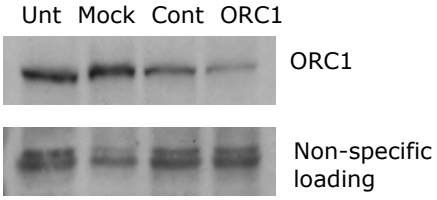

Figure 5.10 RNAi Depletion of ORC1 in MG63 osteosarcoma weed cells impairs ATR-dependent G2/M arrest

a) MG63 osteosarcoma cells were untransfected (Unt), mock transfected (Mock) or transfected with control (Cont) or ORC1 siRNA oligonucleotides for 72hrs and cells were then examined for G2/M arrest 2hrs after exposure to 5J/m^2 UV or 3 Gy IR. A decrease in the number of mitotic cells was taken as indicative of a G2/M arrest. Graph represents the mean of three independent experiments. Error bars represent the standard deviation.

b) Western blot confirming ORC1 depletion. A non-specific band was used as a loading control.

In conclusion, in this chapter I have shown that the mutations identified in *ORC1L* patients result in reduced levels of ORC1 protein and reduced localisation of ORC1 and other preRC components to the chromatin. This leads to defects in S phase progression, possibly due to reduced origin availability and compromised replication fork stability. ATR-dependent G2/M checkpoint activation is also defective and cells harbour supernumerary mitotic centrosomes. The G2/M checkpoint defect can be corrected by expression of WT ORC1 in patient cells and recapitulated by depletion of ORC1 in weed cells, demonstrating that ORC1 is required for ATR-dependent G2/M checkpoint activation.

5.3 DISCUSSION

In this chapter I have described the functional characterisation of a cell line with mutations in *ORC1L* and novel defects in replication origin licensing. This is the first time that mutations in a preRC component have been implicated in human disease.

At the same time as the data presented in this chapter was published, two other reports of preRC mutations were reported. Further mutations in *ORC1, ORC4, ORC6, CDT1* and *CDC6* were reported in patients presenting with Meier-Gorlin syndrome (MGS) (Bicknell *et al.*, 2011a) and another group reported mutations in *ORC4* in MGS (Guernsey *et al*., 2011). MGS is a microcephalic primordial dwarfism disorder, similar to SS, and has been discussed in the introduction section of this thesis. These patients present with microcephaly, short stature, absent patellae and small external ears.

The data presented in this chapter implicates impaired origin licensing as a possible cause of microcephalic dwarfism. A reduction in origin licensing, as evidenced by reduced levels of preRC proteins bound to the chromatin and the presence of smaller replication intermediates (Figure 5.11), has an impact on S-phase progression. Entry into S-phase was also found to be delayed in ORC1 deficient cells (Bicknell *et al.*, 2011b) suggesting that these cells require a longer time in G1 phase in order to assemble sufficient preRC's to enter into S-phase.

How does reduced origin licensing impact on cell cycle kinetics? If fewer origins are licensed due to limiting ORC1 levels, the time taken for cells to build up enough licensed origins to enter S phase will be increased. The 'licensing checkpoint' has been shown to prevent cells from entering S phase until they have sufficient numbers of licensed origins (Shreeram *et al.*, 2002, Blow and Gillespie, 2008).

Therefore the G1 phase in ORC1 cells is prolonged while origin licensing proceeds to the required level for S phase entry. It has been demonstrated that cells entering S phase with too few licensed origins synthesize their DNA at a reduced rate and accumulate DNA damage (Nevis *et al.*, 2009).

S phase progression could slow as there are less origins fired in any one stretch of DNA. Thus, forks have to travel further to complete replication, potentially making them less stable and more prone to stalling (Pruitt *et al.*, 2007, Shima *et al.*, 2007). If there are reduced licensed origins available, the firing of dormant origins may also be compromised with a failure to complete S phase in a timely manner. Conversely, more dormant origins may be fired than in a WT scenario due to the longer distance travelled by each fork. Dormant origins may be passively replicated (and inactivated) before they have a chance to fire. If fork progression is slowed, the dormant origins are more likely to fire as it takes longer for them to be inactivated (Blow and Ge, 2009). DNA fibre analysis would suggest that possibly more origins are fired within an 'active replication cluster' in ORC cells than WT cells, although this aspect requires further study. Indeed Chk1 depleted cells have been reported to show slow fork progression coupled with increased origin firing (Seiler *et al.*, 2007).

Another possibility is that the fork speed in ORC1 cells is reduced due to the reduction of components such as the MCM helicase bound to the chromatin. MCM moves along with the replication fork, unwinding the DNA ahead of the polymerase. Could reduced levels of MCM helicase lead to a slowing of the replication fork? This question could be addressed by analysis of fork speed from combed DNA fibres.

Although the changes in cell cycle kinetics described above do not seem to affect growth of cells in culture (data not shown), they could be important in development. In early neurogenesis, total cell cycle duration can be as short as 8 hrs with periods of rapid replication (Takahashi *et al.*, 1995). Increases in length of G1 phase in neuronal progenitor cells have been implicated in the switch from symmetric to asymmetric cell division, potentially decreasing the total number of neurons produced (Arai *et a*l., 2011). These authors also found that S phase duration was an important factor in the ability of progenitor cells to either continue to proliferate or to differentiate.

A perhaps surprising phenotype conferred by mutation in ORC1 is the loss of the ATR-dependent G2/M checkpoint. This phenotype is common to all SS cell lines

tested in our laboratory but why should a mutation in a pre-replication complex component result in a checkpoint defect? ORC1 has been shown to be required for control of centrosome numbers and to be localised to the centrosome (Hemerly *et al.*, 2009). We have previously identified mutations in centrosome components, such as PCNT, in SS patients and further mutations have been identified in CEP152 (Kalay *et al.*, 2011) and CENPJ (Al-Dosari *et al.*, 2010) in SS patients and in Primary Microcephaly patients. The centrosome is now regarded as an important organelle involved in cell cycle control (Doxsey *et al.*, 2005). It is possible that ORC1 that is localised at the centrosome plays some role in G2/M checkpoint regulation.

CDC6, another important preRC component interacts with ORC1 and is proposed to act as a monitor to ensure that replication is complete before cells enter mitosis (Lau *et al.*, 2006). Overexpression of CDC6 in G2 phase human cells prevents entry into mitosis but this block can be overcome by the use of a Chk1 inhibitor. The ability of CDC6 to block mitotic entry may be regulated by the phosphorylation of CDC6 at serine74 (Clay-Farrace *et al.*, 2003). These authors postulated that when CDC6 is not inactivated, Chk1 activation occurs and cells are not able to enter mitosis. It is possible that the function of CDC6 as a mitotic inhibitor requires its localisation at the chromatin or the centrosome through an interaction with ORC1.

CDC6 also interacts with ATR in a manner that is stimulated by Cdk phosphorylation (Yoshida *et al.*, 2010). These authors demonstrated that CDC6 is required for an ATR-dependent replication checkpoint after exposure to low doses of HU, representing low levels of replication stress. However they found no requirement for CDC6 after higher HU doses or after treatment with UV. CDC6 is, however, polyubiquitinated by the ubiquitin ligase Huwe1 upon exposure to UV and is subsequently degraded (Hall *et al.*, 2007).

In this chapter I have demonstrated that ORC1 deficiency leads to reduced origin licensing and a slowing of S-phase progression. I have presented data that ORC1 deficiency results in a defective UV-induced ATR-dependent G2/M checkpoint response in these cells. Supernumerary mitotic centrosomes are also observed in these cells, similar to other SS cell lines examined. Which of these cellular phenotypes correlate with the clinical features of the patients? The later two phenotypes are common to other microcephaly disorders such as Primary Microcephaly, therefore, in the next chapter I will attempt to examine the molecular

basis of the defective G2/M checkpoint response in cell lines derived from patients with MPD disorders.

CHAPTER SIX

RESULTS IV: Dissecting the molecular basis of the defective ATR-dependent G2/M checkpoint response in various MPD patient derived cell lines: Roles of Aurora A kinase and Polo-like kinase 1

6.1 INTRODUCTION

The cell lines that I have examined in this thesis have been shown to harbour mutations in proteins with diverse functions such as structural centrosomal proteins (PCNT), PreRC proteins (ORC1) and DNA damage response proteins (ATR-ATRIP). Each of the cell lines are derived from patients with MPD, although the precise clinical description of the patients varies from MGS to MOPDII to SS. All of these patients display microcephaly and growth retardation to varying degrees. One of the cellular phenotypes that all of these cell lines have in common is a defective ATR-dependent G2/M checkpoint response.

Control of mitotic entry is ultimately governed by levels and activity of the Cyclin dependent kinase, Cdk1 in complex with cyclin B. When DNA is damaged and mitotic entry must be delayed, the Chk1/Chk2 kinases have a well-established role in activating a G2/M checkpoint response, via their activation through ATM/ATR. This is achieved through the inhibition of the Cdc25 family of phosphatases, which are then unable to activate Cdk1. A further important mechanism existing in cells is regulation of the Aurora A kinase (AurA) and polo-like kinase 1 (PLK1). These kinases also play an important role in the control of mitotic entry. They are considered important for the 'commitment' step for entry into mitosis and regulate cyclinB-Cdk1 activation.

6.1.1 Aurora A Kinase (AurA)

AurA is a serine/threonine mitotic kinase (Figure 6.1) and is often overexpressed in tumours (Zhou *et al.*, 1998, Yang *et al.*, 2007, Otto *et al.*, 2009). It is localised to the centrosome during interphase, via interactions with centrosomin (CDK5RAP2) (Terada *et al.*, 2003) and CEP192 (Gomez-Ferreria *et al.*, 2007). It is also localised

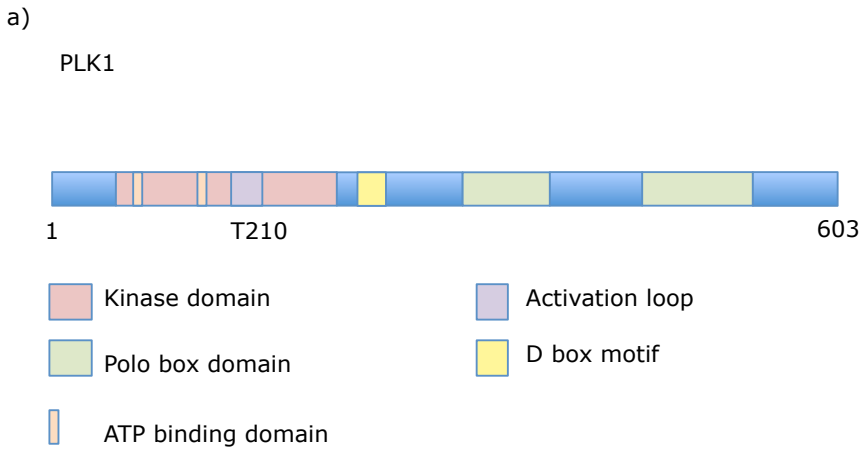

Figure 6.1 Protein schematic showing conserved domains

a) Polo-like kinase 1 (PLK1)
b) Aurora A Kinase (AurA)

at the spindle during mitosis via an interaction with Targeting Protein for Xenopus kinesin-like protein 2 (TPX2) (Kufer *et al.*, 2002). The localisation of AurA to the centrosome is promoted by PLK1 (van de Weerdt *et al.*, 2008). Depletion of CEP192 leads to a mis-localisation of AurA at the centrosomes of mitotic cells (Gomez-Ferreria *et al.*, 2007). Once located at the centrosome, AurA undergoes dimerisation and becomes activated, as evidenced by T288 autophosphorylation. CEP192 is not essential for this dimerisation process (Joukov *et al.*, 2010).

The full activation of AurA is complex, involving many cofactor proteins and activation steps. Phosphorylation of the T loop of AurA at threonine 288 (T288) results in a marked increase in kinase activity (Walter *et al.*, 2000). In Xenopus extracts, TPX2 stimulates AurA autophosphorylation at T295 (equivalent to T288 in humans) (Eyers *et al.*, 2003). In humans, the binding of TPX2 to AurA induces a conformational change in AurA and the T loop containing T288 becomes inaccessible to the PP1 phosphatase (Bayliss *et al.*, 2003), which dephosphorylates this site during interphase to inhibit AurA (Eyers *et al.*, 2003). The binding of TPX2 confers a protective effect to AurA, preventing its degradation and enabling the accumulation of AurA levels during G2 phase. However, the earliest centrosomal pool of AurA, detected at this location in interphase, does not require this TPX2-dependent stabilisation (Giubettini *et al.*, 2011). TPX2 binding may therefore be more important for localizing AurA to the spindle, rather than the centrosome, to perform its role in spindle formation (Kufer *et al.*, 2002).

In human cells, Ajuba interacts with AurA at the centrosome during G2 and mitosis, promotes the phosphorylation of AurA at T288 and is required for the activation of AurA at the centrosomes. Active AurA can first be detected in late G2 phase at the centrosomes, before full activation in early mitosis and appears to be required for the initial recruitment of cyclinB-Cdk1 to the centrosome (Hirota *et al.*, 2003). This initial activation of AurA at the centrosome is Cdk1 independent. In Drosophila neuroblasts Ajuba was shown to be important in maintaining active AurA at the centrosome but was not required for the activation of AurA (Sabino *et al.*, 2011).

In contrast to this initial activation of AurA in G2, full mitotic activation of AurA is Cdk1 dependent with positive feedback loops of Cdk1, AurA and PLK1 leading to swift co-activation of these kinases (Figure 6.2) (Van Horn *et al.*, 2010). However, several studies have indicated that AurA and PLK1 are not essential for mitotic entry under normal cell cycle conditions, although they can accelerate entry into mitosis (van Vugt *et al.*, 2004). These kinases only become essential for mitotic entry following recovery from DNA damage-induced arrest (van Vugt *et al.*, 2004,

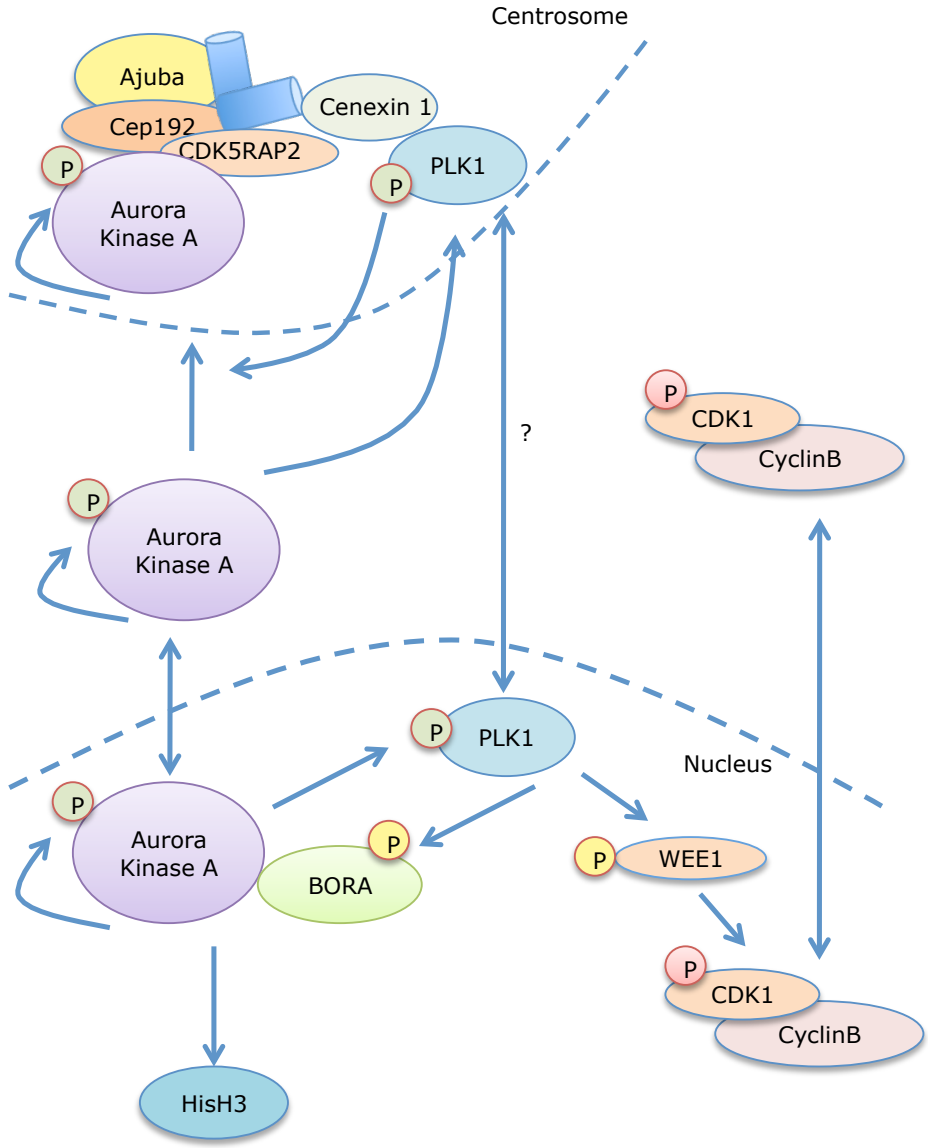

Figure 6.2 PLK1 and AurA function during mitotic entry

Green phosphates (P) are activating, red are inhibitory and yellow prime the protein for degradation. In late G2 AurA and PLK1 are recruited to the centrosome. PLK1 is recruited by cenexin1 and promotes the recruitment of AurA. AurA binds to CDK5RAP2. Cep192 and Ajuba are also important to localise AurA to the centrosome. AurA once located at the centrosome undergoes dimerisation and can be activated by autophosphorylation. AurA activity is enhanced by BORA. AurA in conjunction with BORA activates PLK1 in G2 but it is unclear whether this occurs in the nucleus, on centrosomes or in the cytoplasm. Active PLK1 can phosphorylate WEE1, which negatively regulates CDK1-CyclinB complexes.

Figure and legend adapted from Lens at al, 2010. Nature Reviews Cancer

Macůrek *et al.*, 2008). Furthermore, overexpression of AurA overrides the G2/M damage-induced checkpoint (Marumoto *et al.*, 2002), whilst depletion of AurA by siRNA treatment leads to a block to mitotic entry in some studies (Hirota *et al.*, 2003) or a delay to mitotic entry in others (Marumoto *et al.*, 2002, Marumoto *et al.*, 2003).

A further interaction partner of AurA in human cells is Bora. Bora is able to bind to AurA and activate the kinase in vitro (Hutterer *et al.*, 2006).The interaction between Bora and AurA is essential for AurA to phosphorylate its target PLK1. Following phosphorylation of Bora on serine 252 by Cdk1 (Chan *et al.*, 2008), Bora binds to PLK1 in G2 and increases the accessibility of the T210 site for phosphorylation by AurA (Seki *et al.*, 2008). PLK1 in turn regulates AurA levels by phosphorylation of a phosphodegron site in Bora. This leads to degradation of Bora by the $SCF^{\beta\text{-}TrCP}$ ubiquitin ligase (Chan *et al.*, 2008), resulting in a reduction in levels of active AurA.

AurA can also be activated in vitro by Protein Kinase A (PKA), which phosphorylates at least three sites including T288 (Eyers and Maller, 2003). Dephosphorylation of T288 by Protein phosphatase 1 (PP1) or Protein phosphatase 2 (PP2) is also known to occur, inhibiting the kinase activity of AurA during interphase (Walter *et al.*, 2000, Katayama *et al.*, 2001).

Interestingly, in terms of SS cell lines and the defective ATR-dependent G2/M checkpoint response observed, AurA kinase activity is inhibited following DNA damage. This occurs in a manner dependent on ATR/ATM signaling through the Chk1 kinase (Krystyniak *et al.*, 2006). No direct interaction between Chk1 and AurA has been detected, suggesting that further proteins could be involved in this signaling pathway. AurA is also known to phosphorylate CDC25B on serine 353, an event that occurs at the centrosome. This phosphorylation event is also inhibited after DNA damage (Cazales *et al.*, 2005).

AurA also binds to BRCA1 and phosphorylates this protein at serine 308. BRCA1 is present at the centrosomes during the G2/M transition and has been postulated to play a role in G2/M progression (Ouchi *et al.*, 2004).

Just before mitotic entry, centrosomes increase in both size and microtubule nucleating capability, in a process termed centrosome maturation (Carmena *et al.*, 2009). AurA contributes to this process by phosphorylation and recruitment of pericentriolar material proteins such as Transforming acidic coiled-coil protein

(TACC) (Barros *et al.*, 2005), Centrosomin (CDK5RAP2) (Hannak *et al.*, 2001), Large tumor suppressor homolog 2 (LATS2) (Toji *et al.*, 2004) and Nuclear distribution element-like 1 (NDEL1) (Mori *et al.*, 2007). PLK1 is also required for the initiation of centrosome maturation and was recently shown to phosphorylate PCNT at the onset of mitosis to facilitate this process (Lee and Rhee, 2011). PLK1 inhibition has also been demonstrated to lead to a reduction in the recruitment of CEP192 and PCNT to the centrosome in mitotic cells although this mechanism does not appear to be important in interphase cells (Haren *et al.*, 2009).

AurA is also localized at the basal body of the primary cilia. It is activated here by human enhancer of filamentation 1 (HEF1), resulting in the phosphorylation of ciliary Histone Deacetylase 6 (HDAC6) (Pugacheva *et al.*, 2007). Ciliary resorption is then induced, a process that has been postulated to be important for cell cycle re-entry (Kim and Tsiokas, 2011). In mammalian cells, Ajuba has also been shown to localize to the basal body and is required for ciliogenesis (Nagai *et al.*, 2010).

AurA is essential for embryonic development as AurA-/- mice are embryonic lethal and early embryos from these mice do not survive beyond the sixteen cell stage of development (Lu *et al.*, 2008b). Fibroblasts from heterozygous AurA+/- mice showed higher levels of aneuploidy and heterozygous mice have an increased incidence of tumour formation compared to WT mice.

6.1.2 Polo-like kinase 1 (PLK1)

PLK1 is a member of the Polo-like kinase family of serine/threonine kinases (Figure 6.1). There are five mammalian PLKs: PLK1, PLK2, PLK3, PLK4 and the recently identified PLK5. They possess a highly conserved N-terminal kinase domain and a C-terminal polo-box domain, which is more divergent (Kishi *et al.*, 2009). PLK1 functions in multiple cellular processes including mitotic entry, centrosome maturation, spindle formation, chromosome segregation, cytokinesis and mitotic exit (Lens *et al.*, 2010).

PLK1 has also recently been demonstrated to participate in the regulation of DNA replication as depletion of PLK1 can disrupt pre-RC formation and reduce DNA synthesis (Yim and Erikson, 2009). PLK1 interacts with pre-RC proteins such as MCM7 (Tsvetkov and Stern, 2005a) and ORC2 (Song *et al.*, 2011). An interaction of PLK1 with Timeless was also observed, predominately in G2/M phase cells and a function for this complex in the coordination of S phase and mitotic events was

proposed (Dheekollu *et al.*, 2011). In Xenopus extracts, the recruitment of Plx1 to the chromatin was shown to be dependent on the phosphorylation of MCM2 by ATR and important for the prevention of replication associated DNA breakage (Trenz *et al.*, 2008).

PLK1, like AurA, is required for embryonic development as PLK1-/- mice are embryonic lethal and early embryos from these mice do not survive beyond the eight cell stage of development (Lu *et al.*, 2008a). In this study, heterozygous PLK1+/- mice also went on to develop tumours, at an incidence that was three-fold higher than WT counterparts.

PLK1 is located at the centrosome in interphase and early prophase via an interaction between the polo-box domain of PLK1 and centrosomal proteins such as cenexin1 (Soung *et al.*, 2006). It is highly dynamic at mitotic centrosomes and complete removal of the kinase domain causes the protein to stably associate with the centrosome, suggesting that the release of PLK1 from the centrosome is facilitated by its kinase activity (Kishi *et al.*, 2009). Later in mitosis PLK1 becomes located at the midbody, spindle and kinetochores. Thus the kinase-dependent release from the centrosomes may be important for the relocation of PLK1 to these structures in late mitosis. Additionally, PLK1 anchored at the centrosome prevents proper mitotic progression, inducing a G2 delay (Kishi *et al.*, 2009).

PLK1 is activated several hours before the onset of mitosis by phosphorylation of threonine 210 in the T loop of the kinase. This phosphorylation is performed by AurA in G2, in concert with Bora (Seki *et al.*, 2008), and active PLK1 is present on the centrosomes in G2. It is not known if the AurA-dependent activation of PLK1 occurs at this location or in the nucleus. Depletion of AurA, however, does reduce the phosphorylation at T210 of centrosomally located PLK1 (Macůrek *et al.*, 2008).

Cdk1 dependent phosphorylation of many target proteins such as WEE1, Myt1 and Cdc25c creates a 'docking site' for PLK1 (Elia *et al.*, 2003a, Elia *et al.*, 2003b), allowing the targeting of PLK1 to many Cdk1 substrates. PLK1 phosphorylates Cdc25C at serine 198, promoting its nuclear translocation (Roshak *et al.*, 2000, Toyoshima-Morimoto *et al.*, 2002), phosphorylates Myt1 and inhibits its kinase activity (Nakajima *et al.*, 2003, Inoue and Sagata, 2005) and phosphorylates WEE1 resulting in its ubiquitination and degradation via the $SCF^{\beta\text{-}TrCP}$ complex (Watanabe *et al.*, 2004). PLK1 also regulates Cdc25B activity by promoting its nuclear localization (Lobjois *et al.*, 2009). CyclinB1 is phosphorylated on serine 147 by PLK1, promoting its accumulation in the nucleus (Toyoshima-Morimoto *et al.*,

2001). PLK1 therefore activates or inhibits many targets involved in cell cycle control in order to facilitate mitotic entry.

Similarly to AurA, the activation of PLK1 is also inhibited after DNA damage (Smits *et al.*, 2000) in a manner dependent on ATM or ATR (van Vugt *et al.*, 2001). Further studies showed that the phosphorylation of PLK1 at S137 and T210 are inhibited in response to DNA damage, in a manner dependent on ATM/ATR and Chk1/Chk2 (Tsvetkov and Stern, 2005b). PLK1 kinase activity is also inhibited in an ATR-dependent manner after topoisomerase II inhibition (Deming *et al.*, 2002). The overexpression of an activated PLK1 T210D phospho-mimetic mutant causes abrogation of the G2/M checkpoint and cells are able to enter and progress through mitosis (Smits *et al.*, 2000). PLK1 is degraded by the APC/C^{Cdh1} after damage, mediated by the Cdh1 binding site on PLK1. This degradation is proposed to be critical for the initiation and maintenance of the G2/M checkpoint and is suggested to be necessary for the inhibition of Cdk1 after damage (Bassermann *et al.*, 2008).

The role of PLK1 in mitotic exit is proposed to be via its regulation of CDC6. The phosphorylation of CDC6 on T37 by PLK1 results in an inhibition of CDK1 and the activation of Separase, promoting chromosome segregation (Yim and Erikson, 2010).

53BP1, a checkpoint mediator protein involved in the G2/M checkpoint response to ionizing radiation, has also been shown to interact with PLK1. It was speculated to act as a scaffold to facilitate an interaction between PLK1 and Chk2. Direct phosphorylation of Chk2 by PLK1 results in a down regulation of Chk2 activity and allows release from the checkpoint (van Vugt *et al.*, 2010).

PLK1 also directly activates Forkhead Box M1 (FoxM1), an enhancer of transcription, which then stimulates the transcription of many genes involved in mitotic entry such as cyclinB1, PLK1 and the Cdc25 phosphatases (Fu *et al.*, 2008).

It has recently been demonstrated in C. Elegans and Drosophila that PLK1, Bora and AurA play a role in asymmetric cell division through acting on PAR and NUMB proteins (Budirahardja and Gönczy, 2008, Wirtz-Peitz *et al.*, 2008, Khazaei and Püschel, 2009, Noatynska *et al.*, 2010). This could highlight a role for these proteins in the maintenance of stem cell populations and brain development.

Due to the above documented links between AurA and PLK1 with the DNA damage response, the centrosomal location of these proteins and their possible role in

asymmetric cell division, I undertook an examination of the regulation of these proteins after damage in a subset of MPD cell lines. G2/M checkpoint defects in response to UV irradiation are a consistently observed phenotype in all MPD cell lines that I have examined. These cell lines carry mutations in diverse proteins such as ATR, ATRIP, PCNT and ORC1. A common feature of all of these proteins is their localization at the centrosome. We have also observed G2/M checkpoint defects in cell lines with mutations in other centrosomal proteins such as MCPH1 (Alderton *et al.*, 2006) and ASPM (data not shown). The ATR-dependent Chk1 phosphorylation in these cell lines is not consistently defective, although the defect may lie downstream of global Chk1 phosphorylation, such as in PCNT mutated cells, where Chk1 is not effectively localized at the centrosome (Chapter Three). The aim of this chapter was to examine a panel of MPD cell lines and attempt to dissect the molecular basis underlying the ATR-dependent G2/M checkpoint defect observed.

6.2 RESULTS

6.2.1 Meier-Gorlin syndrome cells fail to activate the ATR-dependent G2/M checkpoint

ATR-Seckel cells have previously been shown to display a defective G2/M checkpoint response both 24 hours (Alderton *et al.*, 2004) and 2 hours (Stiff *et al.*, 2008) post UV irradiation. ORC1-MPD (Chapter Five) and PCNT mutated cells (Griffith *et al.*, 2008) have also been shown to display a defective G2/M checkpoint response to UV exposure. Due to the unexpected finding that ORC1 may be required for efficient ATR-dependent G2/M checkpoint arrest, LBL cells from patients with MGS with further mutations in preRC components (Table 8) were assessed for the ability to arrest at the G2/M checkpoint 24 hr after exposure to UV irradiation. LBL's with mutations in *CDC6, CDT1, ORC4* and *ORC6* all failed to arrest at the G2/M checkpoint following UV exposure, similar to the ATR-S line and in contrast to the WT cell line (Figure 6.3). This result suggests that all of the preRC components examined are required for an efficient ATR-dependent G2/M checkpoint response.

6.2.2 Phosphorylation of Chk1 after UV exposure is defective in Cdc6-MGS patient cell lines

Cdc6 interacts with ATR (Chung and Bunz, 2010, Yoshida *et al.*, 2010) and is able to arrest cells in G2 in a Chk1 dependent manner (Clay-Farrace *et al.*, 2003). In

Gene	Amino Acid Alterations	Current Height (SD)	Current OFC (SD)	Microtia	Absent/small Patellae
ORC1	R105Q + V667fsX24	-9.6	-9.8	+	+
ORC4	Y174C	-4.2	-2.1	+	-
ORC6	F86X + Y232S	-3.3	-1.6	+	+
CDT1	R462Q + Y520X	-1.6	+1.7	+	+
CDC6	T323R	-4.1	-3.3	+	+

Table 8 PreRC mutations in MGS patients

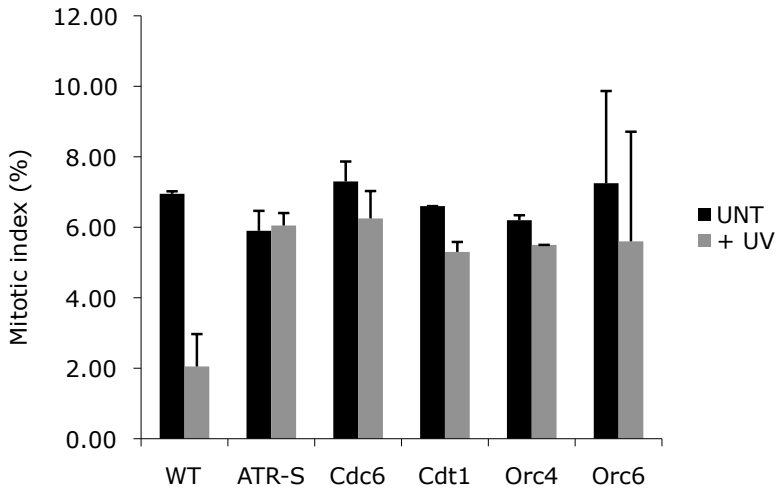

Figure 6.3 Meier-Gorlin Syndrome cells display a defective UV-induced G2/M checkpoint.

WT, ATR-S and Meier-Gorlin Syndrome cell lines with mutations in pre-replication complex components were examined for G2/M checkpoint arrest 24hrs after treatment with 5J/m2 UV irradiation and in the presence of 1.5μM Nocodazole. A decrease in the number of mitotic cells was taken as indicative of a G2/M arrest.

The graph represents the mean of three independent experiments. The error bars represent the standard deviation.

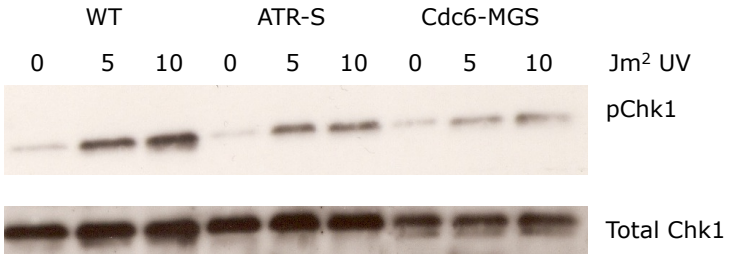

Figure 6.4 Chk1 phosphorylation after UV exposure is defective in the Cdc6 MGS cell line

WT, ATR-S and Cdc6-MGS LBL patient cell lines were treated with 5 or 10 J-m^2 UV and cell pellets harvested 1hr later. Whole cell extracts were then resolved on a 8% SDS-PAGE and transferred onto a PVDF membrane. Membranes were then probed with an anti-phospho Chk1 (ser317) antibody. Total Chk1 levels were used as a loading control.

order to determine at which point in the ATR signaling pathway Cdc6 could be functioning, the phosphorylation of Chk1 after UV irradiation was examined. Cdc6-MGS patient LBL's were assessed for their ability to phosphorylate Chk1 at ser317 after exposure to UV irradiation using western blotting. After both 5J and 10J of UV irradiation, Chk1 phosphorylation in the Cdc6 cell line was found to be reduced compared to the WT response and similar to the ATR-S line (Figure 6.4). This result suggests that Cdc6 is required for the efficient ATR-dependent phosphorylation of Chk1.

6.2.3 Inhibition of PLK1 can rescue the ATR-dependent G2/M checkpoint defect in several MPD cell lines

Several MPD cell lines that have already been characterized in this thesis were chosen for further study. Why should lines with mutations in proteins of diverse function such as centrosomal proteins and pre-replication complex proteins all result in G2/M checkpoint defects? As described in the introduction to this chapter, PLK1 is inhibited after damage in a manner dependent on ATR/ATM (van Vugt *et al.*, 2001). We therefore considered the possibility that as PLK1 must be inhibited in order to prevent mitotic entry following DNA damage, ATR-dependent PLK1 inhibition may not occur efficiently in these MPD cell lines. In order to test this hypothesis, cell lines with ATR-dependent G2/M checkpoint defects were treated with PLK1 inhibitor BI2536 for 15 minutes prior to UV treatment and maintained for two hours post UV exposure. Cultures were also treated with Colcemid in order to block cells at metaphase, thus eliminating the influence of the checkpoint exit function of PLK1 on the data. Cells were then examined for the ability to arrest at the G2/M checkpoint by analysis of mitotic index. Treatment with the PLK1 inhibitor rescued the ATR-dependent G2/M checkpoint defect observed in all cell lines tested, ATR-S, PCNT-S, ORC1-P1 and CDC6 (Figure 6.5a). The PLK1 inhibitor failed to rescue the G2/M checkpoint defect observed in ATM deficient LBL cells following exposure to IR, indicating a role for PLK1 in the ATR-dependent checkpoint pathway specifically (Figure 6.5b). The number of mitotic cells with monopolar spindles increased after PLK1 inhibition from 3.4% to 94.8% (data not shown), indicating that PLK1 was effectively inhibited under these experimental conditions.

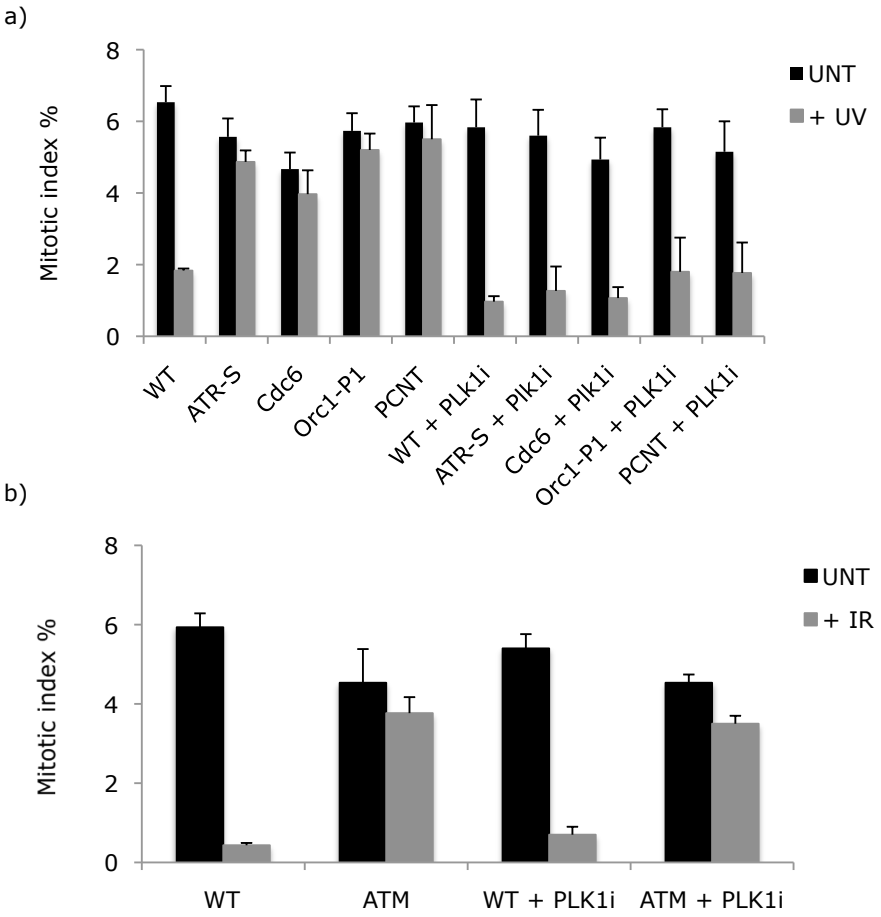

Figure 6.5 PLK1 inhibition rescues the UV induced G2/M checkpoint defect observed in Seckel Syndrome and Meier-Gorlin Syndrome cell lines but fails to rescue the IR-induced G2/M checkpoint defect observed in an ATM deficient cell line.

a) WT, ATR-S, ORC1-P1-S, PCNT-S and Meier-Gorlin Syndrome Cdc6 LBL cell lines were examined for G2/M checkpoint arrest, 2hrs after treatment with 5J/m^2 UV irradiation and in the presence of 0.2µg/mL Colcemid. PLK1 inhibitor BI2536 (PLK1i) 100nM was added to indicated cultures 15 min prior to UV exposure and maintained for 2hrs prior to harvest. A decrease in the number of mitotic cells was taken as indicative of a G2/M arrest.

b) WT and ATM deficient LBL's were examined for G2/M checkpoint arrest 2hrs after treatment with 3Gy Ionising Radiation and in the presence of 0.2µg/mL Colcemid. PLK1 inhibitor BI2536 (PLK1i) 100nM was added to the indicated cultures 15 min prior to IR exposure and maintained for 2hrs prior to harvest. A decrease in the number of mitotic cells was taken as indicative of a G2/M arrest.

Each graph represents the mean of three independent experiments. The error bars represent the standard deviation.

6.2.4 Inhibition of AurA can rescue the ATR-dependent G2/M checkpoint defect in several MPD cell lines

AurA, the upstream kinase that phosphorylates PLK1, is also inhibited following DNA damage, in a manner dependent on ATR/ATM and Chk1 (Krystyniak *et al.*, 2006). In order to determine whether the inhibition of AurA after DNA damage is similarly inefficient in the MPD cell lines examined, the Aurora kinase inhibitor MLN8237 was added to cell cultures prior to UV treatment and maintained for two hours post treatment. Cells were examined for the ability to arrest at the G2/M checkpoint by analysis of mitotic index. Again, treatment with the AurA inhibitor rescued the ATR-dependent G2/M checkpoint defect observed in all cell lines tested, ATR-S, PCNT-S, ORC1-P1 and CDC6 (Figure 6.6a). The AurA inhibitor failed to rescue the G2/M checkpoint defect observed in ATM deficient LBL cells following exposure to IR, indicating that AurA also plays a role in the ATR-dependent checkpoint pathway specifically (Figure 6.6b). The number of mitotic cells with monopolar spindles in AurA inhibited cultures increased from 2% to 19.2% (data not shown), indicating that AurA was effectively inhibited under these experimental conditions.

6.2.5 Phosphorylated PLK1 T210 levels are not appropriately downregulated following UV exposure in ORC1-P1 MPD patient cell lines

Phosphorylation of the PLK1 T210 site is inhibited after DNA damage (Tsvetkov and Stern, 2005b) in a manner dependent on ATR/ATM and Chk1/Chk2. In order to determine how PLK1 T210 phosphorylation is regulated in MPD LBL's, WT and ORC1-P1 cells were treated with $30Jm^{-2}$ UV and then cells harvested 30 minutes or 2 hours later. Extracts were prepared and levels of PLK1 phosphorylated at threonine 210 were examined by western blotting. In WT cells, inhibition of this phosphorylation could be clearly seen 30 minutes after UV exposure and levels of phosphorylation were still diminished at 2 hours post UV exposure (Figure 6.7). In ORC1-P1 cells, some inhibition was observed but levels of phosphorylated T210 PLK1 remained at higher levels than that seen in the WT at both 30 minutes and 2 hours post UV exposure. This raises the possibility that in ORC1-P1 cells, there is a failure to inhibit the phosphorylation of PLK1 at threonine 210 after DNA damage caused by UV irradiation. This suggests that PLK1 activity remains high, contributing to an inability to activate the G2/M checkpoint and allowing cells to enter mitosis even in the presence of DNA damage.

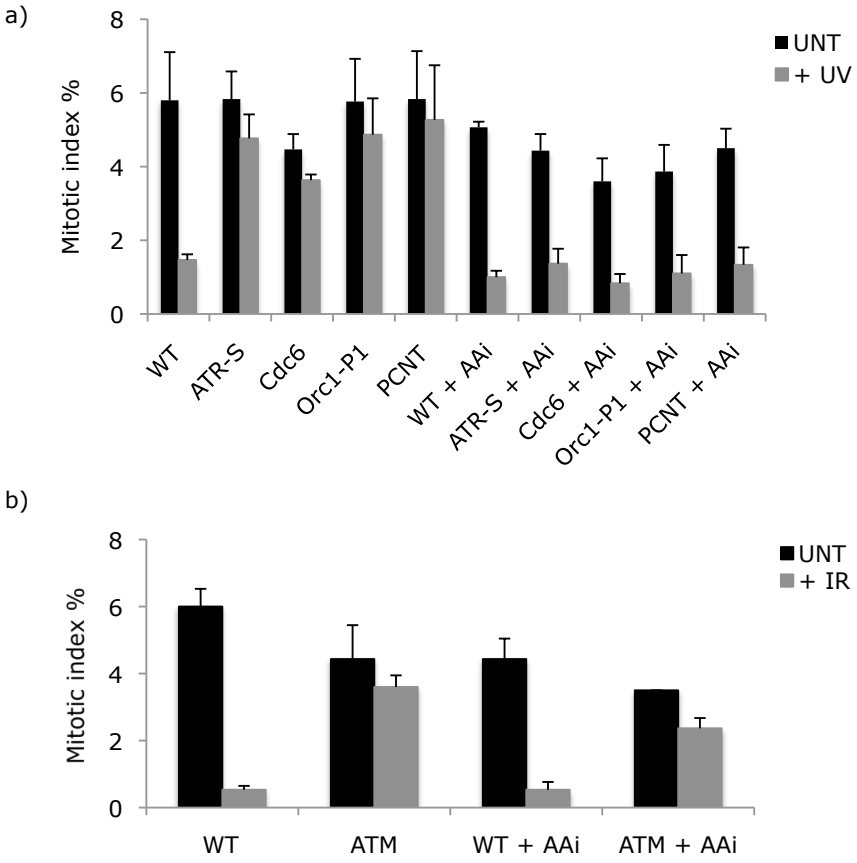

Figure 6.6 Aurora A Kinase inhibition rescues the UV induced G2/M checkpoint defect observed in Seckel Syndrome and Meier-Gorlin Syndrome cell lines but fails to rescue the IR-induced G2/M checkpoint defect observed in an ATM deficient cell line.

a) WT, ATR-S, ORC1-P1, PCNT and Meier-Gorlin Syndrome Cdc6 LBL's were examined for G2/M checkpoint arrest, 2hrs after treatment with 5J/m^2 UV irradiation and in the presence of 0.2µg/mL Colcemid. Aurora A Kinase inhibitor MLN8237 (AAi) 250nM was added to indicated cultures 15 min prior to UV exposure and maintained for 2hrs prior to harvest. A decrease in the number of mitotic cells was taken as indicative of a G2/M arrest.

b) WT and ATM deficient LBL's were examined for G2/M checkpoint arrest 2hrs after treatment with 3Gy ionising radiation and in the presence of 0.2µg/mL Colcemid. Aurora A Kinase inhibitor MLN8237 (AAi) 250nM was added to the indicated cultures 15 min prior to IR exposure and maintained for 2hrs prior to harvest. A decrease in the number of mitotic cells was taken as indicative of a G2/M arrest.

Each graph represents the mean of three independent experiments. The error bars represent the standard deviation.

a)

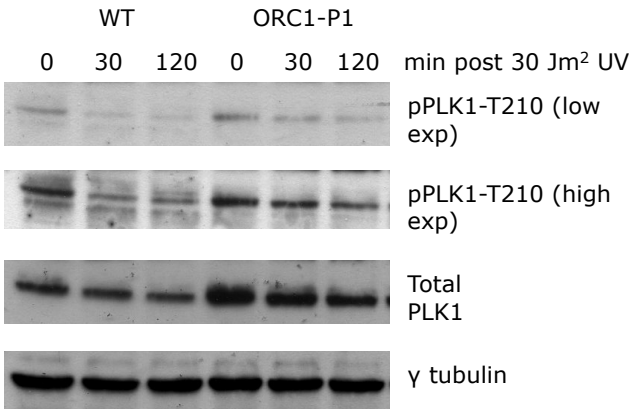

b)

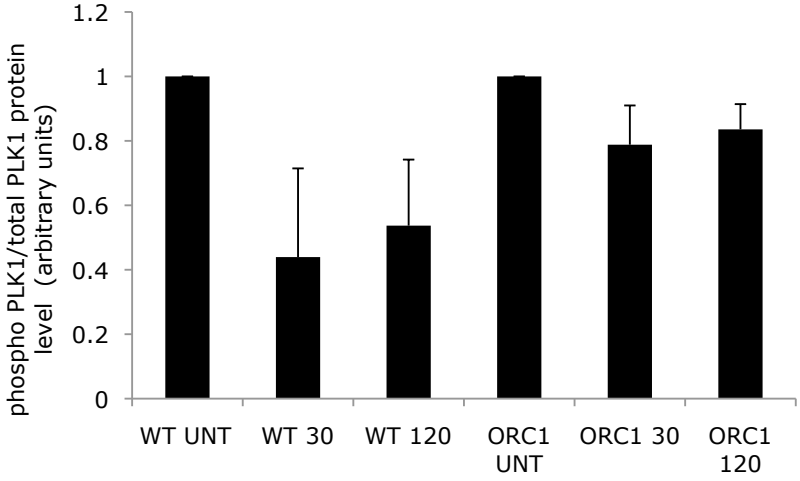

Figure 6.7 Phosphorylated PLK1 T210 levels are not appropriately downregulated following UV exposure in an ORC1-P1 MPD cell line

a) WT and ORC1-P1 MPD patient LBL's were treated with 30 Jm^2 UV and cell pellets harvested 30 min and 2 hr later. Whole cell extracts were then resolved on a 8% SDS-PAGE and transferred onto a PVDF membrane. Membranes were then probed with an anti-phospho PLK1 (Thr210) antibody. Total PLK1 levels were also examined. γ tubulin was used as a loading control.

b) Protein levels of phospho PLK1 (Thr210) were quantified from two independent immunoblotting experiments. Protein levels of total PLK1 were quantified from one immunoblotting experiment. The graph shows the phospho PLK1 (T210) protein levels relative to total PLK1 protein levels. Error bars represent the standard deviation.

6.2.6 Phosphorylated Aurora A T288 levels at the centrosome are not appropriately regulated following UV exposure in MPD cell lines.

In order to confirm and extend the finding that PLK1 T210 phosphorylation is not appropriately inhibited following damage in ORC-P1 MPD cells, an examination of the regulation of AurA phosphorylation at the centrosome was undertaken. Cells were treated with $30Jm^{-2}$ UV irradiation and slides prepared 30 min later. Slides were stained using techniques to visualize centrosomes, using γ-tubulin as a centrosomal marker and co-staining with an antibody towards AurA phosphorylated at threonine 288, or an antibody for Total AurA. The T288 site is an autophosphorylation site on AurA and indicates that the kinase is activated (Walter *et al.*, 2000). AurA was found to be present only at those cells containing two centrosomes, and highly expressed in mitotic cells. As the role of AurA in G2/M checkpoint regulation was of interest, mitotic cells were excluded from further analysis. Z series of 0.2μM stack images were acquired using softWorX software on a Deltavision microscope. Images were then imported into ImageJ software and a standard region of interest for the centrosomes defined. A Z-projection of the stack images was performed and a summed intensity measured at each centrosome in at least 20 cells per experiment. An intensity measurement was taken within each cell, outside the centrosome, and subtracted as background. In WT cells UV treatment resulted in a reduction in signal intensity of AurA phosphorylated on T288, but not of total AurA protein at the centrosome. The intensity of phosphorylated AurA signal decreased by approximately 50% in three independent experiments (Figure 6.8) and this reduction was statistically significant (Figure 6.9). In contrast, the phosphorylation of AurA at T288 did not decrease after treatment with UV irradiation in any of the MPD cell lines examined. In the ATR-S line there was a small, statistically significant, increase in total AurA at the centrosome following exposure to UV irradiation. The reason for this is unclear, however, the levels of phosphorylated T288 AurA at the centrosome remain unchanged in the ATR-S line after damage. Overall, this result indicates that there is a failure to inhibit the phosphorylation of AurA at T288 after DNA damage in MPD patient cell lines, suggesting that this kinase remains active in these cells. This could again contribute to the failure of these cells to activate a G2/M checkpoint in response to DNA damage.

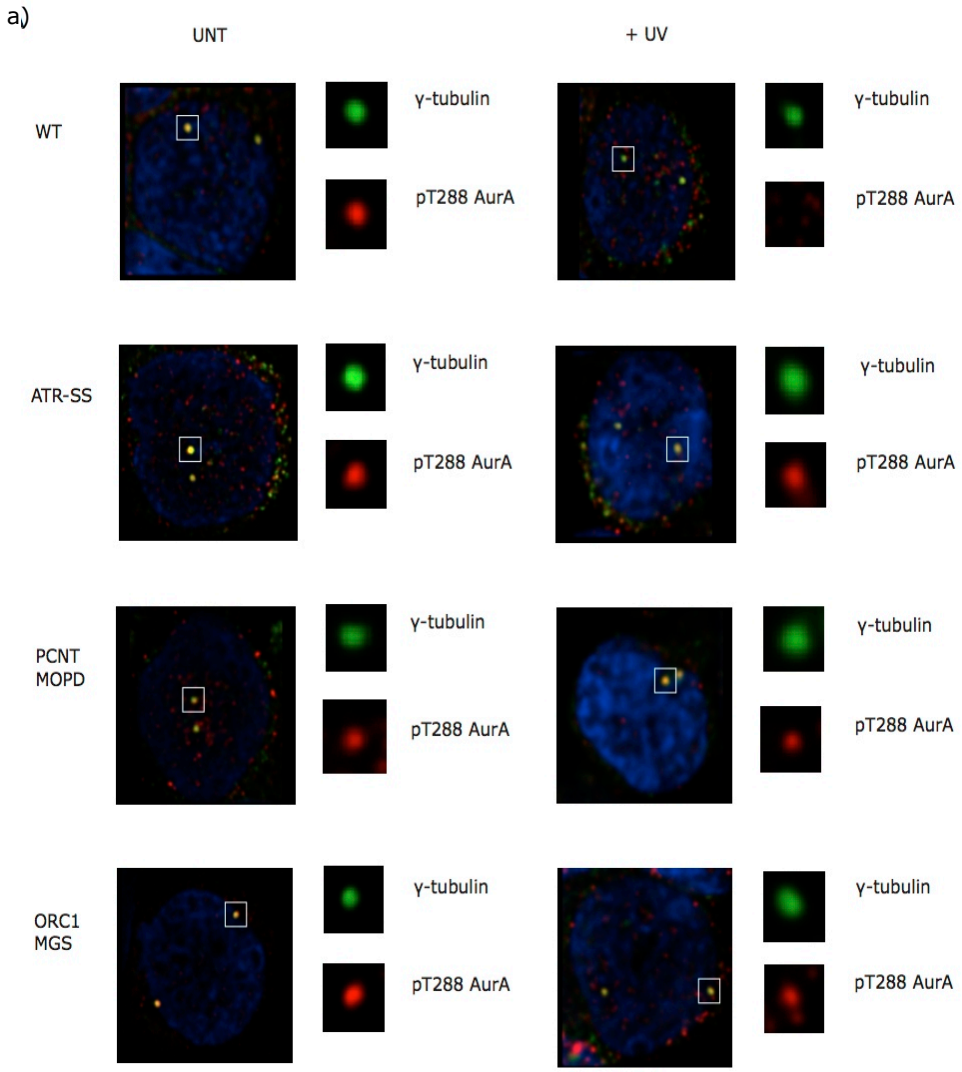

Figure 6.8a Phosphorylation of Aurora A at the centrosome is not appropriately regulated following exposure to UV in Seckel syndrome cells

WT, ATR-S, PCNT and ORC1 LBL cell lines were untreated (UNT) or treated with 30 J/m^2 UV and slides prepared after 30 min. Slides were stained using techniques to identify the centrosomal pool of phosphorylated Aurora A (red). Centrosomes were identified by co-staining with a γ-tubulin marker (green). Aurora A signal was only detected in cells possessing two centrosomes. Deconvolved images from Deltavision stacks.

b)

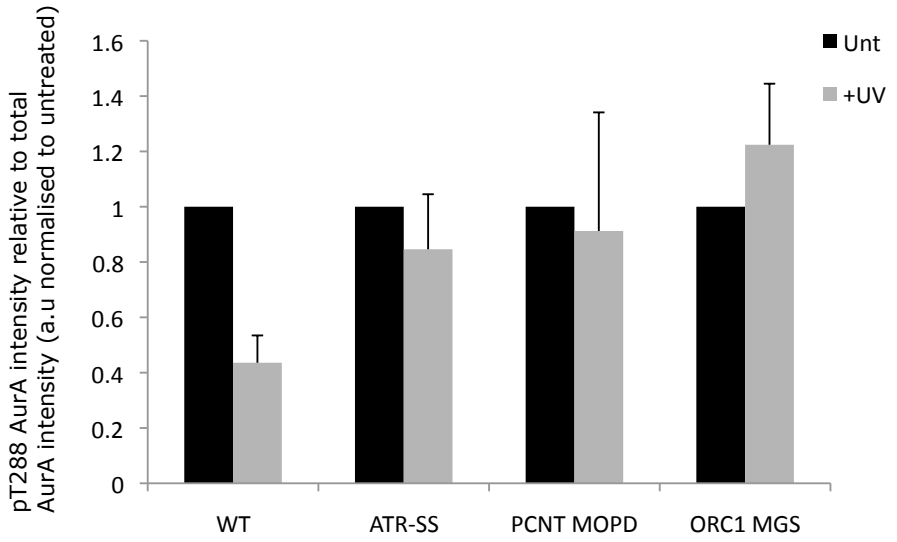

Figure 6.8b Phosphorylation of Aurora A at the centrosome is not appropriately regulated following exposure to UV in Seckel syndrome cells

The level of phosphorylated Aurora A at the centrosome was quantified in 20 cells in three independent experiments. The level of total Aurora A at the centrosome was also quantified in 20 cells in three independent experiments. Mitotic cells were not included in this analysis. The graph represents the normalised mean intensity of phospho AurA relative to total AurA signal. Error bars represent the standard deviation.

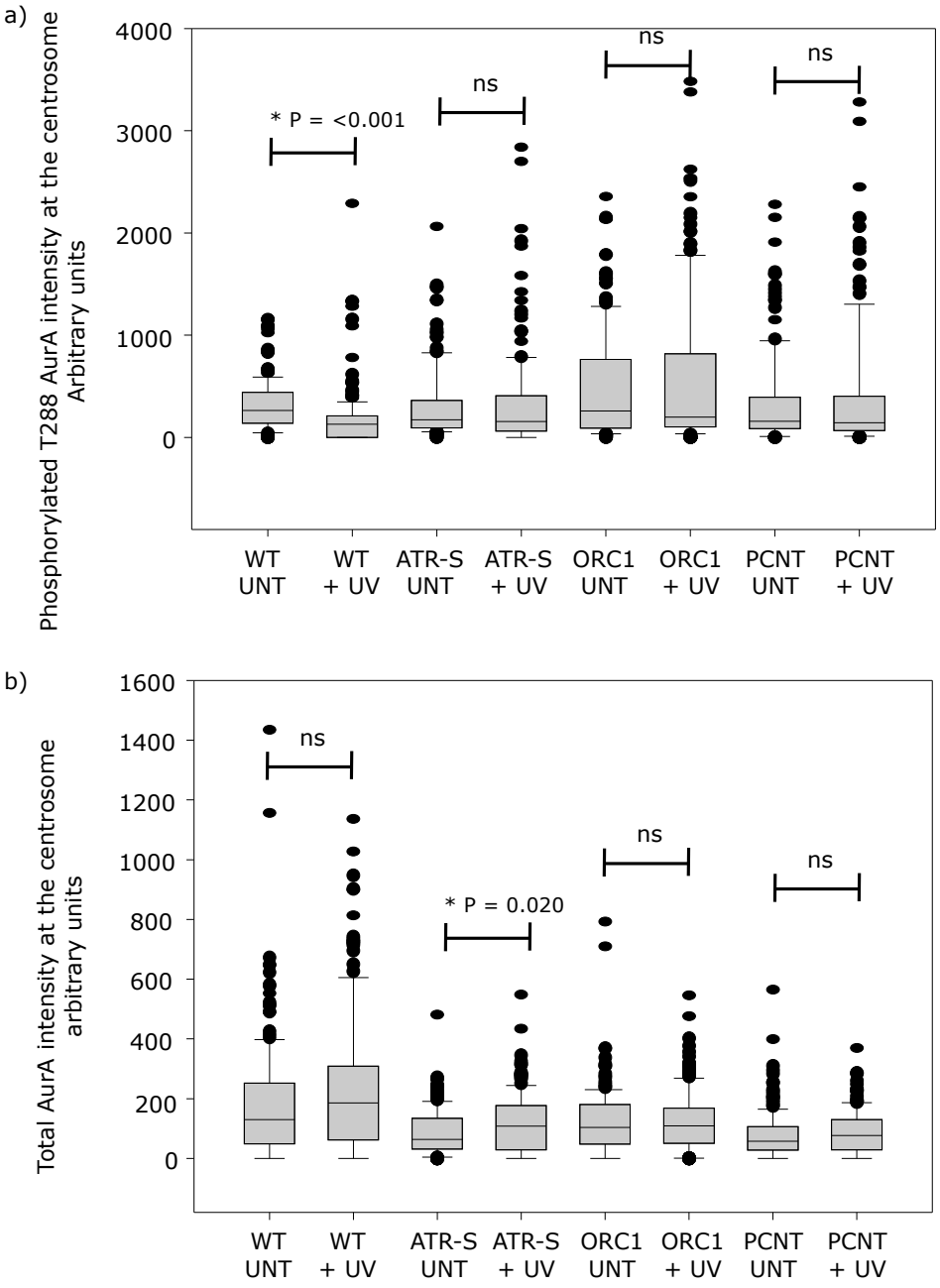

Figure 6.9 Box plots of AurA intensity at the centrosome

a) Box plot of quantification of phosphorylated AurA T288 intensity at the centrosome as shown in figure 6.8. Data shown from three independent experiments.
b) Box plot of quantification of total AurA at the centrosome as shown in figure 6.8. Data shown from three independent experiments.

Statistics performed were Shapiro-Wilk normality test followed by Mann-Whitney Rank Sum test. Statistically significant differences are indicated by *. ns = not statistically significant

6.2.7 Depletion of CEP192 results in an ATR-dependent G2/M checkpoint defect

CEP192 interacts with AurA and localizes it to the centrosome (Gomez-Ferreria *et al.*, 2007). CEP192 also interacts with PCNT and these proteins are partially co-dependent on each other for localization to the centrosome (Gomez-Ferreria *et al.*, 2007). In order to determine whether CEP192 is also required for ATR-dependent G2/M checkpoint responses, CEP192 was depleted in HeLa cells for 72hrs and the G2/M checkpoint response to UV and IR examined. Western blotting to confirm depletion levels was not possible due to unavailability of commercial antibodies at the time of experimentation. However, in CEP192 siRNA treated samples, cells failed to arrest efficiently after UV treatment but arrested proficiently after exposure to IR (Figure 6.10), although not to the same extent as untransfected cells. This indicates that CEP192 may be involved in the ATR-dependent damage response to UV but is not required for the damage response to IR.

In conclusion, in this chapter I have shown that further MGS lines with mutations in preRC components display a defective ATR-dependent UV-induced G2/M checkpoint response, similarly to all MPD line that I have examined in this thesis. I have investigated the molecular basis underlying the G2/M checkpoint defect and have shown that the phosphorylation of AurA kinase and PLK1 at the centrosome is mis-regulated after UV exposure in all MPD lines examined.

6.3 DISCUSSION

The results presented in this chapter reveal an interesting impact of AurA and PLK1 in the ATR-dependent damage response. Published data suggests that PLK1 can regulate mitotic entry via phosphorylation of CDC25C (Roshak *et al.*, 2000, Toyoshima-Morimoto *et al.*, 2002) and CDC25B (Lobjois *et al.*, 2009), promoting the nuclear translocation of these proteins. It has been proposed that PLK1 and CDC25B are required for recovery from a G2 arrest following DNA damage but are dispensable for mitotic entry in unperturbed cell cycles (Van vugt *et al.,* 2004). Further, PLK1 activity, via AurA regulation, is down regulated in an ATR-dependent manner after damage (Tsvetkov and Stern, 2005b).
My results confirm and extend these findings with the observations that:

1. AurA phosphorylation is not efficiently down regulated at the centrosome in MPD patient derived cell lines deficient in ATR, PCNT or ORC1.

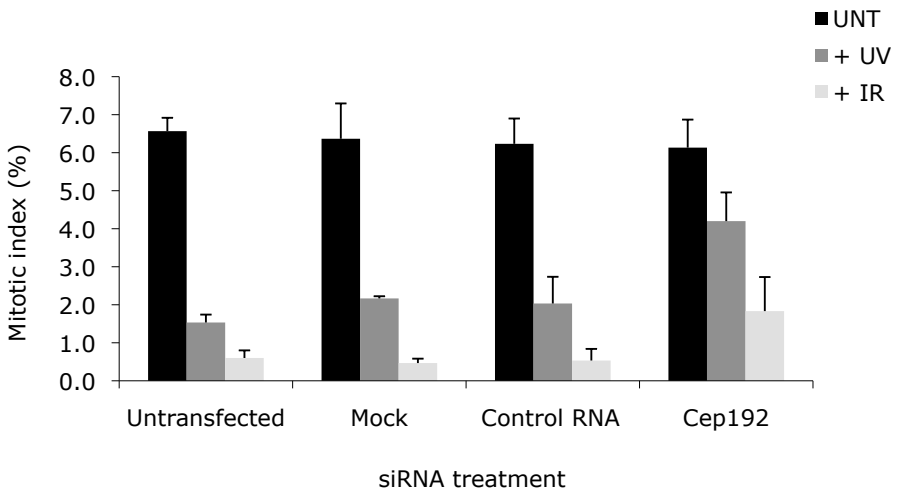

Figure 6.10 Depletion of Cep192 results in an ATR-dependent G2/M checkpoint defect

Cep192 was depleted in Hela cells for 72hrs and then cells were examined for G2/M arrest 2hrs after exposure to 5J/m^2 UV or 3 Gy IR. A decrease in the number of mitotic cells was taken as indicative of a G2/M arrest.

Graph represents the mean of three independent experiments. Error bars represent the standard deviation.

2. In these cell lines, ATR-dependent UV induced checkpoint induction is compromised, however, inhibition of AurA or PLK1 can re-establish the checkpoint arrest

The phosphorylation of both AurA and PLK1 at the centrosome is clearly mis-regulated following exposure to UV radiation in a panel of MPD lines. Results presented in this chapter suggest that ATR-dependent inhibition of AurA, and consequently PLK1, is required in order to proficiently activate the G2/M checkpoint response after UV exposure. The process requires the centrosome as defects in centrosome proteins, such as in the PCNT deficient line, result in an inability for this ATR-dependent regulation to occur. In ATR deficient cells, where the phosphorylation of Chk1 after UV exposure is not efficient, Cdc25 is therefore not efficiently inhibited by direct phosphorylation by Chk1 (Alderton *et al*., 2006), although residual protein present in the patient cells makes interpretation of the level of residual activity difficult. However, inhibition of PLK1 in this context can still result in checkpoint activation, suggesting that the inhibition of PLK1 after damage is a critical step in establishing the checkpoint. In undamaged cells, treatment with AurA or PLK1 inhibitors did not significantly affect mitotic entry, suggesting that these proteins are indeed dispensable for mitotic entry in the absence of damage. After damage, mitotic entry becomes dependent on PLK1, suggesting that the regulation of mitotic entry in this context is different.

A model for regulation of AurA and PLK1 after UV irradiation is presented in Figure 6.11. There are two possible interpretations for the role of AurA and PLK1 in G2/M checkpoint control. The first model is that Chk1, activated by ATR, can control Cdc25 regulation both by direct phosphorylation and also indirectly via the inhibition of PLK1. The second model is that ATR regulates PLK1 via an, as yet undefined, Chk1-independent mechanism. Data from our laboratory (T. Stiff, personal communication) suggests that Chk1 inhibition combined with PLK1 inhibition nevertheless results in checkpoint arrest, suggesting that the first model is correct.

AurA is required for the initial localization of Cdk1-CyclinB to the centrosome. As AurA is inappropriately active at the centrosome in MPD lines it is possible that Cdk1-CyclinB is also inappropriately located at the centrosome. Premature Chromosome Condensation (PCC's) is a hallmark of cells that enter mitosis prematurely, possibly due to increased Cdk1-CyclinB activity (Alderton *et al.*, 2006). I have not observed PCC's in the cell lines examined here, although it is a

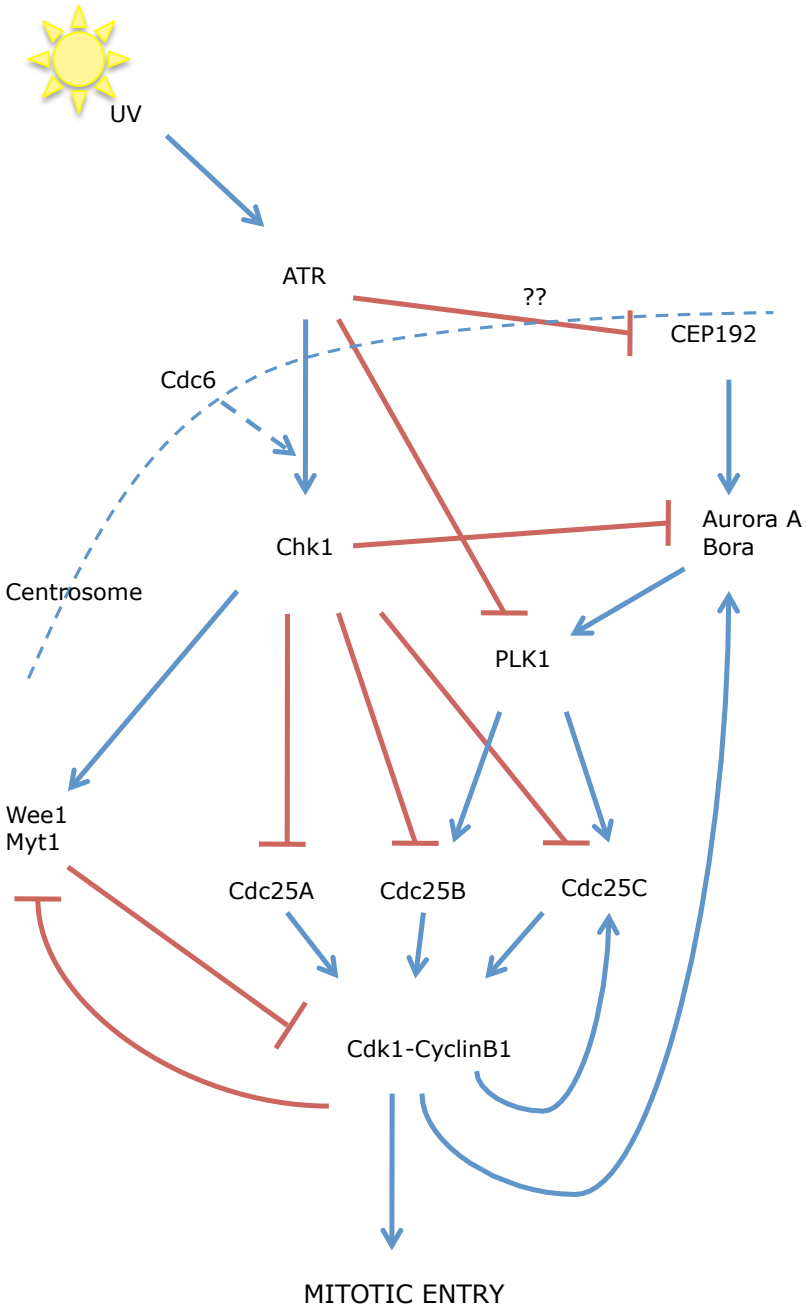

Figure 6.11 AurA and PLK1 in the ATR-dependent damage response at the centrosome

Upon UV exposure, ATR becomes activated and phosphorylates Chk1 at the centrosome, possibly in concert with Cdc6. Active Chk1 inhibits the Cdc25s which are then unable to activate Cdk1-CyclinB, inhibiting mitotic entry. In parallel, ATR inhibits the phosphorylation of Aurora A and PLK1 at the centrosome, either via a mechanism involving Chk1 or potentially via regulation of CEP192. Inhibition of PLK1 prevents the activation of Cdc25B and C and further inhibits Cdk1-CyclinB1 activation and mitotic entry.

feature of some microcephalic cell lines such as Primary Microcephaly patients with mutations in MCPH1 (Alderton *et al.*, 2006).

A minimal level of AurA activity is sufficient for cells to enter mitosis (Hirota *et al.*, 2003), therefore even a small amount of mis-regulation after damage could account for the loss of the G2/M checkpoint. In many of these lines, Chk1 is either not phosphorylated efficiently after damage (ATR-S) or is not localized at the centrosome sufficiently (PCNT mutated), resulting in inappropriate Cdc25 activation. If AurA/PLK1 are also inappropriately activating the Cdc25s, the levels of active Cdk1-CyclinB will be high and cells will enter mitosis. If Chk1 at the centrosome is involved in regulation of AurA phosphorylation, it is possible that reduced Chk1 at the centrosome in the PCNT line results in an inability to inhibit AurA at centrosome. Chk1 could also regulate the function of CEP192 at the centrosome after DNA damage, resulting in reduced localization of AurA at centrosomes. It is possible that an important function of the G2/M checkpoint response is also to inhibit centrosome maturation, ensuring that the centrosome cycle and nuclear cell cycle remain coupled.

Further work to confirm and extend the findings presented here could include the use of AurA inhibitors to determine if the excess signal detected at the centrosome after UV exposure in MPD lines could be reduced. Chk1 inhibitor treatment of the WT cell line could determine if the UV-induced inhibition of AurA at the centrosome is Chk1 dependent. Immunoprecipitation experiments could address the possibility that ATR or Chk1 interacts with CEP192 and/or AurA. Does ATR or Chk1 phosphorylate CEP192 and inhibit it after damage, contributing to the inhibition of AurA activity at the centrosome?

PLK1 also phoshorylates ORC2 following exposure to UV radiation. Increased replication stress in the ORC1 cell line could lead to an increase in PLK1 phosphorylation on T210 in order for PLK1 to then phosphorylate ORC2. Slow S phase progression has been detected when PLK1 is inhibited or depleted, but PLK1 is not required for DNA replication unless cells encounter replication stress (Song *et al.*, 2011).

The question still remains: how are ORC1 and Cdc6, pre-replication complex components, involved in G2/M checkpoint regulation after UV exposure? ORC1 has a role outside of replication, at the centrosome and is involved in the control of centriole duplication (Hemerly *et al.*, 2009). However, there is no evidence as yet for centrosomal localization of Cdc6. Is Cdc6 localised to the centrosome via its

interaction with ORC1? It is possible that the centrosomally located pools of these proteins are important in contributing to checkpoint control.

Cdc6 is phosphorylated by Cdks during the cell cycle, resulting in its nuclear export (Petersen *et al.*, 1999). A phosphorylation site mutant Cdc6 S74A is not able to arrest cells in G2 (Clay-Farrace *et al.*, 2003). Cdc6 null yeast cells still enter mitosis even without fully completing replication of the DNA (Piatti *et al.*, 1995). Cdc6 is therefore postulated to play a role in a checkpoint that couples completion of DNA replication and entry into mitosis. In human cells, depletion of Cdc6 causes cells to enter mitosis without activating the ATR-dependent checkpoint and also results in increased apoptosis (Lau *et al.*, 2006). In Xenopus, Cdc6 is required for the activation of Chk1 following replication fork stalling induced by aphidicolin (Oehlmann *et al.*, 2004). I have also observed an ATR-dependent G2/M checkpoint defect in Cdc6 depleted Hela cells (data not shown). Only one experiment was conducted and the result needs confirming, however this recapitulates the phenotype observed in the Cdc6 mutated MGS cell line.

Chromatin bound Cdc6 interacts with MCM7 (Kneissl *et al.*, 2003, Shin *et al.*, 2003). MCM7 interacts with ATRIP and depletion of Mcm7 results in defective Chk1 phosphorylation (Cortez *et al.*, 2004). It is possible therefore that Cdc6 is involved in the upstream steps of checkpoint activation. My results also suggest that Cdc6 is somehow required for the phosphorylation of Chk1 after UV exposure. This aspect of ATR-dependent signalling requires further investigation.

In this chapter I have explored the molecular basis underlying the ATR-dependent G2/M checkpoint defect in a panel of MPD lines. I have shown that the phosphorylation of AurA and PLK1 at the centrosome is not inhibited in MPD lines after exposure to UV, to the same extent that it is inhibited in WT lines. These results highlight an important role for AurA and PLK1 at the centrosome in the ATR-dependent DNA damage response.

CHAPTER SEVEN

7.1 DISCUSSION

In this thesis I have examined multiple genetically uncharacterised cell lines from patients with MPD disorders for ATR-dependent DNA damage response signalling and have contributed to the identification of the underlying genetic defects. I have further shown that the mutations identified in *PCNT*, *ATRIP* and *ORC1L* result in defects in ATR-dependent DNA damage response signalling. I have explored the molecular basis of the defective ATR-dependent G2/M checkpoint response exhibited by various MPD patient derived cell lines and highlight an important role for AurA and PLK1 at the centrosome in the ATR-dependent DNA damage response.

7.1.1 PCNT mutation and defects in ATR-dependent G2/M checkpoint activation

I have shown that a subset of patients with MPD harbour mutations in *PCNT* with accompanying defects in ATR-dependent DNA damage responses. Prior to this work, mutations in centrosomal proteins had already been indentified in Primary Microcephaly patients (Bond *et al.*, 2005, Gul *et al.*, 2006), however the results presented in this thesis provide further evidence of a link between mutations in proteins that localise to this organelle and the incidence of MPD. This work also provides the first evidence that mutations in a structural centrosomal protein can impact on the ATR-dependent DNA damage response. Further centrosomal protein mutations have since been identified in MPD and Primary Microcephaly patients, such as CENPJ (Al-Dosari *et al.*, 2010) and CEP152 (Kalay *et al.*, 2011). Could centrosome defects therefore be the sole cause of these patients' clinical features? All SS lines studied to date possess supernumerary mitotic centrosomes, indicating that problems in centrosome duplication or segregation occur in the patient cells. It is likely that these cells either die in a 'mitotic catastrophe' event or continue cycling and become aneuploid or polyploid. In developmental terms, if the cells die in sufficient numbers during brain development then this could deplete the stem cell population number, resulting in an overall reduction in brain volume, hence resulting in microcephaly. A similar effect on overall cellular proliferation could result in the overall growth retardation observed in these patients both pre- and post-natally. We have also conducted G2/M checkpoint analysis on patient cell lines with mutations in other centrosomal associated proteins such as CENPJ and ASPM. All cell lines examined show a defective ATR-dependent G2/M checkpoint response,

raising the possibility that events at the centrosome are indeed required to co-ordinate this signalling event. These results extend the findings of Jackman *et al*., 2003, who showed that the first detectable active Cdk1-CyclinB is localised at the centrosome and proposed that pathways for the negative and positive regulation of mitotic entry may be located at the centrosome.

How does the absence of PCNT result in an inability to down regulate AurA/PLK1 activity? PCNT has been shown to interact with Chk1 and tether it at the centrosome (Tibelius *et al.,* 2009). Chk1 levels at the centrosome are reduced in these cells, resulting in reduced inhibitory phosphorylation of Cdc25B. This coupled with the mis-regulation of AurA phosphorylation at the centrosome that I have observed could result in an inability to inhibit PLK1 after damage. This could result in inappropriate activation of Cdc25 and therefore an inability to effectively inhibit Cdk1-CyclinB1 complexes and lead to inappropriate mitotic entry. Indeed, reduced Chk1 activity at the centrosome has been demonstrated to result in G2/M checkpoint defects (Löffler *et al.*, 2007). A direct interaction between Chk1 and AurA has not been shown, although if Chk1 does negatively regulate AurA kinase activity, this could be compromised by the reduced levels of Chk1 at the centrosome in these cells. After exposure to ionising radiation, Cdc25 activation is also inhibited, either by Chk2 or Chk1, to activate the G2/M checkpoint. However, I have not observed defects in checkpoint activation after exposure to IR in patient cell lines, suggesting that the centrosome is not required for checkpoint activation in this context. These results suggest that the regulation of PLK1 could be the step in checkpoint control that occurs at the centrosome and that this is critical for checkpoint activation following exposure to UV but not IR.

It is possible that the UV-induced checkpoint arrest is not as efficient as that induced after IR exposure, as I have observed that a substantial number of control cells still enter mitosis after UV exposure, compared to a negligible number of cells after IR. This could suggest that either the activation of ATR, or the ability of ATR to inhibit Cdc25 after UV exposure is not efficient. In this context, the concomitant down regulation of PLK1 becomes critical to activate the checkpoint. After IR, it is possible that the down regulation of PLK1 is not critical as the Cdc25s are inhibited more efficiently.

Both AurA and PCNT also interact with CEP192, therefore it could be expected that a reduced level of PCNT at the centrosome would result in reduced amounts of CEP192 and therefore a reduction in AurA levels at the centrosome would be

observed. I have not observed this in the patient cells, although the residual protein present may account for this. It is possible that ATR also regulates CEP192 after damage, by inhibiting the localisation of AurA to the centrosome. ATR phosphorylates CEP63 after chromosome breakage, resulting in the inhibition of spindle assembly (Smith *et al.*, 2009), demonstrating the existence of important links between control of the centrosome control and control of the nuclear cell cycle by the DNA damage response.

The centrosome is also important for the correct orientation of the spindle during neurogenesis, influencing the decision between asymmetric and symmetric cell division (Higginbotham and Gleeson, 2007). Defects in spindle orientation were observed in PCNT-MOPDII patients (Rauch *et al.*, 2008), and PCNT depletion leads to loss of astral microtubules (Zimmerman *et al.*, 2004). It is possible that spindle orientation defects in PCNT mutated cells could cause a shift from symmetric division to asymmetric division, resulting in an overall decrease in the progenitor stem cell population (Cox *et al.*, 2006).

7.1.2 ORC1 mutation and defects in ATR-dependent signalling

The identification of mutations in *ORC1* in further MPD patients in this thesis has provided evidence for an important link between replication origin licensing and ATR-dependent signalling. This has also opened up a new avenue for the identification of further genetic defects in other replication-associated proteins. Indeed, further mutations in preRC components, such as CDC6, CDT1 and further ORC members were also uncovered in patients with MGS (Bicknell *et al*., 2011a). Defects in origin licensing and S-phase progression were observed in an ORC1 deficient patient cell line. One model, which was suggested in our publication of this work is that ORC1 deficiency could be important during development when cell cycle phase and replication rate is rapid. During development, the cell cycle phases are shorter than for mammalian cells in culture (Takahashi *et al.*, 1995). Therefore the defect in origin licensing, observed in the patient cells, may become rate-limiting in the context of the shorter cell cycle. This phenotype, coupled with an increased time taken to complete S phase due to the observed defect in S-phase progression, could result in a slowing of overall cellular proliferation. This could therefore reduce the overall cell number, leading to a reduction in overall brain and body size (Klingseisen *et al.,* 2011). The rescue of growth retardation in ORC1 zebrafish by the introduction of WT ORC1 but not by an ORC1 that cannot efficiently bind to origins (Kuo *et al.*, 2012) suggests that origin licensing is indeed

important during development and perturbation of cell-cycle progression in this context could cause the clinical features observed in MGS.

The above model demonstrating an impact of reduced origin licensing capability in the patient cell line reflects the canonical function of ORC1 in the regulation of replication. However my results provide potential alternative or additional impacts of deficiency in ORC1.

A surprising phenotype conferred by ORC1 deficiency is the defect observed in the ATR-dependent G2/M checkpoint response. ORC1 is known to play a role in the prevention of centrosome duplication at the centrosome (Hemerly *et al.*, 2009), and it is postulated that the centrosome acts as a scaffold for the coordination of centrosome and nuclear cycle events (Doxsey *et al.*, 2005). Therefore the absence of ORC1 may cause centrosome duplication as well as a loss of G2/M checkpoint control if these two events are somehow related or regulated by the same machinery. The completion of replication before the decision to undergo mitosis is undertaken may also be co-ordinated by the centrosome. CDC6 has been postulated to be involved in this regulation (Clay-Farrace *et al.,* 2003). However, a centrosomal location for this protein has not been established. It does however interact with ORC1 (Saha *et al.,* 1998) raising the possibility that a centrosome link to CDC6 exists. If centrosome defects in the ORC1 patients also cause spindle mis-orientation, a premature switch from symmetric to asymmetric cell division could also result in a decrease in the progenitor stem cell population, leading to microcephaly (Cox *et al.*, 2006).

In the ORC1 deficient cell line Chk1 appears to be phosphorylated normally, yet AurA and PLK1 remain inappropriately activated after damage. It is possible that if Chk1 regulates AurA/PLK1 activity, then the defect lies downstream of Chk1 phosphorylation in this pathway.

Unpublished data from our laboratory has shown that mutations in ORC1, and other preRC proteins, also lead to defects in cilia function. We consider that this could be due to impairments in centrosome biology, raising the possiblility that a further non-canonical function of ORC1 might have a clinical impact in the patients and be a further cause of microcephaly.

7.1.3 Basis underlying MPD

Overall, which of the cellular phenotypes observed could be causal in the clinical features observed in MPD patients with mutations in *ATR, ATRIP, PCNT* and *ORC1*? There are a number of possible explanations, which I will now address:

1. Replication stress during development, leading to increased levels of apoptosis has been shown in the $ATR^{s/s}$ mouse (Murga *et al.,* 2009) and ATR mutations in the patient cells also likely result in problems in progression though replication, as evidenced by a decrease in the stability of replication forks (Alderton *et al.*, 2006). Defects in replication dynamics are also observed in the ORC1 patient lines. These cells however, also display supernumerary mitotic centrosomes and G2/M checkpoint defects making it somewhat difficult to ascribe the clinical features purely to replication stress alone. High levels of apoptosis due to replication stress during development could lead to depletion of progenitor cell populations.
2. Mutations in centrosome proteins are increasingly observed in various MPD patients (Al-Dosari *et al.*, 2010, Bond *et al.*, 2005, Gul *et al.*, 2006, (Kalay *et al.*, 2011) providing a compelling link between defects at this organelle and these disorders. Defects in centrosome biology could result in an inappropriate switch from symmetric to asymmetric cell division, leading to depleted progenitor cell populations and resulting in microcephaly and growth retardation (Cox *et al*.,2006).
3. The link between the centrosome and the primary cilia is also interesting in terms of the skeletal defects commonly observed both in MPD disorders and ciliopathies (Duldulao *et al.*, 2010), for instance fifth finger clinodactyly is a clinical feature common to both sets of disorders. Defects in both cilia formation and function have been observed in many MPD cell lines in our laboratory (T.Stiff, personal communication) suggesting this could also be an important phenotype contributing to the clinical features observed. However, as the cilia are formed from the centrosome it is not trivial to distinguish if centrosome defects are causal of cilia defects or vice versa.

In addition, as described above, the G2/M checkpoint defect is also a common phenotype observed in most MPD lines examined to date. Do centrosomal mutations always confer ATR-dependent G2/M checkpoint defects? The two phenotypes do seem to correlate in all the MPD patients examined to date, indicative of some connection. It is possible that for all the MPD cell lines examined

in this thesis, a small amount of mis-regulation of Cdk1-CyclinB1 activity, even in unperturbed cell cycles, results in a 'edging towards' mitotic entry rather than not. In terms of the bistability hysteresis model (Lindqvist *et al.*, 2009), detailed in the introduction to this thesis, the level of Cdk1-CyclinB1 that is in an active state could be consistently higher in these cells, due to aberrant CDC25 regulation, and therefore the tendency is for cells to enter mitosis rather than not enter. After DNA damage, this becomes more evident as checkpoints are not activated efficiently.

It is likely that the clinical features observed in the patients are due to a combination of all of the cellular phenotypes described above, resulting in overall impaired cell cycle progression during development. To what degree each separate phenotype contributes to the clinical features observed is not clear, and indeed the explanation may be different in each of the different patients. Further studies could provide insight into the overall mechanisms regulating growth during development.

7.1.4 MPD patient classification

An interesting problem highlighted in this work has been the clinical classification of patients. Some *PCNT*-mutated patients were originally classified as SS and then re-classified to MOPDII (Willems *et al*., 2010). Patients with *ORC1* mutation were included in our mapping studies as SS but are now regarded as MGS with further mutations in preRC components identified in this disorder (Bicknell *et al*., 2011a). The identification of further ATR/ATRIP Seckel patients may aid in delineating the clinical spectrum of Seckel Syndrome but there is certainly considerable overlap between MGS, MOPDII and Seckel. Indeed, it is possible that they are all the same MPD disorder but with varying degrees of severity. Patients with *ORC1* mutations do appear to be more severely microcephalic than the other MGS patients. It is possible that the identification of any molecular differences in the phenotypes of patient cells, if indeed they exist, may be the only means of distinguishing between these disorders. This may be desirable from a clinical point of view in terms of management of the patients. MOPDII patients may need monitoring due to the increased risk of vascular problems, such as moya-moya disease that could result in death (Hall *et al.,* 2004). It is also possible that the genetic deficiency may impact in different ways in different tissues, e.g. MGS patients display severe problems in patellae development (Faqeih *et al.*, 2005). Identification of genetic defects coupled with an understanding of the role of each protein during development may aid in patient diagnosis and treatment.

7.1.5 MPD patients and cancer

Given the role of ATR in the maintenance of genomic stability through the stabilisation of replication forks and checkpoint control, are Seckel or other MPD patients more prone to cancers? Although the number of patients is small it appears that the incidence of cancer is not significantly increased over the general population. Acute Myeloid Leukaemia (AML) has been observed in one Seckel syndrome patient to date (Hayani *et al.,* 1994). No MOPDII related malignancies have been reported and none have been reported in MGS patients. In the context of reduced ATR function, the lack of an efficient G2/M checkpoint response may actually be beneficial to these patients. In rapidly replicating tumour cells, where there is extensive replication stress induced DNA damage, with efficient G2/M checkpoint activation, the cell may attempt to repair the damage and this could lead to mutagenesis. In the absence of an efficient G2/M checkpoint response, the cell enters mitosis with a level of DNA damage that makes the cell unviable. Cells would therefore either undergo apoptosis or die in mitosis and are therefore eliminated. Therefore the level of genomic instability is potentially kept to a minimum and the number of cells likely to cause cancer is reduced. Indeed, the ATR mouse engineered with the SS mutation does not form tumours within the six-month timeframe examined (Murga *et al.,* 2009). When these authors produced a double mutant mouse lacking both ATR and p53, they saw a synthetic lethal effect with an increased amount of apoptosis in embryos. It is possible therefore that extreme down regulation of the ATR DNA damage response confers a tumour suppressive effect. Indeed, a recent study showed that inhibition of ATR could inhibit the growth of murine cancers (Schoppy *et al.*, 2012). A further ATR knockdown mouse does not die prematurely and also does not show an elevated tumour incidence (Ruzankina *et al*., 2008). The ATR+/- mouse from an early study to obtain a knockout mouse model, did however, show a small increase in tumour formation (Brown *et al.,* 2000). It would be interesting to obtain embryonic fibroblasts from these heterozygous animals to examine G2/M checkpoint responses and possibly determine if this correlates with tumour incidence. In this context it would also be interesting to determine if heterozygous SS family members are prone to a higher incidence of cancers than the general population. Again, however, the small numbers of people available for examination could prove an obstacle to this kind of study.

7.1.6 MPD patients and premature aging

Accelerated aging has been observed in mouse models of ATR deficiency, with phenotypes such as greying of hair, osteoporosis and kyphosis (Murga *et al.,* 2009). In the $ATR^{s/s}$ mouse the hematopoietic stem cell (HSC) compartment of the animals was assessed and found to be lacking in multipotent progenitor cells indicating a loss of specific stem cell niches, as would be found in older animals (Murga *et al.,* 2009). It was proposed that this aging phenotype is a result of 'intrauterine programming' where insult to the embryo, in this case increased replicative stress, manifests as problems in adulthood. Premature aging has not been a striking feature manifesting in MPD patients although some features such as kyphosis are present in a few patients.

7.1.7 Final summary

In summary, the data I have presented in this thesis has contributed to the identification of the underlying genetic defects in various patients with MPD disorders. I have shown that novel mutations in *ATRIP, PCNT* and *ORC1* impact on ATR-dependent DNA damage response signalling. I have also demonstrated an important mechanism involving the inhibition of the phosphorylation of AurA at the centrosome in ATR-dependent UV-induced checkpoint activation.

REFERENCES

Al-Dosari, M.S., Shaheen, R., Colak, D. & Alkuraya, F.S. (2010) Novel CENPJ mutation causes Seckel syndrome. *J Med Genet,* Vol. 47 (6) 411-4.

Alderton, G.K., Galbiati, L., Griffith, E., Surinya, K.H., Neitzel, H., Jackson, A.P., Jeggo, P.A. & O'driscoll, M. (2006) Regulation of mitotic entry by microcephalin and its overlap with ATR signalling. *Nat Cell Biol,* Vol. 8 (7) 725-33.

Alderton, G.K., Joenje, H., Varon, R., Børglum, A.D., Jeggo, P.A. & O'driscoll, M. (2004) Seckel syndrome exhibits cellular features demonstrating defects in the ATR-signalling pathway. *Hum Mol Genet,* Vol. 13 (24) 3127-38.

Ammazzalorso, F., Pirzio, L.M., Bignami, M., Franchitto, A. & Pichierri, P. (2010) ATR and ATM differently regulate WRN to prevent DSBs at stalled replication forks and promote replication fork recovery. *EMBO J,* Vol. 29 (18) 3156-69.

Andreassen, P.R., D'andrea, A.D. & Taniguchi, T. (2004) ATR couples FANCD2 monoubiquitination to the DNA-damage response. *Genes Dev,* Vol. 18 (16) 1958-63.

Arai, Y., Pulvers, J.N., Haffner, C., Schilling, B., Nüsslein, I., Calegari, F. & Huttner, W.B. (2011) Neural stem and progenitor cells shorten S-phase on commitment to neuron production. *Nat Commun,* Vol. 2 (1) 154.

Bakkenist, C.J. & Kastan, M.B. (2003) DNA damage activates ATM through intermolecular autophosphorylation and dimer dissociation. *Nature,* Vol. 421 (6922) 499-506.

Ball, H.L. & Cortez, D. (2005) ATRIP oligomerization is required for ATR-dependent checkpoint signaling. *J Biol Chem,* Vol. 280 (36) 31390-6.

Ball, H.L., Ehrhardt, M.R., Mordes, D.A., Glick, G.G., Chazin, W.J. & Cortez, D. (2007) Function of a conserved checkpoint recruitment domain in ATRIP proteins. *Mol Cell Biol,* Vol. 27 (9) 3367-77.

Ball, H.L., Myers, J.S. & Cortez, D. (2005) ATRIP binding to replication protein A-single-stranded DNA promotes ATR-ATRIP localization but is dispensable for Chk1 phosphorylation. *Mol Biol Cell,* Vol. 16 (5) 2372-81.

Barros, T.P., Kinoshita, K., Hyman, A.A. & Raff, J.W. (2005) Aurora A activates D-TACC-Msps complexes exclusively at centrosomes to stabilize centrosomal microtubules. *J Cell Biol,* Vol. 170 (7) 1039-46.

Bartram, C.R., Koske-Westphal, T. & Passarge, E. (1976) Chromatid exchanges in ataxia telangiectasia, Bloom syndrome, Werner syndrome, and xeroderma pigmentosum. *Ann Hum Genet,* Vol. 40 (1) 79-86.

Bassermann, F., Frescas, D., Guardavaccaro, D., Busino, L., Peschiaroli, A. & Pagano, M. (2008) The Cdc14B-Cdh1-Plk1 axis controls the G2 DNA-damage-response checkpoint. *Cell,* Vol. 134 (2) 256-67.

Bassing, C.H., Chua, K.F., Sekiguchi, J., Suh, H., Whitlow, S.R., Fleming, J.C., Monroe, B.C., Ciccone, D.N., Yan, C., Vlasakova, K., Livingston, D.M., Ferguson, D.O., Scully, R. & Alt, F.W. (2002) Increased ionizing radiation sensitivity and genomic instability in the absence of histone H2AX. *Proc Natl Acad Sci U S A,* Vol. 99 (12) 8173-8.

Bayliss, R., Sardon, T., Vernos, I. & Conti, E. (2003) Structural basis of Aurora-A activation by TPX2 at the mitotic spindle. *Mol Cell,* Vol. 12 (4) 851-62.

Ben-Yehoyada, M., Gautier, J. & Dupré, A. (2007) The DNA damage response during an unperturbed S-phase. *DNA Repair (Amst),* Vol. 6 (7) 914-22.

Berquist, B.R. & Wilson, D.M. (2012) Pathways for repairing and tolerating the spectrum of oxidative DNA lesions. *Cancer Lett*.

Bicknell, L.S., Bongers, E.M., Leitch, A., Brown, S., Schoots, J., Harley, M.E., Aftimos, S., Al-Aama, J.Y., Bober, M., Brown, P.A., Van Bokhoven, H., Dean, J., Edrees, A.Y., Feingold, M., Fryer, A., Hoefsloot, L.H., Kau, N., Knoers, N.V., Mackenzie, J., Opitz, J.M., Sarda, P., Ross, A., Temple, I.K., Toutain, A., Wise, C.A., Wright, M. & Jackson, A.P. (2011a) Mutations in the pre-replication complex cause Meier-Gorlin syndrome. *Nat Genet*.

Bicknell, L.S., Walker, S., Klingseisen, A., Stiff, T., Leitch, A., Kerzendorfer, C., Martin, C.A., Yeyati, P., Al Sanna, N., Bober, M., Johnson, D., Wise, C., Jackson, A.P., O'driscoll, M. & Jeggo, P.A. (2011b) Mutations in ORC1, encoding the largest subunit of the origin recognition complex, cause microcephalic primordial dwarfism resembling Meier-Gorlin syndrome. *Nat Genet*.

Blow, J.J. & Ge, X.Q. (2008) Replication forks, chromatin loops and dormant replication origins. *Genome Biol,* Vol. 9 (12) 244.

Blow, J.J. & Ge, X.Q. (2009) A model for DNA replication showing how dormant origins safeguard against replication fork failure. *EMBO Rep,* Vol. 10 (4) 406-12.

Blow, J.J. & Gillespie, P.J. (2008) Replication licensing and cancer--a fatal entanglement? *Nat Rev Cancer,* Vol. 8 (10) 799-806.

Bond, J., Roberts, E., Mochida, G.H., Hampshire, D.J., Scott, S., Askham, J.M., Springell, K., Mahadevan, M., Crow, Y.J., Markham, A.F., Walsh, C.A. & Woods, C.G. (2002) ASPM is a major determinant of cerebral cortical size. *Nat Genet,* Vol. 32 (2) 316-20.

Bond, J., Roberts, E., Springell, K., Lizarraga, S.B., Lizarraga, S., Scott, S., Higgins, J., Hampshire, D.J., Morrison, E.E., Leal, G.F., Silva, E.O., Costa, S.M., Baralle, D., Raponi, M., Karbani, G., Rashid, Y., Jafri, H., Bennett, C., Corry, P., Walsh, C.A. & Woods, C.G. (2005) A centrosomal mechanism involving CDK5RAP2 and CENPJ controls brain size. *Nat Genet,* Vol. 37 (4) 353-5.

Bonnet, J., Coopman, P. & Morris, M.C. (2008) Characterization of centrosomal localization and dynamics of Cdc25C phosphatase in mitosis. *Cell Cycle,* Vol. 7 (13) 1991-8.

Boulaire, J., Fotedar, A. & Fotedar, R. (2000) The functions of the cdk-cyclin kinase inhibitor p21WAF1. *Pathol Biol (Paris),* Vol. 48 (3) 190-202.

Boutros, R., Dozier, C. & Ducommun, B. (2006) The when and wheres of CDC25 phosphatases. *Curr Opin Cell Biol,* Vol. 18 (2) 185-91.

Brancati, F., Castori, M., Mingarelli, R. & Dallapiccola, B. (2005) Majewski osteodysplastic primordial dwarfism type II (MOPD II) complicated by stroke: clinical report and review of cerebral vascular anomalies. *Am J Med Genet A,* Vol. 139 (3) 212-5.

Branzei, D. & Foiani, M. (2005) The DNA damage response during DNA replication. *Curr Opin Cell Biol,* Vol. 17 (6) 568-75.

Branzei, D. & Foiani, M. (2008) Regulation of DNA repair throughout the cell cycle. *Nat Rev Mol Cell Biol,* Vol. 9 (4) 297-308.

Bringmann, H. & Hyman, A.A. (2005) A cytokinesis furrow is positioned by two consecutive signals. *Nature,* Vol. 436 (7051) 731-4.

Brown, E.J. & Baltimore, D. (2000) ATR disruption leads to chromosomal fragmentation and early embryonic lethality. *Genes Dev,* Vol. 14 (4) 397-402.

Buchman, J.J., Tseng, H.C., Zhou, Y., Frank, C.L., Xie, Z. & Tsai, L.H. (2010) Cdk5rap2 interacts with pericentrin to maintain the neural progenitor pool in the developing neocortex. *Neuron,* Vol. 66 (3) 386-402.

Budirahardja, Y. & Gönczy, P. (2008) PLK-1 asymmetry contributes to asynchronous cell division of C. elegans embryos. *Development,* Vol. 135 (7) 1303-13.

Burrows, A.E. & Elledge, S.J. (2008) How ATR turns on: TopBP1 goes on ATRIP with ATR. *Genes Dev,* Vol. 22 (11) 1416-21.

Busch, C., Barton, O., Morgenstern, E., Götz, C., Günther, J., Noll, A. & Montenarh, M. (2007) The G2/M checkpoint phosphatase cdc25C is located within centrosomes. *Int J Biochem Cell Biol,* Vol. 39 (9) 1707-13.

Busino, L., Donzelli, M., Chiesa, M., Guardavaccaro, D., Ganoth, D., Dorrello, N.V., Hershko, A., Pagano, M. & Draetta, G.F. (2003) Degradation of Cdc25A by beta-TrCP during S phase and in response to DNA damage. *Nature,* Vol. 426 (6962) 87-91.

Børglum, A.D., Balslev, T., Haagerup, A., Birkebaek, N., Binderup, H., Kruse, T.A. & Hertz, J.M. (2001) A new locus for Seckel syndrome on chromosome 18p11.31-q11.2. *Eur J Hum Genet,* Vol. 9 (10) 753-7.

Caldecott, K.W. (2008) Single-strand break repair and genetic disease. *Nat Rev Genet,* Vol. 9 (8) 619-31.

Carmena, M., Ruchaud, S. & Earnshaw, W.C. (2009) Making the Auroras glow: regulation of Aurora A and B kinase function by interacting proteins. *Curr Opin Cell Biol,* Vol. 21 (6) 796-805.

Cazales, M., Schmitt, E., Montembault, E., Dozier, C., Prigent, C. & Ducommun, B. (2005) CDC25B phosphorylation by Aurora-A occurs at the G2/M transition and is inhibited by DNA damage. *Cell Cycle,* Vol. 4 (9) 1233-8.

Celeste, A., Petersen, S., Romanienko, P.J., Fernandez-Capetillo, O., Chen, H.T., Sedelnikova, O.A., Reina-San-Martin, B., Coppola, V., Meffre, E., Difilippantonio, M.J., Redon, C., Pilch, D.R., Olaru, A., Eckhaus, M., Camerini-Otero, R.D., Tessarollo, L., Livak, F., Manova, K., Bonner, W.M., Nussenzweig, M.C. & Nussenzweig, A. (2002) Genomic instability in mice lacking histone H2AX. *Science,* Vol. 296 (5569) 922-7.

Cerosaletti, K., Wright, J. & Concannon, P. (2006) Active role for nibrin in the kinetics of atm activation. *Mol Cell Biol,* Vol. 26 (5) 1691-9.

Chan, E.H., Santamaria, A., Silljé, H.H. & Nigg, E.A. (2008) Plk1 regulates mitotic Aurora A function through betaTrCP-dependent degradation of hBora. *Chromosoma,* Vol. 117 (5) 457-69.

Chanoux, R.A., Yin, B., Urtishak, K.A., Asare, A., Bassing, C.H. & Brown, E.J. (2009) ATR and H2AX cooperate in maintaining genome stability under replication stress. *J Biol Chem,* Vol. 284 (9) 5994-6003.

Chen, C.Y., Olayioye, M.A., Lindeman, G.J. & Tang, T.K. (2006) CPAP interacts with 14-3-3 in a cell cycle-dependent manner. *Biochem Biophys Res Commun,* Vol. 342 (4) 1203-10.

Chen, D., Purohit, A., Halilovic, E., Doxsey, S.J. & Newton, A.C. (2004) Centrosomal anchoring of protein kinase C betaII by pericentrin controls microtubule organization, spindle function, and cytokinesis. *J Biol Chem,* Vol. 279 (6) 4829-39.

Cheng, X., Kelso, C., Hornak, V., De Los Santos, C., Grollman, A.P. & Simmerling, C. (2005) Dynamic behavior of DNA base pairs containing 8-oxoguanine. *J Am Chem Soc,* Vol. 127 (40) 13906-18.

Chini, C.C. & Chen, J. (2006) Repeated phosphopeptide motifs in human Claspin are phosphorylated by Chk1 and mediate Claspin function. *J Biol Chem,* Vol. 281 (44) 33276-82.

Cho, J.H., Chang, C.J., Chen, C.Y. & Tang, T.K. (2006) Depletion of CPAP by RNAi disrupts centrosome integrity and induces multipolar spindles. *Biochem Biophys Res Commun,* Vol. 339 (3) 742-7.

Chung, J.H. & Bunz, F. (2010) Cdk2 is required for p53-independent G2/M checkpoint control. *PLoS Genet,* Vol. 6 (2) e1000863.

Cimprich, K.A. & Cortez, D. (2008) ATR: an essential regulator of genome integrity. *Nat Rev Mol Cell Biol,* Vol. 9 (8) 616-27.

Cizmecioglu, O., Arnold, M., Bahtz, R., Settele, F., Ehret, L., Haselmann-Weiss, U., Antony, C. & Hoffmann, I. (2010) Cep152 acts as a scaffold for recruitment of Plk4 and CPAP to the centrosome. *J Cell Biol,* Vol. 191 (4) 731-9.

Clay-Farrace, L., Pelizon, C., Santamaria, D., Pines, J. & Laskey, R.A. (2003) Human replication protein Cdc6 prevents mitosis through a checkpoint mechanism that implicates Chk1. *EMBO J,* Vol. 22 (3) 704-12.

Cleaver, J.E., Lam, E.T. & Revet, I. (2009) Disorders of nucleotide excision repair: the genetic and molecular basis of heterogeneity. *Nat Rev Genet,* Vol. 10 (11) 756-68.

Cliby, W.A., Roberts, C.J., Cimprich, K.A., Stringer, C.M., Lamb, J.R., Schreiber, S.L. & Friend, S.H. (1998) Overexpression of a kinase-inactive ATR protein causes sensitivity to DNA-damaging agents and defects in cell cycle checkpoints. *EMBO J,* Vol. 17 (1) 159-69.

Collis, S.J., Barber, L.J., Clark, A.J., Martin, J.S., Ward, J.D. & Boulton, S.J. (2007) HCLK2 is essential for the mammalian S-phase checkpoint and impacts on Chk1 stability. *Nat Cell Biol,* Vol. 9 (4) 391-401.

Collis, S.J., Ciccia, A., Deans, A.J., Horejsí, Z., Martin, J.S., Maslen, S.L., Skehel, J.M., Elledge, S.J., West, S.C. & Boulton, S.J. (2008) FANCM and FAAP24 function in ATR-mediated checkpoint signaling independently of the Fanconi anemia core complex. *Mol Cell,* Vol. 32 (3) 313-24.

Cook, J.G. (2009) Replication licensing and the DNA damage checkpoint. *Front Biosci,* Vol. 14 5013-30.

Cortez, D., Glick, G. & Elledge, S.J. (2004) Minichromosome maintenance proteins are direct targets of the ATM and ATR checkpoint kinases. *Proc Natl Acad Sci U S A,* Vol. 101 (27) 10078-83.

Cortez, D., Guntuku, S., Qin, J. & Elledge, S.J. (2001) ATR and ATRIP: partners in checkpoint signaling. *Science,* Vol. 294 (5547) 1713-6.

Costanzo, V., Robertson, K., Ying, C.Y., Kim, E., Avvedimento, E., Gottesman, M., Grieco, D. & Gautier, J. (2000) Reconstitution of an ATM-dependent checkpoint that inhibits chromosomal DNA replication following DNA damage. *Mol Cell,* Vol. 6 (3) 649-59.

Cox, J., Jackson, A.P., Bond, J. & Woods, C.G. (2006) What primary microcephaly can tell us about brain growth. *Trends Mol Med,* Vol. 12 (8) 358-66.

Darvish, H., Esmaeeli-Nieh, S., Monajemi, G.B., Mohseni, M., Ghasemi-Firouzabadi, S., Abedini, S.S., Bahman, I., Jamali, P., Azimi, S., Mojahedi, F., Dehghan, A., Shafeghati, Y., Jankhah, A., Falah, M., Soltani Banavandi, M.J., Ghani-Kakhi, M., Garshasbi, M., Rakhshani, F., Naghavi, A., Tzschach, A., Neitzel, H., Ropers, H.H., Kuss, A.W., Behjati, F., Kahrizi, K. & Najmabadi, H. (2010) A clinical and molecular genetic study of 112 Iranian families with primary microcephaly. *J Med Genet,* Vol. 47 (12) 823-8.

Delaval, B. & Doxsey, S.J. (2010) Pericentrin in cellular function and disease. *J Cell Biol,* Vol. 188 (2) 181-90.

Deming, P.B., Flores, K.G., Downes, C.S., Paules, R.S. & Kaufmann, W.K. (2002) ATR enforces the topoisomerase II-dependent G2 checkpoint through inhibition of Plk1 kinase. *J Biol Chem,* Vol. 277 (39) 36832-8.

Derheimer, F.A. & Kastan, M.B. (2010) Multiple roles of ATM in monitoring and maintaining DNA integrity. *FEBS Lett,* Vol. 584 (17) 3675-81.

Dhar, S.K., Yoshida, K., Machida, Y., Khaira, P., Chaudhuri, B., Wohlschlegel, J.A., Leffak, M., Yates, J. & Dutta, A. (2001) Replication from oriP of Epstein-Barr virus requires human ORC and is inhibited by geminin. *Cell,* Vol. 106 (3) 287-96.

Dheekollu, J., Wiedmer, A., Hayden, J., Speicher, D., Gotter, A.L., Yen, T. & Lieberman, P.M. (2011) Timeless links replication termination to mitotic kinase activation. *PLoS One,* Vol. 6 (5) e19596.

Diviani, D., Langeberg, L.K., Doxsey, S.J. & Scott, J.D. (2000) Pericentrin anchors protein kinase A at the centrosome through a newly identified RII-binding domain. *Curr Biol,* Vol. 10 (7) 417-20.

Dobyns, W.B., Reiner, O., Carrozzo, R. & Ledbetter, D.H. (1993) Lissencephaly. A human brain malformation associated with deletion of the LIS1 gene located at chromosome 17p13. *JAMA,* Vol. 270 (23) 2838-42.

Doil, C., Mailand, N., Bekker-Jensen, S., Menard, P., Larsen, D.H., Pepperkok, R., Ellenberg, J., Panier, S., Durocher, D., Bartek, J., Lukas, J. & Lukas, C. (2009) RNF168 binds and amplifies ubiquitin conjugates on damaged chromosomes to allow accumulation of repair proteins. *Cell,* Vol. 136 (3) 435-46.

Donzelli, M., Busino, L., Chiesa, M., Ganoth, D., Hershko, A. & Draetta, G.F. (2004) Hierarchical order of phosphorylation events commits Cdc25A to betaTrCP-dependent degradation. *Cell Cycle,* Vol. 3 (4) 469-71.

Doxsey, S., Mccollum, D. & Theurkauf, W. (2005a) Centrosomes in cellular regulation. *Annu Rev Cell Dev Biol,* Vol. 21 411-34.

Doxsey, S., Zimmerman, W. & Mikule, K. (2005b) Centrosome control of the cell cycle. *Trends Cell Biol,* Vol. 15 (6) 303-11.

Duldulao, N.A., Li, J. & Sun, Z. (2010) Cilia in cell signaling and human disorders. *Protein Cell,* Vol. 1 (8) 726-36.

Dutertre, S., Cazales, M., Quaranta, M., Froment, C., Trabut, V., Dozier, C., Mirey, G., Bouché, J., Theis-Febvre, N., Schmitt, E., Monsarrat, B., Prigent, C. & Ducommun, B. (2004a) Phosphorylation of CDC25B by Aurora-A at the centrosome contributes to the G2-M transition. *J Cell Sci,* Vol. 117 (Pt 12) 2523-31.

Dutertre, S., Cazales, M., Quaranta, M., Froment, C., Trabut, V., Dozier, C., Mirey, G., Bouché, J.P., Theis-Febvre, N., Schmitt, E., Monsarrat, B., Prigent, C. & Ducommun, B. (2004b) Phosphorylation of CDC25B by Aurora-A at the centrosome contributes to the G2-M transition. *J Cell Sci,* Vol. 117 (Pt 12) 2523-31.

Duursma, A. & Agami, R. (2005) p53-Dependent regulation of Cdc6 protein stability controls cellular proliferation. *Mol Cell Biol,* Vol. 25 (16) 6937-47.

Elia, A.E., Cantley, L.C. & Yaffe, M.B. (2003a) Proteomic screen finds pSer/pThr-binding domain localizing Plk1 to mitotic substrates. *Science,* Vol. 299 (5610) 1228-31.

Elia, A.E., Rellos, P., Haire, L.F., Chao, J.W., Ivins, F.J., Hoepker, K., Mohammad, D., Cantley, L.C., Smerdon, S.J. & Yaffe, M.B. (2003b) The molecular basis for phosphodependent substrate targeting and regulation of Plks by the Polo-box domain. *Cell,* Vol. 115 (1) 83-95.

Endoh-Yamagami, S., Karkar, K.M., May, S.R., Cobos, I., Thwin, M.T., Long, J.E., Ashique, A.M., Zarbalis, K., Rubenstein, J.L. & Peterson, A.S. (2010) A mutation in the pericentrin gene causes abnormal interneuron migration to the olfactory bulb in mice. *Dev Biol,* Vol. 340 (1) 41-53.

Eyers, P.A., Erikson, E., Chen, L.G. & Maller, J.L. (2003) A novel mechanism for activation of the protein kinase Aurora A. *Curr Biol,* Vol. 13 (8) 691-7.

Eyers, P.A. & Maller, J.L. (2003) Regulating the regulators: Aurora A activation and mitosis. *Cell Cycle,* Vol. 2 (4) 287-9.

Fabbro, M., Savage, K., Hobson, K., Deans, A.J., Powell, S.N., Mcarthur, G.A. & Khanna, K.K. (2004) BRCA1-BARD1 complexes are required for p53Ser-15

phosphorylation and a G1/S arrest following ionizing radiation-induced DNA damage. *J Biol Chem,* Vol. 279 (30) 31251-8.

Faivre, L., Le Merrer, M., Lyonnet, S., Plauchu, H., Dagoneau, N., Campos-Xavier, A.B., Attia-Sobol, J., Verloes, A., Munnich, A. & Cormier-Daire, V. (2002) Clinical and genetic heterogeneity of Seckel syndrome. *Am J Med Genet,* Vol. 112 (4) 379-83.

Falck, J., Coates, J. & Jackson, S.P. (2005) Conserved modes of recruitment of ATM, ATR and DNA-PKcs to sites of DNA damage. *Nature,* Vol. 434 (7033) 605-11.

Falck, J., Petrini, J.H., Williams, B.R., Lukas, J. & Bartek, J. (2002) The DNA damage-dependent intra-S phase checkpoint is regulated by parallel pathways. *Nat Genet,* Vol. 30 (3) 290-4.

Faqeih, E., Sakati, N. & Teebi, A.S. (2005) Meier-Gorlin (ear-patella-short stature) syndrome: growth hormone deficiency and previously unrecognized findings. *Am J Med Genet A,* Vol. 137A (3) 339-41.

Farkas, L.M. & Huttner, W.B. (2008) The cell biology of neural stem and progenitor cells and its significance for their proliferation versus differentiation during mammalian brain development. *Curr Opin Cell Biol,* Vol. 20 (6) 707-15.

Feijoo, C., Hall-Jackson, C., Wu, R., Jenkins, D., Leitch, J., Gilbert, D.M. & Smythe, C. (2001) Activation of mammalian Chk1 during DNA replication arrest: a role for Chk1 in the intra-S phase checkpoint monitoring replication origin firing. *J Cell Biol,* Vol. 154 (5) 913-23.

Ferguson, R.L. & Maller, J.L. (2010) Centrosomal localization of cyclin E-Cdk2 is required for initiation of DNA synthesis. *Curr Biol,* Vol. 20 (9) 856-60.

Fernandez-Capetillo, O., Celeste, A. & Nussenzweig, A. (2003) Focusing on foci: H2AX and the recruitment of DNA-damage response factors. *Cell Cycle,* Vol. 2 (5) 426-7.

Fish, J.L., Kosodo, Y., Enard, W., Pääbo, S. & Huttner, W.B. (2006) Aspm specifically maintains symmetric proliferative divisions of neuroepithelial cells. *Proc Natl Acad Sci U S A,* Vol. 103 (27) 10438-43.

Flory, M.R. & Davis, T.N. (2003) The centrosomal proteins pericentrin and kendrin are encoded by alternatively spliced products of one gene. *Genomics,* Vol. 82 (3) 401-5.

Fong, K.W., Hau, S.Y., Kho, Y.S., Jia, Y., He, L. & Qi, R.Z. (2009) Interaction of CDK5RAP2 with EB1 to track growing microtubule tips and to regulate microtubule dynamics. *Mol Biol Cell,* Vol. 20 (16) 3660-70.

Foray, N., Marot, D., Gabriel, A., Randrianarison, V., Carr, A.M., Perricaudet, M., Ashworth, A. & Jeggo, P. (2003) A subset of ATM- and ATR-dependent phosphorylation events requires the BRCA1 protein. *EMBO J,* Vol. 22 (11) 2860-71.

Fragkos, M., Jurvansuu, J. & Beard, P. (2009) H2AX is required for cell cycle arrest via the p53/p21 pathway. *Mol Cell Biol,* Vol. 29 (10) 2828-40.

Fu, Z., Malureanu, L., Huang, J., Wang, W., Li, H., Van Deursen, J.M., Tindall, D.J. & Chen, J. (2008) Plk1-dependent phosphorylation of FoxM1 regulates a

transcriptional programme required for mitotic progression. *Nat Cell Biol,* Vol. 10 (9) 1076-82.

Fukasawa, K. (2007) Oncogenes and tumour suppressors take on centrosomes. *Nat Rev Cancer,* Vol. 7 (12) 911-24.

Galasso, C., Lo-Castro, A., Lalli, C., Cerminara, C. & Curatolo, P. (2008) Neurologic aspects of microcephalic osteodysplastic primordial dwarfism type II. *Pediatr Neurol,* Vol. 38 (6) 435-8.

Ganem, N.J., Godinho, S.A. & Pellman, D. (2009) A mechanism linking extra centrosomes to chromosomal instability. *Nature,* Vol. 460 (7252) 278-82.

Ge, X.Q. & Blow, J.J. (2009) The licensing checkpoint opens up. *Cell Cycle,* Vol. 8 (15) 2320-2.

Ge, X.Q. & Blow, J.J. (2010) Chk1 inhibits replication factory activation but allows dormant origin firing in existing factories. *J Cell Biol,* Vol. 191 (7) 1285-97.

Giubettini, M., Asteriti, I.A., Scrofani, J., De Luca, M., Lindon, C., Lavia, P. & Guarguaglini, G. (2011) Control of Aurora-A stability through interaction with TPX2. *J Cell Sci,* Vol. 124 (Pt 1) 113-22.

Gomez-Ferreria, M.A., Rath, U., Buster, D.W., Chanda, S.K., Caldwell, J.S., Rines, D.R. & Sharp, D.J. (2007) Human Cep192 is required for mitotic centrosome and spindle assembly. *Curr Biol,* Vol. 17 (22) 1960-6.

Goodarzi, A.A., Jonnalagadda, J.C., Douglas, P., Young, D., Ye, R., Moorhead, G.B., Lees-Miller, S.P. & Khanna, K.K. (2004) Autophosphorylation of ataxia-telangiectasia mutated is regulated by protein phosphatase 2A. *EMBO J,* Vol. 23 (22) 4451-61.

Goodarzi, A.A., Noon, A.T., Deckbar, D., Ziv, Y., Shiloh, Y., Löbrich, M. & Jeggo, P.A. (2008) ATM signaling facilitates repair of DNA double-strand breaks associated with heterochromatin. *Mol Cell,* Vol. 31 (2) 167-77.

Gorlin, R.J. (1992) Microtia, absent patellae, short stature, micrognathia syndrome. *J Med Genet,* Vol. 29 (7) 516-7.

Graser, S., Stierhof, Y.D. & Nigg, E.A. (2007) Cep68 and Cep215 (Cdk5rap2) are required for centrosome cohesion. *J Cell Sci,* Vol. 120 (Pt 24) 4321-31.

Greenberg, R.A., Sobhian, B., Pathania, S., Cantor, S.B., Nakatani, Y. & Livingston, D.M. (2006) Multifactorial contributions to an acute DNA damage response by BRCA1/BARD1-containing complexes. *Genes Dev,* Vol. 20 (1) 34-46.

Greer, D.A., Besley, B.D., Kennedy, K.B. & Davey, S. (2003) hRad9 rapidly binds DNA containing double-strand breaks and is required for damage-dependent topoisomerase II beta binding protein 1 focus formation. *Cancer Res,* Vol. 63 (16) 4829-35.

Griffith, E., Walker, S., Martin, C.A., Vagnarelli, P., Stiff, T., Vernay, B., Al Sanna, N., Saggar, A., Hamel, B., Earnshaw, W.C., Jeggo, P.A., Jackson, A.P. & O'driscoll, M. (2008) Mutations in pericentrin cause Seckel syndrome with defective ATR-dependent DNA damage signaling. *Nat Genet,* Vol. 40 (2) 232-6.

Guernsey, D.L., Jiang, H., Hussin, J., Arnold, M., Bouyakdan, K., Perry, S., Babineau-Sturk, T., Beis, J., Dumas, N., Evans, S.C., Ferguson, M., Matsuoka, M., Macgillivray, C., Nightingale, M., Patry, L., Rideout, A.L., Thomas, A., Orr, A., Hoffmann, I., Michaud, J.L., Awadalla, P., Meek, D.C., Ludman, M. & Samuels, M.E. (2010) Mutations in centrosomal protein CEP152 in primary microcephaly families linked to MCPH4. *Am J Hum Genet,* Vol. 87 (1) 40-51.

Guernsey, D.L., Matsuoka, M., Jiang, H., Evans, S., Macgillivray, C., Nightingale, M., Perry, S., Ferguson, M., Leblanc, M., Paquette, J., Patry, L., Rideout, A.L., Thomas, A., Orr, A., Mcmaster, C.R., Michaud, J.L., Deal, C., Langlois, S., Superneau, D.W., Parkash, S., Ludman, M., Skidmore, D.L. & Samuels, M.E. (2011) Mutations in origin recognition complex gene ORC4 cause Meier-Gorlin syndrome. *Nat Genet*.

Gul, A., Hassan, M.J., Hussain, S., Raza, S.I., Chishti, M.S. & Ahmad, W. (2006) A novel deletion mutation in CENPJ gene in a Pakistani family with autosomal recessive primary microcephaly. *J Hum Genet,* Vol. 51 (9) 760-4.

Götz, M. & Huttner, W.B. (2005) The cell biology of neurogenesis. *Nat Rev Mol Cell Biol,* Vol. 6 (10) 777-88.

Hagting, A., Karlsson, C., Clute, P., Jackman, M. & Pines, J. (1998) MPF localization is controlled by nuclear export. *EMBO J,* Vol. 17 (14) 4127-38.

Hall, J.G., Flora, C., Scott, C.I., Pauli, R.M. & Tanaka, K.I. (2004) Majewski osteodysplastic primordial dwarfism type II (MOPD II): natural history and clinical findings. *Am J Med Genet A,* Vol. 130A (1) 55-72.

Hall, J.R., Kow, E., Nevis, K.R., Lu, C.K., Luce, K.S., Zhong, Q. & Cook, J.G. (2007) Cdc6 stability is regulated by the Huwe1 ubiquitin ligase after DNA damage. *Mol Biol Cell,* Vol. 18 (9) 3340-50.

Hanashiro, K., Kanai, M., Geng, Y., Sicinski, P. & Fukasawa, K. (2008) Roles of cyclins A and E in induction of centrosome amplification in p53-compromised cells. *Oncogene,* Vol. 27 (40) 5288-302.

Hanasoge, S. & Ljungman, M. (2007) H2AX phosphorylation after UV irradiation is triggered by DNA repair intermediates and is mediated by the ATR kinase. *Carcinogenesis,* Vol. 28 (11) 2298-304.

Hanawalt, P.C., Ford, J.M. & Lloyd, D.R. (2003) Functional characterization of global genomic DNA repair and its implications for cancer. *Mutat Res,* Vol. 544 (2-3) 107-14.

Hannak, E., Kirkham, M., Hyman, A.A. & Oegema, K. (2001) Aurora-A kinase is required for centrosome maturation in Caenorhabditis elegans. *J Cell Biol,* Vol. 155 (7) 1109-16.

Haren, L., Stearns, T. & Lüders, J. (2009) Plk1-dependent recruitment of gamma-tubulin complexes to mitotic centrosomes involves multiple PCM components. *PLoS One,* Vol. 4 (6) e5976.

Harper, J.W. & Elledge, S.J. (2007) The DNA damage response: ten years after. *Mol Cell,* Vol. 28 (5) 739-45.

Hayani, A., Suarez, C.R., Molnar, Z., Lebeau, M. & Godwin, J. (1994) Acute myeloid leukaemia in a patient with Seckel syndrome. *J Med Genet,* Vol. 31 (2) 148-9.

Hayon, I.L. & Haupt, Y. (2002) p53: an internal investigation. *Cell Cycle,* Vol. 1 (2) 111-6.

Heffernan, T.P., Unsal-Kaçmaz, K., Heinloth, A.N., Simpson, D.A., Paules, R.S., Sancar, A., Cordeiro-Stone, M. & Kaufmann, W.K. (2007) Cdc7-Dbf4 and the human S checkpoint response to UVC. *J Biol Chem,* Vol. 282 (13) 9458-68.

Hemerly, A.S., Prasanth, S.G., Siddiqui, K. & Stillman, B. (2009) Orc1 controls centriole and centrosome copy number in human cells. *Science,* Vol. 323 (5915) 789-93.

Herring, M., Davenport, N., Stephan, K., Campbell, S., White, R., Kark, J. & Wolkow, T.D. (2010) Fission yeast Rad26ATRIP delays spindle-pole-body separation following interphase microtubule damage. *J Cell Sci,* Vol. 123 (Pt 9) 1537-45.

Higginbotham, H.R. & Gleeson, J.G. (2007) The centrosome in neuronal development. *Trends Neurosci,* Vol. 30 (6) 276-83.

Higgins, J., Midgley, C., Bergh, A.M., Bell, S.M., Askham, J.M., Roberts, E., Binns, R.K., Sharif, S.M., Bennett, C., Glover, D.M., Woods, C.G., Morrison, E.E. & Bond, J. (2010) Human ASPM participates in spindle organisation, spindle orientation and cytokinesis. *BMC Cell Biol,* Vol. 11 85.

Hinchcliffe, E.H., Miller, F.J., Cham, M., Khodjakov, A. & Sluder, G. (2001) Requirement of a centrosomal activity for cell cycle progression through G1 into S phase. *Science,* Vol. 291 (5508) 1547-50.

Hirota, T., Kunitoku, N., Sasayama, T., Marumoto, T., Zhang, D., Nitta, M., Hatakeyama, K. & Saya, H. (2003) Aurora-A and an interacting activator, the LIM protein Ajuba, are required for mitotic commitment in human cells. *Cell,* Vol. 114 (5) 585-98.

Huang-Doran, I., Bicknell, L.S., Finucane, F.M., Rocha, N., Porter, K.M., Tung, Y.C., Szekeres, F., Krook, A., Nolan, J.J., O'driscoll, M., Bober, M., O'rahilly, S., Jackson, A.P., Semple, R.K. & Group, F.T.M.O.P.D.S. (2011) Genetic Defects in Human Pericentrin Are Associated With Severe Insulin Resistance and Diabetes. *Diabetes,* Vol. 60 (3) 925-935.

Hung, L.Y., Tang, C.J. & Tang, T.K. (2000) Protein 4.1 R-135 interacts with a novel centrosomal protein (CPAP) which is associated with the gamma-tubulin complex. *Mol Cell Biol,* Vol. 20 (20) 7813-25.

Hutterer, A., Berdnik, D., Wirtz-Peitz, F., Zigman, M., Schleiffer, A. & Knoblich, J.A. (2006) Mitotic activation of the kinase Aurora-A requires its binding partner Bora. *Dev Cell,* Vol. 11 (2) 147-57.

Huttner, W.B. & Kosodo, Y. (2005) Symmetric versus asymmetric cell division during neurogenesis in the developing vertebrate central nervous system. *Curr Opin Cell Biol,* Vol. 17 (6) 648-57.

Inoue, D. & Sagata, N. (2005) The Polo-like kinase Plx1 interacts with and inhibits Myt1 after fertilization of Xenopus eggs. *EMBO J,* Vol. 24 (5) 1057-67.

Ira, G., Pellicioli, A., Balijja, A., Wang, X., Fiorani, S., Carotenuto, W., Liberi, G., Bressan, D., Wan, L., Hollingsworth, N.M., Haber, J.E. & Foiani, M. (2004) DNA end

resection, homologous recombination and DNA damage checkpoint activation require CDK1. *Nature,* Vol. 431 (7011) 1011-7.

Ishiai, M., Kitao, H., Smogorzewska, A., Tomida, J., Kinomura, A., Uchida, E., Saberi, A., Kinoshita, E., Kinoshita-Kikuta, E., Koike, T., Tashiro, S., Elledge, S.J. & Takata, M. (2008) FANCI phosphorylation functions as a molecular switch to turn on the Fanconi anemia pathway. *Nat Struct Mol Biol,* Vol. 15 (11) 1138-46.

Jackman, M., Lindon, C., Nigg, E. & Pines, J. (2003a) Active cyclin B1-Cdk1 first appears on centrosomes in prophase. *Nat Cell Biol,* Vol. 5 (2) 143-8.

Jackman, M., Lindon, C., Nigg, E.A. & Pines, J. (2003b) Active cyclin B1-Cdk1 first appears on centrosomes in prophase. *Nat Cell Biol,* Vol. 5 (2) 143-8.

Jackson, A.P., Eastwood, H., Bell, S.M., Adu, J., Toomes, C., Carr, I.M., Roberts, E., Hampshire, D.J., Crow, Y.J., Mighell, A.J., Karbani, G., Jafri, H., Rashid, Y., Mueller, R.F., Markham, A.F. & Woods, C.G. (2002) Identification of microcephalin, a protein implicated in determining the size of the human brain. *Am J Hum Genet,* Vol. 71 (1) 136-42.

Jazayeri, A., Falck, J., Lukas, C., Bartek, J., Smith, G.C., Lukas, J. & Jackson, S.P. (2006) ATM- and cell cycle-dependent regulation of ATR in response to DNA double-strand breaks. *Nat Cell Biol,* Vol. 8 (1) 37-45.

Jin, C., Lan, H., Attie, A.D., Churchill, G.A., Bulutuglo, D. & Yandell, B.S. (2004) Selective phenotyping for increased efficiency in genetic mapping studies. *Genetics,* Vol. 168 (4) 2285-93.

Jin, J., Ang, X.L., Ye, X., Livingstone, M. & Harper, J.W. (2008) Differential roles for checkpoint kinases in DNA damage-dependent degradation of the Cdc25A protein phosphatase. *J Biol Chem,* Vol. 283 (28) 19322-8.

Joukov, V., De Nicolo, A., Rodriguez, A., Walter, J.C. & Livingston, D.M. (2010) Centrosomal protein of 192 kDa (Cep192) promotes centrosome-driven spindle assembly by engaging in organelle-specific Aurora A activation. *Proc Natl Acad Sci U S A,* Vol. 107 (49) 21022-7.

Jowsey, P., Morrice, N., Hastie, C., Mclauchlan, H., Toth, R. & Rouse, J. (2007a) Characterisation of the sites of DNA damage-induced 53BP1 phosphorylation catalysed by ATM and ATR. *DNA Repair (Amst),* Vol. 6 (10) 1536-44.

Jowsey, P., Morrice, N.A., Hastie, C.J., Mclauchlan, H., Toth, R. & Rouse, J. (2007b) Characterisation of the sites of DNA damage-induced 53BP1 phosphorylation catalysed by ATM and ATR. *DNA Repair (Amst),* Vol. 6 (10) 1536-44.

Jurczyk, A., Gromley, A., Redick, S., San Agustin, J., Witman, G., Pazour, G.J., Peters, D.J. & Doxsey, S. (2004) Pericentrin forms a complex with intraflagellar transport proteins and polycystin-2 and is required for primary cilia assembly. *J Cell Biol,* Vol. 166 (5) 637-43.

Jurczyk, A., Pino, S.C., O'sullivan-Murphy, B., Addorio, M., Lidstone, E.A., Diiorio, P., Lipson, K.L., Standley, C., Fogarty, K., Lifshitz, L., Urano, F., Mordes, J.P., Greiner, D.L., Rossini, A.A. & Bortell, R. (2010) A novel role for the centrosomal protein, pericentrin, in regulation of insulin secretory vesicle docking in mouse pancreatic beta-cells. *PLoS One,* Vol. 5 (7) e11812.

Kalay, E., Yigit, G., Aslan, Y., Brown, K.E., Pohl, E., Bicknell, L.S., Kayserili, H., Li, Y., Tüysüz, B., Nürnberg, G., Kiess, W., Koegl, M., Baessmann, I., Buruk, K., Toraman, B., Kayipmaz, S., Kul, S., Ikbal, M., Turner, D.J., Taylor, M.S., Aerts, J., Scott, C., Milstein, K., Dollfus, H., Wieczorek, D., Brunner, H.G., Hurles, M., Jackson, A.P., Rauch, A., Nürnberg, P., Karagüzel, A. & Wollnik, B. (2011) CEP152 is a genome maintenance protein disrupted in Seckel syndrome. *Nat Genet,* Vol. 43 (1) 23-6.

Katayama, H., Zhou, H., Li, Q., Tatsuka, M. & Sen, S. (2001) Interaction and feedback regulation between STK15/BTAK/Aurora-A kinase and protein phosphatase 1 through mitotic cell division cycle. *J Biol Chem,* Vol. 276 (49) 46219-24.

Kee, Y. & D'andrea, A.D. (2010) Expanded roles of the Fanconi anemia pathway in preserving genomic stability. *Genes Dev,* Vol. 24 (16) 1680-94.

Kemp, M.G., Akan, Z., Yilmaz, S., Grillo, M., Smith-Roe, S.L., Kang, T.H., Cordeiro-Stone, M., Kaufmann, W.K., Abraham, R.T., Sancar, A. & Unsal-Kaçmaz, K. (2010) Tipin-replication protein A interaction mediates Chk1 phosphorylation by ATR in response to genotoxic stress. *J Biol Chem,* Vol. 285 (22) 16562-71.

Khazaei, M.R. & Püschel, A.W. (2009) Phosphorylation of the par polarity complex protein Par3 at serine 962 is mediated by aurora a and regulates its function in neuronal polarity. *J Biol Chem,* Vol. 284 (48) 33571-9.

Khodjakov, A. & Rieder, C.L. (2001) Centrosomes enhance the fidelity of cytokinesis in vertebrates and are required for cell cycle progression. *J Cell Biol,* Vol. 153 (1) 237-42.

Kim, H., Chen, J. & Yu, X. (2007a) Ubiquitin-binding protein RAP80 mediates BRCA1-dependent DNA damage response. *Science,* Vol. 316 (5828) 1202-5.

Kim, H., Huang, J. & Chen, J. (2007b) CCDC98 is a BRCA1-BRCT domain-binding protein involved in the DNA damage response. *Nat Struct Mol Biol,* Vol. 14 (8) 710-5.

Kim, H.S., Li, H., Cevher, M., Parmelee, A., Fonseca, D., Kleiman, F.E. & Lee, S.B. (2006) DNA damage-induced BARD1 phosphorylation is critical for the inhibition of messenger RNA processing by BRCA1/BARD1 complex. *Cancer Res,* Vol. 66 (9) 4561-5.

Kim, S. & Tsiokas, L. (2011) Cilia and cell cycle re-entry: More than a coincidence. *Cell Cycle,* Vol. 10 (16) 2683-90.

Kishi, K., Van Vugt, M.A., Okamoto, K., Hayashi, Y. & Yaffe, M.B. (2009) Functional dynamics of Polo-like kinase 1 at the centrosome. *Mol Cell Biol,* Vol. 29 (11) 3134-50.

Kneissl, M., Pütter, V., Szalay, A.A. & Grummt, F. (2003) Interaction and assembly of murine pre-replicative complex proteins in yeast and mouse cells. *J Mol Biol,* Vol. 327 (1) 111-28.

Knoblich, J.A. (2010) Asymmetric cell division: recent developments and their implications for tumour biology. *Nat Rev Mol Cell Biol,* Vol. 11 (12) 849-60.

Kondo, T., Kobayashi, M., Tanaka, J., Yokoyama, A., Suzuki, S., Kato, N., Onozawa, M., Chiba, K., Hashino, S., Imamura, M., Minami, Y., Minamino, N. &

Asaka, M. (2004) Rapid degradation of Cdt1 upon UV-induced DNA damage is mediated by SCFSkp2 complex. *J Biol Chem,* Vol. 279 (26) 27315-9.

Kosodo, Y., Röper, K., Haubensak, W., Marzesco, A.M., Corbeil, D. & Huttner, W.B. (2004) Asymmetric distribution of the apical plasma membrane during neurogenic divisions of mammalian neuroepithelial cells. *EMBO J,* Vol. 23 (11) 2314-24.

Kuo, A.J., Song, J., Cheung, P., Ishibe-Murakami, S., Yamazoe, S., Chen, J.K., Patel, D.J. & Gozani, O. (2012) The BAH domain of ORC1 links H4K20me2 to DNA replication licensing and Meier-Gorlin syndrome. *Nature,* Vol. 484 (7392) 115-9.

Krause, D.R., Jonnalagadda, J.C., Gatei, M.H., Sillje, H.H., Zhou, B.B., Nigg, E.A. & Khanna, K. (2003) Suppression of Tousled-like kinase activity after DNA damage or replication block requires ATM, NBS1 and Chk1. *Oncogene,* Vol. 22 (38) 5927-37.

Krystyniak, A., Garcia-Echeverria, C., Prigent, C. & Ferrari, S. (2006) Inhibition of Aurora A in response to DNA damage. *Oncogene,* Vol. 25 (3) 338-48.

Krämer, A., Maier, B. & Bartek, J. (2011) Centrosome clustering and chromosomal (in)stability: a matter of life and death. *Mol Oncol,* Vol. 5 (4) 324-35.

Krämer, A., Mailand, N., Lukas, C., Syljuåsen, R., Wilkinson, C., Nigg, E., Bartek, J. & Lukas, J. (2004a) Centrosome-associated Chk1 prevents premature activation of cyclin-B-Cdk1 kinase. *Nat Cell Biol,* Vol. 6 (9) 884-91.

Krämer, A., Mailand, N., Lukas, C., Syljuåsen, R.G., Wilkinson, C.J., Nigg, E.A., Bartek, J. & Lukas, J. (2004b) Centrosome-associated Chk1 prevents premature activation of cyclin-B-Cdk1 kinase. *Nat Cell Biol,* Vol. 6 (9) 884-91.

Kufer, T.A., Silljé, H.H., Körner, R., Gruss, O.J., Meraldi, P. & Nigg, E.A. (2002) Human TPX2 is required for targeting Aurora-A kinase to the spindle. *J Cell Biol,* Vol. 158 (4) 617-23.

Kumagai, A. & Dunphy, W.G. (2000) Claspin, a novel protein required for the activation of Chk1 during a DNA replication checkpoint response in Xenopus egg extracts. *Mol Cell,* Vol. 6 (4) 839-49.

Kumagai, A., Lee, J., Yoo, H.Y. & Dunphy, W.G. (2006) TopBP1 activates the ATR-ATRIP complex. *Cell,* Vol. 124 (5) 943-55.

Kwon, S.H. & Workman, J.L. (2008) The heterochromatin protein 1 (HP1) family: put away a bias toward HP1. *Mol Cells,* Vol. 26 (3) 217-27.

Lacey, K.R., Jackson, P.K. & Stearns, T. (1999) Cyclin-dependent kinase control of centrosome duplication. *Proc Natl Acad Sci U S A,* Vol. 96 (6) 2817-22.

Lau, E., Zhu, C., Abraham, R.T. & Jiang, W. (2006) The functional role of Cdc6 in S-G2/M in mammalian cells. *EMBO Rep,* Vol. 7 (4) 425-30.

Lee, J.E. & Gleeson, J.G. (2011) Cilia in the nervous system: linking cilia function and neurodevelopmental disorders. *Curr Opin Neurol,* Vol. 24 (2) 98-105.

Lee, K. & Rhee, K. (2011) PLK1 phosphorylation of pericentrin initiates centrosome maturation at the onset of mitosis. *J Cell Biol,* Vol. 195 (7) 1093-101.

Lee, Y., Shull, E.R., Frappart, P.O., Katyal, S., Enriquez-Rios, V., Zhao, J., Russell, H.R., Brown, E.J. & Mckinnon, P.J. (2012) ATR maintains select progenitors during nervous system development. *EMBO J,* Vol. 31 (5) 1177-89.

Lempiäinen, H. & Halazonetis, T.D. (2009) Emerging common themes in regulation of PIKKs and PI3Ks. *EMBO J,* Vol. 28 (20) 3067-73.

Lens, S.M., Voest, E.E. & Medema, R.H. (2010) Shared and separate functions of polo-like kinases and aurora kinases in cancer. *Nat Rev Cancer,* Vol. 10 (12) 825-41.

Li, C.J. & Depamphilis, M.L. (2002) Mammalian Orc1 protein is selectively released from chromatin and ubiquitinated during the S-to-M transition in the cell division cycle. *Mol Cell Biol,* Vol. 22 (1) 105-16.

Li, C.J., Vassilev, A. & Depamphilis, M.L. (2004) Role for Cdk1 (Cdc2)/cyclin A in preventing the mammalian origin recognition complex's largest subunit (Orc1) from binding to chromatin during mitosis. *Mol Cell Biol,* Vol. 24 (13) 5875-86.

Lieber, M.R. (2010) The mechanism of double-strand DNA break repair by the nonhomologous DNA end-joining pathway. *Annu Rev Biochem,* Vol. 79 181-211.

Lieber, M.R. & Wilson, T.E. (2010) SnapShot: Nonhomologous DNA end joining (NHEJ). *Cell,* Vol. 142 (3) 496-496.e1.

Lindqvist, A., Rodríguez-Bravo, V. & Medema, R.H. (2009) The decision to enter mitosis: feedback and redundancy in the mitotic entry network. *J Cell Biol,* Vol. 185 (2) 193-202.

Lindqvist, A., Van Zon, W., Karlsson Rosenthal, C. & Wolthuis, R.M. (2007) Cyclin B1-Cdk1 activation continues after centrosome separation to control mitotic progression. *PLoS Biol,* Vol. 5 (5) e123.

Liu, H., Takeda, S., Kumar, R., Westergard, T.D., Brown, E.J., Pandita, T.K., Cheng, E.H. & Hsieh, J.J. (2010) Phosphorylation of MLL by ATR is required for execution of mammalian S-phase checkpoint. *Nature,* Vol. 467 (7313) 343-6.

Liu, P., Barkley, L.R., Day, T., Bi, X., Slater, D.M., Alexandrow, M.G., Nasheuer, H.P. & Vaziri, C. (2006) The Chk1-mediated S-phase checkpoint targets initiation factor Cdc45 via a Cdc25A/Cdk2-independent mechanism. *J Biol Chem,* Vol. 281 (41) 30631-44.

Liu, Q., Guntuku, S., Cui, X.S., Matsuoka, S., Cortez, D., Tamai, K., Luo, G., Carattini-Rivera, S., Demayo, F., Bradley, A., Donehower, L.A. & Elledge, S.J. (2000) Chk1 is an essential kinase that is regulated by Atr and required for the G(2)/M DNA damage checkpoint. *Genes Dev,* Vol. 14 (12) 1448-59.

Liu, S., Shiotani, B., Lahiri, M., Maréchal, A., Tse, A., Leung, C.C., Glover, J.N., Yang, X.H. & Zou, L. (2011) ATR autophosphorylation as a molecular switch for checkpoint activation. *Mol Cell,* Vol. 43 (2) 192-202.

Lobjois, V., Jullien, D., Bouché, J.P. & Ducommun, B. (2009) The polo-like kinase 1 regulates CDC25B-dependent mitosis entry. *Biochim Biophys Acta,* Vol. 1793 (3) 462-8.

Lovejoy, C.A. & Cortez, D. (2009) Common mechanisms of PIKK regulation. *DNA Repair (Amst),* Vol. 8 (9) 1004-8.

Lu, B., Jan, L. & Jan, Y.N. (2000) Control of cell divisions in the nervous system: symmetry and asymmetry. *Annu Rev Neurosci,* Vol. 23 531-56.

Lu, L.Y., Wood, J.L., Minter-Dykhouse, K., Ye, L., Saunders, T.L., Yu, X. & Chen, J. (2008a) Polo-like kinase 1 is essential for early embryonic development and tumor suppression. *Mol Cell Biol,* Vol. 28 (22) 6870-6.

Lu, L.Y., Wood, J.L., Ye, L., Minter-Dykhouse, K., Saunders, T.L., Yu, X. & Chen, J. (2008b) Aurora A is essential for early embryonic development and tumor suppression. *J Biol Chem,* Vol. 283 (46) 31785-90.

Löffler, H., Bochtler, T., Fritz, B., Tews, B., Ho, A., Lukas, J., Bartek, J. & Krämer, A. (2007a) DNA damage-induced accumulation of centrosomal Chk1 contributes to its checkpoint function. *Cell Cycle,* Vol. 6 (20) 2541-8.

Löffler, H., Bochtler, T., Fritz, B., Tews, B., Ho, A.D., Lukas, J., Bartek, J. & Krämer, A. (2007b) DNA damage-induced accumulation of centrosomal Chk1 contributes to its checkpoint function. *Cell Cycle,* Vol. 6 (20) 2541-8.

Löffler, H., Rebacz, B., Ho, A.D., Lukas, J., Bartek, J. & Krämer, A. (2006) Chk1-dependent regulation of Cdc25B functions to coordinate mitotic events. *Cell Cycle,* Vol. 5 (21) 2543-7.

Macůrek, L., Lindqvist, A., Lim, D., Lampson, M.A., Klompmaker, R., Freire, R., Clouin, C., Taylor, S.S., Yaffe, M.B. & Medema, R.H. (2008) Polo-like kinase-1 is activated by aurora A to promote checkpoint recovery. *Nature,* Vol. 455 (7209) 119-23.

Mailand, N., Bekker-Jensen, S., Faustrup, H., Melander, F., Bartek, J., Lukas, C. & Lukas, J. (2007) RNF8 ubiquitylates histones at DNA double-strand breaks and promotes assembly of repair proteins. *Cell,* Vol. 131 (5) 887-900.

Mailand, N., Podtelejnikov, A.V., Groth, A., Mann, M., Bartek, J. & Lukas, J. (2002) Regulation of G(2)/M events by Cdc25A through phosphorylation-dependent modulation of its stability. *EMBO J,* Vol. 21 (21) 5911-20.

Majewski, F. & Goecke, T. (1982) Studies of microcephalic primordial dwarfism I: approach to a delineation of the Seckel syndrome. *Am J Med Genet,* Vol. 12 (1) 7-21.

Marumoto, T., Hirota, T., Morisaki, T., Kunitoku, N., Zhang, D., Ichikawa, Y., Sasayama, T., Kuninaka, S., Mimori, T., Tamaki, N., Kimura, M., Okano, Y. & Saya, H. (2002) Roles of aurora-A kinase in mitotic entry and G2 checkpoint in mammalian cells. *Genes Cells,* Vol. 7 (11) 1173-82.

Marumoto, T., Honda, S., Hara, T., Nitta, M., Hirota, T., Kohmura, E. & Saya, H. (2003) Aurora-A kinase maintains the fidelity of early and late mitotic events in HeLa cells. *J Biol Chem,* Vol. 278 (51) 51786-95.

Matsumoto, Y. & Maller, J. (2004a) A centrosomal localization signal in cyclin E required for Cdk2-independent S phase entry. *Science,* Vol. 306 (5697) 885-8.

Matsumoto, Y. & Maller, J.L. (2004b) A centrosomal localization signal in cyclin E required for Cdk2-independent S phase entry. *Science,* Vol. 306 (5697) 885-8.

Matsuo, K., Nishimura, T., Hayakawa, A., Ono, Y. & Takahashi, M. (2010) Involvement of a centrosomal protein kendrin in the maintenance of centrosome cohesion by modulating Nek2A kinase activity. *Biochem Biophys Res Commun,* Vol. 398 (2) 217-23.

Matsusaka, T. & Pines, J. (2004) Chfr acts with the p38 stress kinases to block entry to mitosis in mammalian cells. *J Cell Biol,* Vol. 166 (4) 507-16.

Maya-Mendoza, A., Petermann, E., Gillespie, D.A., Caldecott, K.W. & Jackson, D.A. (2007) Chk1 regulates the density of active replication origins during the vertebrate S phase. *EMBO J,* Vol. 26 (11) 2719-31.

Mazón, G., Mimitou, E.P. & Symington, L.S. (2010) SnapShot: Homologous recombination in DNA double-strand break repair. *Cell,* Vol. 142 (4) 646, 646.e1.

Mcnairn, A.J., Okuno, Y., Misteli, T. & Gilbert, D.M. (2005) Chinese hamster ORC subunits dynamically associate with chromatin throughout the cell-cycle. *Exp Cell Res,* Vol. 308 (2) 345-56.

Mikule, K., Delaval, B., Kaldis, P., Jurcyzk, A., Hergert, P. & Doxsey, S. (2007) Loss of centrosome integrity induces p38-p53-p21-dependent G1-S arrest. *Nat Cell Biol,* Vol. 9 (2) 160-70.

Miyoshi, K., Onishi, K., Asanuma, M., Miyazaki, I., Diaz-Corrales, F.J. & Ogawa, N. (2006) Embryonic expression of pericentrin suggests universal roles in ciliogenesis. *Dev Genes Evol,* Vol. 216 (9) 537-42.

Mohammad, M.M., Donti, T.R., Sebastian Yakisich, J., Smith, A.G. & Kapler, G.M. (2007) Tetrahymena ORC contains a ribosomal RNA fragment that participates in rDNA origin recognition. *EMBO J,* Vol. 26 (24) 5048-60.

Mordes, D.A., Glick, G.G., Zhao, R. & Cortez, D. (2008) TopBP1 activates ATR through ATRIP and a PIKK regulatory domain. *Genes Dev,* Vol. 22 (11) 1478-89.

Mori, D., Yano, Y., Toyo-Oka, K., Yoshida, N., Yamada, M., Muramatsu, M., Zhang, D., Saya, H., Toyoshima, Y.Y., Kinoshita, K., Wynshaw-Boris, A. & Hirotsune, S. (2007) NDEL1 phosphorylation by Aurora-A kinase is essential for centrosomal maturation, separation, and TACC3 recruitment. *Mol Cell Biol,* Vol. 27 (1) 352-67.

Moshous, D., Callebaut, I., De Chasseval, R., Corneo, B., Cavazzana-Calvo, M., Le Deist, F., Tezcan, I., Sanal, O., Bertrand, Y., Philippe, N., Fischer, A. & De Villartay, J.P. (2001) Artemis, a novel DNA double-strand break repair/V(D)J recombination protein, is mutated in human severe combined immune deficiency. *Cell,* Vol. 105 (2) 177-86.

Murga, M., Bunting, S., Montaña, M.F., Soria, R., Mulero, F., Cañamero, M., Lee, Y., Mckinnon, P.J., Nussenzweig, A. & Fernandez-Capetillo, O. (2009) A mouse model of ATR-Seckel shows embryonic replicative stress and accelerated aging. *Nat Genet,* Vol. 41 (8) 891-8.

Myers, J.S., Zhao, R., Xu, X., Ham, A.J. & Cortez, D. (2007) Cyclin-dependent kinase 2 dependent phosphorylation of ATRIP regulates the G2-M checkpoint response to DNA damage. *Cancer Res,* Vol. 67 (14) 6685-90.

Méndez, J., Zou-Yang, X.H., Kim, S.Y., Hidaka, M., Tansey, W.P. & Stillman, B. (2002) Human origin recognition complex large subunit is degraded by ubiquitin-mediated proteolysis after initiation of DNA replication. *Mol Cell,* Vol. 9 (3) 481-91.

Nagai, Y., Asaoka, Y., Namae, M., Saito, K., Momose, H., Mitani, H., Furutani-Seiki, M., Katada, T. & Nishina, H. (2010) The LIM protein Ajuba is required for ciliogenesis and left-right axis determination in medaka. *Biochem Biophys Res Commun,* Vol. 396 (4) 887-93.

Nakajima, H., Toyoshima-Morimoto, F., Taniguchi, E. & Nishida, E. (2003) Identification of a consensus motif for Plk (Polo-like kinase) phosphorylation reveals Myt1 as a Plk1 substrate. *J Biol Chem,* Vol. 278 (28) 25277-80.

Nam, E.A., Zhao, R., Glick, G.G., Bansbach, C.E., Friedman, D.B. & Cortez, D. (2011) Thr-1989 phosphorylation is a marker of active ataxia telangiectasia-mutated and Rad3-related (ATR) kinase. *J Biol Chem,* Vol. 286 (33) 28707-14.

Namiki, Y. & Zou, L. (2006) ATRIP associates with replication protein A-coated ssDNA through multiple interactions. *Proc Natl Acad Sci U S A,* Vol. 103 (3) 580-5.

Nevis, K.R., Cordeiro-Stone, M. & Cook, J.G. (2009) Origin licensing and p53 status regulate Cdk2 activity during G(1). *Cell Cycle,* Vol. 8 (12) 1952-63.

Nicholas, A.K., Swanson, E.A., Cox, J.J., Karbani, G., Malik, S., Springell, K., Hampshire, D., Ahmed, M., Bond, J., Di Benedetto, D., Fichera, M., Romano, C., Dobyns, W.B. & Woods, C.G. (2009) The molecular landscape of ASPM mutations in primary microcephaly. *J Med Genet,* Vol. 46 (4) 249-53.

Nigg, E.A. & Raff, J.W. (2009) Centrioles, centrosomes, and cilia in health and disease. *Cell,* Vol. 139 (4) 663-78.

Niida, H., Katsuno, Y., Banerjee, B., Hande, M.P. & Nakanishi, M. (2007) Specific role of Chk1 phosphorylations in cell survival and checkpoint activation. *Mol Cell Biol,* Vol. 27 (7) 2572-81.

Niida, H., Tsuge, S., Katsuno, Y., Konishi, A., Takeda, N. & Nakanishi, M. (2005) Depletion of Chk1 leads to premature activation of Cdc2-cyclin B and mitotic catastrophe. *J Biol Chem,* Vol. 280 (47) 39246-52.

Nishitani, H. & Lygerou, Z. (2002) Control of DNA replication licensing in a cell cycle. *Genes Cells,* Vol. 7 (6) 523-34.

Nishitani, H., Sugimoto, N., Roukos, V., Nakanishi, Y., Saijo, M., Obuse, C., Tsurimoto, T., Nakayama, K.I., Nakayama, K., Fujita, M., Lygerou, Z. & Nishimoto, T. (2006) Two E3 ubiquitin ligases, SCF-Skp2 and DDB1-Cul4, target human Cdt1 for proteolysis. *EMBO J,* Vol. 25 (5) 1126-36.

Noatynska, A., Panbianco, C. & Gotta, M. (2010) SPAT-1/Bora acts with Polo-like kinase 1 to regulate PAR polarity and cell cycle progression. *Development,* Vol. 137 (19) 3315-25.

Noguchi, K., Vassilev, A., Ghosh, S., Yates, J.L. & Depamphilis, M.L. (2006) The BAH domain facilitates the ability of human Orc1 protein to activate replication origins in vivo. *EMBO J,* Vol. 25 (22) 5372-82.

Noon, A.T., Shibata, A., Rief, N., Löbrich, M., Stewart, G.S., Jeggo, P.A. & Goodarzi, A.A. (2010) 53BP1-dependent robust localized KAP-1 phosphorylation is essential for heterochromatic DNA double-strand break repair. *Nat Cell Biol,* Vol. 12 (2) 177-84.

Nouspikel, T. (2009) DNA repair in mammalian cells : Nucleotide excision repair: variations on versatility. *Cell Mol Life Sci,* Vol. 66 (6) 994-1009.

O'driscoll, M., Cerosaletti, K.M., Girard, P.M., Dai, Y., Stumm, M., Kysela, B., Hirsch, B., Gennery, A., Palmer, S.E., Seidel, J., Gatti, R.A., Varon, R., Oettinger, M.A., Neitzel, H., Jeggo, P.A. & Concannon, P. (2001) DNA ligase IV mutations identified in patients exhibiting developmental delay and immunodeficiency. *Mol Cell,* Vol. 8 (6) 1175-85.

O'driscoll, M., Jackson, A.P. & Jeggo, P.A. (2006) Microcephalin: a causal link between impaired damage response signalling and microcephaly. *Cell Cycle,* Vol. 5 (20) 2339-44.

O'driscoll, M. & Jeggo, P.A. (2006) The role of double-strand break repair - insights from human genetics. *Nat Rev Genet,* Vol. 7 (1) 45-54.

O'driscoll, M. & Jeggo, P.A. (2008) The role of the DNA damage response pathways in brain development and microcephaly: insight from human disorders. *DNA Repair (Amst),* Vol. 7 (7) 1039-50.

O'driscoll, M., Ruiz-Perez, V.L., Woods, C.G., Jeggo, P.A. & Goodship, J.A. (2003) A splicing mutation affecting expression of ataxia-telangiectasia and Rad3-related protein (ATR) results in Seckel syndrome. *Nat Genet,* Vol. 33 (4) 497-501.

Oehlmann, M., Score, A.J. & Blow, J.J. (2004) The role of Cdc6 in ensuring complete genome licensing and S phase checkpoint activation. *J Cell Biol,* Vol. 165 (2) 181-90.

Ohta, S., Tatsumi, Y., Fujita, M., Tsurimoto, T. & Obuse, C. (2003) The ORC1 cycle in human cells: II. Dynamic changes in the human ORC complex during the cell cycle. *J Biol Chem,* Vol. 278 (42) 41535-40.

Okuno, Y., Mcnairn, A.J., Den Elzen, N., Pines, J. & Gilbert, D.M. (2001) Stability, chromatin association and functional activity of mammalian pre-replication complex proteins during the cell cycle. *EMBO J,* Vol. 20 (15) 4263-77.

Olson, E., Nievera, C.J., Klimovich, V., Fanning, E. & Wu, X. (2006) RPA2 is a direct downstream target for ATR to regulate the S-phase checkpoint. *J Biol Chem,* Vol. 281 (51) 39517-33.

Otto, T., Horn, S., Brockmann, M., Eilers, U., Schüttrumpf, L., Popov, N., Kenney, A.M., Schulte, J.H., Beijersbergen, R., Christiansen, H., Berwanger, B. & Eilers, M. (2009) Stabilization of N-Myc is a critical function of Aurora A in human neuroblastoma. *Cancer Cell,* Vol. 15 (1) 67-78.

Ouchi, M., Fujiuchi, N., Sasai, K., Katayama, H., Minamishima, Y.A., Ongusaha, P.P., Deng, C., Sen, S., Lee, S.W. & Ouchi, T. (2004) BRCA1 phosphorylation by Aurora-A in the regulation of G2 to M transition. *J Biol Chem,* Vol. 279 (19) 19643-8.

Paulsen, R.D. & Cimprich, K.A. (2007) The ATR pathway: fine-tuning the fork. *DNA Repair (Amst),* Vol. 6 (7) 953-66.

Peng, C.Y., Graves, P.R., Thoma, R.S., Wu, Z., Shaw, A.S. & Piwnica-Worms, H. (1997) Mitotic and G2 checkpoint control: regulation of 14-3-3 protein binding by phosphorylation of Cdc25C on serine-216. *Science,* Vol. 277 (5331) 1501-5.

Petermann, E., Maya-Mendoza, A., Zachos, G., Gillespie, D.A., Jackson, D.A. & Caldecott, K.W. (2006) Chk1 requirement for high global rates of replication fork progression during normal vertebrate S phase. *Mol Cell Biol,* Vol. 26 (8) 3319-26.

Petersen, B.O., Lukas, J., Sørensen, C.S., Bartek, J. & Helin, K. (1999) Phosphorylation of mammalian CDC6 by cyclin A/CDK2 regulates its subcellular localization. *EMBO J,* Vol. 18 (2) 396-410.

Petersen, B.O., Wagener, C., Marinoni, F., Kramer, E.R., Melixetian, M., Lazzerini Denchi, E., Gieffers, C., Matteucci, C., Peters, J.M. & Helin, K. (2000) Cell cycle- and cell growth-regulated proteolysis of mammalian CDC6 is dependent on APC-CDH1. *Genes Dev,* Vol. 14 (18) 2330-43.

Piatti, S., Lengauer, C. & Nasmyth, K. (1995) Cdc6 is an unstable protein whose de novo synthesis in G1 is important for the onset of S phase and for preventing a 'reductional' anaphase in the budding yeast Saccharomyces cerevisiae. *EMBO J,* Vol. 14 (15) 3788-99.

Prasanth, S.G., Prasanth, K.V., Siddiqui, K., Spector, D.L. & Stillman, B. (2004) Human Orc2 localizes to centrosomes, centromeres and heterochromatin during chromosome inheritance. *EMBO J,* Vol. 23 (13) 2651-63.

Prasanth, S.G., Prasanth, K.V. & Stillman, B. (2002) Orc6 involved in DNA replication, chromosome segregation, and cytokinesis. *Science,* Vol. 297 (5583) 1026-31.

Prasanth, S.G., Shen, Z., Prasanth, K.V. & Stillman, B. (2010) Human origin recognition complex is essential for HP1 binding to chromatin and heterochromatin organization. *Proc Natl Acad Sci U S A,* Vol. 107 (34) 15093-8.

Pruitt, S.C., Bailey, K.J. & Freeland, A. (2007) Reduced Mcm2 expression results in severe stem/progenitor cell deficiency and cancer. *Stem Cells,* Vol. 25 (12) 3121-32.

Pugacheva, E.N., Jablonski, S.A., Hartman, T.R., Henske, E.P. & Golemis, E.A. (2007) HEF1-dependent Aurora A activation induces disassembly of the primary cilium. *Cell,* Vol. 129 (7) 1351-63.

Pulvers, J.N., Bryk, J., Fish, J.L., Wilsch-Bräuninger, M., Arai, Y., Schreier, D., Naumann, R., Helppi, J., Habermann, B., Vogt, J., Nitsch, R., Tóth, A., Enard, W., Pääbo, S. & Huttner, W.B. (2010) Mutations in mouse Aspm (abnormal spindle-like microcephaly associated) cause not only microcephaly but also major defects in the germline. *Proc Natl Acad Sci U S A,* Vol. 107 (38) 16595-600.

Purohit, A., Tynan, S.H., Vallee, R. & Doxsey, S.J. (1999) Direct interaction of pericentrin with cytoplasmic dynein light intermediate chain contributes to mitotic spindle organization. *J Cell Biol,* Vol. 147 (3) 481-92.

Qvist, P., Huertas, P., Jimeno, S., Nyegaard, M., Hassan, M.J., Jackson, S.P. & Børglum, A.D. (2011) CtIP Mutations Cause Seckel and Jawad Syndromes. *PLoS Genet,* Vol. 7 (10) e1002310.

Rastogi, R.P., Richa, Kumar, A., Tyagi, M.B. & Sinha, R.P. (2010) Molecular mechanisms of ultraviolet radiation-induced DNA damage and repair. *J Nucleic Acids,* Vol. 2010 592980.

Rauch, A., Thiel, C., Schindler, D., Wick, U., Crow, Y., Ekici, A., Van Essen, A., Goecke, T., Al-Gazali, L., Chrzanowska, K., Zweier, C., Brunner, H., Becker, K., Curry, C., Dallapiccola, B., Devriendt, K., Dörfler, A., Kinning, E., Megarbane, A., Meinecke, P., Semple, R., Spranger, S., Toutain, A., Trembath, R., Voss, E., Wilson, L., Hennekam, R., De Zegher, F., Dörr, H. & Reis, A. (2008a) Mutations in the pericentrin (PCNT) gene cause primordial dwarfism. *Science,* Vol. 319 (5864) 816-9.

Rauch, A., Thiel, C.T., Schindler, D., Wick, U., Crow, Y.J., Ekici, A.B., Van Essen, A.J., Goecke, T.O., Al-Gazali, L., Chrzanowska, K.H., Zweier, C., Brunner, H.G., Becker, K., Curry, C.J., Dallapiccola, B., Devriendt, K., Dörfler, A., Kinning, E., Megarbane, A., Meinecke, P., Semple, R.K., Spranger, S., Toutain, A., Trembath, R.C., Voss, E., Wilson, L., Hennekam, R., De Zegher, F., Dörr, H.G. & Reis, A. (2008b) Mutations in the pericentrin (PCNT) gene cause primordial dwarfism. *Science,* Vol. 319 (5864) 816-9.

Rendtlew Danielsen, J.M., Larsen, D.H., Schou, K.B., Freire, R., Falck, J., Bartek, J. & Lukas, J. (2009) HCLK2 is required for activity of the DNA damage response kinase ATR. *J Biol Chem,* Vol. 284 (7) 4140-7.

Riballo, E., Kühne, M., Rief, N., Doherty, A., Smith, G.C., Recio, M.J., Reis, C., Dahm, K., Fricke, A., Krempler, A., Parker, A.R., Jackson, S.P., Gennery, A., Jeggo, P.A. & Löbrich, M. (2004) A pathway of double-strand break rejoining dependent upon ATM, Artemis, and proteins locating to gamma-H2AX foci. *Mol Cell,* Vol. 16 (5) 715-24.

Rogakou, E.P., Boon, C., Redon, C. & Bonner, W.M. (1999) Megabase chromatin domains involved in DNA double-strand breaks in vivo. *J Cell Biol,* Vol. 146 (5) 905-16.

Rogakou, E.P., Nieves-Neira, W., Boon, C., Pommier, Y. & Bonner, W.M. (2000) Initiation of DNA fragmentation during apoptosis induces phosphorylation of H2AX histone at serine 139. *J Biol Chem,* Vol. 275 (13) 9390-5.

Roos, W.P. & Kaina, B. (2012) DNA damage-induced apoptosis: From specific DNA lesions to the DNA damage response and apoptosis. *Cancer Lett*.

Roshak, A.K., Capper, E.A., Imburgia, C., Fornwald, J., Scott, G. & Marshall, L.A. (2000) The human polo-like kinase, PLK, regulates cdc2/cyclin B through phosphorylation and activation of the cdc25C phosphatase. *Cell Signal,* Vol. 12 (6) 405-11.

Roy, R., Chun, J. & Powell, S.N. (2012) BRCA1 and BRCA2: different roles in a common pathway of genome protection. *Nat Rev Cancer,* Vol. 12 (1) 68-78.

Rudner, A.D. & Murray, A.W. (1996) The spindle assembly checkpoint. *Curr Opin Cell Biol,* Vol. 8 (6) 773-80.

Ruzankina, Y., Pinzon-Guzman, C., Asare, A., Ong, T., Pontano, L., Cotsarelis, G., Zediak, V.P., Velez, M., Bhandoola, A. & Brown, E.J. (2007) Deletion of the developmentally essential gene ATR in adult mice leads to age-related phenotypes and stem cell loss. *Cell Stem Cell,* Vol. 1 (1) 113-26.

Sabino, D., Brown, N.H. & Basto, R. (2011) Drosophila Ajuba is not an Aurora-A activator but is required to maintain Aurora-A at the centrosome. *J Cell Sci,* Vol. 124 (Pt 7) 1156-66.

Saha, T., Ghosh, S., Vassilev, A. & Depamphilis, M.L. (2006) Ubiquitylation, phosphorylation and Orc2 modulate the subcellular location of Orc1 and prevent it from inducing apoptosis. *J Cell Sci,* Vol. 119 (Pt 7) 1371-82.

Sakasai, R. & Tibbetts, R. (2008) RNF8-dependent and RNF8-independent regulation of 53BP1 in response to DNA damage. *J Biol Chem,* Vol. 283 (20) 13549-55.

Sancar, A., Lindsey-Boltz, L.A., Unsal-Kaçmaz, K. & Linn, S. (2004) Molecular mechanisms of mammalian DNA repair and the DNA damage checkpoints. *Annu Rev Biochem,* Vol. 73 39-85.

Sartori, A.A., Lukas, C., Coates, J., Mistrik, M., Fu, S., Bartek, J., Baer, R., Lukas, J. & Jackson, S.P. (2007) Human CtIP promotes DNA end resection. *Nature,* Vol. 450 (7169) 509-14.

Schmitt, E., Boutros, R., Froment, C., Monsarrat, B., Ducommun, B. & Dozier, C. (2006) CHK1 phosphorylates CDC25B during the cell cycle in the absence of DNA damage. *J Cell Sci,* Vol. 119 (Pt 20) 4269-75.

Schoppy, D.W., Ragland, R.L., Gilad, O., Shastri, N., Peters, A.A., Murga, M., Fernandez-Capetillo, O., Diehl, J.A. & Brown, E.J. (2012) Oncogenic stress sensitizes murine cancers to hypomorphic suppression of ATR. *J Clin Invest,* Vol. 122 (1) 241-52.

Sebastian, B., Kakizuka, A. & Hunter, T. (1993) Cdc25M2 activation of cyclin-dependent kinases by dephosphorylation of threonine-14 and tyrosine-15. *Proc Natl Acad Sci U S A,* Vol. 90 (8) 3521-4.

Seckel, H.P.G. (1960) *Bird-Headed Dwarfs.* Basel: S Karger.

Seiler, J.A., Conti, C., Syed, A., Aladjem, M.I. & Pommier, Y. (2007) The intra-S-phase checkpoint affects both DNA replication initiation and elongation: single-cell and -DNA fiber analyses. *Mol Cell Biol,* Vol. 27 (16) 5806-18.

Seki, A., Coppinger, J.A., Jang, C.Y., Yates, J.R. & Fang, G. (2008) Bora and the kinase Aurora a cooperatively activate the kinase Plk1 and control mitotic entry. *Science,* Vol. 320 (5883) 1655-8.

Sengupta, S., Robles, A.I., Linke, S.P., Sinogeeva, N.I., Zhang, R., Pedeux, R., Ward, I.M., Celeste, A., Nussenzweig, A., Chen, J., Halazonetis, T.D. & Harris, C.C. (2004) Functional interaction between BLM helicase and 53BP1 in a Chk1-mediated pathway during S-phase arrest. *J Cell Biol,* Vol. 166 (6) 801-13.

Shechter, D., Costanzo, V. & Gautier, J. (2004) Regulation of DNA replication by ATR: signaling in response to DNA intermediates. *DNA Repair (Amst),* Vol. 3 (8-9) 901-8.

Shen, Z., Sathyan, K.M., Geng, Y., Zheng, R., Chakraborty, A., Freeman, B., Wang, F., Prasanth, K.V. & Prasanth, S.G. (2010) A WD-repeat protein stabilizes ORC binding to chromatin. *Mol Cell,* Vol. 40 (1) 99-111.

Shibata, A., Barton, O., Noon, A.T., Dahm, K., Deckbar, D., Goodarzi, A.A., Löbrich, M. & Jeggo, P.A. (2010) Role of ATM and the damage response mediator proteins 53BP1 and MDC1 in the maintenance of G(2)/M checkpoint arrest. *Mol Cell Biol,* Vol. 30 (13) 3371-83.

Shigechi, T., Tomida, J., Sato, K., Kobayashi, M., Eykelenboom, J.K., Pessina, F., Zhang, Y., Uchida, E., Ishiai, M., Lowndes, N.F., Yamamoto, K., Kurumizaka, H., Maehara, Y. & Takata, M. (2012) ATR-ATRIP kinase complex triggers activation of the Fanconi anemia DNA repair pathway. *Cancer Res,* Vol. 72 (5) 1149-56.

Shima, N., Alcaraz, A., Liachko, I., Buske, T.R., Andrews, C.A., Munroe, R.J., Hartford, S.A., Tye, B.K. & Schimenti, J.C. (2007) A viable allele of Mcm4 causes chromosome instability and mammary adenocarcinomas in mice. *Nat Genet,* Vol. 39 (1) 93-8.

Shin, J.H., Grabowski, B., Kasiviswanathan, R., Bell, S.D. & Kelman, Z. (2003) Regulation of minichromosome maintenance helicase activity by Cdc6. *J Biol Chem,* Vol. 278 (39) 38059-67.

Shreeram, S., Hee, W.K. & Bulavin, D.V. (2008) Cdc25A serine 123 phosphorylation couples centrosome duplication with DNA replication and regulates tumorigenesis. *Mol Cell Biol,* Vol. 28 (24) 7442-50.

Shreeram, S., Sparks, A., Lane, D.P. & Blow, J.J. (2002) Cell type-specific responses of human cells to inhibition of replication licensing. *Oncogene,* Vol. 21 (43) 6624-32.

Siddiqui, K. & Stillman, B. (2007) ATP-dependent assembly of the human origin recognition complex. *J Biol Chem,* Vol. 282 (44) 32370-83.

Sii-Felice, K., Etienne, O., Hoffschir, F., Mathieu, C., Riou, L., Barroca, V., Haton, C., Arwert, F., Fouchet, P., Boussin, F.D. & Mouthon, M.A. (2008) Fanconi DNA repair pathway is required for survival and long-term maintenance of neural progenitors. *EMBO J,* Vol. 27 (5) 770-81.

Siliciano, J.D., Canman, C.E., Taya, Y., Sakaguchi, K., Appella, E. & Kastan, M.B. (1997) DNA damage induces phosphorylation of the amino terminus of p53. *Genes Dev,* Vol. 11 (24) 3471-81.

Silkworth, W.T., Nardi, I.K., Scholl, L.M. & Cimini, D. (2009) Multipolar spindle pole coalescence is a major source of kinetochore mis-attachment and chromosome mis-segregation in cancer cells. *PLoS One,* Vol. 4 (8) e6564.

Silljé, H.H. & Nigg, E.A. (2001) Identification of human Asf1 chromatin assembly factors as substrates of Tousled-like kinases. *Curr Biol,* Vol. 11 (13) 1068-73.

Smith, E., Dejsuphong, D., Balestrini, A., Hampel, M., Lenz, C., Takeda, S., Vindigni, A. & Costanzo, V. (2009) An ATM- and ATR-dependent checkpoint inactivates spindle assembly by targeting CEP63. *Nat Cell Biol,* Vol. 11 (3) 278-85.

Smits, V.A., Klompmaker, R., Arnaud, L., Rijksen, G., Nigg, E.A. & Medema, R.H. (2000) Polo-like kinase-1 is a target of the DNA damage checkpoint. *Nat Cell Biol,* Vol. 2 (9) 672-6.

Smits, V.A., Reaper, P.M. & Jackson, S.P. (2006) Rapid PIKK-dependent release of Chk1 from chromatin promotes the DNA-damage checkpoint response. *Curr Biol,* Vol. 16 (2) 150-9.

So, S., Davis, A.J. & Chen, D.J. (2009) Autophosphorylation at serine 1981 stabilizes ATM at DNA damage sites. *J Cell Biol,* Vol. 187 (7) 977-90.

Song, B., Liu, X.S., Davis, K. & Liu, X. (2011) Plk1 phosphorylation of Orc2 promotes DNA replication under conditions of stress. *Mol Cell Biol,* Vol. 31 (23) 4844-56.

Soung, N.K., Kang, Y.H., Kim, K., Kamijo, K., Yoon, H., Seong, Y.S., Kuo, Y.L., Miki, T., Kim, S.R., Kuriyama, R., Giam, C.Z., Ahn, C.H. & Lee, K.S. (2006) Requirement of hCenexin for proper mitotic functions of polo-like kinase 1 at the centrosomes. *Mol Cell Biol,* Vol. 26 (22) 8316-35.

Stewart, G.S., Wang, B., Bignell, C.R., Taylor, A.M. & Elledge, S.J. (2003) MDC1 is a mediator of the mammalian DNA damage checkpoint. *Nature,* Vol. 421 (6926) 961-6.

Stiff, T., Cerosaletti, K., Concannon, P., O'driscoll, M. & Jeggo, P.A. (2008) Replication independent ATR signalling leads to G2/M arrest requiring Nbs1, 53BP1 and MDC1. *Hum Mol Genet,* Vol. 17 (20) 3247-53.

Stiff, T., O'driscoll, M., Rief, N., Iwabuchi, K., Löbrich, M. & Jeggo, P.A. (2004) ATM and DNA-PK function redundantly to phosphorylate H2AX after exposure to ionizing radiation. *Cancer Res,* Vol. 64 (7) 2390-6.

Stiff, T., Reis, C., Alderton, G.K., Woodbine, L., O'driscoll, M. & Jeggo, P.A. (2005) Nbs1 is required for ATR-dependent phosphorylation events. *EMBO J,* Vol. 24 (1) 199-208.

Suter, B., Tong, A., Chang, M., Yu, L., Brown, G.W., Boone, C. & Rine, J. (2004) The origin recognition complex links replication, sister chromatid cohesion and transcriptional silencing in Saccharomyces cerevisiae. *Genetics,* Vol. 167 (2) 579-91.

Syljuåsen, R.G., Sørensen, C.S., Hansen, L.T., Fugger, K., Lundin, C., Johansson, F., Helleday, T., Sehested, M., Lukas, J. & Bartek, J. (2005) Inhibition of human Chk1 causes increased initiation of DNA replication, phosphorylation of ATR targets, and DNA breakage. *Mol Cell Biol,* Vol. 25 (9) 3553-62.

Takahashi, M., Yamagiwa, A., Nishimura, T., Mukai, H. & Ono, Y. (2002) Centrosomal proteins CG-NAP and kendrin provide microtubule nucleation sites by anchoring gamma-tubulin ring complex. *Mol Biol Cell,* Vol. 13 (9) 3235-45.

Takahashi, T., Nowakowski, R.S. & Caviness, V.S. (1995) The cell cycle of the pseudostratified ventricular epithelium of the embryonic murine cerebral wall. *J Neurosci,* Vol. 15 (9) 6046-57.

Takahashi, T.S., Yiu, P., Chou, M.F., Gygi, S. & Walter, J.C. (2004) Recruitment of Xenopus Scc2 and cohesin to chromatin requires the pre-replication complex. *Nat Cell Biol,* Vol. 6 (10) 991-6.

Takeda, D.Y. & Dutta, A. (2005) DNA replication and progression through S phase. *Oncogene,* Vol. 24 (17) 2827-43.

Tassan, J.P., Schultz, S.J., Bartek, J. & Nigg, E.A. (1994) Cell cycle analysis of the activity, subcellular localization, and subunit composition of human CAK (CDK-activating kinase). *J Cell Biol,* Vol. 127 (2) 467-78.

Tatsumi, Y., Ohta, S., Kimura, H., Tsurimoto, T. & Obuse, C. (2003) The ORC1 cycle in human cells: I. cell cycle-regulated oscillation of human ORC1. *J Biol Chem,* Vol. 278 (42) 41528-34.

Terada, Y., Uetake, Y. & Kuriyama, R. (2003) Interaction of Aurora-A and centrosomin at the microtubule-nucleating site in Drosophila and mammalian cells. *J Cell Biol,* Vol. 162 (5) 757-63.

Thornton, G.K. & Woods, C.G. (2009) Primary microcephaly: do all roads lead to Rome? *Trends Genet,* Vol. 25 (11) 501-10.

Tibelius, A., Marhold, J., Zentgraf, H., Heilig, C.E., Neitzel, H., Ducommun, B., Rauch, A., Ho, A.D., Bartek, J. & Krämer, A. (2009) Microcephalin and pericentrin regulate mitotic entry via centrosome-associated Chk1. *J Cell Biol,* Vol. 185 (7) 1149-57.

Toji, S., Yabuta, N., Hosomi, T., Nishihara, S., Kobayashi, T., Suzuki, S., Tamai, K. & Nojima, H. (2004) The centrosomal protein Lats2 is a phosphorylation target of Aurora-A kinase. *Genes Cells,* Vol. 9 (5) 383-97.

Toyoshima, F., Moriguchi, T., Wada, A., Fukuda, M. & Nishida, E. (1998) Nuclear export of cyclin B1 and its possible role in the DNA damage-induced G2 checkpoint. *EMBO J,* Vol. 17 (10) 2728-35.

Toyoshima, F. & Nishida, E. (2007) Integrin-mediated adhesion orients the spindle parallel to the substratum in an EB1- and myosin X-dependent manner. *EMBO J,* Vol. 26 (6) 1487-98.

Toyoshima-Morimoto, F., Taniguchi, E. & Nishida, E. (2002) Plk1 promotes nuclear translocation of human Cdc25C during prophase. *EMBO Rep,* Vol. 3 (4) 341-8.

Toyoshima-Morimoto, F., Taniguchi, E., Shinya, N., Iwamatsu, A. & Nishida, E. (2001) Polo-like kinase 1 phosphorylates cyclin B1 and targets it to the nucleus during prophase. *Nature,* Vol. 410 (6825) 215-20.

Trenz, K., Errico, A. & Costanzo, V. (2008) Plx1 is required for chromosomal DNA replication under stressful conditions. *EMBO J,* Vol. 27 (6) 876-85.

Tripathi, V., Kaur, S. & Sengupta, S. (2008) Phosphorylation-dependent interactions of BLM and 53BP1 are required for their anti-recombinogenic roles during homologous recombination. *Carcinogenesis,* Vol. 29 (1) 52-61.

Tsubuki, S., Saito, Y., Tomioka, M., Ito, H. & Kawashima, S. (1996) Differential inhibition of calpain and proteasome activities by peptidyl aldehydes of di-leucine and tri-leucine. *J Biochem,* Vol. 119 (3) 572-6.

Tsvetkov, L. & Stern, D.F. (2005a) Interaction of chromatin-associated Plk1 and Mcm7. *J Biol Chem,* Vol. 280 (12) 11943-7.

Tsvetkov, L. & Stern, D.F. (2005b) Phosphorylation of Plk1 at S137 and T210 is inhibited in response to DNA damage. *Cell Cycle,* Vol. 4 (1) 166-71.

Uetake, Y. & Sluder, G. (2004) Cell cycle progression after cleavage failure: mammalian somatic cells do not possess a "tetraploidy checkpoint". *J Cell Biol,* Vol. 165 (5) 609-15.

Unsal-Kaçmaz, K., Mullen, T.E., Kaufmann, W.K. & Sancar, A. (2005) Coupling of human circadian and cell cycles by the timeless protein. *Mol Cell Biol,* Vol. 25 (8) 3109-16.

Van De Weerdt, B.C., Littler, D.R., Klompmaker, R., Huseinovic, A., Fish, A., Perrakis, A. & Medema, R.H. (2008) Polo-box domains confer target specificity to the Polo-like kinase family. *Biochim Biophys Acta,* Vol. 1783 (6) 1015-22.

Van Horn, R.D., Chu, S., Fan, L., Yin, T., Du, J., Beckmann, R., Mader, M., Zhu, G., Toth, J., Blanchard, K. & Ye, X.S. (2010) Cdk1 activity is required for mitotic activation of aurora A during G2/M transition of human cells. *J Biol Chem,* Vol. 285 (28) 21849-57.

Van Vugt, M.A., Brás, A. & Medema, R.H. (2004) Polo-like kinase-1 controls recovery from a G2 DNA damage-induced arrest in mammalian cells. *Mol Cell,* Vol. 15 (5) 799-811.

Van Vugt, M.A., Gardino, A.K., Linding, R., Ostheimer, G.J., Reinhardt, H.C., Ong, S.E., Tan, C.S., Miao, H., Keezer, S.M., Li, J., Pawson, T., Lewis, T.A., Carr, S.A., Smerdon, S.J., Brummelkamp, T.R. & Yaffe, M.B. (2010) A mitotic phosphorylation feedback network connects Cdk1, Plk1, 53BP1, and Chk2 to inactivate the G(2)/M DNA damage checkpoint. *PLoS Biol,* Vol. 8 (1) e1000287.

Van Vugt, M.A., Smits, V.A., Klompmaker, R. & Medema, R.H. (2001) Inhibition of Polo-like kinase-1 by DNA damage occurs in an ATM- or ATR-dependent fashion. *J Biol Chem,* Vol. 276 (45) 41656-60.

Vashee, S., Cvetic, C., Lu, W., Simancek, P., Kelly, T.J. & Walter, J.C. (2003) Sequence-independent DNA binding and replication initiation by the human origin recognition complex. *Genes Dev,* Vol. 17 (15) 1894-908.

Vashee, S., Simancek, P., Challberg, M.D. & Kelly, T.J. (2001) Assembly of the human origin recognition complex. *J Biol Chem,* Vol. 276 (28) 26666-73.

Venere, M., Snyder, A., Zgheib, O. & Halazonetis, T.D. (2007) Phosphorylation of ATR-interacting protein on Ser239 mediates an interaction with breast-ovarian cancer susceptibility 1 and checkpoint function. *Cancer Res,* Vol. 67 (13) 6100-5.

Walter, A.O., Seghezzi, W., Korver, W., Sheung, J. & Lees, E. (2000) The mitotic serine/threonine kinase Aurora2/AIK is regulated by phosphorylation and degradation. *Oncogene,* Vol. 19 (42) 4906-16.

Wang, B., Matsuoka, S., Ballif, B.A., Zhang, D., Smogorzewska, A., Gygi, S.P. & Elledge, S.J. (2007) Abraxas and RAP80 form a BRCA1 protein complex required for the DNA damage response. *Science,* Vol. 316 (5828) 1194-8.

Wang, Q., Hirohashi, Y., Furuuchi, K., Zhao, H., Liu, Q., Zhang, H., Murali, R., Berezov, A., Du, X., Li, B. & Greene, M.I. (2004) The centrosome in normal and transformed cells. *DNA Cell Biol,* Vol. 23 (8) 475-89.

Wang, X., Zou, L., Lu, T., Bao, S., Hurov, K.E., Hittelman, W.N., Elledge, S.J. & Li, L. (2006) Rad17 phosphorylation is required for claspin recruitment and Chk1 activation in response to replication stress. *Mol Cell,* Vol. 23 (3) 331-41.

Ward, I.M. & Chen, J. (2001) Histone H2AX is phosphorylated in an ATR-dependent manner in response to replicational stress. *J Biol Chem,* Vol. 276 (51) 47759-62.

Watanabe, N., Arai, H., Nishihara, Y., Taniguchi, M., Hunter, T. & Osada, H. (2004) M-phase kinases induce phospho-dependent ubiquitination of somatic Wee1 by SCFbeta-TrCP. *Proc Natl Acad Sci U S A,* Vol. 101 (13) 4419-24.

Willems, M., Geneviève, D., Borck, G., Baumann, C., Baujat, G., Bieth, E., Edery, P., Farra, C., Gerard, M., Héron, D., Leheup, B., Le Merrer, M., Lyonnet, S., Martin-Coignard, D., Mathieu, M., Thauvin-Robinet, C., Verloes, A., Colleaux, L., Munnich, A. & Cormier-Daire, V. (2010) Molecular analysis of pericentrin gene (PCNT) in a series of 24 Seckel/microcephalic osteodysplastic primordial dwarfism type II (MOPD II) families. *J Med Genet,* Vol. 47 (12) 797-802.

Wilsker, D., Petermann, E., Helleday, T. & Bunz, F. (2008) Essential function of Chk1 can be uncoupled from DNA damage checkpoint and replication control. *Proc Natl Acad Sci U S A,* Vol. 105 (52) 20752-7.

Wirtz-Peitz, F., Nishimura, T. & Knoblich, J.A. (2008) Linking cell cycle to asymmetric division: Aurora-A phosphorylates the Par complex to regulate Numb localization. *Cell,* Vol. 135 (1) 161-73.

Wood, J.L., Singh, N., Mer, G. & Chen, J. (2007) MCPH1 functions in an H2AX-dependent but MDC1-independent pathway in response to DNA damage. *J Biol Chem,* Vol. 282 (48) 35416-23.

Woodward, A.M., Göhler, T., Luciani, M.G., Oehlmann, M., Ge, X., Gartner, A., Jackson, D.A. & Blow, J.J. (2006) Excess Mcm2-7 license dormant origins of replication that can be used under conditions of replicative stress. *J Cell Biol,* Vol. 173 (5) 673-83.

Wu, L.C., Wang, Z.W., Tsan, J.T., Spillman, M.A., Phung, A., Xu, X.L., Yang, M.C., Hwang, L.Y., Bowcock, A.M. & Baer, R. (1996) Identification of a RING protein that can interact in vivo with the BRCA1 gene product. *Nat Genet,* Vol. 14 (4) 430-40.

Wu, X., Mondal, G., Wang, X., Wu, J., Yang, L., Pankratz, V.S., Rowley, M. & Couch, F.J. (2009) Microcephalin regulates BRCA2 and Rad51-associated DNA double-strand break repair. *Cancer Res,* Vol. 69 (13) 5531-6.

Xie, Z., Moy, L.Y., Sanada, K., Zhou, Y., Buchman, J.J. & Tsai, L.H. (2007) Cep120 and TACCs control interkinetic nuclear migration and the neural progenitor pool. *Neuron,* Vol. 56 (1) 79-93.

Xu, Y., Ashley, T., Brainerd, E.E., Bronson, R.T., Meyn, M.S. & Baltimore, D. (1996) Targeted disruption of ATM leads to growth retardation, chromosomal fragmentation during meiosis, immune defects, and thymic lymphoma. *Genes Dev,* Vol. 10 (19) 2411-22.

Yang, S.B., Zhou, X.B., Zhu, H.X., Quan, L.P., Bai, J.F., He, J., Gao, Y.N., Cheng, S.J. & Xu, N.Z. (2007) Amplification and overexpression of Aurora-A in esophageal squamous cell carcinoma. *Oncol Rep,* Vol. 17 (5) 1083-8.

Yim, H. & Erikson, R.L. (2009) Polo-like kinase 1 depletion induces DNA damage in early S prior to caspase activation. *Mol Cell Biol,* Vol. 29 (10) 2609-21.

Yim, H. & Erikson, R.L. (2010) Cell division cycle 6, a mitotic substrate of polo-like kinase 1, regulates chromosomal segregation mediated by cyclin-dependent kinase 1 and separase. *Proc Natl Acad Sci U S A,* Vol. 107 (46) 19742-7.

Yoshida, K., Sugimoto, N., Iwahori, S., Yugawa, T., Narisawa-Saito, M., Kiyono, T. & Fujita, M. (2010) CDC6 interaction with ATR regulates activation of a replication checkpoint in higher eukaryotic cells. *J Cell Sci,* Vol. 123 (Pt 2) 225-35.

Yun, M.H. & Hiom, K. (2009) CtIP-BRCA1 modulates the choice of DNA double-strand-break repair pathway throughout the cell cycle. *Nature,* Vol. 459 (7245) 460-3.

Zhadanov, A.B., Provance, D.W., Speer, C.A., Coffin, J.D., Goss, D., Blixt, J.A., Reichert, C.M. & Mercer, J.A. (1999) Absence of the tight junctional protein AF-6 disrupts epithelial cell-cell junctions and cell polarity during mouse development. *Curr Biol,* Vol. 9 (16) 880-8.

Zhan, Q., Antinore, M.J., Wang, X.W., Carrier, F., Smith, M.L., Harris, C.C. & Fornace, A.J. (1999) Association with Cdc2 and inhibition of Cdc2/Cyclin B1 kinase activity by the p53-regulated protein Gadd45. *Oncogene,* Vol. 18 (18) 2892-900.

Zhang, S., Hemmerich, P. & Grosse, F. (2007) Centrosomal localization of DNA damage checkpoint proteins. *J Cell Biochem,* Vol. 101 (2) 451-65.

Zhao, H., Watkins, J.L. & Piwnica-Worms, H. (2002) Disruption of the checkpoint kinase 1/cell division cycle 25A pathway abrogates ionizing radiation-induced S and G2 checkpoints. *Proc Natl Acad Sci U S A,* Vol. 99 (23) 14795-800.

Zhong, X., Liu, L., Zhao, A., Pfeifer, G.P. & Xu, X. (2005) The abnormal spindle-like, microcephaly-associated (ASPM) gene encodes a centrosomal protein. *Cell Cycle,* Vol. 4 (9) 1227-9.

Zhou, H., Kuang, J., Zhong, L., Kuo, W.L., Gray, J.W., Sahin, A., Brinkley, B.R. & Sen, S. (1998) Tumour amplified kinase STK15/BTAK induces centrosome amplification, aneuploidy and transformation. *Nat Genet,* Vol. 20 (2) 189-93.

Zimmerman, W.C., Sillibourne, J., Rosa, J. & Doxsey, S.J. (2004) Mitosis-specific anchoring of gamma tubulin complexes by pericentrin controls spindle organization and mitotic entry. *Mol Biol Cell,* Vol. 15 (8) 3642-57.

Zou, L., Cortez, D. & Elledge, S.J. (2002) Regulation of ATR substrate selection by Rad17-dependent loading of Rad9 complexes onto chromatin. *Genes Dev,* Vol. 16 (2) 198-208.

Zou, L. & Elledge, S.J. (2003) Sensing DNA damage through ATRIP recognition of RPA-ssDNA complexes. *Science,* Vol. 300 (5625) 1542-8.

APPENDIX

List of publications:

Griffith, E., Walker, S., Martin, C.A., Vagnarelli, P., Stiff, T., Vernay, B., Al Sanna, N., Saggar, A., Hamel, B., Earnshaw, W.C., Jeggo, P.A., Jackson, A.P. & O'driscoll, M. (2008) Mutations in pericentrin cause Seckel syndrome with defective ATR-dependent DNA damage signaling. *Nat Genet,* Vol. 40 (2) 232-6.

Bicknell, L.S., Walker, S., Klingseisen, A., Stiff, T., Leitch, A., Kerzendorfer, C., Martin, C.A., Yeyati, P., Al Sanna, N., Bober, M., Johnson, D., Wise, C., Jackson, A.P., O'driscoll, M. & Jeggo, P.A. (2011b) Mutations in ORC1, encoding the largest subunit of the origin recognition complex, cause microcephalic primordial dwarfism resembling Meier-Gorlin syndrome. *Nat Genet*.

Ogi T, Walker S, Stiff T, Hobson E, Limsirichaikul S, Carpenter G, Prescott K, Suri M, Byrd PJ, Matsuse M, Mitsutake N, Nakazawa Y, Vasudevan P, Barrow M, Stewart GS, Taylor AM, O'Driscoll M, Jeggo PA. (2012) Identification of the First ATRIP-Deficient Patient and Novel Mutations in ATR Define a Clinical Spectrum for ATR-ATRIP Seckel Syndrome. PLoS Genet. Nov;8(11)

nature genetics

© 2008 Nature Publishing Group http://www.nature.com/naturegenetics

Mutations in pericentrin cause Seckel syndrome with defective ATR-dependent DNA damage signaling

Elen Griffith[1,7], Sarah Walker[2,7], Carol-Anne Martin[1], Paola Vagnarelli[3], Tom Stiff[2], Bertrand Vernay[1], Nouriya Al Sanna[4], Anand Saggar[5], Ben Hamel[6], William C Earnshaw[3], Penny A Jeggo[2], Andrew P Jackson[1] & Mark O'Driscoll[2]

Large brain size is one of the defining characteristics of modern humans. Seckel syndrome (MIM 210600), a disorder of markedly reduced brain and body size[1,2], is associated with defective ATR-dependent DNA damage signaling[3]. Only a single hypomorphic mutation of ATR has been identified in this genetically heterogeneous condition[4]. We now report that mutations in the gene encoding pericentrin (PCNT)—resulting in the loss of pericentrin from the centrosome, where it has key functions anchoring both structural and regulatory proteins—also cause Seckel syndrome[5,6]. Furthermore, we find that cells of individuals with Seckel syndrome due to mutations in *PCNT* (PCNT-Seckel) have defects in ATR-dependent checkpoint signaling, providing the first evidence linking a structural centrosomal protein with DNA damage signaling. These findings also suggest that other known microcephaly genes implicated in either DNA repair responses[7] or centrosomal function[8,9] may act in common developmental pathways determining human brain and body size.

Seckel syndrome is an autosomal recessive disorder of intrauterine growth retardation, severe proportionate short stature and marked microcephaly[1,2]. The ataxia-telangiectasia and Rad3-related *(ATR)* gene is mutated in some individuals with Seckel syndrome (ATR-Seckel)[4], and it encodes a phosphatidylinositol 3-kinase-like kinase that has distinct but overlapping functions with ATM in coordinating the response to DNA damage[10]. ATR is activated by single-stranded DNA, whereas ATM responds to DNA double-strand breaks. MCPH1, encoded by another gene whose mutations cause severe (primary) microcephaly, also acts in the ATR damage response pathway[7]. Furthermore, cell lines of other individuals with Seckel syndrome but without a mutation in *ATR* also show ATR-pathway dysfunction[3], suggesting that mutation of additional genes encoding proteins involved in this DNA damage response cascade may also cause this disorder.

To identify such components, we carried out a SNP-microarray genome-wide homozygosity scan on two consanguineous families from the Middle East that include individuals clinically diagnosed with Seckel syndrome (**Supplementary Figs. 1** and **2** online) and showing cellular evidence of defective ATR signaling. Through multipoint linkage analysis, we identified a new locus, *Sckl4*, with a maximum lod score of 4.03 at 70.9 cM on chromosome 21q22.3 between rs1598206 and rs2330591 (**Fig. 1** and **Supplementary Fig. 2**). Within this interval were 55 RefSeq-annotated genes, including pericentrin (*PCNT*), which encodes a centrosomal protein. As mutations in several centrosomal genes, *CENPJ*, *ASPM* and *CDK5RAP2*, cause a related condition, primary microcephaly[8,9], we postulated that *PCNT* might be the causative gene and therefore sequenced its 47 coding exons in affected individuals from both families.

We identified a homozygous nonsense mutation in exon 4 of family 1 (E220X). A homozygous single–base pair deletion in exon 12 in family 2 (S629fs; **Fig. 1c,d**) led to a frameshift, which was predicted to result in premature protein truncation after an additional 65 amino acids. Both mutations segregated with the disease in each family, with all parents of affected individuals being heterozygous for the respective mutations. From screening of additional cases, we identified a further individual with a homozygous single–base pair insertion in exon 18, resulting in a frameshift at codon 1190 (C1190fs). Neither this insertion nor the other two mutations were present in over 200 control alleles screened. Collectively, these mutations disrupt all described mammalian protein isoforms of PCNT[11,12]. We therefore concluded that homozygous truncating mutations in *PCNT* cause Seckel syndrome.

Pericentrin (also known as kendrin) is a huge (360-kDa) coiled-coil protein with a C-terminal PACT domain that targets it to the centrosome (**Fig. 1d**). Two protein isoforms have been described in humans[11]: the full-length protein, pericentrin B, and a C-terminally truncated isoform, pericentrin A. Pericentrin localizes to the pericentriolar material (PCM), where it interacts with several structural centrosomal proteins, including γ-tubulin and PCM1 (refs. 13,14) and plays an important role in microtubular nucleation and spindle organization[15,16]. Antibodies to pericentrin disrupt mitosis, suggesting that it is essential for mitotic

[1]Medical Research Council (MRC) Human Genetics Unit, Western General Hospital, Crewe Road, Edinburgh EH4 2XU, UK. [2]Genome Damage and Stability Centre, University of Sussex, East Sussex BN1 9RQ, UK. [3]Wellcome Trust Centre for Cell Biology, School of Biological Sciences, University of Edinburgh, Kings Buildings, Mayfield Road, Edinburgh EH9 3JR, UK. [4]Pediatric Services Division, Box 76, Dhahran Health Center, Saudi Arabia. [5]Southwest Thames Regional Genetics Service, St. George's Hospital Medical School, London, SW17 ORE UK. [6]Radboud University Nijmegen Medical Center, Department of Human Genetics 417, Geert Grooteplein 20, 6525GA, Nijmegen, The Netherlands. [7]These authors contributed equally to this work. Correspondence should be addressed to A.P.J. (andrew.jackson@hgu.mrc.ac.uk).

Received 29 October; accepted 13 December; published online 23 December 2007; doi:10.1038/ng.2007.80

© 2008 Nature Publishing Group http://www.nature.com/naturegenetics

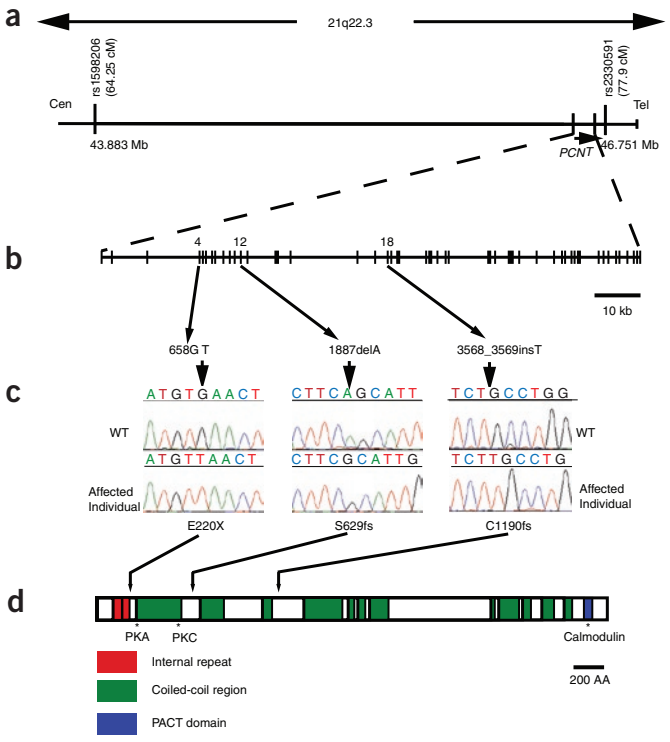

Figure 1 Schematic of the *Sckl4* critical region and the *PCNT* gene depicting location of identified mutations. (**a**) Genetic map of chromosome 21q22.3 with the refined *Sckl4* locus, defined by overlapping homozygous chromosomal segments in two consanguineous families and extending over a 2.9-Mb interval between SNP markers rs1598206 and rs2330591 (43,883,204–46,751,852, UCSC Browser, March 2006 Assembly). Genetic distances, deCODE genetic map. (**b**) *PCNT* spans 122 kb of genomic sequence in 47 exons and encodes a 3,336-amino-acid protein. (**c**) Sequence electropherograms of *PCNT* mutations. (**d**) Schematic of the pericentrin protein indicating position of identified mutations and protein structure. Pericentrin contains internal repeats (red), coiled-coil regions (green) and a PACT domain (blue). Protein structural regions as predicted by SMART. Sites of interaction with PKA, PKC βII and calmodulin indicated by asterisks.

progression[15]. However, its *Drosophila melanogaster* homolog, D-PLP, though required for timely recruitment of PCM components, is apparently dispensable for cell division[17]. Furthermore, in addition to its structural roles, pericentrin acts as a scaffold to recruit signaling proteins, such as protein kinase A (PKA) and protein kinase CβII, to the centrosome[5,18].

All mutations identified were homozygous and substantially truncated the protein, suggesting that they are functionally 'null' alleles. To test this prediction, we examined pericentrin localization in lymphoblastoid cell lines (LCLs) of affected individuals. Centrosomal pericentrin staining was lost in three independent LCLs, in contrast to control cell lines (**Fig. 2a** and **Supplementary Fig. 3** online), both in interphase and mitosis. We also examined protein expression by immunoblotting (**Fig. 2b**). Two bands were detected in controls (wild-type (WT) and heterozygous relatives ($PCNT^{E220X/+}$ and $PCNT^{S629fs/+}$)), representing two isoforms of pericentrin, which were not present in mutant LCLs. A smaller ~170-kDa band was present in $PCNT^{E220X}$ lymphoblastoid cells (potentially representing an aberrant truncated PCNT protein product), whereas no significant PCNT protein was apparent in the other two mutant cell lines, supporting the molecular genetic findings that protein function is considerably, if not completely, disrupted.

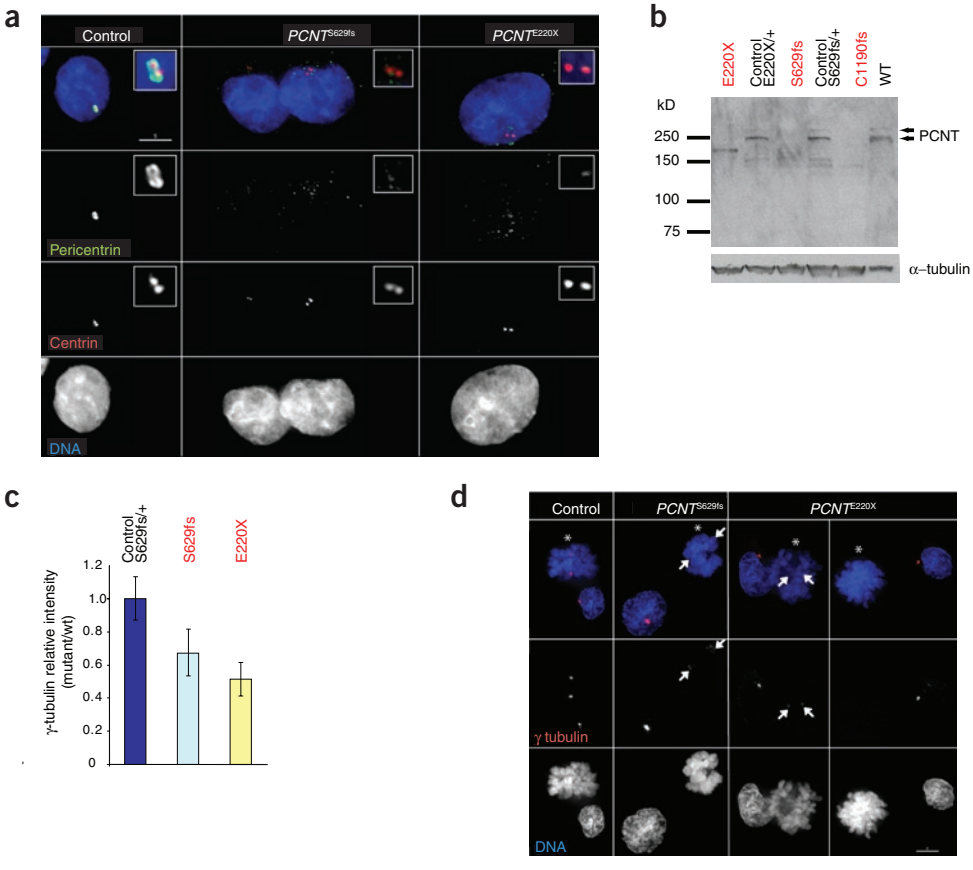

Figure 2 Pericentrin localization and function is disrupted in PCNT-Seckel cell lines. (**a**) Pericentrin is not localized to the pericentriolar material in PCNT-Seckel cells. Deconvolved immunofluorescent images from PCNT-Seckel and control lymphoblastoid cell lines, showing pericentrin (ab448-100, green) and centrin (red). Scale bar, 5 μm. Control, heterozygote relative, $PCNT^{220X/+}$. (**b**) Immunoblot of LCL cell lysates with pericentrin ab448-100 antibody, which detects both pericentrin A and B isoforms. Two pericentrin (arrowheads) isoforms are absent from PCNT-Seckel cells but present in control lymphoblastoid cells from heterozygous relatives. A smaller protein product of ~170 kDa is detected in the $PCNT^{220X}$ cell line, which might represent an aberrant truncated PCNT protein product. Loading control, α-tubulin. (**c**,**d**) γ-tubulin localization is frequently reduced or absent during mitosis in PCNT-Seckel cells. (**c**) Quantification of γ-tubulin signal in PCNT-Seckel mitotic cells at prometaphase and metaphase, relative to WT. $n = 20$. Error bars, s.d. γ-tubulin signal intensity is significantly reduced relative to WT cells ($P < 0.05$, S629fs; $P < 0.001$, E220X). (**d**) In PCNT-Seckel mitotic cells (asterisks), γ–tubulin centrosomal staining is reduced (arrows) or absent, relative to centrosomal staining in adjacent interphase cells or in control cells from a heterozygous relative.

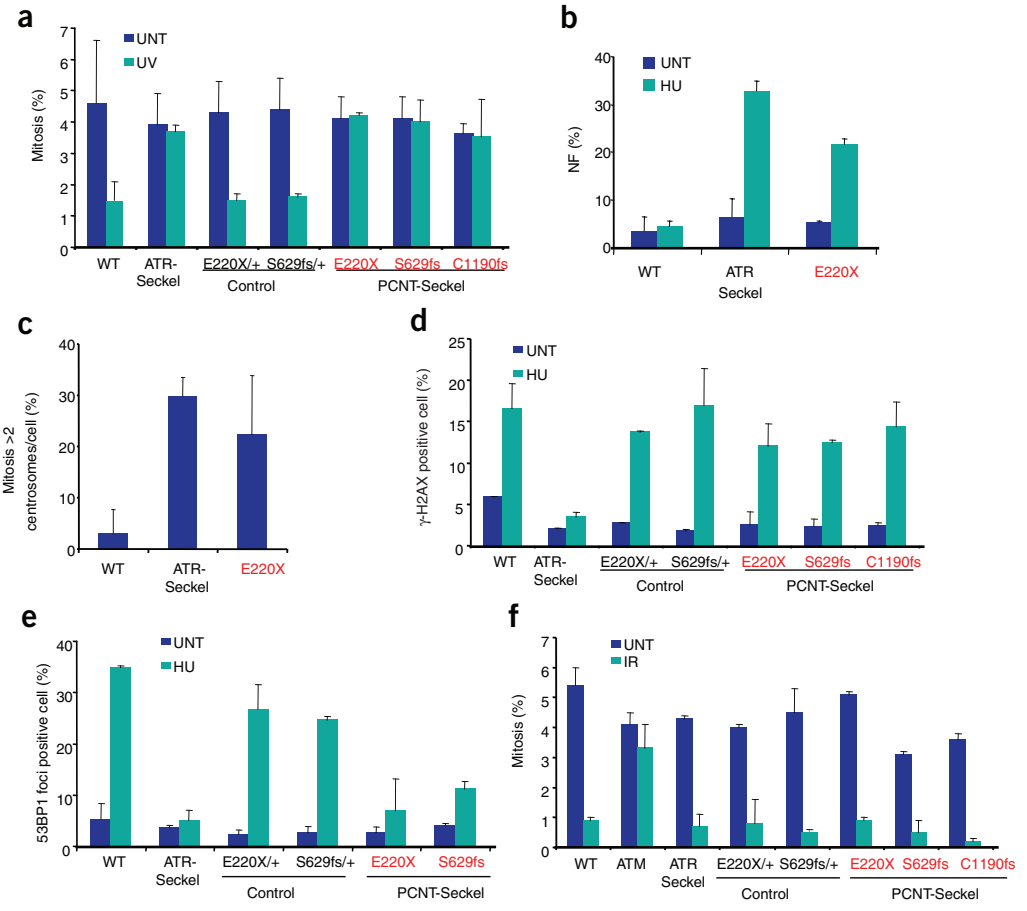

Figure 3 PCNT is required for ATR-dependent DNA damage signaling. (**a**) G2-M checkpoint arrest was observed 2 h after UV treatment in control but not in ATR- or PCNT-Seckel LCLs. The mitotic index was examined 2 h after treatment with 5 J m^{-2} UV. Average of three experiments; error bars, s.d. Controls: heterozygote relatives *PCNT*$^{E220X/+}$ and *PCNT*$^{S629fs/+}$ and an unrelated wild-type (WT) cell line. UNT, untreated; UV, UV-C treated. Mitotic index is significantly increased in PCNT-Seckel cells compared with wild-type cells after UV treatment ($P < 0.001$, E220X; $P < 0.01$, S629fs; $P < 0.05$, C1190fs). (**b**) ATR- and PCNT-Seckel LCL cells have increased hydroxyurea-induced nuclear fragmentation. Nuclear fragmentation was examined 24 h after treatment with 5 mM hydroxyurea (HU). Percentage of cells showing nuclear fragmentation (NF) is shown ($P < 0.001$ WT versus PCNT-Seckel E220X). (**c**) ATR- and PCNT-Seckel LCL cells show elevated levels of supernumerary centrosomes in mitosis. Percentage of mitotic (phospho-histoneH3 (Ser10)–positive cells) with more than two γ-tubulin stained foci (centrosomes) determined after 24-h incubation with nocodazole ($P < 0.05$ WT versus E220X). (**d**) γH2AX foci formation is normal in PCNT-Seckel LCLs. Phosphorylation of the histone H2AX (termed γH2AX) by the PI3K-kinases is one of the earliest detectable responses to DNA damage and is ATR-signaling specific after hydroxyurea treatment. Percentage of γH2AX foci was determined 2 h after treatment with 5 mM hydroxyurea. (**e**) ATR- and PCNT-Seckel cells show significantly reduced 53BP1 foci formation after treatment with 5 mM hydroxyurea for 2 h, reflecting impairment in ATR/Chk1-dependent signaling. Immunofluorescence staining with anti-BrdU confirmed that all LCLs had equivalent S-phase populations (range, 20–23%) before exposure to hydroxyurea ($P < 0.005$ E220X; $P < 0.001$, S629fs versus WT after hydroxyurea). (**f**) G2-M checkpoint arrest after ionizing radiation (IR) is normal in PCNT-Seckel and ATR-Seckel LCLs but not in ataxia telangiectasia–mutated (ATM) LCLs.

We next examined other components of the centrosome in order to establish whether they were affected by the absence of pericentrin. ASPM, PCM-1, ninein and centrin were all localized normally (**Fig. 2a** and **Supplementary Fig. 4** online). However, during mitosis, γ-tubulin was significantly reduced or absent at prometaphase and metaphase (**Fig. 2c**,**d**), consistent with the results of previous RNAi experiments[6].

Other individuals with Seckel syndrome have defects in the ATR DNA damage response pathway[3]. We therefore assessed PCNT-Seckel cell lines to see whether loss of this key centrosomal protein is associated with the defects in ATR signaling previously described for this disorder[3,4]. Indeed, PCNT-Seckel (*PCNT*^{C1190fs}, *PCNT*^{E220X} and *PCNT*^{S629fs}) LCLs showed defective UV-induced G2-M checkpoint arrest, similar to that seen in ATR-Seckel LCLs (**Fig. 3a**), in contrast to cell lines established from heterozygote relatives (*PCNT*$^{E220X/+}$, *PCNT*$^{S629fs/+}$) and an unrelated WT control. This suggested that mutations in *PCNT* affect ATR-dependent cell cycle checkpoint activation. Similarly, PCNT-Seckel LCLs also showed elevated nuclear fragmentation after replication-fork stalling (**Fig. 3b**) and supernumerary mitotic 'centrosomes' after prolonged mitotic arrest with nocodazole (**Fig. 3c**), two additional cellular phenotypes caused by impaired ATR signaling[3].

As these findings suggested a direct role for PCNT in ATR-dependent DNA damage response signaling, we examined further steps in this signaling cascade in PCNT-Seckel cells. We found that ATR-dependent γH2AX formation was normal in PCNT-Seckel LCLs, similar to controls (**Fig. 3d**). This was distinct from what was observed in ATR-Seckel LCLs and suggested that ATR is able to phosphorylate a key substrate in PCNT-Seckel cells. Thus, pericentrin functions downstream of ATR kinase activation in this pathway.

We next examined hydroxyurea-induced 53BP1 foci formation in PCNT-Seckel cell lines. Notably, both PCNT-Seckel and ATR-Seckel LCLs did not form such foci, in contrast to control cell lines (**Fig. 3e**). This phenotype is dependent on both ATR and Chk1 kinases[19], indicating that PCNT has a downstream role in ATR-pathway function.

To determine whether *PCNT* mutations affect other DNA damage responses, we assessed the G2-M checkpoint response to DNA double-strand breaks induced by ionizing radiation. This response is specifically dependent on ATM and not ATR signaling. PCNT-Seckel LCLs arrested as efficiently as control LCLs under these conditions. ATR-Seckel LCLs, unlike ATM-mutant LCLs, also had a normal response, confirming that this assay was ATR independent (**Fig. 3f**). Therefore, we concluded that mutations in *PCNT* have specific effects on the

© 2008 Nature Publishing Group http://www.nature.com/naturegenetics

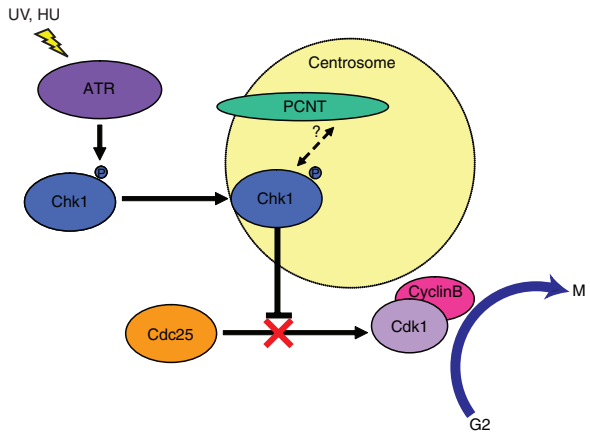

Figure 4 Model of pericentrin's role in ATR-dependent G2-M checkpoint arrest. Low-dose UV and hydroxyurea activate ATR kinase, which then phosphorylates downstream targets including Chk1 kinase. Activating phosphorylation is required for accumulation of Chk1 at the centrosome after DNA damage[28]. Direct or indirect binding of Chk1 by pericentrin could mediate localization of Chk1 to the centrosome. Chk1 localization at the centrosome inhibits Cdc25, preventing cyclin B/Cdk1 activation[27] and thus the transition from G2 to mitosis.

downstream stage of the ATR pathway, including G2-M checkpoint activation.

We also carried out siRNA experiments in HeLa cells to provide confirmatory evidence that PCNT is required for ATR-dependent signaling. siRNA depletion of PCNT also results in defective ATR-dependent (UV) checkpoint activation (**Supplementary Fig. 5** online), as we had observed in PCNT-Seckel LCLs. Furthermore, we did not find any defects in ATM-dependent checkpoint response after ionizing radiation. These results substantiate our findings indicating that *PCNT* mutations cause impaired ATR signaling.

PCNT is a key structural centrosomal protein nucleating microtubular assembly during mitosis[15,16]. It was thus surprising to identify homozygous truncating mutations that seem to cause absence of known forms of PCNT protein from centrosomes. So, notably, PCNT would seem to be dispensable for most aspects of human development. Pericentrin mutations do, however, markedly reduce both body and brain size by ~8 s.d. below the norm. Other centrosomal genes (*ASPM*, *CDK5RAP2* and *CENPJ*) have been implicated in determining human brain size, as they are mutated in primary microcephaly. They are presumed to act through effects on neurogenic mitosis[8,9,20], perhaps modulating symmetric versus asymmetric cell division. Given the role of PCNT in mitotic spindle assembly[15,16], perturbation of cell division may similarly result in globally reduced cell number, thus additionally causing reduced body size. However, for the *ATR*, *MCPH1* and now *PCNT* genes, there is a specific correlation between defects in ATR signaling and reduced brain and body size[4,7]. This suggests an alternative explanation—impaired ATR signaling might cause these phenotypes directly, through impaired mitotic progression or reduced cell survival.

Primary microcephaly genes have undergone considerable adaptive evolution in primates, suggesting that functional alterations in the proteins they encode may have contributed to the evolution of human brain size[21]. Morphologically, Seckel syndrome also has evolutionary parallels. *Homo floresiensis,* the recently described Indonesian hominid, has similarly marked reduced brain and body size (cranial volume –6.1 s.d, height –9.5 s.d, relative to modern humans)[22]. Consequently, changes in *PCNT* or similar genes could underlie the anatomical differences seen in this hominid[23].

By studying a human disease phenotype, we have, for the first time, implicated a structural protein of the centrosome in the ATR-dependent DNA damage response. Centrosomes have a central role in regulating cell cycle progression[24], and pericentrin has an established role in recruiting regulatory proteins to the centrosome[5,18]. Therefore, a role in checkpoint signaling would be consistent with its known functions. Components of the ATR pathway have been observed to localize to the centrosome[25], most notably Chk1 (refs. 26,27). Chk1 centrosomal localization, mediated by activating phosphorylation at Ser317 and Ser345 residues[28], is enhanced by DNA damage. At the centrosome, Chk1 is thought to delay G2-M transition through inhibiting activation of Cyclin B-Cdk1 by Cdc25 (ref. 27). Notably, fusion of Chk1 with a PACT domain prevents G2-M mitotic progression[27], suggesting that endogenous pericentrin, one of only two PACT domain containing proteins, could provide the means of Chk1 localization to mediate G2-M checkpoint arrest (model, **Fig. 4**). Alternatively, PCNT may not be required for localization of Chk1, but may be necessary for Chk1 to transmit its signal to downstream centrosomally localized components to effect G2-M arrest. Future investigations based on these possibilities will be valuable in understanding the mechanism of Chk1 relocalization and activation at the centrosome.

The identification of pericentrin mutations in Seckel syndrome also provides an interesting convergence between microcephaly genes implicated in ATR signaling (*MCPH1* and *ATR)* and those involved in centrosomal function (*ASPM, CDK5RAP2* and *CENPJ*). This suggests that further biochemical and developmental investigation is likely to be fruitful in delineating common cellular pathways responsible for the brain and body size phenotypes in these syndromes.

METHODS

Affected individuals with Seckel syndrome. All affected individuals included in this study were diagnosed with Seckel syndrome and had intrauterine growth retardation, severe proportionate short stature, marked microcephaly and developmental delay. Blood samples were obtained with informed consent from affected children, parents and unaffected siblings. We established lymphoblastoid cell lines by EBV transformation and extracted genomic DNA using standard methods. The study was approved by the Scottish Multicentre Research Ethics Committee (04:MRE00/19) and the University of Sussex School of Life Sciences Research Governance Committee.

Genotyping and linkage analysis. SNP microarray genotyping was done by AROS Applied Biotechnology (Denmark) using Affymetrix Human Mapping 50K Xba240 Genechips. We analyzed SNP genotypes using Alohomora[29] and carried out multipoint linkage with GENEHUNTER (version 2.0β) under a model of autosomal recessive inheritance with full penetrance, using a disease-allele frequency estimated at 1 in 1,000. We used deCODE genetic map distances and Affymetrix SNP allele frequencies.

Mutation detection. We designed primers using the ExonPrimer tool in the University of California Santa Cruz Genome Browser to amplify coding exons of pericentrin (primer sequences listed in **Supplementary Table 1** online). Purified PCR amplification products were sequenced using dye-terminator chemistry and electrophoresed on an ABI 3730 capillary sequencer (Applied Biosystems). Mutation analysis was done using Mutation Surveyor (Softgenetics). Anonymous control samples were screened by sequencing.

Cell lines and cell culture. LBLs were cultured in RPMI 1640 with 15% FCS (FCS). We used wild-type (WT; GM02188), ATR-Seckel (DK0064) and ataxia telangiectasia–mutated (ATM; GM03189D) cell lines, all of which have been described previously[4,7]. $PCNT^{E220X}$ (cell-line identifier: CV1559; affected Seckel, PCNT 658G>T); $PCNT^{E220X/+}$ (cell-line identifier: CV1584; unaffected brother of CV1559); $PCNT^{S629fs}$ (cell-line identifier: CV1576; affected Seckel, PCNT 1887delA); $PCNT^{S629fs/+}$ (cell-line identifier: CV1582; unaffected mother of CV1576) and $PCNT^{C1190fs}$ (12061; affected Seckel, PCNT 3568_3569insT).

© 2008 Nature Publishing Group http://www.nature.com/naturegenetics

Immunofluorescence and protein blotting. Immunostaining was done as previously described[30]. We used antibodies at the following dilutions: anti-pericentrin (Abcam, ab448-100), 1:1,000; anti-pericentrin (N-20) (Santa Cruz Biotechnology) 1:100; anti–γ-tubulin (Sigma), 1:1,000; anti-centrin (20H5, J. Salisbury), 1:1,000; anti–PCM-1 (A. Merdes), 1:1,000; anti-ASPM (Bethyl Labs, IHC-00058), 1:250; anti-ninein (A. Merdes), 1:100. Secondary antibodies were conjugated to FITC or Texas Red (Jackson ImmunoResearch Lab) and used at 1:200. Three-dimensional datasets were collected with a DeltaVision system (Applied Precision) on the basis of an Olympus IX-70 with a Chroma Technology Sedat filter set driven by SoftWorx software under standard conditions. All images were archived as raw (r3d) and deconvolved (d3d) files. Images were subjected to standard deconvolution algorithm. Three-dimensional datasets were converted to Quick Projections in SoftWorx and then converted to TIFF files and imported into Adobe Photoshop for final presentation. For the quantification of γ-tubulin staining in mitosis, we used a defined volume containing the centrosome to measure the total intensity of the signal. The same volume was used to identify the background noise as intensity outside the cells and also the non-centrosomal γ-tubulin within the cells. We averaged the ratios of centrosome-bound and dispersed γ-tubulin for each slide after background subtraction and calculated the relative intensity in comparison to the WT control slide.

Immunoblotting was done using anti-pericentrin (Abcam, ab448-100) at 1:1,000, and horseradish peroxidase (HRP)–conjugated anti–rabbit IgG secondary antibody, 1:5,000 (Cell Signaling 7074), detected with ECL-Plus (Amersham).

DNA damage response assays. For ATR-dependent G2-M arrest, cells were untreated (UNT) or irradiated with 5 J/m^2 UV-C (UV) and immediately seeded into complete medium and incubated for 2 h before being cytospun onto poly-D-lysine–coated slides and stained with 4,6-diamidino-2-phenylindole (DAPI) and anti–phospho-histoneH3, as previously described[7]. For the ATM-dependent G2-M arrest, cells were either untreated (UNT) or irradiated with 2 Gy of ionizing radiation (IR) and processed as above. For γH2AX formation and 53BP1 foci formation, cells were either untreated (UNT) or treated with 5 mM hydroxyurea (HU) for 2 h and processed for immunofluorescence (IF) staining as previously described[3]. Cells were also pulse labeled (15 min) with 50 μM BrdU to allow quantification of cells in S phase using anti-BrdU by immunofluorescence. Supernumerary mitotic centrosomes were determined after treatment with 1.5 μM nocodazole for 24 h as previously described[7]. We used the following antibodies: anti-γH2AX (Upstate Technology), anti-53BP1 (BL181; Universal Biologicals), anti-BrdU (Autogen Bioclear) and anti–γ-tubulin (Sigma-Aldrich).

RNAi. HeLa cells were transfected with 10 nmol of Invitrogen Stealth duplex oligoribonucleotides using siPORT *Neo*FX Transfection Agent (Ambion, standard protocol). siRNA oligonucleotide sequences are listed in **Supplementary Table 1**. After 72 h, we carried out G2-M checkpoint assays, as outlined above.

URLs. UCSC Human Genome Browser, http://genome.ucsc.edu; SMART (Simple Modular Architecture Research Tool), http://smart.embl-heidelberg.de/.

GenBank accession codes. Pericentrin transcript, NM_006031.4; protein, NP_006022.

Note: Supplementary information is available on the Nature Genetics website.

ACKNOWLEDGMENTS

We thank the families and their clinicians for their participation in this study; C. Hayward for contributing control samples; S. McKay and the MRC HGU core sequencing service for advice and technical support; C. Nicol for help with figure preparation; X. Fant, V. Van Heyningen and N. Hastie for discussions and comments; W. Fergusson (St. Mary's Hospital, Manchester) for LCL transformation; and A. Merdes and J. Salisbury for kindly sharing antibody reagents. A.P.J.'s laboratory is funded by the MRC, M.O'D.'s laboratory is funded by CRUK and the MRC, and P.A.J.'s laboratory is funded by the MRC, UK LRF, IACR and EU grants (FIGH-CT-200200207) (DNA repair) and FI6R-CT-2003-508842 (RiscRad). P.V. and W.C.E. are funded by the Wellcome Trust, of which W.C.E. is a Principal Research Fellow. A.P.J. is an MRC Senior Clinical Fellow and M.O'D. is a CRUK Senior Cancer Research Fellow.

AUTHOR CONTRIBUTIONS

E.G., C.-A.M. and A.P.J. performed the mutation screening and sequencing of controls; A.P.J., linkage analysis; P.V., immunostaining analysis of LCLs and C.-A.M., immunoblotting. S.W., T.S., M.O'D. and P.A.J. designed and performed the DNA damage response assays and RNAi experiments. N.A.S., A.S. and B.H. provided clinical samples and data. E.G. and A.P.J. wrote the paper with M.O'D., P.A.J., B.V. and W.C.E.

Published online at http://www.nature.com/naturegenetics
Reprints and permissions information is available online at http://npg.nature.com/reprintsandpermissions

1. Majewski, F. *et al.* Studies of microcephalic primordial dwarfism I: approach to a delineation of the Seckel syndrome. *Am. J. Med. Genet.* **12**, 7–21 (1982).
2. Seckel, H.P.G. Bird-headed Dwarfs: Studies in Developmental Anthropology Including Human Proportions (Charles C. Thomas, Springfield, Illinois, 1960).
3. Alderton, G.K. *et al.* Seckel syndrome exhibits cellular features demonstrating defects in the ATR-signalling pathway. *Hum. Mol. Genet.* **13**, 3127–3138 (2004).
4. O'Driscoll, M. *et al.* A splicing mutation affecting expression of ataxia-telangiectasia and Rad3-related protein (ATR) results in Seckel syndrome. *Nat. Genet.* **33**, 497–501 (2003).
5. Diviani, D. *et al.* Pericentrin anchors protein kinase A at the centrosome through a newly identified RII-binding domain. *Curr. Biol.* **10**, 417–420 (2000).
6. Zimmerman, W.C. *et al.* Mitosis-specific anchoring of gamma tubulin complexes by pericentrin controls spindle organization and mitotic entry. *Mol. Biol. Cell* **15**, 3642–3657 (2004).
7. Alderton, G.K. *et al.* Regulation of mitotic entry by microcephalin and its overlap with ATR signalling. *Nat. Cell Biol.* **8**, 725–733 (2006).
8. Bond, J. *et al.* ASPM is a major determinant of cerebral cortical size. *Nat. Genet.* **32**, 316–320 (2002).
9. Bond, J. *et al.* A centrosomal mechanism involving CDK5RAP2 and CENPJ controls brain size. *Nat. Genet.* **37**, 353–355 (2005).
10. Shiloh, Y. ATM and ATR: networking cellular responses to DNA damage. *Curr. Opin. Genet. Dev.* **11**, 71–77 (2001).
11. Flory, M.R. *et al.* The centrosomal proteins pericentrin and kendrin are encoded by alternatively spliced products of one gene. *Genomics* **82**, 401–405 (2003).
12. Miyoshi, K. *et al.* Characterization of pericentrin isoforms in vivo. *Biochem. Biophys. Res. Commun.* **351**, 745–749 (2006).
13. Li, Q. *et al.* Kendrin/pericentrin-B, a centrosome protein with homology to pericentrin that complexes with PCM-1. *J. Cell Sci.* **114**, 797–809 (2001).
14. Dictenberg, J.B. *et al.* Pericentrin and gamma-tubulin form a protein complex and are organized into a novel lattice at the centrosome. *J. Cell Biol.* **141**, 163–174 (1998).
15. Doxsey, S.J. *et al.* Pericentrin, a highly conserved centrosome protein involved in microtubule organization. *Cell* **76**, 639–650 (1994).
16. Purohit, A. *et al.* Direct interaction of pericentrin with cytoplasmic dynein light intermediate chain contributes to mitotic spindle organization. *J. Cell Biol.* **147**, 481–492 (1999).
17. Martinez-Campos, M. *et al.* The *Drosophila* pericentrin-like protein is essential for cilia/flagella function, but appears to be dispensable for mitosis. *J. Cell Biol.* **165**, 673–683 (2004).
18. Chen, D. *et al.* Centrosomal anchoring of protein kinase C betaII by pericentrin controls microtubule organization, spindle function, and cytokinesis. *J. Biol. Chem.* **279**, 4829–4839 (2004).
19. Sengupta, S. *et al.* Functional interaction between BLM helicase and 53BP1 in a Chk1-mediated pathway during S-phase arrest. *J. Cell Biol.* **166**, 801–813 (2004).
20. Woods, C.G. *et al.* Autosomal recessive primary microcephaly (MCPH): a review of clinical, molecular, and evolutionary findings. *Am. J. Hum. Genet.* **76**, 717–728 (2005).
21. Ponting, C. *et al.* Evolution of primary microcephaly genes and the enlargement of primate brains. *Curr. Opin. Genet. Dev.* **15**, 241–248 (2005).
22. Brown, P. *et al.* A new small-bodied hominin from the Late Pleistocene of Flores, Indonesia. *Nature* **431**, 1055–1061 (2004).
23. Martin, R.D. *et al.* Flores hominid: new species or microcephalic dwarf? *Anat. Rec. A Discov. Mol. Cell. Evol. Biol.* **288**, 1123–1145 (2006).
24. Doxsey, S. *et al.* Centrosomes in cellular regulation. *Annu. Rev. Cell Dev. Biol.* **21**, 411–434 (2005).
25. Zhang, S. *et al.* Centrosomal localization of DNA damage checkpoint proteins. *J. Cell. Biochem.* **101**, 451–465 (2007).
26. Loffler, H. *et al.* DNA damage–induced accumulation of centrosomal Chk1 contributes to its checkpoint function. *Cell Cycle* **6**, 2541–2518 (2007).
27. Kramer, A. *et al.* Centrosome-associated Chk1 prevents premature activation of cyclin-B-Cdk1 kinase. *Nat. Cell Biol.* **6**, 884–891 (2004).
28. Niida, H. *et al.* Specific role of Chk1 phosphorylations in cell survival and checkpoint activation. *Mol. Cell. Biol.* **27**, 2572–2581 (2007).
29. Ruschendorf, F. *et al.* ALOHOMORA: a tool for linkage analysis using 10K SNP array data. *Bioinformatics* **21**, 2123–2125 (2005).
30. Dodson, H. *et al.* Centrosome amplification induced by DNA damage occurs during a prolonged G2 phase and involves ATM. *EMBO J.* **23**, 3864–3873 (2004).

© 2008 Nature Publishing Group http://www.nature.com/naturegenetics

nature genetics

Mutations in *ORC1*, encoding the largest subunit of the origin recognition complex, cause microcephalic primordial dwarfism resembling Meier-Gorlin syndrome

Louise S Bicknell[1,8], Sarah Walker[2,8], Anna Klingseisen[1], Tom Stiff[2], Andrea Leitch[1], Claudia Kerzendorfer[3], Carol-Anne Martin[1], Patricia Yeyati[1], Nouriya Al Sanna[4], Michael Bober[5], Diana Johnson[6], Carol Wise[7], Andrew P Jackson[1], Mark O'Driscoll[3] & Penny A Jeggo[2]

© 2011 Nature America, Inc. All rights reserved.

Studies into disorders of extreme growth failure (for example, Seckel syndrome and Majewski osteodysplastic primordial dwarfism type II) have implicated fundamental cellular processes of DNA damage response signaling and centrosome function in the regulation of human growth. Here we report that mutations in *ORC1*, encoding a subunit of the origin recognition complex, cause microcephalic primordial dwarfism resembling Meier-Gorlin syndrome. We establish that these mutations disrupt known ORC1 functions including pre-replicative complex formation and origin activation. ORC1 deficiency perturbs S-phase entry and S-phase progression. Additionally, we show that Orc1 depletion in zebrafish is sufficient to markedly reduce body size during rapid embryonic growth. Our data suggest a model in which *ORC1* mutations impair replication licensing, slowing cell cycle progression and consequently impeding growth during development, particularly at times of rapid proliferation. These findings establish a novel mechanism for the pathogenesis of microcephalic dwarfism and show a surprising but important developmental impact of impaired origin licensing.

Severely impaired growth beginning from early fetal life is the defining feature of microcephalic primordial dwarfism, a group of disorders with autosomal recessive inheritance. The group encompasses several distinct disease entities, including Seckel syndrome[1], microcephalic osteodysplastic primordial dwarfism type II (MOPD II)[2] and Meier-Gorlin syndrome (MGS)[3], which share common features of intrauterine growth retardation, severe postnatal short stature and marked microcephaly. Three genes have been implicated in Seckel syndrome and MOPD II[4–7]; to date, no gene has been identified for MGS. Mutations in *ATR* (the ataxia-telangiectasia and Rad3-related gene), which encodes a DNA damage response kinase, have been found in related families with Seckel syndrome[4]. Mutations in *PCNT* have been identified in MOPD II and in individuals originally classified as having Seckel syndrome[5,6,8]. *PCNT* encodes pericentrin, a core centrosomal protein that facilitates nucleation of the mitotic spindle[9]. *PCNT*-deficient cells from affected individuals also show impaired ATR-dependent checkpoint arrest, connecting the centrosome with DNA damage-response signaling[5,10]. Recently, mutation of *CENPJ*, another centrosomal gene (originally identified as causing primary microcephaly), has been reported to cause Seckel syndrome[7].

To identify further genes regulating human growth, we performed SNP array genome-wide homozygosity mapping on nine members of a consanguineous Saudi-Arabian family with two children who had microcephalic primordial dwarfism. We identified a single large homozygous region on chromosome 1p32 which was refined by microsatellite genotyping to a 15.6-cM region containing 105 annotated genes (**Supplementary Figs. 1** and **2**). Screening of candidate genes encoding DNA damage response or centrosomal proteins (*PIK3R3, RAD54L, KIF2C* and *STIL*) did not identify pathogenic mutations. We then evaluated *ORC1* as a candidate gene, in part because the encoded protein, ORC1, regulates centrosome duplication[11]. Sequencing the 16 coding exons of *ORC1* in the affected siblings revealed a homozygous A>G transition (c.314A>G) in exon 4 generating a non-conservative amino acid substitution (p.Glu127Gly). Screening of 204 additional individuals with microcephalic primordial dwarfism identified a further three families with biallelic missense mutations in *ORC1*. All mutations segregated appropriately in the respective families for an autosomal recessive disorder and were not present in 380 controls (**Table 1**). The majority of the mutations, including a recurrent mutation resulting in p.Arg105Gln, occurred within conserved residues of the N-terminal BAH domain (**Supplementary Fig. 1**), a protein-protein interaction

[1]Medical Research Council (MRC) Human Genetics Unit (HGU), Institute for Genetics and Molecular Medicine, Western General Hospital, Edinburgh, UK. [2]DNA Double Strand Break Repair Laboratory, Genome Damage and Stability Centre, University of Sussex, Brighton, UK. [3]Human DNA Damage Response Disorders Group, Genome Damage and Stability Centre, University of Sussex, Brighton, UK. [4]Pediatric Services Division, Dhahran Health Center, Dhahran, Saudi Arabia. [5]Division of Genetics, Department of Pediatrics, A.I. DuPont Hospital for Children, Wilmington, Delaware, USA. [6]Sheffield Children's Hospital, Sheffield, UK. [7]Sarah M. and Charles E. Seay Center for Musculoskeletal Research, Texas Scottish Rite Hospital for Children, Dallas, Texas, USA. [8]These authors contributed equally to this work. Correspondence should be addressed to M.O'D. (m.o-driscoll@sussex.ac.uk) or A.P.J. (andrew.jackson@hgu.mrc.ac.uk).

Received 2 August 2010; accepted 25 January 2011; published online 27 February 2011; doi:10.1038/ng.776

Table 1 Clinical summary of the individuals with *ORC1* mutations

Subject	Family Country of origin	Sex	Alteration (mutation)	Gestation[a]/wgt[b] (s.d.)	Postnatal morphometric details[c] Age Height Weight OFC	Intellect	Facial features	Other notable clinical history	Skeletal analysis
P1	Family 1 Saudi Arabia (consanguineous)	M	p.Glu127Gly (c.380A>G)	40/2.64 (–1.9)	4.5 85.5 (–4.5) 9.6 (–5.9) 42 (–7.1)	Normal	Small chin, mildly small ears, full lips.	46XY. Mild, nonspecific icythyosis. Suboptimal growth hormone stimulation test. Normal IGF1. No response GH therapy.	–
P2	Family 1	F	p.Glu127Gly (c.380A>G)	39/2.18 (–2.5)	0.66 52 (–7.6) 3.1 (–9.3) 36 (–7.6)	Normal	Small anterior fontanelle, relatively small ears.	46XX. Gastro-oesophageal reflux. Normal brain MRI.	–
P3	Family 2 Syria/USA (consanguineous)	F	p.Phe89Ser (c.266T>C)	40/1.58 (–4.5)	4.5 73 (–7.6) 5.9 (–11) 38.5 (–11)	Normal	Mild micrognathia small ears, mild synophrys, full lips.	Bronchomalacia. Gastro-oesophageal reflux. Craniosynostosis surgery.	Hyper-extended dislocated knees at birth. Tibia posteriorly dislocated and surgically corrected, patella present.
P4	Family 3 USA	F	p.Arg105Gln, p.Arg720Gln (c.314G>A, c.2159G>A)	36/1.46 (–3.2)	7.1 94 (–5.3) 10.9 (–6.6) 46.2 (–5.4)	Normal	Normally shaped ears with small lobules, narrow auricular canals, normal teeth, bifid uvula, full lips No micrognathia, nose slightly prominent.	46XX. Normal sister chromatid exchange analysis. Severe conductive hearing loss. High-pitched voice. Normal muscle biopsy, metabolic screen, endocrine screen, normal brain MRI.	Skeletal survey mildly gracile long bones, minimal metaphyseal widening, some undertubulation in the midshaft for some long bones. Delayed bone age. Patella present.
P5	Family 4 UK	M	p.Arg105Gln (c.314G>A)	28/1.00 (–0.6)	13 102.9 (–6.6) 18.4 (–6.1) 43.5 (–7.3)	Moderate learning difficulty	Normal or large ear size, short philtrum, normal teeth, full lips.	Lobectomy for lobar emphysema. Severe prematurity, consequently associated with intraventricular hemorrhage resulting in left hemiplegia.	Slender long bones, cupped distal metaphyses of metacarpals, short fourth metacarpal. Patella present.

GH, growth hormone; MRI, magnetic resonance imaging.
[a]Gestation in weeks. [b]Weight in kilograms. [c]Age in years, height in centimeters, weight in kilograms, OFC in centimeters.

© 2011 Nature America, Inc. All rights reserved.

domain implicated in ORC1 chromatin binding[12]. All individuals with *ORC1* mutations had very marked growth retardation (–6.5 standard deviations (s.d.) from the age-related normal population mean with proportionate microcephaly (–6.9 s.d.) and had received diagnoses of MOPD, Seckel syndrome or unspecified microcephalic dwarfism (**Table 1** and **Supplementary Fig. 3**).

ORC1 is a component of the origin recognition complex (ORC), which encompasses six subunits (ORC1–ORC6). ORC binds to replication origins, licensing them for the initiation of replication[13]. The assembled ORC complex recruits CDC6 and CDT1 and promotes MCM2–MCM7 loading, generating the pre-replicative complex (pre-RC)[14]. ORC assembly therefore defines where replication can begin.

To assess the cellular consequences of *ORC1* mutations, we established a lymphoblastoid cell line (LBL), ORC1-P1, from subject 1 (p.Glu127Gly) and a skin fibroblast line, ORC1-P4, from subject 4 (p.Arg105Gln). We also generated a telomerase-immortalized derivative (ORC1-P4 hTERT). Immunoblotting of ORC1-P1 cells using two ORC1 antibodies (**Fig. 1a**) revealed substantially reduced levels of ORC1 in comparison to control cells, both in soluble and insoluble fractions (the latter containing chromatin-bound proteins). Parental lines had partially reduced chromatin-bound ORC1 (**Fig. 1b**). Additionally, ORC1 was dramatically reduced in chromatin-enriched fractions generated by micrococcal nuclease digestion (**Fig. 1c**). Additional pre-RC complex components, ORC2 and MCM2, were also reduced in the chromatin-enriched fractions, showing impaired pre-RC complex assembly on chromatin. Although immunoblotting of ORC1-P4 fibroblasts showed normal ORC1 protein levels (**Fig. 1d**), reduced chromatin-bound ORC1 and ORC2 were evident in chromatin-enriched insoluble extracts. ORC1-P1 has biallelic mutations in the BAH domain, and reduced protein stability in this line is consistent with a previous mutagenesis study on the BAH domain[12]. Importantly, pre-RC assembly was diminished in both cell lines irrespective of protein stability.

We next assessed whether reduced pre-RC complex formation impairs licensing capacity using a previously described assay that monitors the replication of Epstein-Barr virus (EBV) episomes from a viral replication origin that requires cellular ORC for licensing[15]. Following transfection of the episome into hTERT immortalized fibroblasts and incubation to allow one population doubling, we extracted episomal DNA and examined it by DNA hybridization with or without *Dpn*I digestion (which specifically degrades unreplicated episomes). Notably, EBV replication was severely reduced in

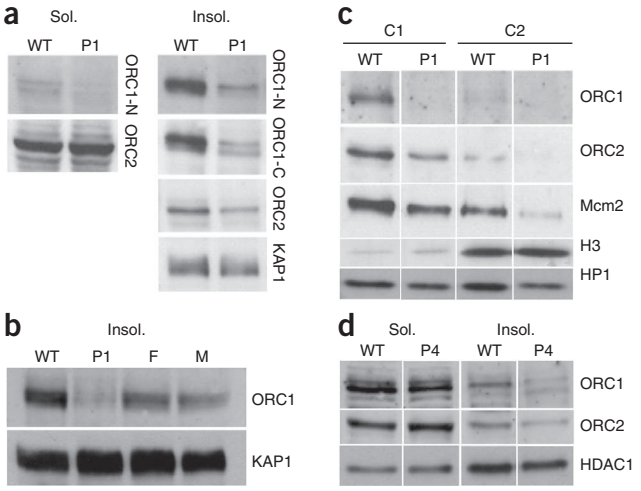

Figure 1 ORC1 expression and pre-RC complex assembly in ORC1-deficient cell lines from affected individuals. (**a**,**b**) ORC1 protein levels are markedly reduced in the ORC1-P1 cell line and less severely reduced in heterozygous parental cell lines. LBL cell extracts from control (WT), subject ORC1-P1 (p.Glu127Gly) (P1), and the subject's mother (M) and father (F) were separated into a soluble (sol.) or insoluble fraction that contained chromatin-bound proteins (insol.) and examined by protein blotting using the indicated antibodies. ORC1-N and ORC1-C detect epitopes at the ORC1 N or C terminus, respectively. KAP1 is a chromatin-bound protein used as a loading control. ORC2 served as a loading control for the soluble fraction. ORC1-N antibody was used subsequently. (**c**) We subjected extracts from control (WT) and ORC1-P1 cells (P1) to a two-step micrococcal nuclease (MNase) extraction procedure to derive chromatin enriched fractions, C1 and C2, of increasing MNase resistance and we examined these fractions by immunoblotting using the indicated antibodies. HP1 and histone H3 are chromatin-bound proteins. Histone H3 is strongly enriched in the C2 fraction, showing the enrichment of chromatin binding proteins. (**d**) We examined cell extracts from ORC1-P4 (p.Arg105Gln) fibroblasts as in **a**.

ORC1-P4 hTERT cells in contrast to the strong band of replicated episomal DNA in control cells (**Fig. 2a–c** and **Supplementary Fig. 4**). These results strongly suggest that ORC1-P4 fails to initiate replication from EBV oriP (origin-containing plasmid) origin.

We used a complementary approach to examine replication licensing in ORC1-P1 LBLs. Although new origin licensing is prevented in the S and G2 phases, nuclei in binucleate cells can undergo re-replication when cytokinesis is abrogated using cytochalasin B[16]. We reasoned that a diminished capacity to license origins might impair such DNA re-replication in binucleate cells. Following cytocholasin B treatment, we pulse labeled control and ORC1-P1 LBLs with BrdU and assessed its incorporation into binucleates (>4n DNA content) by fluorescence-activated cell sorting (FACS) (**Fig. 2d**). ORC1-P1 cells showed reduced BrdU incorporation in binucleates compared to control cells (**Fig. 2d**,**e**). These two approaches strongly suggest that the reduced pre-RC assembly observed by analysis of chromatin-bound ORC complex formation manifests as a reduced capacity to activate replication origins.

Only a fraction of licensed pre-RC complexes are utilized during replication. Thus, although ORC1 is essential, it is likely that markedly reduced ORC1 function may suffice for growth. However, because origin reutilization in the S phase is prevented[13], we considered that reduced licensing capacity might impair the rate of S-phase progression. Although the cultured ORC1 cells from the affected subjects grew well, we considered that subtle changes in cell cycle progression could have a developmental impact. We therefore examined the time taken for control and ORC1-P1 LBLs to progress through S phase following pulse labeling with BrdU (**Fig. 3a**,**b**). We monitored the rate of loss of early S-phase cells (identified by their BrdU and DNA content) to determine the speed of S-phase progression (**Fig. 3b**). ORC-P1 cells progressed more slowly through S phase compared to control LBLs (**Fig. 3a**,**b**).

To confirm and extend this finding, we used sucrose gradient sedimentation to monitor the size of replication intermediates following pulse labeling with [^{3}H]-TdR. Following a 15-min pulse of [^{3}H]-TdR, the DNA sedimentation profile was similar for control and ORC-P1 LBLs (**Fig. 3c**). However, following 60 min of growth in [^{3}H]-TdR, markedly less labeled DNA from ORC1-P1 LBLs had moved to a higher molecular weight size compared to control LBLs. This and the previous experiment have two possible explanations: a reduced rate of fork progression from multiple origins or reduced origin usage (see **Fig. 3d** legend for an explanation). The latter explanation is consistent with the described defect in origin licensing.

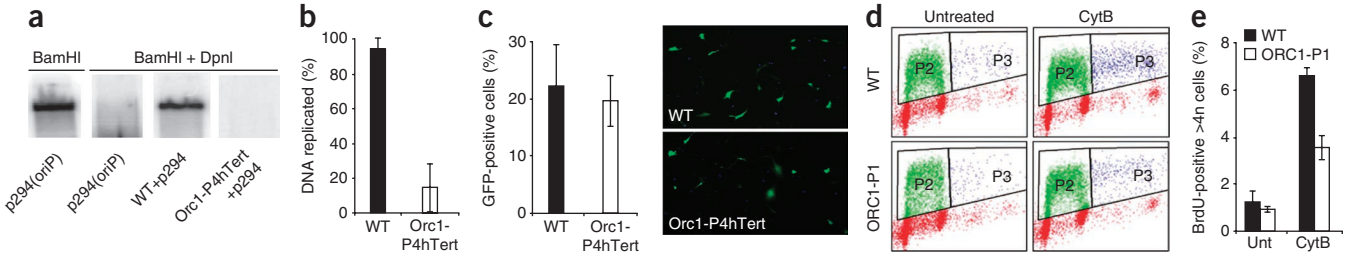

Figure 2 ORC1-deficient cells fail to efficiently activate replication origins. (**a**–**c**) ORC1-P4 cells showed impaired licensing of an Epstein-Barr virus (EBV) oriP origin. EBV uses virally encoded EBNA-1 and oriP and the host cell origin licensing complex. Consequently, EBNA-1-dependent EBV replication utilizes cellular ORC[15,19]. ORC1 activity was monitored as the replication capacity of plasmid-294 (p294(OriP)), which encodes OriP and EBNA-1, in control (WT; 1BR3 hTERT) and ORC1-P4 hTERT fibroblasts. Following transfection with plasmid-294 and incubation to allow one population doubling (1 day for WT and 4 days for ORC1-P4), we extracted plasmid DNA examined it using DNA blotting following *BamH*I or *BamH*I+*Dpn*I digestion using plasmid-294 as the probe. *Dpn*I degrades unreplicated plasmids that retain bacterial Dam-dependent methylation. (**a**) Southern blot of plasmid-294 (p294(OriP)) and plasmid extracted from WT and ORC1-P4 cells. Non-transfected cells gave no signal (data not shown). (**b**) Quantification expressed as percent replicated DNA (*BamH*I+*Dpn*I/*BamH*I) (values are mean ± s.d. of three experiments). (**c**) Percent transfection frequency of WT hTERT and ORC1-P4 hTERT cells following transfection with GFP-expressing plasmid (values are mean ± s.d. of three experiments), showing a similar transfection frequency. The greater impact on EBV replication compared to cellular replication is likely because the plasmid contains a single origin, whereas human DNA has redundant origins. (**d**,**e**) Control (WT) and ORC1-P1 LBLs were treated with cytochalasin B (0.75 μg/ml) for 24 h to accumulate binucleate cells that failed to undergo cytokinesis. We added BrdU (20 μM) for 1 h, and BrdU incorporation into >4n cells (P3 compartment) was taken to represent re-replication in binucleate cells; (**e**) quantification of (**d**) mean ± s.d. of three experiments.

© 2011 Nature America, Inc. All rights reserved.

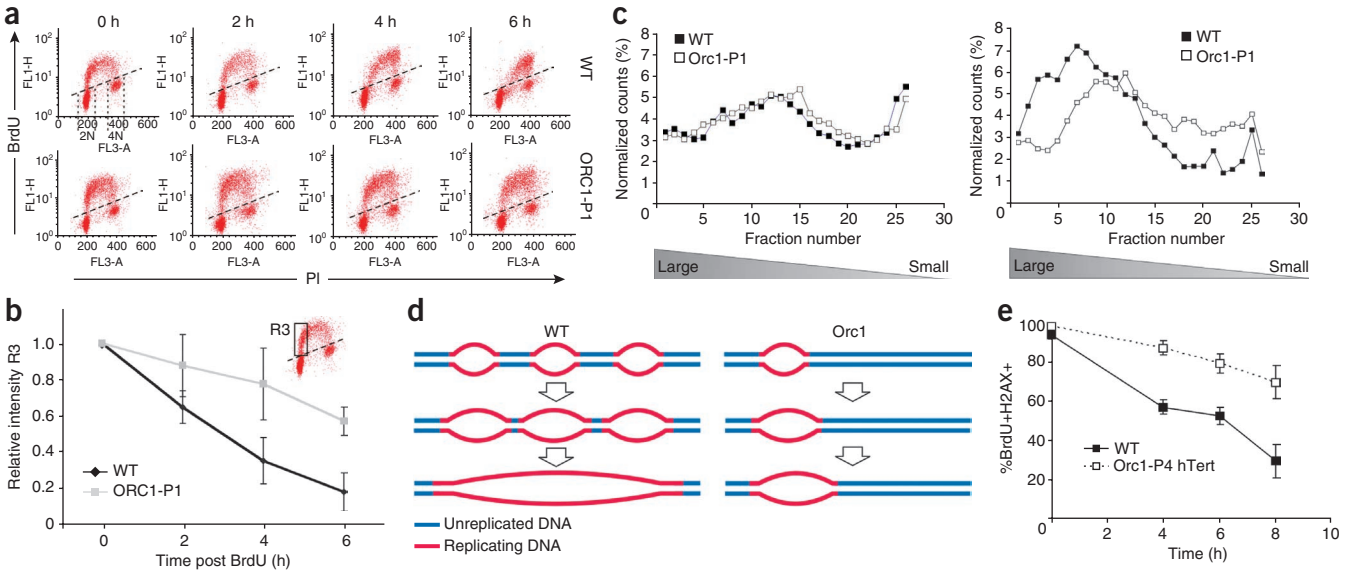

Figure 3 ORC1-deficient cells show slow S-phase progression. (**a**) Control (WT) or ORC1-P1 LBLs were BrdU labeled for 30 min and incubated for varying times before fluorescence-activated cell sorting. Early S-phase cells (above the 2N compartment) progress to late S phase (above the 4N compartment) over time. The rate of loss of BrdU+ early S-phase cells represents S-phase progression. (**b**) Quantification of early S-phase cells (highlighted as R3) (values are mean ± s.d. of three experiments). (**c**) WT or ORC1-P1 LBLs were labeled with [^{3}H]TdR for 15 min (left) or 1 h (right) and subjected to sucrose-gradient sedimentation following fragmentation and concurrent lysis. Newly fired origins sediment within fractions 25–30, precluding an estimation of new origin firing. DNA from WT LBLs increases in size more rapidly compared to ORC1-P1 DNA. Plots show a representative profile from three experiments. (**d**) A diagram showing how smaller replication intermediates arise when origin firing is limited. Slow fork progression will also generate smaller replication intermediates. (**e**) Control or ORC1-P4 hTERT fibroblasts were BrdU-labeled for 15 min and analyzed by immunofluorescence. We enumerated pan-nuclear γH2AX+ (S-phase cells at time of analysis) and/or BrdU+ cells (S-phase at time of labeling). γH2AX+ cells lose γH2AX staining in the G2 phase; BrdU+ cells remain BrdU+ in the G2 phase. Results show BrdU+ γH2AX+/total BrdU+ cells, indicating the percentage of BrdU+ cells still in S phase when sampled (values are mean ± s.d. of three experiments). The slope of the graph represents the rate of S-phase progression. Note that pan-nuclear γH2AX+ cells represent S-phase cells; we did not score defined γH2AX foci, a marker of DSBs.

© 2011 Nature America, Inc. All rights reserved.

As further confirmation, we used an immunofluorescence approach to examine S-phase progression in ORC1-P4 hTERT fibroblasts. We used BrdU pulse labeling and pan-nuclear γH2AX immunostaining to distinguish cells that are actively replicating from those that have progressed through S phase (see **Fig. 3e** legend for details). This approach showed that ORC1-P4 hTERT fibroblasts also progress slowly through S phase (**Fig. 3e**). For all these approaches, transfection with exogenous DNA slowed S-phase progression, precluding examination of complementation by ORC1 complementary DNA expression. In summary, these combined approaches provide strong evidence that ORC1 deficiency impairs the rate of S-phase progression, a previously unknown phenotype conferred by ORC1 deficiency.

Pre-RC complex assembly starts upon G1-phase entry, and a 'licensing checkpoint' acts to preclude S-phase entry until a critical level of licensed origins assemble[17,18]. Therefore, we examined whether ORC1 deficiency prolongs the G1 phase. We synchronized primary fibroblasts in G0 by serum starvation, and we promoted G1 phase entry by serum addition. We added BrdU after serum addition to monitor S-phase entry by immunofluorescence. ORC1-P4 fibroblasts showed

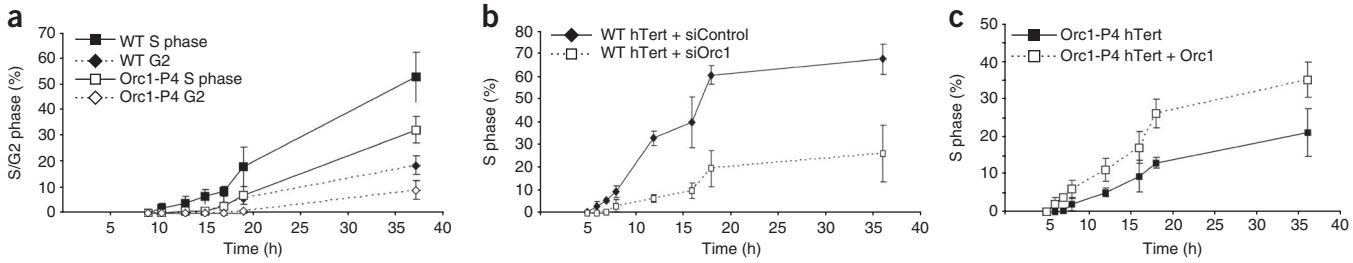

Figure 4 ORC1-deficient cells show delayed G1 to S progression. All values represent mean ± s.d. of three experiments. (**a**) ORC1-P4 cells showed delayed G1/S phase entry following serum starvation. We serum starved control (WT) or ORC1-P4 primary fibroblasts for 3 days. We added serum and BrdU (20 μM) at time 0 to monitor S-phase entry by immunofluorescence. We estimated the percent of BrdU+ cells, representing cells that have entered S phase, at the indicated time points by immunofluorescence. The solid lines represent the time of entry from G1 into S phase. We also monitored entry into G2 by measuring CENPF+ cells (dotted lines). ORC1-P4 cells showed delayed entry into S phase following re-entry into G1 phase. (**b**) We treated 1BR3-hTERT cells (a control WT hTERT immortalized fibroblast) with control or ORC1 siRNA and analyzed them as in **a**. (**c**) We transfected ORC1-P4 hTERT fibroblasts with empty vector or ORC1 complementary DNA plasmids and examined them as in **b** (note that the actual timing of S-phase entry was faster in both hTERT cell lines, but the delayed entry in ORC1-deficient cells remained). We also examined WT, ORC1-P1 and ATM$^{-/-}$ LBLs for chromosome aberrations in untreated cells and 24 h after exposure to 3 Gray (Gy) X-rays. ORC1-P1 LBLs showed a normal frequency of endogenous and radiation-induced chromosome aberrations; ATM$^{-/-}$ LBLs showed a tenfold increase in radiation-induced chromosome aberrations compared to control LBLs.

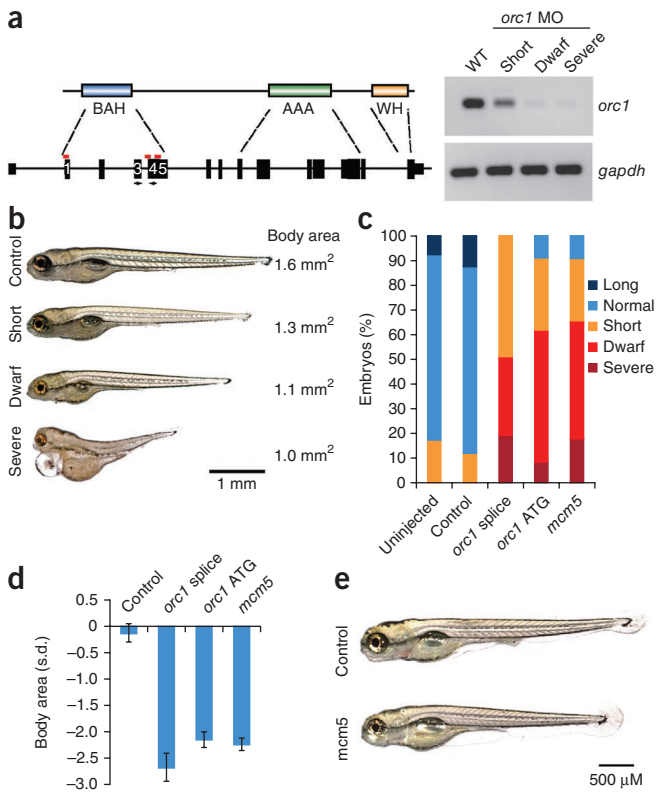

Figure 5 Depletion of Orc1 causes dwarfism in zebrafish. (**a**) Schematic of *orc1* zebrafish protein and gene intron-exon structure. Red bars are the position of morpholino oligonucleotide (MO) target sites and the arrows are PCR primers. RT-PCR of *orc1* MO from 3 days post fertilization (dpf) zebrafish embryos sorted according to phenotypic categories; WT, wild-type uninjected embryos. (**b**) Injection of splice-site targeted MOs to *orc1* caused marked reduction in body size compared to standard control embryos or uninjected wild-type zebrafish. 'Dwarf' *orc1* zebrafish were globally reduced in size and essentially otherwise normal aside from some subtle craniofacial features (hypoplasia of jaw cartilage, reduction in number or fusion of otoliths and smaller eye size). Severe embryos additionally had altered body curvature and decreased viability. (**c**) Quantification of phenotypes of MO-injected zebrafish. We defined categories with respect to zebrafish size: short, less than −1 s.d.; dwarf less than −2 s.d.; severe, less than −3 s.d. with additional body curvature. We defined normal as −1 to 1 s.d. and long as >1 s.d. (**d**) Body surface area of zebrafish injected with *orc1*, *mcm5* or control MOs expressed as s.d. relative to uninjected wild-type (AB) zebrafish embryos from the same matings. $P < 0.001$ for *orc1*-sp, *orc1*-atg or mcm5 MO versus control MO. Error bars, s.e.m. ($n = 23$ for control; $n = 41$ for *orc1*-sp; $n = 66$ for *orc1*-atg; and $n = 65$ for mcm5 MOs). *orc1*-sp, pooled splice-site targeted *orc1* Mos; *orc1*-atg; translational blocking orc MO. (**e**) mcm5 MO zebrafish (5 dpf) also have reduced body size and are morphologically similar to *orc1* MO zebrafish. Body surface area is significantly reduced ($P < 0.001$ mcm5 versus control MO). Quantification of mcm5 MO phenotype, see **c**,**d**.

substantially delayed S-phase entry compared to control fibroblasts (**Fig. 4a**). Small interfering RNA (siRNA) knockdown and complementation analysis using hTERT fibroblasts confirmed these findings (**Fig. 4b**,**c**). Finally, we also examined chromosome aberrations in ORC1-P1 LBLs because chromosome instability is a feature of many disorders with impaired DNA metabolism. We observed a normal frequency of chromosome aberrations (**Fig. 4** legend). In summary, these data show that ORC1 deficiency in affected individuals delays S-phase entry, thereby prolonging the G1 phase, consistent with previous analysis of an ORC2-deficient cancer cell line[19].

Previous developmental studies have not examined the consequence of reduced ORC function on organism growth. To examine whether ORC1 deficiency could specifically reduce overall body size, we established a zebrafish morphant model. Injecting morpholino oligonucleotides targeting *orc1* into one-cell-stage embryos substantially reduced embryo size at 5 days after fertilization (**Fig. 5a**,**b**). Over 80% of injected embryos were structurally normal and viable with a general reduction in size of all tissues (**Fig. 5**). The remaining embryos displayed a 'severe' phenotype with abnormal body curvature and reduced viability (**Fig. 5b**,**c**), and phenotype correlated with the degree of orc1 transcript-level depletion (**Fig. 5a**). Similarities to a lethal amorphic *mcm5* mutant[20] led us to also deplete *mcm5*, and we found that these *mcm5* morphants had an identical phenotype to our viable 'dwarf' Orc1 zebrafish and exhibited similar levels of growth retardation (**Fig. 5d**,**e**). The finding of a similar phenotype between Mcm5- and Orc1-depleted zebrafish suggests that the phenotype might be a direct consequence of impaired origin licensing rather than an indirect consequence of any additional function of Orc1 distinct from its role in origin licensing.

Collectively, our cellular and developmental studies implicate impaired origin licensing as a cause of microcephalic dwarfism. We establish that reduced origin licensing in ORC1 cells is associated with alterations in cell-cycle kinetics with a prolonged G1 phase and delayed S-phase entry and S-phase progression. Although redundancy in origin usage allows efficient growth in cell culture, Orc1 reduction could be developmentally important. Cell-cycle timings vary markedly during development, with some stages being rapid. For example, in early neurogenesis, cell cycle length (in neural progenitors) is only 8 h[21]. Furthermore, neuronal stem cells have a markedly truncated G1 phase in which impaired pre-RC assembly could become rate limiting. As the result of prolonged cell cycle times, even small changes in the number of cell divisions of progenitor and stem cells could have dramatic effects on eventual tissue and organ size[22].

Given that defects in origin licensing causes primordial dwarfism (**Supplementary Fig. 5**), we screened *ORC2–ORC6* in our general cohort of individuals with microcephalic dwarfism but did not identify any mutations. However, based on some potential overlapping features of the individuals with MGS with *ORC1* mutations (for example, subject 3; P3 **Table 1**), we screened a specific cohort of individuals with MGS and identified further mutations in *ORC1* as well as in additional licensing proteins. This work is described in the accompanying paper[23]. A summary of the features of individuals with MGS with *ORC1* mutations is shown here (**Supplementary Table 1**) to allow direction comparison. Based on these two papers, we conclude that *ORC1* mutations cause a broad spectrum of phenotypes that includes MGS and cases of microcephalic dwarfism.

URLs. Alohomora, http://gmc.mdc-berlin.de/alohomora/; Pedcheck, http://watson.hgen.pitt.edu/register/docs/pedcheck.html; MERLIN, http://www.sph.umich.edu/csg/abecasis/Merlin; Allegro, http://www.decode.com/software/.

METHODS

Methods and any associated references are available in the online version of the paper at http://www.nature.com/naturegenetics/.

Accession codes. The data from this study are deposited in the RefSeq database under the following accession codes: *ORC1*, NM_004153.3 and *orc1*, NM_199933.1.

Note: Supplementary information is available on the Nature Genetics website.

© 2011 Nature America, Inc. All rights reserved.

ACKNOWLEDGMENTS

We thank the families and clinicians for their involvement; S. McKay, K. Erskine and the MRC HGU core sequencing service for advice and technical support; D. Fitzpatrick, J. Blow, E. Patton, V. van Heyningen, N. Hastie and T. Carr for discussions and comments; A. Sinclair for p294(oriP); A. Oliver for structural modeling; and S. Devroy for subject enrollment and sample collection. The A.P.J. laboratory is funded by the MRC and the Lister Insitute for Preventive Medicine, the M.O'D. laboratory is funded by Cancer Research UK and the MRC, and the P.A.J. laboratory is funded by the MRC, Association for International Cancer Research and the Wellcome Research Trust. A.P.J. is an MRC Senior Clinical Fellow and Lister Institute Prize fellow. M.O'D. is a CRUK Senior Cancer Research Fellow.

AUTHOR CONTRIBUTIONS

L.S.B. and A.P.J. designed and performed the genetics experiments. A.K., A.L., C.-A.M., P.Y. and A.P.J. performed the zebrafish studies. S.W., T.S., C.K., M.O'D. and P.A.J. designed and performed the functional cell biology experiments. N.A.S., D.J., M.B. and C.W. provided clinical samples and data. P.A.J., A.P.J., L.S.B. and M.O'D. wrote the paper.

COMPETING FINANCIAL INTERESTS

The authors declare no competing financial interests.

Published online at http://www.nature.com/naturegenetics/.
Reprints and permissions information is available online at http://npg.nature.com/reprintsandpermissions/.

1. Majewski, F. & Goecke, T. Studies of microcephalic primordial dwarfism I: approach to a delineation of the Seckel syndrome. *Am. J. Med. Genet.* **12**, 7–21 (1982).
2. Hall, J.G., Flora, C., Scott, C.I. Jr., Pauli, R.M. & Tanaka, K.I. Majewski osteodysplastic primordial dwarfism type II (MOPD II): Natural history and clinical findings. *Am. J. Med. Genet.* **130A**, 55–72 (2004).
3. Gorlin, R.J. Microtia, absent patellae, short stature, micrognathia syndrome. *J. Med. Genet.* **29**, 516–517 (1992).
4. O'Driscoll, M., Ruiz-Perez, V.L., Woods, C.G., Jeggo, P.A. & Goodship, J.A. A splicing mutation affecting expression of ataxia-telangiectasia and Rad3-related protein (ATR) results in Seckel syndrome. *Nat. Genet.* **33**, 497–501 (2003).
5. Griffith, E. *et al.* Mutations in pericentrin cause Seckel syndrome with defective ATR-dependent DNA damage signaling. *Nat. Genet.* **40**, 232–236 (2008).
6. Rauch, A. *et al.* Mutations in the Pericentrin (PCNT) gene cause primordial dwarfism. *Science* **319**, 816–819 (2008).
7. Al-Dosari, M.S., Shaheen, R., Colak, D. & Alkuraya, F.S. Novel *CENPJ* mutation causes Seckel syndrome. *J. Med. Genet.* **47**, 411–414 (2010).
8. Willems, M. *et al.* Molecular analysis of Pericentrin gene (*PCNT*) in a series of 24 Seckel/ MOPD II families. *J. Med. Genet.* **47**, 797–802 (2010).
9. Doxsey, S.J., Stein, P., Evans, L., Calarco, P.D. & Kirschner, M. Pericentrin, a highly conserved centrosome protein involved in microtubule organization. *Cell* **76**, 639–650 (1994).
10. Tibelius, A. *et al.* Microcephalin and pericentrin regulate mitotic entry via centrosome-associated Chk1. *J. Cell Biol.* **185**, 1149–1157 (2009).
11. Hemerly, A.S., Prasanth, S.G., Siddiqui, K. & Stillman, B. Orc1 controls centriole and centrosome copy number in human cells. *Science* **323**, 789–793 (2009).
12. Noguchi, K., Vassilev, A., Ghosh, S., Yates, J.L. & DePamphilis, M.L. The BAH domain facilitates the ability of human Orc1 protein to activate replication origins *in vivo*. *EMBO J.* **25**, 5372–5382 (2006).
13. Bell, S.P. & Stillman, B. ATP-dependent recognition of eukaryotic origins of DNA-replication by a multiprotein complex. *Nature* **357**, 128–134 (1992).
14. Nishitani, H., Lygerou, Z., Nishimoto, T. & Nurse, P. The Cdt1 protein is required to license DNA for replication in fission yeast. *Nature* **404**, 625–628 (2000).
15. Dhar, S.K. *et al.* Replication from oriP of Epstein-Barr virus requires human ORC and is inhibited by geminin. *Cell* **106**, 287–296 (2001).
16. Uetake, Y. & Sluder, G. Cell cycle progression after cleavage failure: mammalian somatic cells do not possess a "tetraploidy checkpoint". *J. Cell Biol.* **165**, 609–615 (2004).
17. Blow, J.J. & Gillespie, P.J. Replication licensing and cancer–a fatal entanglement? *Nat. Rev. Cancer* **8**, 799–806 (2008).
18. Ge, X.Q. & Blow, J.J. The licensing checkpoint opens up. *Cell Cycle* **8**, 2320–2322 (2009).
19. Teer, J.K. *et al.* Proliferating human cells hypomorphic for origin recognition complex 2 and pre-replicative complex formation have a defect in p53 activation and Cdk2 kinase activation. *J. Biol. Chem.* **281**, 6253–6260 (2006).
20. Ryu, S., Holzschuh, J., Erhardt, S., Ettl, A.K. & Driever, W. Depletion of minichromosome maintenance protein 5 in the zebrafish retina causes cell-cycle defect and apoptosis. *Proc. Natl. Acad. Sci. USA* **102**, 18467–18472 (2005).
21. Takahashi, T., Nowakowski, R.S. & Caviness, V.S. Jr. The cell cycle of the pseudostratified ventricular epithelium of the embryonic murine cerebral wall. *J. Neurosci.* **15**, 6046–6057 (1995).
22. Rakic, P. A small step for the cell, a giant leap for mankind: a hypothesis of neocortical expansion during evolution. *Trends Neurosci.* **18**, 383–388 (1995).
23. Bicknell, L.S. *et al.* Mutations in the pre-replication complex cause Meier-Gorlin syndrome. *Nat. Genet.* advance online publication, doi:10.1038/ng.775 (27 February 2011).

© 2011 Nature America, Inc. All rights reserved.

ONLINE METHODS

Research subjects. Genomic DNA was isolated from peripheral blood from the affected children and their family members. All individuals screened in the study fulfilled the inclusion criteria of head circumference less than −4 s.d. and height less than −4 s.d and included individuals with diagnoses of Seckel syndrome and MOPD as well as unspecified microcephalic dwarfism. Informed consent was obtained from all participating families, and the studies were approved by the Scottish Multicentre Research Ethics Committee (04:MRE00/19), the University of Sussex School of Life Sciences Research Governance Committee or the University of Texas Southwestern Medical Center at Dallas (IRB #032008-066). Permission to publish photographs was obtained.

Clinical features of individuals with microcephalic primordial dwarfism with mutations in *ORC1*. The average height of the affected subjects was −6.5 s.d. ± 1.7 s.d. and the average head circumference was −6.9 s.d. ± 1.0 s.d. All affected subjects were referred with diagnoses of microcephalic osteodysplastic primordial dwarfism (MOPD), Seckel syndrome or unspecified microcephalic dwarfism. Subsequently, we also found *ORC1* mutations in a cohort of individuals with a prior diagnosis of Meier-Gorlin syndrome (MGS), and retrospective assessment suggests some similarities between individuals with MGS and the individuals described here. First, ear size was reduced in several of our subjects (for example, individual P1; **Supplementary Fig. 3**), though to a lesser extent than that generally associated with MGS. Additionally, individuals P3 and P5 had a malformation also described in individuals with MGS in the accompanying paper (**Supplementary Table 1**; genu recurvatum and congenital lobar emphysema, respectively).

Mutation detection. Primers were designed using the ExonPrimer tool in the UCSC Genome Browser to amplify coding exons. Purified PCR amplification products were sequenced using dye-terminator chemistry and electrophoresed on an ABI 3730 capillary sequencer (Applied Biosystems). Mutation analysis was performed using Mutation Surveyor (Softgenetics). Anonymized control samples were screened by sequencing. Sequencing primers are detailed in **Supplementary Table 2**.

Genetic mapping. Genome-wide genotyping was performed by AROS Applied Biotechnology (Denmark) using Affymetrix Human Mapping SNP 5.0 GeneChips. SNP genotypes were analyzed using Alohomora, Pedcheck and MERLIN, and multipoint linkage analysis was performed with Allegro (see URLs) under a model of autosomal recessive inheritance with full penetrance and using a disease allele frequency estimated at 1 in 1,000. DeCODE genetic map distances and Affymetrix SNP allele frequencies were used. The region of homozygosity on chromosome 1 was confirmed through high-resolution haplotype analysis using microsatellite markers.

Bioinformatics. Genetic locations are based on NCBI genome assembly build 36. Sequence alignments were performed by ClustalW.

Vector construction. The coding sequence of *ORC1* from the open reading frame shuttle clone IOH9757 (ImaGene) was cloned into an N-terminal T7 epitope–tagged mammalian expression vector using Gateway cloning (Invitrogen).

Cell culture. EBV-transformed control (GM2188), ORC1-P1 and parental LBLs (ORC1-M; ORC1-F) were grown in Roswell Park Memorial Institute (RPMI) medium supplemented with 15% fetal calf serum (FCS), penicillin and streptomycin. Primary human control fibroblasts (1BR.3), ORC1-P4 fibroblasts and hTERT derivatives (WT: 1BRhTERT; ORC1-P4hTERT) were grown in minimal essential medium (MEM) with 15% FCS, 1% non-essential amino acids (NEAA) and 1% antibiotics. For synchronization, fibroblasts were serum starved for 3–4 days in MEM containing 0.5% (primary) or 0.1% (hTERT) FCS to promote G0. Cells were released into the G1 phase by addition of FCS-containing MEM. We added 10 μM BrdU (Becton Dickinson) or 20 μM CldU (MP Biomedicals) to identify S-phase cells.

Antibodies. ORC1 antibodies raised against the N (N17) or C terminus (H80), ORC2 (H300), MCM2 (N19), CDT11 (H300) and HP1 (FL191) were from Santa Cruz Biotechnology. KAP1 (Ab10484), HDAC1 (Ab19845) and Histone H3 (Y173) were from Abcam.

Chromatin extraction. Cells were lysed for 1 hour in buffer A (50 mM Tris-HCl, 150 mM NaCl, 2 mM EDTA, 2 mM EGTA, 25 mM NaF, 25 mM β-glycerolphosphate, 0.1 mM NaOrthovanadate, 0.2% Triton X-100, 0.3% NP-40, plus protease inhibitor cocktail (Roche)) at 4 °C and pelleted. The insoluble pellet was re-suspended in buffer A containing 300 mM NaCl and sonicated for 15 min in a sonicating waterbath. For micrococcal nuclease (MNase), cells were extracted as above but the insoluble pellet was subjected to increasing MNase digestion. For C1, digestion was 10 U/ml MNase for 10 min at 37 °C. For C2, the pellet from C1 was digested with 100 U/ml MNase for 45 min at 37 °C and then an equal volume of solubilization buffer was added (2% NP-40, 2% Triton X-100, 600mM NaCl) before sonication.

Fluorescence-activated cell sorting analysis. BrdU-labeled cells were fixed in 70% ethanol (−20 °C), treated with 2 M HCl in PBS for 20 min, washed in PBS/1% FCS, incubated in 0.1 M Na-tetraborate for 2 min, re-washed in PBS/1% FCS and incubated with fluorescein isothiocyanate (FITC)-conjugated monoclonal anti-BrdU (Becton Dickinson). Cells were counterstained with 10 μg/ml propidium iodide with 0.5 mg/ml RNase in PBS for 30 min. Cytocholasin B treatment was 0.75 μg/ml for 24 h.

Nascent DNA sucrose gradient. Cells were pulse labeled with [3H]-thymidine (0.1 millicurie (mCi)) as indicated, harvested into PBS containing 0.17 M EDTA and then irradiated with 20 Gray (Gy) to minimize DNA entanglement. Cells were laid onto a layer of lysis buffer (2% SDS, 0.02 M EDTA) on a 2.5 ml 5–20% alkaline sucrose gradient (5–20% sucrose, 0.1M NaOH, 0.1 M NaCl) and ultracentrifuged (Beckman XL-90) at r_{avg} 139,500 (141,000 *g*) for 70 min. Gradient fractions (100 μl) were collected onto a 3MM filter paper strip, fixed with 70% ethanol, washed in 5% TCA and then ethanol before quantification by liquid scintillation counting.

DNA blotting. We transfected 1×10^7 cells with the EBNA-containing plasmid p294(oriP) using Metafectene (Biontex). Plasmid DNA was isolated after one population doubling at the time indicated using the modified Hirt extraction procedure. Plasmid DNA was linearized with BamHI and half was also digested with DpnI. DNA was cleaned using MinElute columns (QIAGEN) and electrophoresed in 0.7% agarose in the absence of ethidium bromide. DNA was blotted onto a Hybond H+ membrane and probed with random primed α-dCTP^{32} labeled p294(oriP) (Rediprime II, GE Healthcare).

Small interfering RNA. Control ON-TARGET*plus* Control pool (Thermo Scientific Dharmacon) and ORC1*Stealth* (Invitrogen) siRNA were used as instructed by the manufacturers. The primers are detailed in **Supplementary Table 2**.

Zebrafish. *orc1* and *mcm5* were knocked down in zebrafish using sequence-specific morpholinos (Gene Tools). For all morpholinos used, a total of 1.5 nl of 0.95 nM/μl morpholino was microinjected into one- cell-stage embryos obtained from natural spawning of wild-type (AB) zebrafish lines. Primers are detailed in **Supplementary Table 2**. Live zebrafish were imaged on a Leica MZFL III stereo microscope, and body surface area was calculated using IPLab software (Biovision).

Statistics. Statistical testing was performed using the Student's *t*-test.

© 2011 Nature America, Inc. All rights reserved.

doi:10.1038/ng.776

OPEN ACCESS Freely available online

PLOS | GENETICS

Identification of the First ATRIP–Deficient Patient and Novel Mutations in ATR Define a Clinical Spectrum for ATR–ATRIP Seckel Syndrome

Tomoo Ogi[1,2☯]*, Sarah Walker[3☯], Tom Stiff[3], Emma Hobson[4], Siripan Limsirichaikul[2¤], Gillian Carpenter[5], Katrina Prescott[4], Mohnish Suri[6], Philip J. Byrd[7], Michiko Matsuse[2], Norisato Mitsutake[1,2], Yuka Nakazawa[1,2], Pradeep Vasudevan[8], Margaret Barrow[8], Grant S. Stewart[7], A. Malcolm R. Taylor[7]*, Mark O'Driscoll[5]*, Penny A. Jeggo[3]*

1 Nagasaki University Research Centre for Genomic Instability and Carcinogenesis (NRGIC), Nagasaki University, Sakamoto, Nagasaki, Japan, **2** Department of Molecular Medicine, Atomic Bomb Disease Institute, Nagasaki University, Sakamoto, Nagasaki, Japan, **3** Double Strand Break Repair Laboratory, Genome Damage and Stability Centre, University of Sussex, Brighton, United Kingdom, **4** Department of Clinical Genetics, Chapel Allerton Hospital, Leeds, United Kingdom, **5** Human DNA Damage Response Disorders Group, Genome Damage and Stability Centre, University of Sussex, Brighton, United Kingdom, **6** Clinical Genetic Service, City Hospital, Nottingham, United Kingdom, **7** School of Cancer Sciences, College of Medical and Dental Sciences, University of Birmingham, Birmingham, United Kingdom, **8** University Hospitals of Leicester NHS Trust, Leicester Royal Infirmary, Leicester, United Kingdom

Abstract

A homozygous mutational change in the *Ataxia-Telangiectasia and RAD3 related* (*ATR*) gene was previously reported in two related families displaying Seckel Syndrome (SS). Here, we provide the first identification of a Seckel Syndrome patient with mutations in *ATRIP*, the gene encoding ATR–Interacting Protein (ATRIP), the partner protein of ATR required for ATR stability and recruitment to the site of DNA damage. The patient has compound heterozygous mutations in *ATRIP* resulting in reduced ATRIP and ATR expression. A nonsense mutational change in one *ATRIP* allele results in a C-terminal truncated protein, which impairs ATR–ATRIP interaction; the other allele is abnormally spliced. We additionally describe two further unrelated patients native to the UK with the same novel, heterozygous mutations in *ATR*, which cause dramatically reduced ATR expression. All patient-derived cells showed defective DNA damage responses that can be attributed to impaired ATR–ATRIP function. Seckel Syndrome is characterised by microcephaly and growth delay, features also displayed by several related disorders including Majewski (microcephalic) osteodysplastic primordial dwarfism (MOPD) type II and Meier-Gorlin Syndrome (MGS). The identification of an ATRIP–deficient patient provides a novel genetic defect for Seckel Syndrome. Coupled with the identification of further ATR–deficient patients, our findings allow a spectrum of clinical features that can be ascribed to the ATR–ATRIP deficient sub-class of Seckel Syndrome. ATR–ATRIP patients are characterised by extremely severe microcephaly and growth delay, microtia (small ears), micrognathia (small and receding chin), and dental crowding. While aberrant bone development was mild in the original ATR–SS patient, some of the patients described here display skeletal abnormalities including, in one patient, small patellae, a feature characteristically observed in Meier-Gorlin Syndrome. Collectively, our analysis exposes an overlapping clinical manifestation between the disorders but allows an expanded spectrum of clinical features for ATR–ATRIP Seckel Syndrome to be defined.

Citation: Ogi T, Walker S, Stiff T, Hobson E, Limsirichaikul S, et al. (2012) Identification of the First ATRIP–Deficient Patient and Novel Mutations in ATR Define a Clinical Spectrum for ATR–ATRIP Seckel Syndrome. PLoS Genet 8(11): e1002945. doi:10.1371/journal.pgen.1002945

Editor: Andrew O. M. Wilkie, University of Oxford, United Kingdom

Received April 25, 2012; **Accepted** July 26, 2012; **Published** November 8, 2012

Copyright: © 2012 Ogi et al. This is an open-access article distributed under the terms of the Creative Commons Attribution License, which permits unrestricted use, distribution, and reproduction in any medium, provided the original author and source are credited.

Funding: This work has been supported by Special Coordination Funds for Promoting Science and Technology from the Japan Science and Technology Agency (JST) to TO and YN; a Global COE Program from the Ministry of Education, Culture, Sports, Sciences, and Technology of Japan to TO, MM, NM, SL, and YN; and by a Grant in Aid for Scientific Research KAKENHI (24681008) from the Japan Society for the Promotion of Science, a science research grant from Inamori Foundation, a medical research grant from Mochida Memorial Founds for Medical and Pharmaceutical Research, a medical research grant from Daiichi-Sankyo Foundation of Life Science, and a medical research grant from Takeda Science Foundation to TO. The PAJ laboratory is supported by the Medical Research Council, the Association for International Cancer Research, and the Wellcome Research Trust. The MO laboratory is supported by Cancer Research UK, Medical Research Council, and Leukaemia Lymphoma Research. MO and GSS are CR-UK Senior Cancer Research Fellows. The funders had no role in study design, data collection and analysis, decision to publish, or preparation of the manuscript.

Competing Interests: The authors have declared that no competing interests exist.

* E-mail: m.o-driscoll@sussex.ac.uk (MO); A.M.R.Taylor@bham.ac.uk (AMRT); p.a.jeggo@sussex.ac.uk (PAJ); togi@nagasaki-u.ac.jp (TO)

¤ Current address: Faculty of Pharmacy, Silpakorn University, Nakhon Pathom, Thailand

☯ These authors contributed equally to this work.

Introduction

Seckel Syndrome (SS) (OMIM 216000) is an autosomal recessive disorder characterised by marked microcephaly, intrauterine and post-natal growth retardation, developmental delay and characteristic facial features, encompassing micrognathia (small and receding chin), receding forehead and pronounced nose [1]. Majewski (microcephalic) osteodysplastic primordial dwarfism (MOPD) type II and Meier-Gorlin Syndrome (MGS) also display microcephaly and primordial dwarfism [2,3]. How-

Author Summary

Seckel Syndrome (SS) is a rare human disorder characterised by small head circumference and delayed growth. Patients can show additional features including abnormal bone development, receding chins, sloping foreheads, and small ears. In 2003, we identified *ataxia telangiectasia and Rad3 related* (*ATR*) as a causal genetic defect in two related families displaying SS. However, additional patients with mutations in *ATR* have not hitherto been identified. Here, we describe two further patients with novel mutations in *ATR*. Additionally, we identify a patient with mutations in *ATRIP*, which encodes an interacting partner of ATR, representing a novel genetic defect causing SS. ATR functions to promote the ability of cells to recover from difficulties encountered during replication. We show that patient-derived cells have reduced ATR and ATRIP protein levels and defective ATR/ATRIP function. Our identification of further ATR–ATRIP defective patients and a consideration of their clinical features aids the characterisation and identification of this form of SS and provides insight into the role played by the ATR–ATRIP complex during development.

ever, each of these disorders display an additional spectrum of features conferring clinical distinction. Despite this, on an individual basis, assigning patients to a specific classification is difficult. Additionally, primary microcephaly represents a disorder displaying pronounced microcephaly without marked impact on growth [4]. Five loci conferring SS have been described with four genes identified [5,6]. The first causal genetic defect identified for SS was the *Ataxia-Telangiectasia and RAD3 related (ATR)* gene [7]. A homozygous mutation in *ATR* was identified in two related SS families and cell-based studies provided strong evidence for an impact on ATR function in patient cell lines. This sub-class of SS was designated ATR–SS. More recently, mutations in *CTIP* were identified in a SS patient as well as in a family described as displaying Jawad Syndrome [8]. Additionally, mutations in CENPJ and CEP152, two centrosomal proteins, have been described in SS patients, although mutations in these genes more frequently confer primary microcephaly [9,10]. Mutations in *PCNT*, which encodes a centrosomal protein, and *ORC1L*, a component of the original licensing complex, were reported in patients originally classified as SS although in both cases retrospective analysis revealed that such mutations more frequently cause MOPD type II or MGS, respectively, highlighting the diagnostic challenge faced in the clinic [11–15]. These studies demonstrate that evaluation of multiple patients is required to provide insight into the spectrum of clinical features conferred by specific gene defects, which ultimately aids an understanding of the role of the defective protein during development. To date all ATR–SS patients belong to one of two related families, which harbour the identical homozygous mutation in *ATR*, thereby limiting the characterisation of the clinical phenotype conferred by ATR deficiency. Furthermore, no patients deficient in ATR interacting protein, ATRIP, which is required for ATR stability, have hitherto been described.

ATR, like the related Ataxia-Telangiectasia mutated (ATM) protein, is a phosphoinositol-3 kinase (PI3)-like kinase that functions at the centre of a signal transduction network activated by DNA damage, and most importantly, by replication fork stalling [16]. ATR and ATM share phosphorylation targets but whilst ATM is activated by DNA double strand breaks (DSBs) that arise, for example, following exposure to ionising radiation (IR), ATR is activated by single stranded (ss) regions of DNA that arise following replication fork stalling or exposure to agents that induce bulky DNA adducts [17,18]. Importantly, since replication fork stalling occurs during most cycles of replication, ATR is essential. ATM, in contrast, is non-essential presumably because endogenous DSBs arise infrequently. ATR forms a stable complex with ATR–interacting protein (ATRIP), which is required for ATR stability [19]. Further, ATRIP is required for ATR localisation to ssDNA regions and hence for ATR activation. Consequently, in a range of organisms loss of ATRIP or its homologue, phenocopies ATR deficiency [17,20–22]. Although ATM and ATR share overlapping substrates, ATR specifically phosphorylates Chk1 whilst ATM phosphorylates the related kinase, Chk2. The major functions of ATR are to activate cell cycle checkpoint arrest, stabilise stalled replication forks and promote replication fork restart, which is achieved through its ability to phosphorylate a range of substrates including p53 and H2AX [18,23,24]. Interestingly, in the context of SS, CtIP promotes DNA end resection, which leads to ss DNA formation, the lesion activating ATR. Hence, CtIP functions in a mechanism leading to ATR activation. It is noteworthy that cells derived from *PCNT*-mutated MOPD type II patients are also defective in ATR–dependent G2/M checkpoint arrest although upstream steps in the ATR–signalling pathway are activated normally [11]. These findings suggest that PCNT is required for an important end-point of ATR function. Additionally, the origin licensing complex, components of which are mutated in MGS, is required for the initiation of replication and *ORC1L*-deficient MGS cell lines display slow S phase progression [13]. Similarly, ATR promotes S phase progression by facilitating recovery from replication fork stalling. Together, these findings demonstrate mechanistic overlap between ATR, PCNT and ORC1L, which may underlie some clinical overlap in the disorders conferred by mutations in the genes encoding these proteins.

Here, we provide the first description of a SS patient with mutations in *ATRIP*. Interestingly, the mutational change in one *ATRIP* allele causes impaired ATR–ATRIP interaction and our extensive cellular analysis confirms a deficiency in ATR signalling and damage responses. Additionally, we describe two further, unrelated patients with mutations in *ATR*. The identification and clinical description of an ATRIP patient and two further ATR patients provides a more definitive characterisation of the clinical phenotype conferred by ATR deficiency.

Results

Cells derived from patient CV1720 display a compromised DNA damage response

Patient CV1720 displayed severe microcephaly, growth delay and dysmorphic facial features and was classified as a SS patient (see Table 1 and Figure S1A for details of the clinical features). Cell line CV1720 is a lymphoblastoid cell line (LBL) derived from the patient; fibroblasts were not available. Cells from the previously described ATR–SS (DK0064) patient display impaired DNA damage responses and phosphorylation of ATR substrates [7]. To determine whether CV1720 cells are defective in ATR–dependent G2/M checkpoint arrest, the mitotic index (MI) was monitored at 2 h following UV exposure, a form of DNA damage known to activate ATR–dependent checkpoint arrest. Whilst WT LBLs show a significantly reduced MI following UV exposure compared to undamaged cells, CV1720 cells showed only a modest decrease similar to that observed in DK0064 (ATR–SS) cells (Figure 1A). Cells from the parents of patient CV1720

Table 1. Clinical features of ATR/ATRIP–deficient patients.

	ATRIP–SS		ATR–SS	27-4BI	19-8BI
Ethnicity	**Gujarati-Indian (consanguineous)**		**Pakistani (consanguineous)**	**English**	**English**
Birth.					
OFC (cm)	27.1		24 *(-8SD)*	27	24.2
Wgt (Kg)	2.06		1.1 *(-3SD)*	1.15	0.77
Hgt (cm)	NR		NR	36	NR
Age.	**14 mts**	**3 yrs 3 mts**	**9 yrs**	**20 mts**	**4.5 yrs**
OFC (cm)	-9SD	-10SD	-12SD	-10SD	-10SD
Wgt (Kg)	-5SD	-6SD	-3.3SD	-8SD	-7SD
Hgt (cm)	-5SD	-6.5SD	NR	-8SD	-8SD
Face	Micrognathia, receding forehead, prominent nose.		Micrognathia, receding forehead, prominent nose.	Micrognathia, prominent nose, hypoplastic alae nasi, low set columella, deep set short palpebral fissures.	Micrognathia, blepharophimosis, short palpebral fissures. Prominent nose; high nasal bridge. High anterior hairline.
Teeth	Dental crowding.		Dental crowding and malocclution.	4 teeth at 20 months.	Dental crowding.
Ears	Small lobes.		Posteriorly rotated with absent lobes.	Small, round, low set with poorly formed antihelix tragus & antitragus. Absent lobes.	Small ears with absent lobes
Hands	Bilateral 5^{th} finger clinodactyly.		Multiple ivory epiphysis.	Small, tapering fingers.	Bilateral 5^{th} finger clinodactyly. 5^{th} metacarpels appear short. Blue colouration to both thenar eminence.
Skeletal Survey	Delayed bone age (wrist & hips), symmetric dwarfism.		Microcrania with fuse sutures. Mild thoracic kyphosis. Ribs angulated posteriorly. Narrow iliac blades, cox valga and minor subluxation of the hips. No disslocation of the radial heads	Symmetric dwarfism. Small patellae. No joint hypermobility or kyphoscoliosis.	Symmetric dwarfism. Copper beaten skull. No ossification of the patellae (age 4 yrs). Marked hip & shoulder flexibility. No kyphosis.
Endo-crinology	Normal IGF1, TFT, LH, FSH & cortisol.		NA	NA	NA
MRI	14 mts:generalised cerebral atrophy, normal ventricular systems. Delayed myelination in the anterior limb of the internal capsule. Pituitary is present though of unusual shape with absent fossa.		NA	NA	2 yrs: abnormal gyration in posterior aspect of the cingulated gyrus extending into the parietal occipital region. Hypoplastic corpus collasum.
Other	NR		Developmental delay. Walked at 7 yrs.	No abnormal skin pigmentation. Small feet with metatarsus adductus	No abnormal skin pigmentation. Developmental delay. Sat at 15 mts, walked at 3 yrs 10 mts. High pitched voice, asthma, multiple chest infections, feeding difficulties-reflux (gastrostomy fed). Multiple liver cysts consistent with Caroli's disease found at 17 mts.

NR; not recorded. NA; not assessed.

doi:10.1371/journal.pgen.1002945.t001

(CV1780 and CV1783) displayed normal G2/M checkpoint arrest.

We have previously observed that cells from other SS patients display defects in ATR–dependent G2/M checkpoint arrest but activate upstream steps in the ATR signalling cascade normally [25]. This is exemplified by cell lines from MOPD type II patients with mutations in *PCNT*, which are defective in ATR–dependent G2/M checkpoint arrest but proficient in ATR phosphorylation events [11]. Therefore, next, we examined whether CV1720 LBLs efficiently activate upstream steps in ATR signalling. Since these assays predominantly reflect the response of replicating phase cells, we first verified that CV1720 and control LBLs harbour a similar percentage of S phase cells (Figure S2). Pan-nuclear phosphorylation of H2AX (γH2AX) after replication fork stalling represents an ATR–specific damage response [24]. Strikingly, whilst exposure to 5 mM HU for 2 h resulted in an elevated number of cells staining positively for γH2AX in WT cells, this was not observed in either CV1720 or DK0064 (ATR–SS) cells (Figure 1B). We note that although previous studies have shown that ATM can be activated and phosphorylate γH2AX at DSBs arising following HU treatment in the absence of ATR due to enhanced fork collapse, this was not observed at 2 h post 5 mM HU exposure in these patient cells most likely due to residual ATR activity and/or the early times examined [26,27]. Chk1 represents an important ATR substrate required for G2/M checkpoint arrest. To examine Chk1 activation, we carried out Western Blotting using p-Chk1 antibodies. Following the same UV exposure conditions (2 h post 5 Jm^{-2}) employed to examine G2/M checkpoint arrest, we

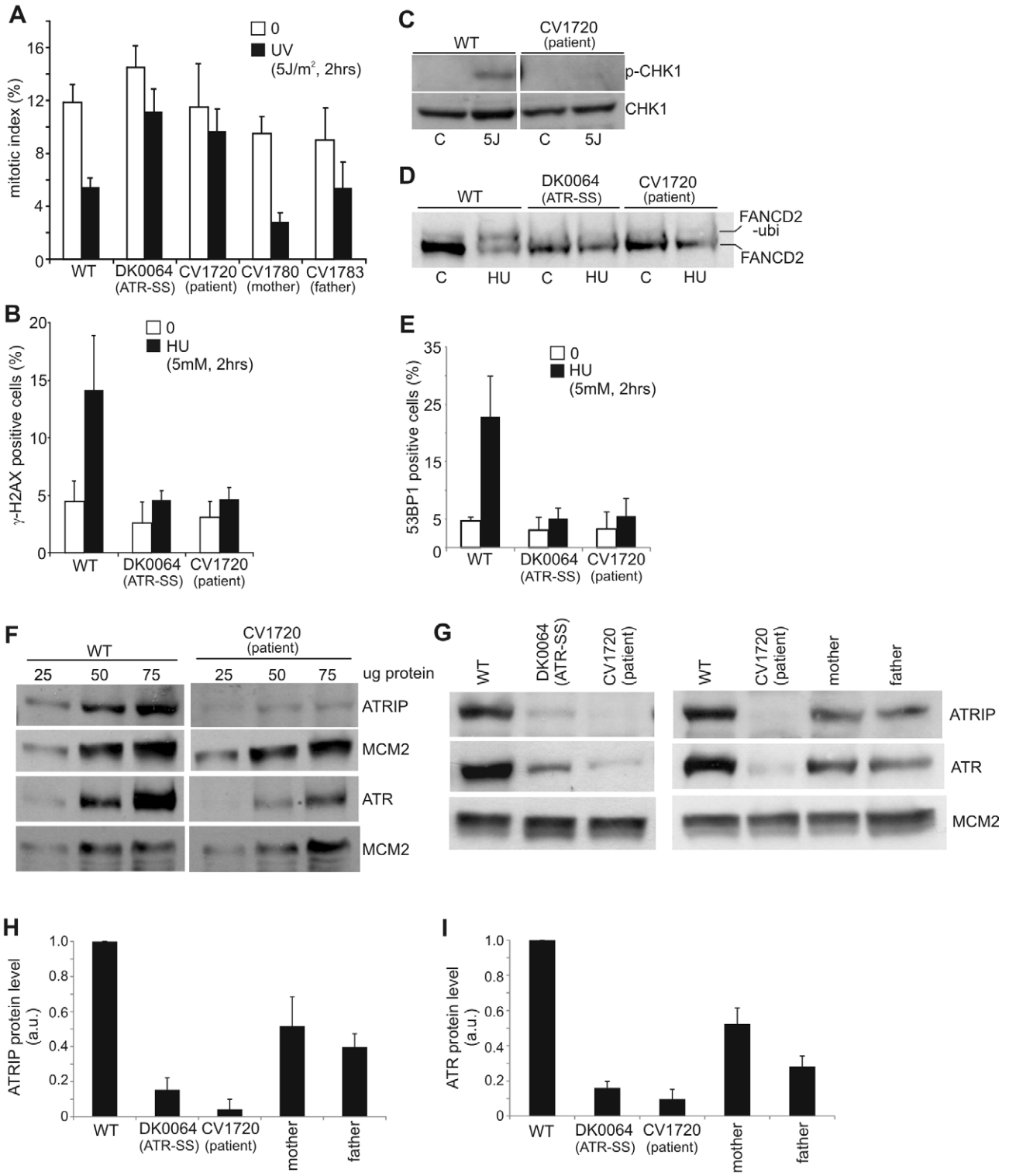

Figure 1. CV1720 cells show impaired ATR–dependent DNA damage responses. A) WT, DK0064 (ATR–SS), CV1720 (patient), CV1780 (patient's mother) and CV1783 (patient's father) cells were exposed to 5 Jm^{-2} UV and the mitotic index (MI) assessed 2 h post exposure. A greater than two fold decrease in mitotic index is observed in WT and both paternal cell lines but not in DK0064 (ATR–SS) or CV1720 (patient) cells. B) Cells were exposed to 5 mM HU for 2 h and the percentage of p-H2AX (γ-H2AX) positive cells assessed by immunofluorescence. Note that HU causes pan nuclear p-H2AX formation rather than defined foci as observed after exposure to ionising radiation. Thus, the percentage of γ-H2AX positive cells was scored. C) Cells were exposed to UV (5 Jm^{-2}) and subjected to Western Blotting (WB) using p-Chk1 (p-Ser317) antibodies at 2 h. Chk1 expression was shown to be similar in WT and patient cells (lower panel). D) Cells were exposed to 3 mM HU for 2 h and whole cell extracts analysed by WB using FANCD2 antibodies. The ubiquitylation of FANCD2, detectable by a product with reduced mobility, is diminished in DK0064 (ATR–SS) and CV1720 cells compared to WT cells. E) Cells were exposed to 5 mM HU and examined for the percentage of cells showing >5 53BP1 foci at 2 h post exposure. 53BP1 foci formation is reduced in DK0064 (ATR–SS) and CV1720 cells compared to WT cells. F–I) The indicated cells were processed by WB using

ATRIP or ATR antibodies. MCM2 was used as a loading control. F shows the analysis of a range of protein levels for accurate comparison. CV1720 (patient) cells show markedly reduced ATR and ATRIP protein levels. G shows that both parental lines have approximately half the level of ATR and ATRIP compared to two WT cell lines. DK0064 (ATR–SS) and CV1720 cells, in contrast, have more dramatically reduced ATR and ATRIP protein levels. 50 ug protein was loaded. WT in all panels was GM2188. Patient, mother and father were as shown in panel A. H and I show the quantification of ATRIP and ATR protein levels from at least three independent WB experiments.
doi:10.1371/journal.pgen.1002945.g001

observed a pronounced p-Chk1 band in WT LBLs but not in CV1720 cells although Chk1 levels were similar in the two lines (Figure 1C). These results provide strong evidence that CV1720 show impaired ATR–dependent substrate phosphorylation.

A further ATR–dependent response is mono-ubiquitylation of FANCD2 following exposure to HU [28]. Mono-ubiquitinated FANCD2 can be detected by the presence of a slowly migrating isoform of FANCD2 generated post exposure to 3 mM HU. Whilst such a product was detected in WT cell extracts, it was absent in CV1720 and DK0064 (ATR–SS) cell extracts (Figure 1D). Finally, ATR also regulates the formation of 53BP1 foci following replication fork stalling via a Chk1-dependent process. We observed a failure to form 53BP1 foci following exposure to 5 mM HU in CV1720 and DK0064 (ATR–SS) LBLs in contrast to WT LBLs (Figure 1E), consistent with the diminished levels of p-Chk1 observed in CV1720 cells.

Collectively, these studies provide strong evidence that CV1720 cells are defective in an upstream step of the ATR–dependent signalling response defining them as distinct to the majority of previously characterised SS cell lines, which, though defective in UV-induced G2/M checkpoint arrest, are proficient in upstream steps of the ATR signalling response [25].

Reduced ATR and ATRIP protein expression in CV1720 cells

Given the overlapping cellular phenotype between CV1720 and DK0064 (ATR–SS) cells, we examined CV1720 cells for expression of ATR and ATRIP protein by Western Blotting. Strikingly, we observed markedly reduced levels of both ATR and ATRIP in CV1720 cells (Figure 1F). Since ATRIP stabilises ATR, this does not distinguish whether the primary defect lies in ATR or ATRIP and indeed a similar reduced level of ATR and ATRIP was observed in DK0064 (ATR–SS) cells (Figure 1G). Significantly, we observed reduced ATRIP and ATR in both parental LBLs (CV1780 and CV1783), which was approximately 50% of the level in WT LBLs (Figure 1G–1I).

Sequencing analysis reveals mutational changes in *ATRIP* in CV1720 cells

To examine whether the causal genetic defect in CV1720 lies in *ATR* or *ATRIP*, we carried out sequencing of the two genes. First, we undertook PCR-based gDNA sequencing of the 47 exons and neighbouring exon-intron boundaries of the human *ATR* gene from CV1720 cells and failed to observe any mutational changes likely to be of functional significance. Next, we undertook gDNA sequencing of *ATRIP* exons and observed a heterozygous mutational change, c.2278C>T, in exon12 which generated a stop codon predicting a truncated protein at position arginine 760 (p.Arg760*) (Figure S3). However, no mutational changes in any other exons were identified although we detected several novel intronic changes that could potentially impact on splicing (Table S1). Significantly, the c.2278C>T mutational change was observed as a heterozygous change in the patient's mother but not in the father (Figure S3).

We also performed RT-PCR sequencing of *ATRIP* cDNA from CV1720 and both parents. These analyses revealed a low level of a smeared PCR product following amplification of the 5′*ATRIP* cDNA region using patient but not control cDNA (data not shown). Following multiple analyses, we found specifically that RT-PCR amplification using primers located in exons 1 and 4, reproducibly yielded a smeared product from CV1720 cDNA with discrete bands at 458 bp (the expected product size) and 325 bp whereas only the 458 bp product was observed using cDNA from WT cells (Figure 2A). Direct sequencing of the gel purified smaller (325 bp) and full-length (458 bp) RT-PCR products showed that the small fragment specifically lacked exon 2. Sequencing analysis of the RT-PCR product of CV1720 cDNA using the same primers revealed the predicted double sequence with the product lacking exon 2 being less than 50% of the product containing exon 2 (Figure 2B). It is notable that there were also some PCR products larger than the full length product although a discrete band was not evident. In sequencing the RT-PCR product, we observed some that harboured intron 2 sequences although these represented a minor product relative to that lacking exon 2. Collectively, these findings strongly suggested that there could be mis-splicing in CV1720 cells with loss of exon 2 being the major product.

To assess this further, qRT-PCR was undertaken using sets of primers that allow selective amplification of the WT and mutant products (c.2278C>T mutant as well as the mis-spliced product). The aim was to determine if the mis-spliced product originated from the paternal allele and if it impacted upon the transcript level. Primer pairs, P1 and P3C, located in exons 12 and 13, respectively, allow selective amplification of the WT (paternal) c.2278C allele whilst primers P2 and P3C selectively amplify the mutated (maternal) c. 2278C>T allele (Figure 2C). As expected, the mutant (c.2278C>T)-allele-specific PCR product (right columns, red bars) was only detected in the patient and mother whereas the WT-specific PCR product (left columns, blue bars) was detected in all samples, demonstrating that the primers distinguished the two alleles (Figure 2C). The results also showed that the c.2278C>T and the WT (c.2278C) alleles were expressed at nearly equal levels (normalised against *HPRT1*) in the mother (compare blue and red bars labelled 'mother' in Figure 2C), suggesting that the c.2278C>T *ATRIP* mRNA is not subject to nonsense mediated RNA decay (NMD) (Figure 2C).

To evaluate the expression level of the mis-spliced *ATRIP* mRNA, we designed primers located at the exon 2/exon 3 boundary (primer P4) and within exon 3 (primer 6C) to allow selective amplification of the correctly spliced mRNA (Figure 2D); primers located at the exon 1/exon 3 boundary (primer P5) and within exon 3 (primer 6C) selectively amplify the mis-spliced mRNA. Whilst the correctly spliced product was amplified to similar (although slightly different) extents from father, mother and patient mRNA (compare the column heights, left panel in Figure 2D), the mis-spliced product was more abundant in the patient and father, suggesting that mis-splicing is a consequence of a mutational change linked to the paternal allele (compare the column heights, right panel in Figure 2D). Since we observed nearly equal expression levels of the wild type (c.2278C) and mutant (c.2278C>T) alleles in the mother (Figure 2C, compare the right and left panels), we considered that the PCR products derived from the mother using primers P4/P6C or P5/P6C would

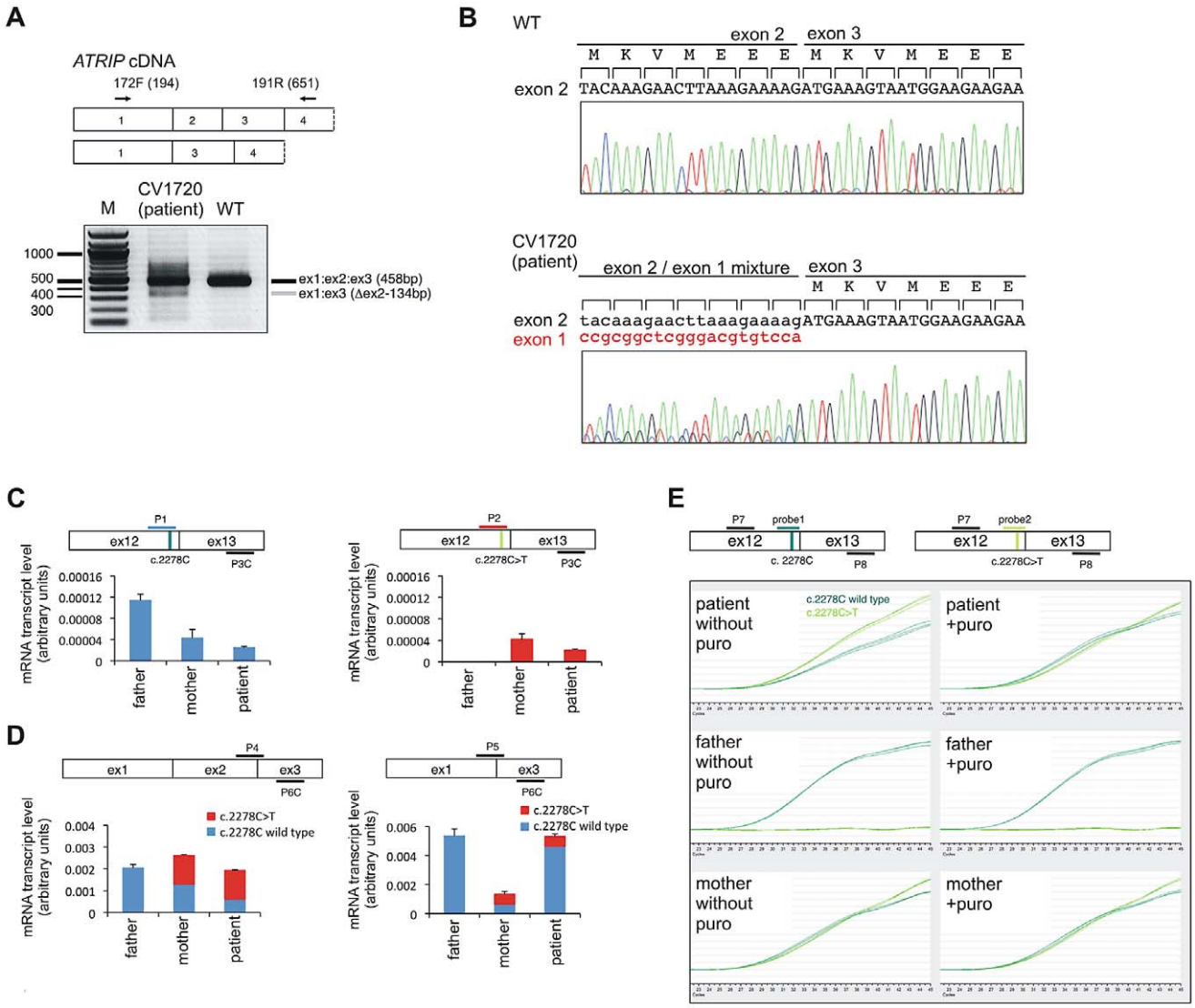

Figure 2. Identification of mutational changes in *ATRIP* in CV1720. A) Upper panel shows primer pairs used to distinguish cDNA products encompassing or lacking exon 2. Lower panel shows RT-PCR products obtained using the primers shown in the upper panel. RT-PCR from patient CV1720 generated a smeared product with a defined band of 458 bp, as observed in WT cells, and a weaker band of 325 bp. The latter band was not detected using cDNA from WT cells (MRC5). A similar single 458 bp band was obtained using the same primers with cDNA derived from a distinct wild type cell line (GM2188; data not shown). (B) Sequencing of the RT-PCR products derived from WT (MRC5) and patient (CV1720) cells. A double sequence pattern at the exon 2–3 boundary is observed using patient CV1720 cDNA. C) Selective quantitative amplification of the WT or 2278C>T *ATRIP* alleles. Primers located in *ATRIP* exon 12 and 13 were designed to selectively amplify the WT (c.2278C) (P1 and P3C) versus the mutated (c.2278C>T) (P2 and P3C) alleles. The WT PCR product is shown in blue and the c.2278C>T PCR product in red. The exon 12 mutated allele is only observed in the patient and mother cDNA whilst the WT allele is observed in the patient, mother and father cDNA although the level is reduced in the patient and mother. D) qRT-PCR analysis of *ATRIP* splicing variants from patient CV1720 and parental cells. qRT-PCR analysis of the level of the normally spliced (encompassing exons 1-2-3) and the aberrantly spliced (Δexon2) *ATRIP* cDNA in the patient and parent cells. PCR primers were designed at the exon2-exon3 or exon1-exon3 boundaries to selectively amplify the splicing variants. Transcripts from *HPRT1* were used as a quantification control. The correctly spliced transcript from the paternal allele of the patient (wild type c.2278C, blue fraction in the cumulative bar labelled, 'patient', at the left panel) was estimated to be ~25% of the normal level. (E) The mis-spliced paternal allele is subject to nonsense mediated mRNA decay (NMD). Cycleave-qPCR confirmed that the *ATRIP* c.2278C>T mutant allele was expressed exclusively in the patient and the mother. The *ATRIP* exon12-13 fragment was amplified with PCR primers P7/P8 as shown in the figure. A set of fluorescent probes were used to distinguish the WT versus c.2278C>T allele (probe1 and probe2, respectively). In the patient, the paternal mRNA transcript level (emerald lines) is low because of NMD (top left). Puromycin treatment eliminated the NMD and the paternal transcript level returned to the normal level. In all panels WT represented MRC5, patient was CV1720 and parents were as shown in Figure 1A.
doi:10.1371/journal.pgen.1002945.g002

be equally derived from the c.2278C and c.2278C>T alleles, which have, therefore, been depicted as equal sized contributions (shown in red or blue in mother columns in Figure 2D). Similarly, the mutant c.2278C>T allele is likely to be expressed at an equal level in the patient as in the mother (shown in red in patient columns in Figure 2D). Based on these assumptions, we estimated that the normally spliced WT mRNA is reduced to around 1/4 of the WT level in the patient and to 3/4 in the father (shown in blue in the left hand panel in Figure 2D). Assuming that the c.2278C>T allele is fully inactivated (see below), the patient

therefore has around 25% of ATRIP activity compared to a normal individual.

The findings above suggested that the mis-spliced mRNA, which generates an out of frame cDNA, is subject to NMD. To examine this and substantiate our findings, qRT-PCR was also carried out using fluorescent cycleave probes with or without exposure to puromycin, an antibiotic which prevents NMD (Figure 2E) [29]. Primers (P7 and P8) and fluorescent probes (probe 1 and 2) were designed to allow amplification of a product encompassing exon 12–13 that distinguished the maternal (probe 2) from the paternal (probe 1) allele. We confirmed detection of the c.2278C>T allele exclusively in the patient and mother as well as the WT allele in all samples (Figure 2E). In the mother, the wild type (c.2278C) and mutant (c.2278C>T) signals were detected at equal levels regardless of whether puromycin was added, indicating that the alleles are equally expressed and are not subjected to NMD. In patient CV1720, the WT product was reduced relative to the mutant product in the absence of puromycin but was at similar levels in the presence of puromycin (Figure 2E). These findings are consistent with the notion that the mRNA expressed from the parental allele is aberrantly spliced and partially subject to NMD. Perhaps surprisingly, we did not detect any obvious difference of the WT product following puromycin treatment in the father; however, in this case, we anticipate a 25% decreased product, which is unlikely to be detected without an internal control. However, despite this, there was evidence for abnormal splicing in the paternal cDNA from analysis of the PCR products spanning exons 1–3 (Figure 2B, 2D).

Finally, to gain insight into the basis underlying mis-splicing, we sequenced introns 1 and 2 from the patient, mother, and father and identified a previously unreported mutational change in intron 2, 13 bp from the intron-exon 2 boundary in the patient and paternal gDNA (Table S1). However, given the modest impact on splicing we did not attempt to examine whether this represented the causal mutational change affecting splicing.

Arg760* ATRIP does not promote ATR–dependent G2/M arrest and reduces ATR–ATRIP interaction

It is likely that *ATRIP* c.2278C>T causes an impacting mutational change since the low levels of ATRIP protein (10–20% WT levels) in CV1720 cells suggest that p.R760* ATRIP is unstable (given that the mRNA level of this allele is normal). To substantiate that p.R760* expression impairs the ATR–dependent response to DNA damage, we examined whether its expression could complement the G2/M checkpoint defect of CV1720 cells. We also examined whether p.R760* might exert a dominant negative impact (since this represented a possible explanation for the low ATRIP protein level in CV1720 cells). The c.2278C>T mutational change was introduced into *ATRIP* cDNA by site directed mutagenesis. cDNA encoding WT *ATRIP* and/or R760* ATRIP was transiently transfected into LBLs and G2/M checkpoint arrest examined at 2 h post exposure to 5 Jm^{-2} UV. Consistent with previous findings, WT but not CV1720 cells showed a G2/M checkpoint arrest (Figure 3A). Whilst transfection with WT *ATRIP* cDNA completely rescued the G2/M checkpoint defect of CV1720 cells, no correction was observed in CV1720 cells following expression of c.2278C>T *ATRIP* cDNA (encoding R760* ATRIP). Surprisingly, expression of WT *ATRIP* cDNA also corrected the G2/M checkpoint defect in DK0064 (ATR–SS) cells, which we propose could result from elevated ATRIP expression causing stabilisation of residual ATR protein, since ATR–SS cells have low ATR and ATRIP expression. Significantly, c.2278C>T *ATRIP* cDNA was unable to rescue ATR–SS cells. Finally expression of c.2278C>T *ATRIP* cDNA in WT cells did not affect G2/M checkpoint arrest demonstrating that p.R760* ATRIP does not exert a dominant negative impact. Collectively, we conclude that p.R760* ATRIP impacts upon ATRIP function.

Next we examined how loss of the ATRIP C-terminus might impact upon ATRIP function. Two studies have previously observed that the C-terminal region of ATRIP is required for interaction with ATR [21,30]. Falck *et al* [30] reported that ATR–ATRIP interaction required the C-terminal 32 amino-acids of ATRIP (769–791) whilst Ball *et al* [21] found that interaction was abolished in a protein that lacked exon 11, which encompasses amino-acids 658–684. Arg760 lies close to these regions. To examine whether p.R760* ATRIP can interact with ATR, HA-tagged *WT* or c.2278C>T (ATRIP R760*) cDNA was co-expressed with untagged WT *ATR* cDNA in HEK293 cells. Following IP with HA-agarose, the level of co-immunoprecipitated ATR was assessed by Western Blotting. Although there was a low level of non-specific ATR binding to the HA beads, the level of ATR present after HA-R760* ATRIP expression (derived from c.2278C>T *ATRIP* cDNA) was substantially lower than after HA-WT ATRIP expression (Figure 3B left panel). Both WT and R760* ATRIP were efficiently expressed, however (Figure 3B right panel). Thus, we conclude that R760* impairs the binding of ATRIP to ATR.

Identification of further patients with mutations in *ATR*

In the course of our functional characterisation of cell lines from SS patients, we examined LBLs derived from two SS patients, 27-4BI and 19-8BI (see Figure 4A, Figure S4, and Table 1 for clinical details). Western Blotting revealed that both cell lines displayed substantially reduced ATR protein whilst showing normal expression of other DNA damage response components, including CtIP, TOPBP1 and RAD17 (Figure 4B). 27-4BI also had reduced ATRIP levels. Additionally, the 27-4BI cell line expressed normal levels of PCNT, excluding MOPD type II as a potential genetic diagnosis, since most of these patients exhibit severely reduced PCNT expression. These findings raised the possibility that the patients could harbour mutations affecting ATR or ATRIP expression. Sequencing of *ATR* cDNA revealed the same c.3477G>T mutational change in both patients (Figure S5A). This change causes an amino acid substitution, p.Met1159Ile, which lies within a conserved UME (NUC010) domain of ATR. UME domains, and particularly the methionine residue within the domain, are highly conserved in ATR species, including yeast although their function is unknown (Figure 4C and 4D).

The second *ATR* mutation identified was c.6897+464C>G;p.Val2300Gly fs75*, which, surprisingly, was also present in both patients. RT-PCR sequencing showed that a 142 bp sequence, which originated from a repeat region present in intron 40, was inserted at the boundary between exon 40 and 41 in both patients (Figure S5C). Genomic sequencing revealed the presence of a single C>G mutation in intron 40, which generates a preferred splice signal causing insertion of the intron sequence to the start of exon 41 (Figure S5D for further details). This insertion causes a frameshift and the generation of a stop codon at c.6978 in exon 41. Sequencing of *ATRIP* cDNA in patient 27-4BI failed to reveal any mutational changes. Thus, our findings provide strong evidence that mutational changes in ATR underlie the reduced ATR/ATRIP expression observed in both patients.

To verify that these mutational changes impact upon ATR function, we examined whether 27-4BI cells could activate UV-induced ATR–dependent G2/M checkpoint arrest. Significantly, we observed an inability to activate UV-induced G2/M checkpoint arrest in 27-4BI cells similar to that observed in DK0064

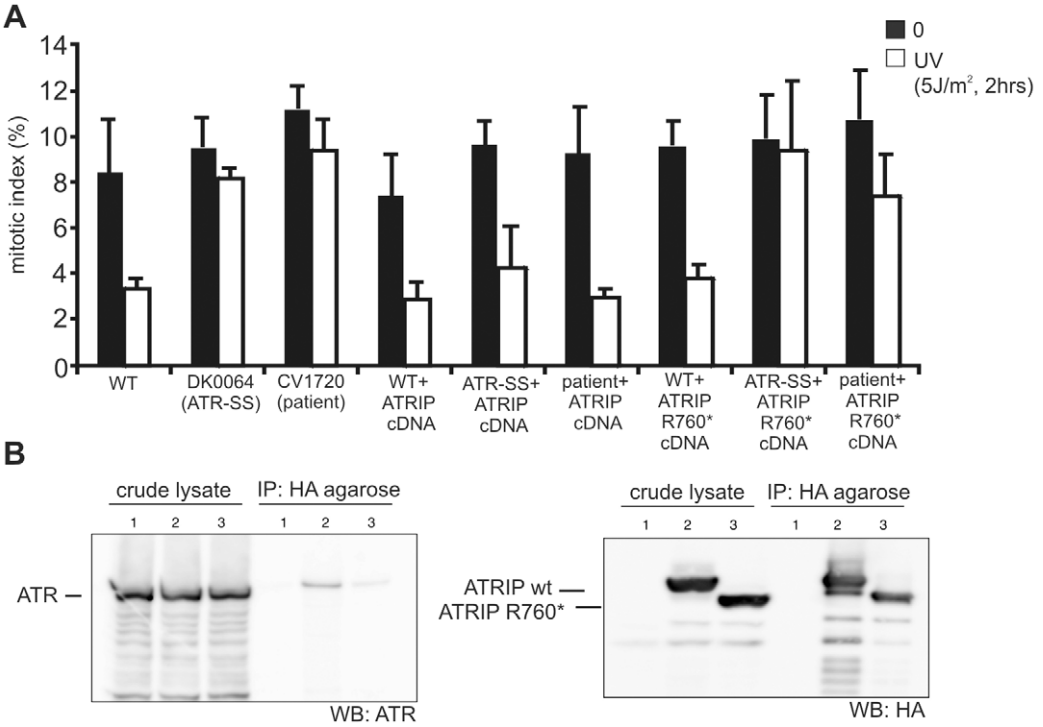

Figure 3. WT ATRIP cDNA but not cDNA encoding p.Arg760* ATRIP complements the G2/M checkpoint defect in CV1720 cells, and p.Arg760*ATRIP impairs ATR–ATRIP protein interaction. A) Analysis of the G2/M checkpoint defect in CV1720 cells following expression of ATRIP cDNA. G2/M checkpoint arrest was examined 2 h post exposure to 5 Jm^{-2} UV. As shown in Figure 1A, WT cells showed proficient checkpoint arrest whilst DK0064 (ATR–SS) and CV1720 (patient) cells are unable to undergo arrest. Expression of WT ATRIP cDNA restored the ability of CV1720 (patient) and DK0064 (ATR–SS) to undergo checkpoint arrest but this was not observed following transfection of cDNA encoding R760* ATRIP. Significantly, expression of ATRIP R760* did not impair checkpoint arrest in WT cells verifying that it does not exert a dominant negative impact. Results represent the mean and SD of three experiments. WT cells were GM2188. ATR–SS represents DK0064 and patient, CV1720. B) R760* ATRIP impairs ATR–ATRIP interaction. Crude lysates were prepared from HEK293T cells and either mock transfected (lane1), transfected with HA-tagged WT *ATRIP* cDNA (lane2), or R760* *ATRIP* cDNA (lane3) (generating p.Arg760* ATRIP protein) together with *ATR* cDNA. The extracts were immunoprecipitated with agarose-conjugated rabbit anti-HA-tag antibody (MBL). Interaction with ATR was examined by immunoblotting with ATR antibodies (left panel). Immunoblotting using the HA-tag (ATRIP; right panel) verified expression of the appropriately sized ATRIP in the samples. 33% of the crude lysate was loaded; IP, immunoprecipitate.
doi:10.1371/journal.pgen.1002945.g003

(ATR–SS) cells (Figure 5A) [7]. Checkpoint arrest after exposure to ionising radiation was activated normally. Additionally, we examined the phosphorylation of a range of ATR substrates following exposure to 0.5 mM HU and observed impaired phosphorylation in both 27-4BI and 19-8BI cells (Figure 5B). Collectively, these functional data substantiate a deficiency in the ATR–dependent DNA damage response in LBLs from these two cases. Thus, we conclude that both patients represent further ATR–SS patients.

Discussion

Although the first causal defect for SS was identified as ATR in 2003, further patients with mutations in *ATR* have not been reported [7]. SS patients are characterised by microcephaly and growth delay, features also observed in other microcephalic, primordial dwarfism syndromes including MOPD type II and MGS. Given that all ATR–SS patients to date share consanguinity, there are limitations in defining the spectrum of clinical features conferred by ATR deficiency to support a clinical distinction between ATR–SS and related disorders such as MOPD type II and MGS as well as other sub-classes of SS [1–3,31].

Here, we describe the novel identification of a patient mutated in ATRIP, the binding partner of ATR. Thus, we identify *ATRIP* as a new causal gene for SS. The mutational change in one *ATRIP* allele lies within a region previously suggested to be required for interaction with ATR, which is consolidated by our work [21,30]. We demonstrate that the second allele is abnormally spliced causing a reduction in *ATRIP* mRNA from that allele. qRT-PCR analysis suggested that there could be 25% residual WT *ATRIP* expressed in the patient cells. Consistent with this, we routinely observed ~10–20% of WT ATRIP protein in CV1720 cells by Western Blotting, although the level was variable between preparations. Although not examined in detail, there appeared to be a correlation between proliferation status and ATRIP levels, with the levels decreasing as proliferation slowed. Thus, differences in the proliferative state of cells at the time of analysis may underlie the apparent difference between Western Blotting and qRT-PCR analysis. Notwithstanding some limitations in quantification, the patient clinical features were marked despite ~10–20% residual ATRIP expression. Similarly, in patient DK0064, residual ATR protein can be readily detected [7]. Thus, we conclude that reduced but detectable levels of ATR/ATRIP protein can confer a clinical phenotype.

Additionally, we identify two further SS patients with ATR mutations in two unrelated families native to the UK. Interestingly, despite being unrelated, 27-4BI and 19-8BI carry the same compound heterozygous mutations, possibly representing founder mutations in the UK population.

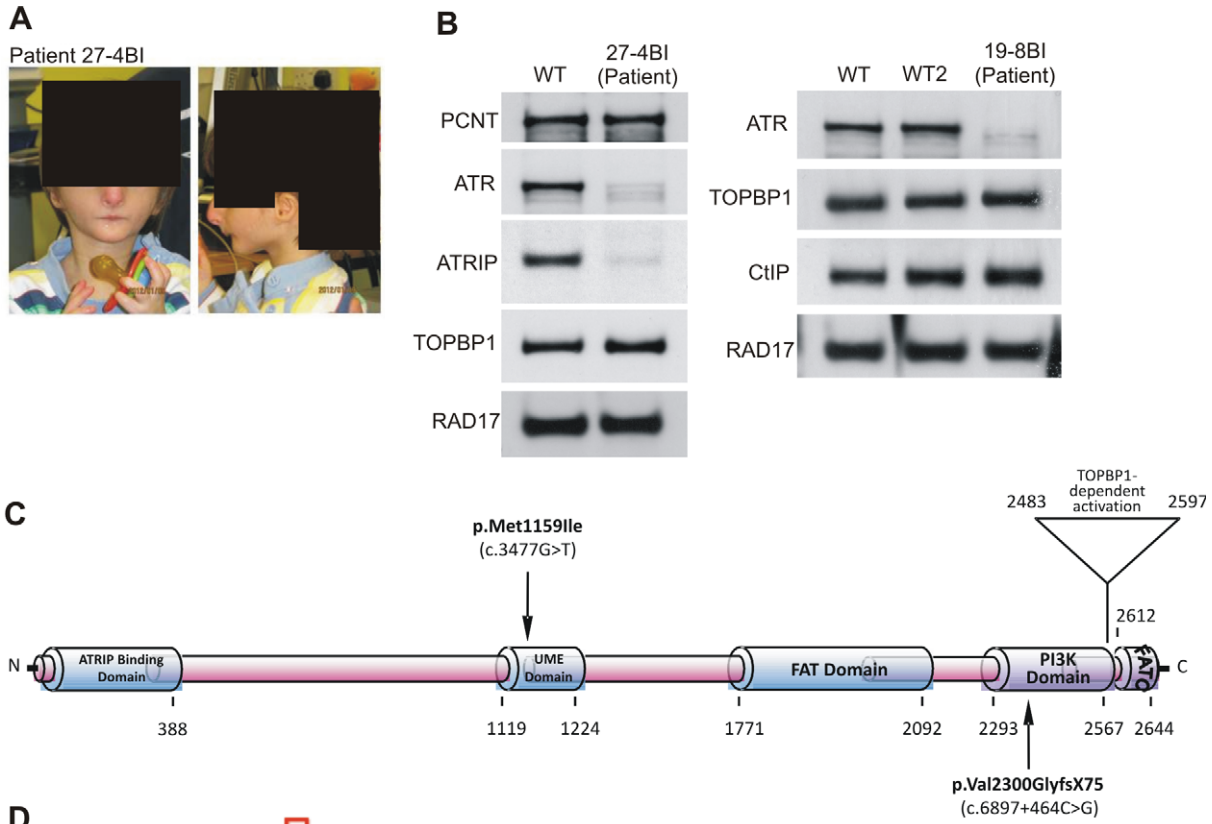

Figure 4. Patients 27-4BI and 19-8BI have reduced ATR and ATRIP expression and mutations in ATR. A) Photographs of patient included with informed consent of parent. B) Cell extracts (50 μg) from LBLs derived from WT (IM257), patient 27-4BI or patient 19-8BI were immunoblotted using the indicated antibodies. Reduced expression of ATR was observed in both patients. 27-4BI also had reduced ATRIP expression. C) Structure of ATR showing the site of the mutations identified and the UME domain. D) The UME domain is conserved between species and the methionine residue within this domain is conserved in yeast.
doi:10.1371/journal.pgen.1002945.g004

All four ATR/ATRIP patients displayed severe microcephaly and growth delay (Table 1). All patients also displayed micrognathia, receding forehead, dental crowding and microtia with small or absent lobes (Figure 4A). Interestingly, an MRI scan of the ATRIP–SS patient revealed an abnormally small pituitary with absent fossa, which could contribute to the delayed growth observed (Figure S1). In distinction to the original ATR–SS patient (DK0064), patients 27-4BI and 19-8BI showed more marked skeletal abnormalities including digital features and aberrant patellae suggesting that ATR deficiency can have a detrimental impact on bone development (Table 1, Figure S4) [32]. Interestingly, aberrant patellae is a clinical feature commonly exhibited by MGS patients suggestive of a biological overlap between the ATR checkpoint pathway and the replication machinery during skeletal development and maintenance. In keeping with this, characterisation of a mouse model harbouring the same mutational change identified in the original ATR–SS patient (DK0064) revealed marked bone abnormalities including kyphosis and osteoporosis [32]. Our findings suggest that ATR–ATRIP SS shows more overlap with MGS than previously recognised (Table 2). However, whereas ATR–ATRIP SS patients tend to have very marked microcephaly, growth delay, dental crowding, small ears and less severe skeletal abnormalities, the spectrum for MGS tends to be less marked microcephaly and growth delay but a striking impact on skeletal development. Nonetheless, there does not appear to be an absolute clinical divide between these two disorders. Significantly, these overlapping clinical features could reflect the fact that both ATR/ATRIP

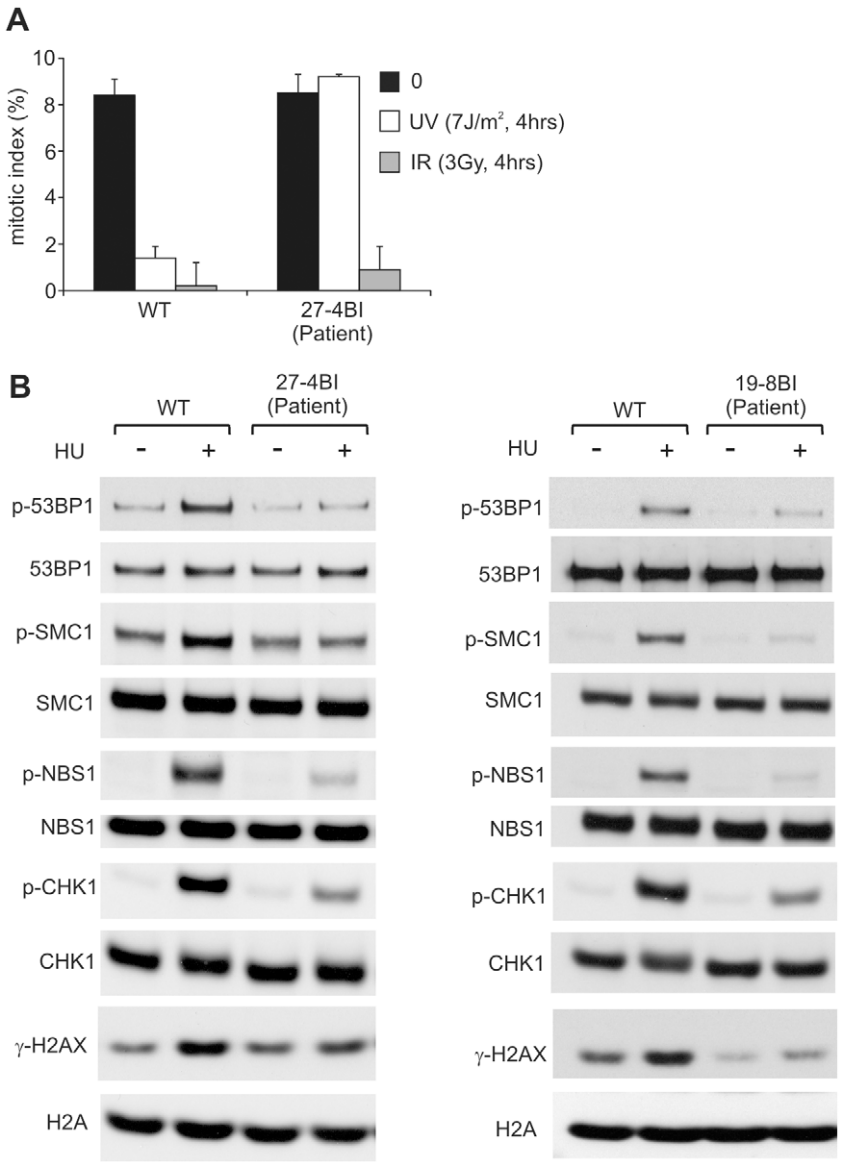

Figure 5. LBLs from patient 27-4BI and 19-8BI showed impaired ATR–dependent damage responses. A) 27-4BI cells were examined for their ability to activate G2/M checkpoint arrest at 4 h following exposure to 7 Jm^{-2} UV. In contrast to WT cells (GM2188), no significant arrest was observed in 27-4BI cells. The checkpoint response to ionizing radiation, which is ATM rather than ATR dependent, was normal. B) LBLs derived from patients 27-4BI and 19-8BI were examined for their ability to phosphorylate the indicated ATR substrates at 1 h following exposure to 0.5 mM HU. WT represents IM257. 27-4BI and control LBLs have a similar cell cycle profile demonstrating that the lack of ATR substrate phosphorylation cannot be attributed to the lack of S phase cells (Figure S2).
doi:10.1371/journal.pgen.1002945.g005

and the origin licensing complex play an essential role in promoting efficient replication and recovery from fork stalling, which may be vital during developmental stages involving rapid replication [13].

In summary, we provide the first report of a SS patient with mutations in *ATRIP*, defining a further novel genetic defect for this disorder, and describe two additional patients native to the UK, with mutations in *ATR*. The description of multiple ATR–ATRIP patients allows us to define a spectrum of clinical features conferred by *ATR–ATRIP* mutations. The clinical characteristics include severe microcephaly and growth delay, small or absent ear lobes, micrognathia and dental crowding. In addition, the novel ATR–mutated cases described here expand the clinical impact of impaired ATR–function to include more marked skeletal involvement.

Methods

Ethics Statement

Ethical approval for the research was granted by the School of Life Sciences Research Governance Committee, University of Sussex. Informed consent was obtained and clinical investigations were conducted according to the principles expressed in the Declaration of Helsinki. Patient material was gathered under conditions of the Human Tissue Authority (HTA licence number 12119).

Patients and cell lines

CV1720 is a SS patient of Gujarati-Indian origin. Patients 27-4BI and 19-8BI are English. The clinical features are described in

Table 2. MGS and Seckel syndrome patient phenotypes.

	ORC1 - MGS	Pre-RC MGS	ATR/ATRIP SS
Number of patients	10	25	4
OFC (cm)*	−5.4 to −11 SD	+1.7 to −5.0 SD	−10 to −12 SD
Height (cm)*	−4.5 to −9.6 SD	−0.4 to −6.4 SD	−5 to −8 SD
Weight (kg)*	0.8 to −11 SD	−0.3 to −9.9 SD	−3.3 to −8 SD
Intellectual disability	Ranges from none to mild/moderate	None	Developmental delay (2/4)
Facial Features	Small and abnormal ears (9/10), micrognathia (5/10), down slanted palpebral fissures (1/10)	Small and abnormal ears(25/25), micrognathia (20/25), down slanted palpebral fissures (8/25)	Small and/or abnormal ears (4/4), micrognathia (4/4), receding forehead (4/4), prominent nose (4/4), short palpebral fissures (2/4)
Skeletal abnormalities	Delayed bone age (3/10), Slender long bones (2/10) , absent patellae (6/10), genu recurvatum (4/10)	Delayed bone age (11/25), slender long bones, absent patellae (24/25)	Delayed bone age (1/4), 5th finger clinodactyly (2/4), symmetric dwarfism (3/4), small/abnormal patellae (2/4), kyphosis (1/4), hip abnormality (2/4), narrow pelvis (iliac blades) (1/4)
MRI	Normal in 2 patients examined	NA	Generalised cerebral atrophy, delayed myelination, abnormal gyration (2 patients examined)
Other	High pitched voice (1/10), full lips (7/10), cryptochordism (2/4 examined), mammary hypoplasia (2/2 examined), feeding and respiratory problems during infancy (8/10)	Full lips (14/25), cryptochordism (7/14 examined), mammary hypoplasia (8/8 examined), feeding (20/25) and respiratory (9/25) problems during infancy	Dental crowding (4/4), feeding and respiratory problems during infancy (1/4)

*standard deviations from the age-related normal population mean, NA = not assessed.
MGS data from [13,14] [33,34].
doi:10.1371/journal.pgen.1002945.t002

Table 1. Lymphoblastoid cell lines (LBLs) were derived from blood following EBV transformation. WT LBLs were GM2188 or LB197 as indicated. All LBLs were grown in RPMI medium supplemented with 10% foetal calf serum, penicillin, and streptomycin. Transfection with *ATRIP* cDNA was with Genejuice Transfection Reagent (Novagen, Merck Millipore, UK) following the manufacturers protocol.

qRT–PCR. Transcript levels of the *ATRIP*–c.2278C (normal) and *ATRIP*–c.2278C>T (p.Arg760*) alleles in LBLs from patient CV1720, and the parents were determined by the cycleave quantitative real time PCR (Cycleave-qPCR, TaKaRa Co. Ltd, Kyoto Japan) as well as standard site specific q-PCR (carried out in triplicate). Transcripts from the *HPRT1* allele were used as a quantification control. In the Cycleave qPCR, RNaseH sensitive fluorescent probes that specifically recognize the c.2278C and c.2278C>T alleles were used for the assay. qPCR results were analyzed by the ΔΔCT method. qPCR primers and probes used for the assay are listed below. (172F, 5′-CTTCACTGCCGAC-GACCTGG-3′; 191R, 5′-TTTGCTCGTTCACTGGTCTG-3′; P1, 5′-GGGGTCAGCATGCTCATCC-3′; P2, 5′-GGGGGTC-AGCATGCTCATCT-3′; P3C, 5′-ACCTCGGGGTCTTCCA-CATC-3′; P4, 5′- -3′; P5, 5′- -3′; P6C, 5′- -3′; P7, 5′-GCC-TATCGCAGAAGGACAAG-3′; P8, 5′-GGGTCTTCCACAT-CGGTTTC-3′; probe1 for c.2278C, 5′Eclipse-CCCTC(rG)GAT-3′FAM; probe2 for c.2278C, 5′Eclipse- GCCCTC(rA)GA-3′ROX)

Co-immunoprecipitation. To investigate the interaction of the ATRIP proteins with ATR, HEK293T cells were transfected with the HA-tagged *ATRIP* cDNA expressing plasmids (wild type and 2278C>T *ATRIP*) together with *ATR* cDNA, followed by 24 h incubation. Whole cell lysates were prepared using CelLytic Nuclear Extraction Kit (Sigma, St. Louis). Co-immunoprecipitation was performed using rabbit anti-HA antibody-conjugated agarose beads (MBL, Nagoya, Japan). Western blotting was carried out using ATR or anti-HA (detecting HA-tagged ATRIP) antibodies. Anti-ATR was N19 (Santa Cruz, Santa Cruz) at 1:200 dilution. Anti-HA-tag antibody, 132-3 (MBL, Nagoya, Japan), was used at 1:1000 dilution.

Immunofluorescence for analysis of γH2AX and 53BP1 staining

Cells were cytospun onto slides, fixed with 3% formaldehyde for 10 min and permeabilized in 0.5% Triton-X100. After antibody treatment and staining with 4,6-diamidino-2-phenylindole (DAPI), coverslips were mounted in Vectashield mounting medium (Vector Laboratories, Burlingame). Samples were incubated with primary antibodies for γ-H2AX (Millipore, Billerica) or 53BP1 (Bethyl, Montgomery). Secondary antibodies were from Sigma (St. Louis).

Western blotting

Cells were lysed for one hour in IPLB (50 mM Tris-HCl, 150 mM NaCl, 2 mM EDTA, 2 mM EGTA, 25 mM NaF, 25 mM β-glycerolphosphate, 0.1 mM NaOrthovanadate, 0.2% Triton X-100, 0.3% NP-40, plus protease inhibitor cocktail (Roche, Basel) at 4°C, centrifuged at 13,000 rpm for 10 minutes. The soluble fraction was subjected to SDS-PAGE and transferred to a nitrocellulose membrane for protein detection.

Antibodies raised against ATR, CHK1 (FL476) and MCM2 (N19) were from Santa Cruz (Santa Cruz). Anti-FANCD2, ATRIP and phospho-Chk1 (Ser317) antibodies were from Novus (Littleton), Bethyl (Montgomery), and Cell Signaling (Beverly, Woburn), respectively.

G2/M checkpoint arrest

Cells were exposed to 5 or 7 Jm^{-2} UV, or 3Gy ionising radiation and incubated for 2 or 4 hours (as indicated) in complete medium containing 0.2 ug/ml Colcemid (Invitrogen, Carlsbad), followed by processing for immunofluorescence as detailed above. Mitotic cells were detected by α-Histone H3-pSer10 antibodies (Millipore, Billerica) and cells were counterstained with DAPI.

Supporting Information

Figure S1 Photograph of limbs and MRI scan of patient CV1720. Left hand photograph showing hands and feet. Right hand photograph shows an MRI scan where a small pituitary is evident.
(TIF)

Figure S2 Cell cycle analysis of WT, DK0064 (ATR–SS), 27-4BI, and CV1720 patient LBLs. A) Asynchronous growing cultures of WT, DK0064 (ATR–SS), 27-4BI and CV1720 patient cells were pelleted, fixed in 70% ice-cold ethanol and stained with propidium iodide prior to FACs analysis. Populations were gated and the proportion of cells in G1, S and G2/M phases of the cell cycle measured. B) WT, DK0064 (ATR–SS), 27-4BI and CV1720 patient cells were treated with nocodazole for 16 h and then fixed and analysed as in a). C) Asynchronous growing cultures of WT, DK0064 (ATR–SS), 27-4BI and CV1720 patient cells were pulse-labelled with 50 μM BrdU for 1 h. Cells were then fixed in 70% ice-cold ethanol and processed for BrdU FACs analysis as described in Bicknell et al, 2011 [13]. The proportion of cells in S phase were gated and measured. Each graph represents the mean of three independent experiments. The error bars represent the standard deviation.
(TIF)

Figure S3 Identification of a truncating mutation in *ATRIP* in patient, CV1720. Genomic DNA sequencing of *ATRIP* exons showed that patient CV1720 and the unaffected mother, CV1780, are heterozygous for a c.2278C>T mutational change in exon12 of *ATRIP*. The father has a WT sequence at this site. 2278C>T generates a primary stop codon predicting a truncated protein at position arginine 760 (p.R760*). WT sequence shown in blue, the mutation is shown in Red.
(TIF)

Figure S4 Photographs of patients 27-4BI and 19-8BI. A) Shows abnormal digits of patient 27-4BI. B) Copper beaten appearance of skull of patient 19-8BI. C) Frontal and Lateral view of left knee of patient 19-8BI showing an absence of ossification of the patella.
(TIF)

Figure S5 Mutational changes observed in *ATR* in patients 27-4BI and 19-8BI. A) c.3477G>T mutational change in patients 27-4BI and 19-8BI. RT-PCR sequencing revealed a heterozygous 3477G>T mutational change in both patients causing an amino acid substitution, p.Met1159Ile, which lies within a conserved UME (NUC010) domain of ATR. B) A double sequence was observed at the boundary between exons 40 and 41 in both patients. Sequencing showed that the double sequence was caused by insertion of a 142 bp region from intron 40. C) A C to G mutational change was observed in intron 41 of both patients converting the sequence CAGCT to CAGGT, a splice site. The insertion causes a frameshift and a stop codon at p.Val2300-Glyfs*75. D) Diagram showing the likely origin of the insertion observed at the exon 40/41 boundary. Sequencing of intron 40 revealed a C>G mutation as indicated creating a cryptic splice site causing splicing of exon 40 to the indicated intronic sequence (which represents an Alu repeat sequence). Thus one ATR allele of the patients harbours a 142 nucleotide insertion between exons 40 and 41. Exons 40 and 41 are highlighted in green and the inserted intronic sequence is shown in red. The intronic C>G change is highlighted in red. The insertion causes a frameshift and a stop codon at c.6978 in exon 41.
(TIF)

Table S1 The table shows the position of single nucleotide polymorphisms identified in intron 1 and 2 in the patient and parental genomic DNA. * The contig position is defined as the position of the single nucleotide variant (SNV) on the contig (NT_022517.17) when counting from the first base (base position = 1). **rs# is the NCBI's reference SNP ID. *** minor allele (indicated as a base) and its frequency (MAF) (second most frequent allele) in a default global population reported in dbSNP database (1000 Genome phase 1, May 2011). N.A. not available.
(DOCX)

Acknowledgments

We thank Dr. E. Riballo and P. Gajwani for contributions to this work and Dr. D. Cortez for providing *ATRIP* cDNA.

Author Contributions

Conceived and designed the experiments: TO GSS AMRT MO PAJ. Performed the experiments: SW TS SL GC MM NM YN. Analyzed the data: TO TS GSS AMRT MO PAJ. Contributed reagents/materials/analysis tools: EH KP MS PJB PV MB. Wrote the paper: PAJ. Aided in writing the paper: MO GSS TO AMRT.

References

1. Majewski F, Goecke T (1982) Studies of microcephalic primordial dwarfism I: approach to a delineation of the Seckel syndrome. Am J Med Genet 12: 7–21.
2. Hall JG, Flora C, Scott CI, Jr., Pauli RM, Tanaka KI (2004) Majewski osteodysplastic primordial dwarfism type II (MOPD II): natural history and clinical findings. Am J Med Genet A 130: 55–72.
3. Gorlin RJ (1992) Microtia, absent patellae, short stature, micrognathia syndrome. J Med Genet 29: 516–517.
4. Thornton GK, Woods CG (2009) Primary microcephaly: do all roads lead to Rome? Trends Genet 25: 501–510.
5. Goodship J, Gill H, Carter J, Jackson A, Splitt M, et al. (2000) Autozygosity mapping of a seckel syndrome locus to chromosome 3q22. 1-q24. Am J Hum Genet 67: 498–503.
6. Borglum AD, Balslev T, Haagerup A, Birkebaek N, Binderup H, et al. (2001) A new locus for Seckel syndrome on chromosome 18p11.31-q11.2. Eur J Hum Genet 9: 753–757.
7. O'Driscoll M, Ruiz-Perez VL, Woods CG, Jeggo PA, Goodship JA (2003) A splicing mutation affecting expression of ataxia-telangiectasia and Rad3-related protein (ATR) results in Seckel syndrome. Nature Genetics 33: 497–501.
8. Qvist P, Huertas P, Jimeno S, Nyegaard M, Hassan MJ, et al. (2011) CtIP Mutations Cause Seckel and Jawad Syndromes. PLoS Genet 7: e1002310. doi:10.1371/journal.pgen.1002310
9. Al-Dosari MS, Shaheen R, Colak D, Alkuraya FS (2010) Novel CENPJ mutation causes Seckel syndrome. J Med Genet 47: 411–414.
10. Kalay E, Yigit G, Aslan Y, Brown KE, Pohl E, et al. (2011) CEP152 is a genome maintenance protein disrupted in Seckel syndrome. Nat Genet 43: 23–26.
11. Griffith E, Walker S, Martin CA, Vagnarelli P, Stiff T, et al. (2008) Mutations in pericentrin cause Seckel syndrome with defective ATR–dependent DNA damage signaling. Nat Genet 40: 232–236.
12. Rauch A, Thiel CT, Schindler D, Wick U, Crow YJ, et al. (2008) Mutations in the pericentrin (PCNT) gene cause primordial dwarfism. Science 319: 816–819.
13. Bicknell LS, Walker S, Klingseisen A, Stiff T, Leitch A, et al. (2011) Mutations in ORC1, encoding the largest subunit of the origin recognition complex, cause microcephalic primordial dwarfism resembling Meier-Gorlin syndrome. Nat Genet 43: 350–355.
14. Bicknell LS, Bongers EM, Leitch A, Brown S, Schoots J, et al. (2011) Mutations in the pre-replication complex cause Meier-Gorlin syndrome. Nat Genet 43: 356–359.
15. Willems M, Genevieve D, Borck G, Baumann C, Baujat G, et al. (2010) Molecular analysis of pericentrin gene (PCNT) in a series of 24 Seckel/microcephalic osteodysplastic primordial dwarfism type II (MOPD II) families. Journal of medical genetics 47: 797–802.
16. Nam EA, Cortez D (2011) ATR signalling: more than meeting at the fork. The Biochemical journal 436: 527–536.
17. Zou L, Elledge SJ (2003) Sensing DNA damage through ATRIP recognition of RPA-ssDNA complexes. Science 300: 1542–1548.
18. Ciccia A, Elledge SJ (2010) The DNA damage response: making it safe to play with knives. Mol Cell 40: 179–204.

19. Cortez D, Guntuku S, Qin J, Elledge SJ (2001) ATR and ATRIP: partners in checkpoint signaling. Science 294: 1713–1716.
20. Namiki Y, Zou L (2006) ATRIP associates with replication protein A-coated ssDNA through multiple interactions. Proceedings of the National Academy of Sciences of the United States of America 103: 580–585.
21. Ball HL, Myers JS, Cortez D (2005) ATRIP binding to replication protein A-single-stranded DNA promotes ATR–ATRIP localization but is dispensable for Chk1 phosphorylation. Molecular biology of the cell 16: 2372–2381.
22. Paciotti V, Clerici M, Lucchini G, Longhese MP (2000) The checkpoint protein Ddc2, functionally related to S. pombe Rad26, interacts with Mec1 and is regulated by Mec1-dependent phosphorylation in budding yeast. Genes Dev 14: 2046–2059.
23. Lakin ND, Jackson SP (1999) Regulation of p53 in response to DNA damage. Oncogene 18: 7644–7655.
24. Ward IM, Chen J (2001) Histone H2AX is phosphorylated in an ATR–dependent manner in response to replicational stress. J Biol Chem 276: 47759–47762.
25. Alderton GK, Joenje H, Varon R, Borglum AD, Jeggo PA, et al. (2004) Seckel syndrome exhibits cellular features demonstrating defects in the ATR signalling pathway. Human Molecular Genetics 13: 3127–3138.
26. Toledo LI, Murga M, Zur R, Soria R, Rodriguez A, et al. (2011) A cell-based screen identifies ATR inhibitors with synthetic lethal properties for cancer-associated mutations. Nature structural & molecular biology 18: 721–727.
27. Chanoux RA, Yin B, Urtishak KA, Asare A, Bassing CH, et al. (2009) ATR and H2AX cooperate in maintaining genome stability under replication stress. The Journal of biological chemistry 284: 5994–6003.
28. Andreassen PR, D'Andrea AD, Taniguchi T (2004) ATR couples FANCD2 monoubiquitination to the DNA damage response. Genes and Development 18: 1958–1963.
29. Noensie EN, Dietz HC (2001) A strategy for disease gene identification through nonsense-mediated mRNA decay inhibition. Nature biotechnology 19: 434–439.
30. Falck J, Coates J, Jackson SP (2005) Conserved modes of recruitment of ATM, ATR and DNA-PKcs to sites of DNA damage. Nature 434: 605–611.
31. Klingseisen A, Jackson AP (2011) Mechanisms and pathways of growth failure in primordial dwarfism. Genes & development 25: 2011–2024.
32. Murga M, Bunting S, Montana MF, Soria R, Mulero F, et al. (2009) A mouse model of ATR–Seckel shows embryonic replicative stress and accelerated aging. Nature genetics 41: 891–898.
33. Guernsey DL, Matsuoka M, Jiang H, Evans S, Macgillivray C, et al. (2011) Mutations in origin recognition complex gene ORC4 cause Meier-Gorlin syndrome. Nat Genet 43: 360–364.
34. de Munnik SA, Bicknell LS, Aftimos S, Al-Aama JY, van Bever Y, et al. (2012) Meier-Gorlin syndrome genotype-phenotype studies: 35 individuals with pre-replication complex gene mutations and 10 without molecular diagnosis. European journal of human genetics : EJHG 20: 598–606.